ADOPTIVE TRANSFER OF *EX VIVO* EXPANDED

GAMMA DELTA T CELLS

TARGETING OSTEOLYTIC CANCER IN THE BONE

ANETA ZYSK B.Sc (Hons)

A thesis submitted in total fulfilment of the requirements

For the degree of Doctor of Philosophy

in

The Discipline of Surgery, School of Medicine

Faculty of Health Sciences

The University of Adelaide

July 2017

Table of Contents

Declaration ix

Acknowledgements x

Abstract xii

Conference proceedings xiii

Publications xv

Manuscripts under review xvi

Prizes Awarded.....xvii

Abbreviations Used xviii

Chapter 1 Introduction.....1

1.1 Cancer in the bone 2

1.1.1 Normal bone metabolism 3

1.2 The 'vicious cycle' of cancer in the bone 6

1.3 Osteosarcoma.....9

1.4 Breast cancer bone metastases.....10

1.5 Focus on aminobisphosphonates 11

1.6 Gamma delta (γδ) T cells.....17

1.7 Activation of Vγ9Vδ2 T cells.....19

1.8 Mechanisms of Vγ9Vδ2 T cell cytotoxicity.....23

1.9 Clinical trials with Vγ9Vδ2 T cells 29

1.9.1 *In vivo* expansion of Vγ9Vδ2 T cells 29

1.9.2 Vγ9Vδ2 T cell adoptive transfer 32

1.10 Combination Therapies 34

1.10.1 Sensitisation with nBPs 34

1.10.2 Chemotherapies 35

1.10.3 Antibodies 37

1.11 Role of Vγ9Vδ2 T cells in osteoimmunology 40

1.12 Aims and significance 41

Chapter 2 Materials and Methods 44

2.1 Cell Lines 45

2.2 Antibodies and Reagents 45

2.3 *Ex vivo* expansion of Vγ9Vδ2 T cells 46

2.4 Enrichment of Vγ9Vδ2 T cells 46

2.5 Enrichment of $CD16^+$ Vγ9Vδ2 T cells 47

2.6 Cell cytotoxicity assay 47

2.7 Luciferase-based viability assay 48

2.8 Measurement of DEVD-caspase activity 48

2.9 Western Blotting 49

2.10 Labelling Vγ9Vδ2 T cells with DiR 49

2.11 Animals 50

2.12 *In vivo* fluorescence and bioluminescence imaging 50

2.13 Intratibial injections of cancer cells 51

2.14 *In vivo* localisation 51

2.15 Assessing the *in vivo* anti-cancer efficacy of a single administration of ZOL and Vγ9Vδ2 T cells 52

2.16 Assessing the *in vivo* anti-cancer efficacy Vγ9Vδ2 T cells in combination with metronomic ZOL 52

2.17 *In vivo* anti-cancer efficacy of ZOL and Vγ9Vδ2 T cells 53

2.18 *Ex vivo* micro-computed tomography (μCT) analysis 53

2.19 Histology 54

2.20 Data analysis and statistics 54

Chapter 3 Optimising adoptive transfer of *ex vivo* expanded Vγ9Vδ2 T cells 55

3.1 Introduction 56

3.2 Results 58

3.2.1 *Ex vivo* expansion and phenotyping of Vγ9Vδ2 T cells 58

3.2.2 ZOL sensitises cancer cells to Vγ9Vδ2 T cell cytotoxicity 63

3.2.3 A single infusion of Vγ9Vδ2 T cells transiently inhibits tumour growth 64

3.2.4 Metronomic ZOL dosing does not potentiate the anti-cancer efficacy of Vγ9Vδ2 T cells 69

3.2.5 ZOL-M shows a trend towards decreasing cancer induced osteolysis 72

3.3 Discussion 75

Chapter 4 Adoptive transfer of *ex vivo* expanded Vγ9Vδ2 T cells in combination with zoledronic acid inhibits cancer growth and limits osteolysis in a murine model of osteolytic breast cancer 77

4.1 Chapter Introduction 78

4.2 Statement of Authorship 79

4.2 Manuscript 84

Chapter 5 Adoptive transfer of Vγ9Vδ2 T cells in combination with zoledronic acid treatment inhibits tumour growth and lung metastases in a murine model of osteolytic osteosarcoma 94

5.1 Chapter Introduction 95

5.2 Statement of Authorship 95

5.3 Abstract 98

5.4 Introduction 98

5.5 Materials and Methods 101

5.5.1 Cells and reagents 101

5.5.2 *Ex vivo* expansion and enrichment of Vγ9Vδ2 T cells 101

5.5.3 Cell cytotoxicity assay 102

5.5.4 Cell viability assay 103

5.5.5 Western Blotting 103

5.5.6 Labelling Vγ9Vδ2 T cells with fluorescent DiR dye 104

5.5.7 Animals 104

5.5.8 *In vivo* localisation 105

5.5.9 *In vivo* anti-tumour efficacy of ZOL and Vγ9Vδ2 T cells 106

5.5.10 *Ex vivo* micro-computed tomography (μCT) analysis 106

5.5.11 Data analysis and statistics 107

5.6 Results.....107

5.6.1 ZOL sensitises osteosarcoma cells to Vγ9Vδ2 T cell cytotoxicity *in vitro* 107

5.7 *Ex vivo* expanded Vγ9Vδ2 T cells localise to tumours in the bone.....110

5.7.1 ZOL potentiates the anti-cancer efficacy of Vγ9Vδ2 T cells against osteosarcoma 111

5.7.2 Vγ9Vδ2 T cells reduce the incidence and tumour burden of lung metastases.....114

5.7.3 ZOL in combination with Vγ9Vδ2 T cells inhibits bone degradation 114

5.8 Discussion.....121

5.9 Conflict of Interest 124

5.10 Acknowledgments 124

Chapter 6 Adoptive transfer of Vγ9Vδ2 T cells has a neutral effect on normal bone homeostasis 125

6.1 Introduction.....126

6.2 Results.....129

6.2.1 Vγ9Vδ2 T cells alone have minimal impact on bone morphometric parameters 129

6.2.2 ZOL alone has a positive effect on bone morphometric parameters... 129

6.2.3 Vγ9Vδ2 T cells in combination with ZOL have no effect on bone morphometric parameters compared to ZOL alone 133

6.3 Discussion.....136

Chapter 7 Vγ9Vδ2 T cells in combination with pro-apoptotic receptor agonists (PARAs) or chemotherapy enhance killing of breast cancer cells.....139

7.1 Introduction.....140

7.2 Results.....142

7.2.1 Phenotypic analysis of impure, CD16 depleted, and CD16 enriched cells 142

7.2.2 Drozitumab does not cross-link with CD16 on Vγ9Vδ2 T cells to elicit ADCC against cancer cells 148

7.2.3 Concurrent treatment of Vγ9Vδ2 T cells in combination with PARAs or chemotherapy enhances killing of cancer cells 151

7.3 Discussion.....154

7.4 Supplementary Figures 161

Chapter 8 Discussion, Future Directions and Conclusion.....165

8.1 Discussion.....166

8.2 Future Directions 175

8.2.1 Vγ9Vδ2 T cell immunotherapy for other cancers in the bone 175

8.2.2 Improving pre-clinical models 177

8.2.3 Enhancing Vγ9Vδ2 T cell adoptive transfer 177

8.2.4 Localised delivery 179

8.2.5 Novel antibodies to enhance anti-cancer efficacy 180

8.3 Conclusion 181

Bibliography 182

Declaration

Name: Aneta Zysk **Program:** PhD

I certify that this work contains no material which has been accepted for the award of any other degree or diploma in my name in any university or other tertiary institution and, to the best of my knowledge and belief, contains no material previously published or written by another person, except where due reference has been made in the text. In addition, I certify that no part of this work will, in the future, be used in a submission in my name for any other degree or diploma in any university or other tertiary institution without the prior approval of the University of Adelaide and where applicable, any partner institution responsible for the joint award of this degree.

I give consent to this copy of my thesis when deposited in the University Library, being made available for loan and photocopying, subject to the provisions of the Copyright Act 1968. The author acknowledges that copyright of published works contained within this thesis resides with the copyright holder(s) of those works. I also give permission for the digital version of my thesis to be made available on the web, via the University's digital research repository, the Library Search and also through web search engines, unless permission has been granted by the University to restrict access for a period of time.

I acknowledge the support I received for my research through the Australian Postgraduate Award.

Signature:…… Date:……..…

Acknowledgements

When most people say their PhD involved blood, sweat, and tears, they usually mean it in a figurative sense. I wish I could say the same. Over the past four years my PhD involved countless vials of blood, working long hours in the laboratory, and of course, many melt downs during moments of weakness. Together these experiences have taught me valuable lessons, not only applicable to scientific research but also to life, making me a stronger person and better researcher in the process. However, none of this growth would have been possible without a strong support network. So, before we delve into the world of Vγ9Vδ2 T cells, there are many people who deserve recognition for their support and the time they have invested in me and my career.

First and foremost, I would like to acknowledge my supervisors, Prof. Andreas Evdokiou and Dr. Mark DeNichilio. Thank you for giving me the opportunity to undertake such an interesting and challenging project. The difficulty of this project is the primary reason I have grown so much as a researcher and why I will continue to seek challenging projects in the future. Thank you for holding my work to a high standard and constantly encouraging me to improve.

Next, I would like to thank the rest of the Breast Cancer Research Unit: Irene Zinonos, Shelley Hay, Bill Panagopolous, and Bill Liapis. You welcomed me with open arms and after a few months I felt like I had been part of the group forever. Thank you all for patiently teaching me new techniques, sharing your scientific knowledge, and being willing volunteers for the Vγ9Vδ2 T cell cause. I would also like to thank the other PhD students, Alex Shoubridge, Chris Difelice, and Bee

Namfon. Good luck in completing your PhDs and I wish you all the best in your future endeavours.

Next, I would like to say a big thank you to my colleagues at the Basil Hetzel Institute. You all made my time here enjoyable and each day in the laboratory a bit more bearable. In particular, I would like to say an extra special thank you to my beautiful friends Alex Shoubridge, Pallave Dasari, Hilary Dorward, and Harshani Piedge. Together you have been my support network during these past few years. As we transition into the next stage of our lives, I will always remember and value our time together at the BHI. I also just wanted to thank you again for organising "Aneta Day" during one of the most stressful periods during my PhD. As Density's Child would say: "All the women, who are independent, throw your hands up at me".

Last, but certainly not least, I would like to thank my closest family and friends. To my wonderful parents Mariola and Wiesław Zysk. The sacrifices you made gave me the opportunity to study and make a better future for myself. I appreciate all your support and encouragement, and my only wish is to make you proud. Z głębi serca, dziękujem wam. To my best friend, Lauren "Mum" Morton. Thank you for all your enthusiasm when listening to me talk about my research, and for being the angel on my shoulder trying to keep me out of trouble since high school. To my wonderful fiancé Daniel Bonini, his parents Anna and Renzo, and brothers Nicholas and Anthony. Thank you all for the support, encouragement, and mlerms you have bought into my life. Daniel, you deserve a special mention as I didn't acknowledge you in my honours thesis as it was early days. Since I met you, you have been my rock, the constant in my life, and I cannot thank you enough for all your love, support, and strength.

Abstract

Bone metastases occur in more than 75% of patients with advanced breast cancer. Cancer in bone is associated with bone destruction and is responsible for high levels of morbidity and mortality but is notoriously difficult to treat. Bone destruction is also the primary cause of morbidity in patients with primary bone cancer, such as osteosarcoma, with metastatic spread to the lungs correlating with poor survival. Therefore, clearly new therapies are desperately required to target cancers in the bone. This study explored the therapeutic potential of gamma delta (Vγ9Vδ2) T cell based adoptive transfer using animal models of osteolytic breast cancer and osteosarcoma. Cytotoxic Vγ9Vδ2 T cells were expanded *ex vivo* from peripheral blood using IL-2 and zoledronic acid (ZOL). *In vitro*, expanded Vγ9Vδ2 T cells were cytotoxic against a panel of breast cancer and osteosarcoma cell lines and pre-treatment with ZOL sensitised all cancer cells to rapid killing by Vγ9Vδ2 T cells. Adoptive transfer of fluorescently labelled *ex vivo* expanded Vγ9Vδ2 T cells into NOD/SCID mice localised to cancer lesions in bone. Multiple infusions of Vγ9Vδ2 T cells reduced breast cancer growth, but had no effect on osteosarcoma growth in the bone marrow. However, in both cases, ZOL pre-treatment potentiated the anti-cancer efficacy of Vγ9Vδ2 T cells in bone, protected the bone from cancer-induced osteolysis and decreased the incidence of pulmonary metastases. Collectively these studies suggest this treatment regimen to be an effective immunotherapeutic approach for the treatment of primary and metastatic bone cancers.

Conference proceedings

Targeting osteolytic cancer in the bone with adoptive transfer of ex vivo expanded gamma delta T-cells in combination with zoledronic acid, University of Adelaide 2016 Florey International Postgraduate Research Conference, Adelaide, SA, Australia, 29th September 2016 **(Poster presentation)**

Targeting osteolytic cancer in the bone with adoptive transfer of ex vivo expanded gamma delta T-cells in combination with zoledronic acid, Gamma Delta Conference 2016, King's College London, UK, 16-19th June 2016 **(Oral and poster presentation)**

Adoptive transfer of ex vivo expanded gamma delta T cells in combination with zoledronic acid to target osteolytic cancer in the bone 2016 Australian Society for Medical Research (ASMR) SA Scientific Meeting, Adelaide, SA, Australia, 8th June 2016 **(Oral presentation)**

Targeting osteosarcoma with adoptive transfer of ex vivo expanded cytotoxic gamma delta T cells in combination with zoledronic acid, The Basil Hetzel Institute and Queen Elizabeth Hospital Research Day 2015, Adelaide, SA, Australia, 16th October 2015 **(Oral presentation)**

Adoptive transfer of ex vivo expanded cytotoxic gamma delta T cells in combination with zoledronic acid against osteolytic osteosarcoma, University of Adelaide 2015 Florey International Postgraduate Research Conference, Adelaide, SA, Australia, 24th September 2015 **(Poster presentation)**

Bad to the Bone, Faculty of Health Sciences Three Minute Thesis, University of Adelaide, Adelaide, SA, Australia, 18th August 2015 **(Oral presentation)**

Targeting breast cancer bone metastases with adoptive transfer of ex vivo expanded cytotoxic gamma delta T cells in combination with zoledronic acid, 2015 Australian Society for Medical Research (ASMR) SA Scientific Meeting, Adelaide, SA, Australia, 3rd June 2015 **(Oral presentation)**

Ex vivo expanded cytotoxic gamma delta T cells localise to tumour lesions in a model of osteolytic breast cancer, The Basil Hetzel Institute and Queen Elizabeth Hospital Research Day 2014, Adelaide, SA, Australia, 17th October 2014 **(Oral presentation)**

Adoptive transfer of ex vivo expanded cytotoxic gamma delta T cells to target breast cancer bone metastases, University of Adelaide 2014 Florey International Postgraduate Research Conference, Adelaide, SA, Australia, 25th September 2014 **(Poster presentation)**

Targeting breast cancer bone metastases with adoptive transfer of ex vivo expanded cytotoxic gamma delta T cells, 10th Asia Pacific Musculoskeletal Tumour Society (APMSTS) meeting, Melbourne, VIC, Australia, 9-11th April 2014 **(Poster presentation)**

Targeting breast cancer bone metastases with ex vivo expanded cytotoxic gamma delta T cells, The Basil Hetzel Institute and Queen Elizabeth Hospital Research Day 2013, Adelaide, SA, Australia, 18th October 2013 **(Oral presentation)**

Targeting breast cancer with ex vivo expanded cytotoxic gamma delta T cells in combination with pro-apoptotic receptor agonists, University of Adelaide 2013 Florey International Postgraduate Research Conference, Adelaide, SA, Australia, 29th August 2013 **(Poster presentation)**

Publications

A. Zysk, M.O. DeNichilo, V. Panagopoulos, I. Zinonos, V. Liapis, S. Hay, W. Ingman, V. Ponomarev, G. Atkins, D. Findlay, A. Zannettino, A. Evdokiou, Adoptive transfer of ex vivo expanded Vgamma9Vdelta2 T cells in combination with zoledronic acid inhibits cancer growth and limits osteolysis in a murine model of osteolytic breast cancer, Cancer Lett, 386 (2017) 141-150 (IF: 5.6)

Y. Wang, I. Zinonos, **A. Zysk**, V. Panagopoulos, G. Kaur, A. Santos, D. Losic, A. Evdokiou, In vivo toxicological assessment of electrochemically engineered anodic alumina nanotubes: a study of biodistribution, subcutaneous implantation and intravenous injection, Journal of Materials Chemistry B, 5 (2017) 2511-2523 (IF: 4.5)

V. Liapis, I. Zinonos, A. Labrinidis, S. Hay, V. Ponomarev, V. Panagopoulos, **A. Zysk**, M. DeNichilo, W. Ingman, G.J. Atkins, D.M. Findlay, A.C. Zannettino, A. Evdokiou, Anticancer efficacy of the hypoxia-activated prodrug evofosfamide (TH-302) in osteolytic breast cancer murine models, Cancer Med, 5 (2016) 534-545 (IF: 2.5)

M. O. DeNichilo, A. J. Shoubridge, V. Panagopoulos, V. Liapis, **A. Zysk**, I. Zinonos, S. Hay, G. J. Atkins, D. M. Findlay, and A. Evdokiou. 2016. Peroxidase Enzymes Regulate Collagen Biosynthesis and Matrix Mineralization by Cultured Human Osteoblasts. *Calcif. Tissue Int.* 98: 294-305. (IF: 2.759)

V. Panagopoulos, I. Zinonos, D.A. Leach, S.J. Hay, V. Liapis, **A. Zysk**, W.V. Ingman, M.O. DeNichilo, A. Evdokiou, Uncovering a new role for peroxidase enzymes as drivers of angiogenesis, Int J Biochem Cell Biol, 68 (2015) 128-138. (IF: 4.240)

Publications continued

Y. Wang, G. Kaur, **A. Zysk**, V. Liapis, S. Hay, A. Santos, D. Losic, A. Evdokiou, Systematic in vitro nanotoxicity study on anodic alumina nanotubes with engineered aspect ratio: understanding nanotoxicity by a nanomaterial model, Biomaterials, 46 (2015) 117-130 (IF: 8.557)

Manuscripts under review

A. Zysk, M. O. DeNichilo, V. Panagopoulos, I. Zinonos, V. Liapis, S. Hay, W. Ingman, G.J. Atkins, D.M. Findlay, A.C. Zannettino, V. Ponomarev, A. Evdokiou, *Adoptive transfer of ex vivo expanded human Vγ9Vδ2 T cells inhibit osteosarcoma growth in bone and pulmonary metastases* (2017) (Manuscript submitted to Cancer Immunology, Immunotherapy, July 2017)

V. Liapis, **A. Zysk**, M. DeNichilo, I. Zinonos, S. Hay, V. Panagopoulos, A. Shoubridge, C. Defelice, V. Ponomarev, W. Ingman, G. J. Atkins, D. M. Findlay, A. CW. Zannettino and A. Evdokiou *Anticancer efficacy of the hypoxia activated prodrug evofosfamide is enhanced in combination with proapoptotic receptor agonists dulanermin and drozitumab against osteosarcoma.* (2016) (Manuscript accepted in Cancer Letters, April 2017)

Prizes Awarded

2016 Wellcome Trust Travel Grant for travel to the Gamma Delta 2016 conference in London

2015 Best Senior PhD Oral Presentation (Laboratory) – The Basil Hetzel Institute and Queen Elizabeth Hospital Research Day 2015

Finalist for the 2015 Ross Wishart Award – 2015 Australian Society for Medical Research (ASMR) SA Scientific Meeting

2014 School of Medicine Poster Presentation Prize – 2014 Florey International Postgraduate Research Conference

Best Lay Description Prize – The Basil Hetzel Institute and Queen Elizabeth Hospital Research Day 2014

SAHMRI Beat Cancer Project Travel Grant 2014

2013 Northern Communities Foundation Prize **–** 2013 Florey International Postgraduate Research Conference

Australian Postgraduate Award

Abbreviations Used

Acronym	Definition	Alternative
2M3B1PP	2-methyl-3-butenyl-1-pyrophosphate	
ADCC	antibody-dependant cellular cytotoxicity	
AICD	activated induced cell death	
BAONJ	bisphosphonate associated osteonecrosis of the jaw	
BMP	bone morphogenetic protein	
BTN	butyrophiln	
BTN3A1	butyrophiln 3A1	CD277
CCR2	C-C chemokine receptor type 2	CD192
CD	cluster of differentiation	
CD16	cluster of differentiation 16	FcγRIII
CLL	chronic lymphocytic leukaemia	
CTGF	connective tissue growth factor	
CTL	cytotoxic T lymphocyte	
DMAPP	dimethylallyl pyrophosphate	
DOT-Cells®	Delta One T cells	
Dox	doxorubicin	
DR4	death receptor 4	Apo2L/TRAIL-R1
DR5	death receptor 5	Apo2L/TRAIL-R2
Droz	drozitumab (Apomab)	
E:T	effector target ratio	
EMT	epithelial to mesenchymal transition	

Acronym	Definition	Alternative
FADD	Fas-associated death domain protein	
FasL	Fas Ligand	
FDA	Food and Drug Administration	
FGF	fibroblast growth factor	
FPP	farnesyl pyrophosphate	
FPPS	farnesyl pyrophosphate synthase	
G-CSF	granulocyte-colony stimulating factor	
GTP	Guanosine-5'-triphosphate	
HER-2	human epidermal growth factor receptor 2	neu
HMBPP	(E)-4-hydroxy-3-methyl-but-2-enyl pyrophosphate	IPH1101
i.p	intraperitoneal	
i.t	intratibial	
i.v	intravenous	
IFN-γ	interferon-gamma	
IGF	insulin-like growth factor	
IL	interleukin	
iNOS	inducible nitric oxide synthase	
iPA	N6-isopentenyladenosine	
IPP	isopentenyl pyrophosphate	
MCP-1	monocyte chemoattractant protein-1	CCL2
M-CSF	macrophage colony stimulating factor	
MHC	major histocompatibility complex	

Acronym	Definition	Alternative
MICA/B	MHC class I polypeptide-related sequence A/B	
MMP	matrix metalloproteinase	
nBP	aminobisphosphonate	
NK	natural killer	
NKG2D	natural killer group 2, member D	
NOD/SCID	nonobese diabetic/severe combined immunodeficiency	
NSG	NOD scid gamma	
ONJ	osteonecrosis of the jaw	
OPG	osteoprotegerin	
PAg	phosphoantigen	
PARA	pro-apoptotic receptor agonist	
PBMC	peripheral blood mononuclear cell	
PRECOG	PREdiction of Clinical Outcomes from Genomic Profiles	
PTHrP	parathyroid hormone-related protein	
RANK	receptor activator of NF-κB	
RANKL	receptor activator of NF-κB ligand	
rhTRAIL	recombinant human TRAIL	
s.c	subcutaneous	
SD	standard deviation	
SEM	standard error of the mean	
SRE	skeletal related event	

Acronym	Definition	Alternative
TAM	tumour associated macrophage	
TB p.f	total bone pattern factor	
Tb.N	trabecular number	
Tb.S	trabecular separation	
Tb.Th	trabecular thickness	
TBV	total bone volume	
T_{CM}	central memory T cell	
TCR	T cell receptor	
T_{EM}	effector memory T cell	
T_{ERMA}	terminally differentiated T cell	
TGA	Therapeutic Goods Administration	
TGF-β	transforming growth factor-beta	
Th1	Type 1 T helper	
$T_{naïve}$	naïve T cell	
TNF-α	tumour necrosis factor-alpha	
Tr p.f	trabecular pattern factor	
TRAIL	tumour necrosis factor related apoptosis inducing ligand	Apo2 Ligand
TrBV	trabecular bone volume	
ULBP	UL16 binding protein	
Vγ9Vδ2 T cell	Vgamma9 Vdelta2 T cell	
Vδ1	Vdelta1	

Acronym	Definition	Alternative
ZOL	zoledronic acid/zoledronate	
ZOL-C	ZOL-conventional	
ZOL-M	ZOL-metronomic	
ZOL-W	ZOL-weekly conventional	
ZOL-XC	ZOL-multiple conventional	
αβ T cell	alpha beta T cell	
γδ T cell	gamma delta T cell	
γδT17	IL-17 producing γδ T cells	

Chapter 1

Introduction

1.1 Cancer in the bone

Primary bone cancer is a heterogeneous group of malignancies which originate in the bone. Primary bone malignancies are generally classified into two groups; multiple myeloma, a haematological malignancy which affects the bone marrow, and sarcoma [1]. Multiple myeloma is the most frequent primary skeletal malignancy, followed by osteosarcoma, chondrosarcoma, Ewing's sarcoma, and others [1, 2]. Although these cancers are extremely rare, accounting for approximately 0.2% of all neoplasms, osteosarcomas, for example are much more common in childhood and adolescence [1, 3].

Although primary bone cancer is relatively rare, the bone is considered a fertile 'soil' for the localisation of disseminated cells from various primary cancers, and thus secondary lesions are far more common [reviewed in 4]. Cancer metastasis is a complicated process which results in the spread of cancer cells to distant sites. Briefly, cancer cells at the primary site undergo complex molecular changes resulting in the loss of adherence properties, resulting in EMT (epithelial to mesenchymal transition) allowing cells to infiltrate blood or lymphatic circulation to disseminate to distant sites where they invade new tissues and re-establish to form micro-metastases [reviewed in 5, 6]. The bone is a highly conducive environment for secondary lesions from breast, prostate, and lung cancer [7, 8].

Lesions from skeletal malignancies can be classed into three phenotypes, based on radiographic appearance; osteolytic (abnormal bone degradation) osteoblastic/osteosclerotic (abnormal bone formation), or mixed (abnormal bone degradation linked to abnormal formation) [9-11]. Abnormal bone destruction causes skeletal related events (SREs) including hypercalcaemia, chronic pain, pathological fractures, spinal cord compression, and impaired mobility, all of which

greatly affect quality of life [1, 8]. Multiple myeloma, bone metastases from breast and lung cancer, and a marginal number of osteosarcomas result in osteolytic lesions [1, 8] Conversely, the majority of osteosarcomas and bone metastases from prostate cancer result in predominately osteoblastic or mixed lesions [1, 8, 12]. To discover new treatments for cancers in the bone, it is important to understand how these lesions form and how to inhibit them.

1.1.1 Normal bone metabolism

Throughout life, bone is being constantly remodelled. Bone homeostasis is achieved by coupling the activities of two main cell types, bone degrading osteoclasts and bone forming osteoblasts. Pre-osteoclasts, cells from the monocyte-macrophage lineage, express RANK (receptor activator of nuclear factor kappa-light-chain-enhancer of activated B cells (NF-κB)) which binds RANKL (RANK ligand), released by osteoblasts and stromal cells [13]. Activation of pre-osteoclasts by RANKL results in the formation of large multi-nucleated cells called osteoclasts which resorb bone [reviewed in 14]. Following bone resorption by osteoclasts, factors including TGF-β (transforming growth factor-beta), IGF-I/II (insulin-like growth factor I/II), FGF (fibroblast growth factor), and BMPs (bone morphogenetic proteins), which are normally sequestered in the bone matrix, are released and activated [15, 16, reviewed in 17], resulting in increased osteoclast activity and liberation of free Ca^{2+} (Figure 1.1). Released growth factors act on mesenchymal progenitor cells, which differentiate into osteoblasts, producing osteoid to form a scaffold for new bone matrix. OPG (osteoprotegerin), a soluble decoy receptor for RANKL, also produced by osteoblasts and stromal cells, regulates osteoclast activity by sequestering the activity of RANKL and downregulating pre-osteoclast differentiation into mature osteoclasts (Figure 1.1).

Figure 1.1 Normal bone remodelling is a balanced process based on the RANKL/RANK/OPG system.

Osteoblasts and stromal cells release RANKL, which binds its receptor RANK on osteoclast precursors, stimulating their differentiation into mature and active osteoclasts. During bone resorption, osteoclasts release factors that can stimulate osteoblast differentiation from mesenchymal progenitor cells, resulting in a coupled increase of bone formation. OPG released by osteoblasts and stromal cells binds to and inhibits RANKL, preventing RANKL binding to osteoclast precursors, inhibiting osteoclast formation.

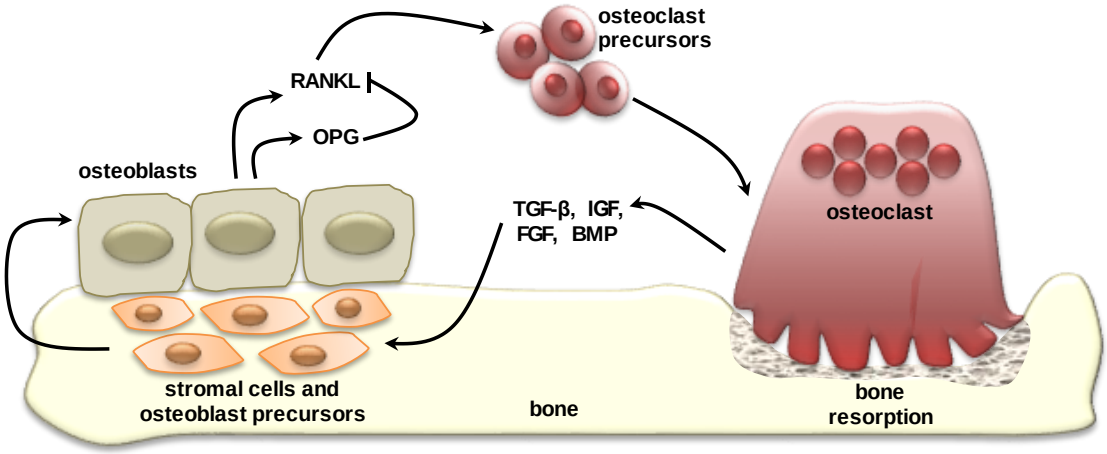
osteoclast
precursors
RANKL
OPG
osteoblasts
TGF-β, IGF,
FGF, BMP
osteoclast
stromal cells and
osteoblast precursors
bone
bone
resorption

1.2 The 'vicious cycle' of cancer in the bone

Cancer lesions in the bone microenvironment disrupt this tightly regulated mechanism and the resulting phenotype depends on factors released by the cancer cells. For example, osteolytic breast cancer cells release factors including RANKL, M-CSF (macrophage colony stimulating factor), and PTHrP (parathyroid hormone-related protein) which directly or indirectly increase the number or activity of osteoclasts [reviewed in 8, 9]. In contrast, prostate cancer cells can release factors including BMP and OPG which promote osteoblasts, as well as RANKL and PTHrP [reviewed in 12]. Depending on which factors are released, abnormal bone formation can lead to predominately osteoblastic lesions or mixed lesions when abnormal bone formation is linked to abnormal bone degradation [reviewed in 8, 12]. Increased bone degradation results in the release of growth factors normally sequestered in the bone matrix, which nourish the cancer cells leading to increased proliferation. In turn, as the tumour grows larger, it releases more factors which can increase osteoclast mediated resorption, leading to what is termed the 'vicious cycle' of cancer growth and bone destruction (Figure 1.2) [reviewed in 18, 19]. Abnormal osteoclast-mediated bone destruction results in SREs including hypercalcaemia, chronic pain, pathological fractures, spinal cord compression, and impaired mobility, all which greatly affect quality of life [reviewed in 1, 8, 20].

Due to the interactions between cancer cells and the bone microenvironment resulting in this 'vicious cycle' of cancer growth and bone degradation, novel therapies need to target both cancer cells to reduce tumour burden, and the bone microenvironment to alleviate symptoms associated with abnormal bone metabolism.

Figure 1.2 Osteolytic cancer cells in the bone microenvironment disrupt normal bone metabolism.

When osteolytic cancer cells are present in the bone microenvironment, they disrupt normal bone remodelling. Cancer cells can release factors which directly and indirectly activate osteoclast precursors, causing an increase in osteoclast number and activity, ultimately resulting in abnormal bone degradation. Growth factors normally sequestered in the bone are then released, which in turn nourish the cancer cells, perpetuating the 'vicious cycle' of cancer growth and bone degradation

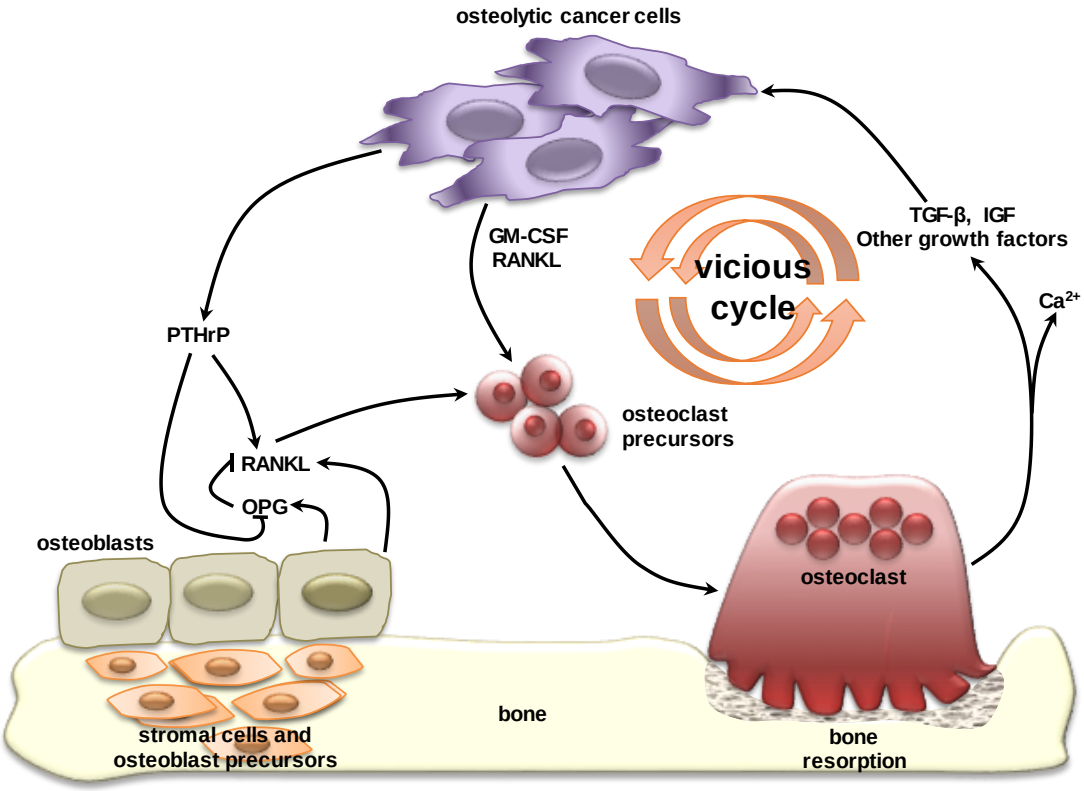
osteolytic cancer cells
GM-CSF
RANKL
TGF-β, IGF
Other growth factors
vicious
cycle
Ca2+
PTHrP
osteoclast
precursors
RANKL
OPG
osteoblasts
osteoclast
bone
stromal cells and
osteoblast precursors
bone
resorption

As cancers that affect the bone are heterogeneous, this thesis will focus primarily on osteolytic osteosarcoma and breast cancer bone metastases, examples of a primary and secondary bone malignancy that result in osteolytic lesions.

1.3 Osteosarcoma

Osteosarcoma is the most frequent primary malignancy of the skeleton in children and adolescents, with over 60% of cases occurring in patients under 25 years old [1]. It most commonly affects the distal femur, proximal tibia, or proximal humerus with ~70% localising around the knee or shoulder [1]. Current treatment regimens involve neoadjuvant (preoperative) chemotherapy in combination with surgery to remove all detectable tumours, resulting in a 10 year overall survival rate of 70-80% for patients with localised osteosarcoma [1, 21]. On face value, this appears to be an acceptable survival rate, however when the average age of diagnosis is taken in account, the outcome is actually quite poor. Additionally, metastatic spread, preferentially to the lungs is seen in 15-20% of presenting patients, correlating with poor survival rates [21-25].

Over the past few decades, the mainstay treatment for osteosarcoma has been chemotherapy in combination with surgery. Patients are given a cocktail of neoadjuvant chemotherapeutic agents including doxorubicin, cisplatin, methotrexate, and isosfamide, followed by limb-salvage surgery to remove the residual tumour mass and any known metastases [26]. While this treatment regimen has greatly improved patient survival compared to surgery alone which was the standard treatment prior to the 1970s, survival rates have now plateaued [reviewed in 27, 28]. Osteosarcoma is generally considered to be radiotherapy resistant and reoccurring lesions can acquire chemotherapy resistance [27, 29]. Lung metastases also present a significant hurdle in the treatment of osteosarcoma [21, 22]. To

prolong survival rates, especially in patients with pulmonary metastases, it is clear that novel therapies are required to target tumour burden in the bone, alleviate symptoms associated with bone lysis, and also target pulmonary metastases.

1.4 Breast cancer bone metastases

As previously discussed, the bone is also considered a fertile 'soil' for the localisation of breast cancer cells, with bone metastases occurring in over 75% of advanced breast cancer patients [9, 30]. Unlike osteosarcoma which is relatively rare, breast cancer is one of the most commonly diagnosed cancers in women worldwide, estimated to affect one in eight women during their lifetime [31]. Over 16,000 Australians were diagnosed with breast cancer in 2016 including more than 15,900 women and approximately 150 men [32]. Prognosis of patients diagnosed with primary breast cancer has improved over the past few years, with overall survival at five years exceeding 89% [33]. In contrast, survival of patients diagnosed with the advanced disease is much lower, with overall survival at five years between 15-40% [34, 35]. This decrease in survival is due to metastatic spread, commonly to the bone, lung, liver and brain [30, 36].

Current treatments for patients with advanced breast cancer include chemotherapies, such as doxorubicin, paclitaxel, cisplatin, and depending on HER-2 status (human epidermal growth factor receptor-2), trastuzumab, either as a monotherapy or in combination with chemotherapy [37, 38]. Chemotherapy can also be used in combination with hormonal treatments, radiotherapy, and if the patient exhibits bone metastases, anti-bone resorptive agents (e.g. aminobisphosphonates (nBPs) or denosumab) [39, 40]. Additionally, quality of life significantly declines due to disease progression and severe adverse effects can be attributed to chemotherapy, such as cardiotoxicity associated with long-term

doxorubicin use [reviewed in 41]. Regardless, in advanced breast cancer all of these treatment options are only palliative, demonstrating the need for novel therapies.

1.5 Focus on aminobisphosphonates

In the last fifteen years, the administration of aminobisphosphonates (nBPs) has emerged as a novel strategy to inhibit osteoclast-mediated bone degradation and alleviate the symptoms associated with bone loss in patients with primary and metastatic skeletal malignancies [42, 43, reviewed in 44]. In the clinic, most frequently used are the second and third-generation nBPs including pamidronate, alendronate, risedronate, and zoledronate. This thesis is primarily focused on zoledronate (zoledronic acid, ZOL), which currently has the most potent anti-resorptive activity [45]. ZOL is approved by the FDA (Food and Drug Administration) and TGA (Therapeutic Goods Administration) under the tradename Zometa (Novartis) and is used for the treatment of osteoporosis, Paget's disease of the bone, and skeletal metastases. The structure of ZOL and other nBPs, allows preferential localisation and binding to the bone matrix [reviewed in 46]. During normal bone resorption osteoclasts internalise nBPs, where they inhibit farnesyl pyrophosphate synthase (FPPS), an enzyme in the mevalonate pathway. FPPS is responsible for the conversion of isopentenyl pyrophosphate (IPP) and its isomer dimethylallyl pyrophosphate (DMPP) to farnesyl pyrophosphate (FPP) (Figure 1.3) [reviewed in 46]. The mevalonate pathway in mammalian cells is the major pathway involved in the synthesis of cholesterol, and in the generation of farnesyl and geranylgeranyl protein prenylation groups. Farnesyl and geranylgeranyl are important for the post-translational modification of small GTPases, which mediate pathways important in survival, adhesion, and migration

Figure 1.3 Inhibition of the mevalonate pathway.

In mammalian cells, the mevalonate pathway, also known as the isoprenoid pathway, is involved in cholesterol synthesis and the production of farnesyl and geranylgeranyl (prenylation) groups necessary for the post-translational modification of small GTPases. Statins, a class of cholesterol lowering drugs inhibit the rate limiting enzyme of the pathway, HMG-CoA reductase. Downstream of HMG-CoA reductase, farnesyl pyrophosphate synthase (FPPS) is inhibited by aminobisphosphonates, such as ZOL, which results in the accumulation of isopentyl pyrophosphate (IPP) and dimethylallyl pyrophosphate (DMAPP). Inhibition of FPPS also decreases prenylation of GTPases, resulting in changes to the morphology of osteoclasts, eventually leading to osteoclast death.

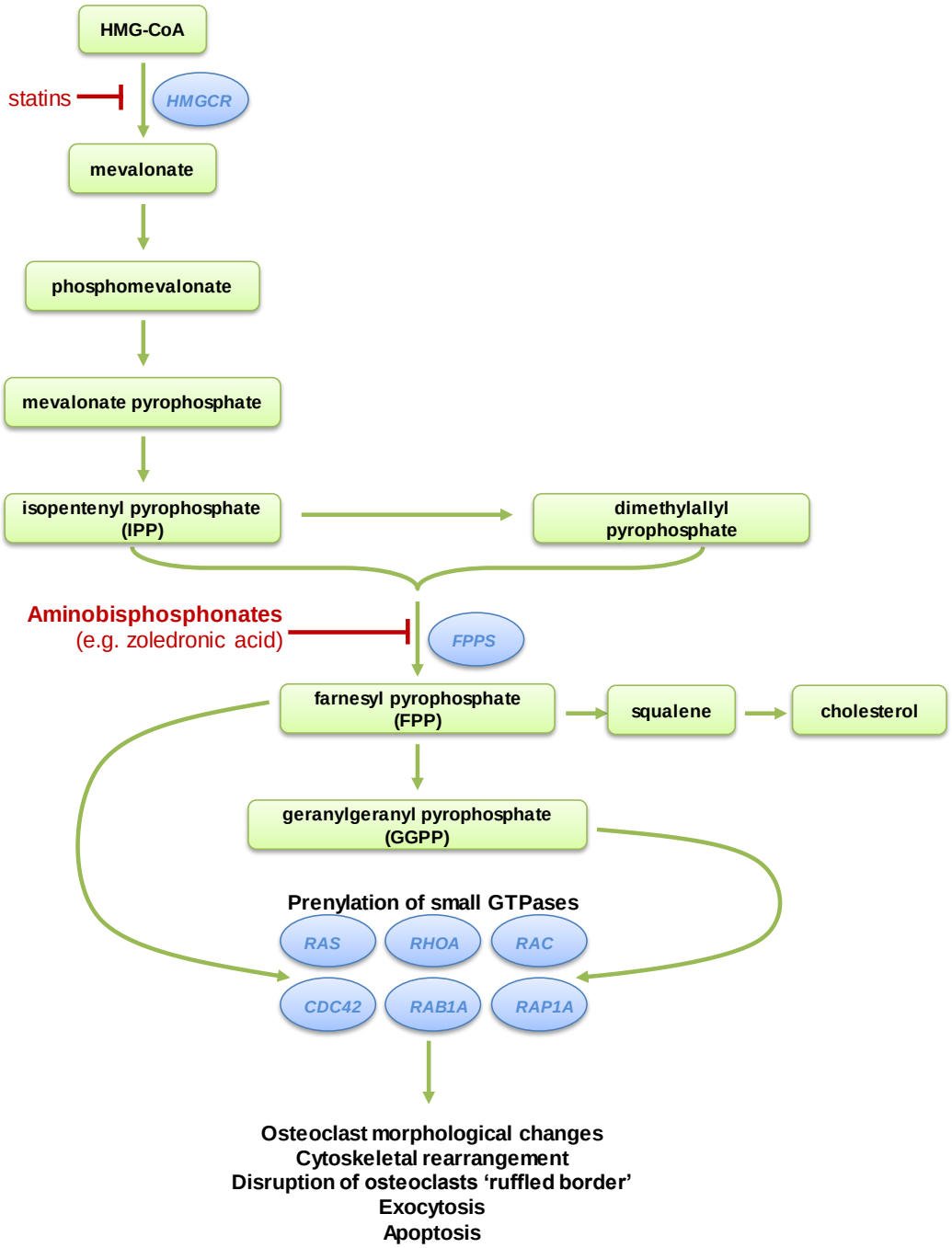
HMG-CoA
statins
HMGCR
mevalonate
phosphomevalonate
mevalonate pyrophosphate
isopentenyl pyrophosphate (IPP)
dimethylallyl pyrophosphate
Aminobisphosphonates
(e.g. zoledronic acid)
FPPS
farnesyl pyrophosphate (FPP)
squalene
cholesterol
geranylgeranyl pyrophosphate (GGPP)
Prenylation of small GTPases
RAS
RHOA
RAC
CDC42
RAB1A
RAP1A
Osteoclast morphological changes
Cytoskeletal rearrangement
Disruption of osteoclasts 'ruffled border'
Exocytosis
Apoptosis

for many cell types, including osteoclasts [46-48]. For example, geranylgeranylation of Rac and Rho are required for maintenance of the correct cytoskeletal arrangement to produce the osteoclast "ruffled border" which is necessary for migration and bone resorption (Figure 1.3 and Figure 1.4) [reviewed in 49]. Inhibition of FPPS by nBPs results in the accumulation of IPP and DMPP, a decrease in farnesyl pyrophosphate (FPP), and consequently a decrease in prenylated proteins. This results in changes to osteoclast cytoskeletal structure, cell adhesion and migration properties, and may eventually cause osteoclasts to undergo apoptosis due to a lack of adhesion to the bone surface (anoikis) (Figure 1.4) [reviewed in 49]. Combined, these outcomes result in the inhibition of bone resorption.

ZOL treatment of patients with primary and metastatic bone cancer inhibits tumour-associated bone loss, increases bone density, and as a result reduces SREs such as fractures and hypercalcaemia [50-53]. Additionally, in patients with early breast cancer, ZOL administration in adjuvant with standard therapies reduces the development of bone metastases and improves disease outcomes in post-menopausal women [54]. However, whether nBP administration in cancer patients increases overall survival is still contradictory.

In addition to the well-characterised ability to inhibit osteoclast-mediated bone degradation, nBPs also have reported anti-cancer properties [reviewed in 55, 56]. ZOL can induce cell death, inhibit proliferation, invasion, and angiogenesis in osteosarcoma [57], fibrosarcoma [58], breast [59, 60], prostate [60, 61], and small cell lung cancer (SCLC) cell lines [62]. Additionally, using chemotherapies such as doxorubicin or etoposide in combination with ZOL further enhances cancer cell death [59, 62]. However, the anti-cancer efficacy of ZOL in pre-clinical trials is

Figure 1.4 Schematic depicting bone metabolism under normal conditions and after zoledronic acid (ZOL) treatment.

A. During normal bone metabolism, small GTPases such as Rac and Rho are actively maintaining adhesions between the bone and the osteoclast to mediate maximum resorption. **B.** Following infusion, ZOL is deposited in the bone and internalised during osteoclast resorption, where it acts on cellular targets including FPPS. This decreases protein prenylation and disrupts adhesions and survival pathways, ultimately decreasing bone resorption and inducing eventual apoptosis

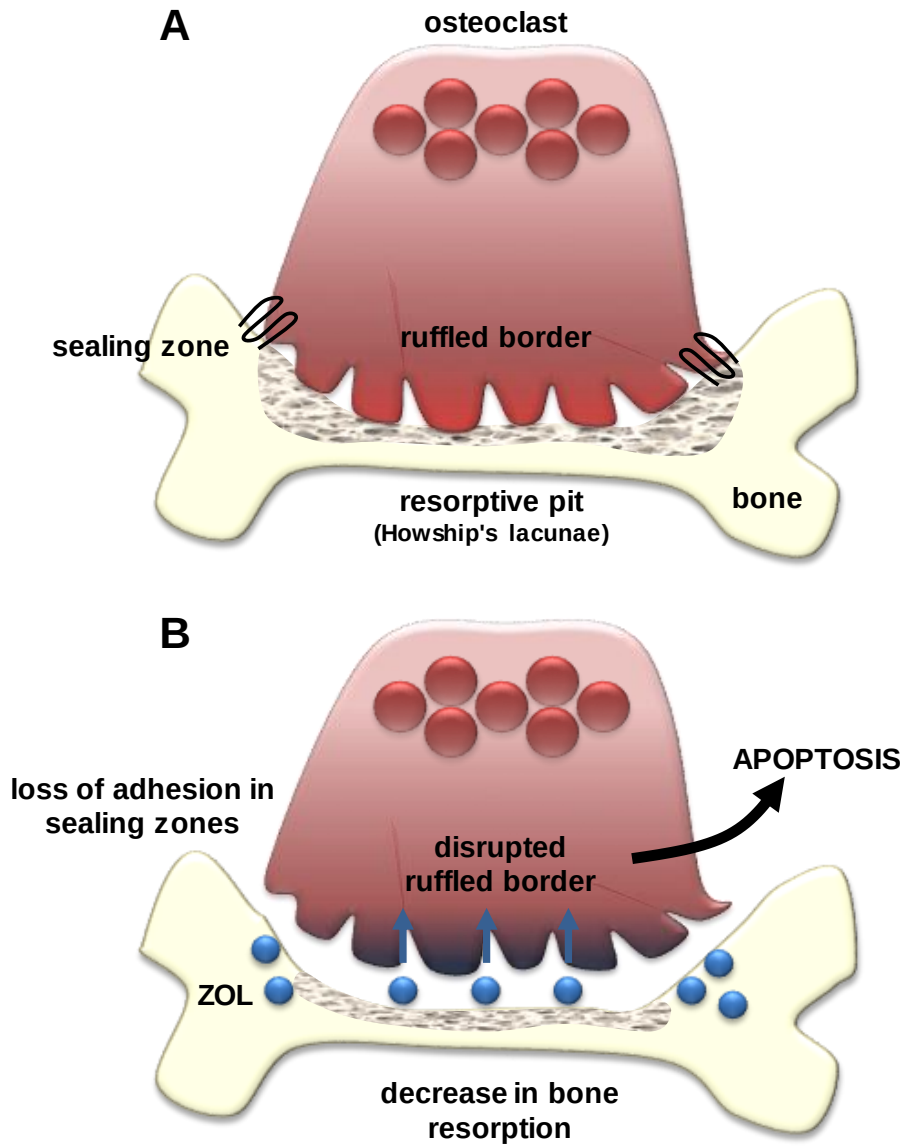
A
osteoclast
sealing zone
ruffled border
resorptive pit
(Howship's lacunae)
bone
B
loss of adhesion in
sealing zones
APOPTOSIS
disrupted
ruffled border
ZOL
decrease in bone
resorption

contradictory. Several studies show that ZOL administration inhibits tumour growth [62, 63], and reduces further lung, liver, and bone metastases [63-66]. In contrast, other studies show that ZOL demonstrate no anti-cancer efficacy, and increases lung metastases [67, 68]. These studies indicate that although ZOL may have some anti-cancer properties *in vitro*, this does not necessarily translate to *in vivo* anti-cancer efficacy. While no clinical trials have assessed the anti-cancer efficacy of ZOL alone, many studies in osteoporosis patients have reported that oral nBPs administration may decrease cancer risk and bone metastases [69-71].

In the clinic, the most frequently observed adverse side effect of intravenous nBPs is a mild fever, which is due to the *in vivo* expansion of a small population of cytotoxic immune cells called gamma delta (γδ) T cells and the associated release of pyrogenic cytokines [72]. Interestingly, the most severe side effect, bisphosphonate-associated osteonecrosis of the jaw (BAONJ) has been correlated to the depletion of γδ T cells in osteoporotic patients [73]. While BAONJ is a very rare adverse event, it is more likely to occur in immune compromised patients, such as cancer patients undergoing chemotherapy, however poor oral hygiene, or oral surgery prior to treatment also appear to be common risk factors [reviewed in 74].

In the last decade, this ability of ZOL and other nBPs to activate and expand γδ T cells has become widely recognised for its exciting potential as novel immunotherapeutic strategy for the treatment of various solid and haematological malignancies [75-83].

1.6 Gamma delta (γδ) T cells

Since their discovery over 30 years ago, the important role of gamma delta (γδ) T cells in immunity has slowly emerged, however less is known about these cytotoxic immune cells compared to the well-characterised alpha beta (αβ) T cells.

Human γδ T cells comprise a small population (1-10%) of circulating peripheral lymphocytes [84] which are stimulated and expanded in response to non-peptic antigens, known as phosphoantigens (PAgs). The majority of human peripheral blood γδ T cells express the Vδ2 TCR (T cell receptor) usually paired with Vγ9 (Vγ9Vδ2 T cells), while the Vδ1 TCR, and to a lesser extent Vδ3 TCR subsets are primarily found in the gut epithelium, dermis, spleen, and liver [85, 86]. While there is some functional overlap between different γδ T cell subtypes, this thesis is primarily focussed on the *ex vivo* expansion of Vγ9Vδ2 T cells from human peripheral blood mononuclear cells (PBMC). PAg stimulated Vγ9Vδ2 T cells are specific to humans and some primates, and the scope of this thesis does not cover γδ T cells from other species (e.g. murine). Therefore, discussion in this thesis will focus primarily on human γδ T cells, specifically Vγ9Vδ2, and if subtype is not specified or information encompasses all subtypes, then γδ T cell will be used.

Similarly to the more well-defined αβ T cells, the γδ TCR is co-expressed with CD3 (cluster of differentiation 3). In contrast, γδ T cells do not express the αβ TCR or MHC (major histocompatibility complex) class I and class II recognition molecules, CD8 and CD4 respectively, which are necessary for detecting cells in a MHC dependant manner. Instead γδ T cells recognise PAgs produced by target cells such as microbial infected, stressed, or transformed (cancer) cells [87]. While the exact mechanisms of PAg detection is still largely unclear, it occurs in an MHC un-restricted manner and has been predicted to occur via the γδ TCR [87]. However, more recently, the importance of the butyrophiln (BTN) family (specifically BTN3A1, also known as CD277) has been implicated as a co-activator required for the activation and expansion of Vγ9Vδ2 T cells, and in the recognition of target cells [88]. The mechanism by which BTN contributes to Vγ9Vδ2 T cell activation

and recognition is not fully understood and is currently under investigation by several research groups. The fact that cancer cells can escape immune surveillance by down-regulating MHC molecules makes adoptive transfer of γδ T cells a more attractive immunotherapeutic approach compared to $CD8^+$ CTLs (cytotoxic T lymphocytes), which require MHC presentation.

1.7 Activation of Vγ9Vδ2 T cells

A variety of natural and synthetic molecules can activate Vγ9Vδ2 T cells to induce their proliferation and activation. Natural PAgs include HMBPP ((E)-4-hydroxy-3-methyl-but-2-enyl pyrophosphate), an intermediate of the non-mevalonate pathway in microbial cells. Host cells infected with pathogenic bacteria and parasites such as *E. coli, Listeria, Mycobacterium, Pseudomonas, Salmonella, Plasmodium,* and *Toxoplasma* produce HMBPP which results in the activation of Vγ9Vδ2 T cells, and the destruction of infected target cells [reviewed in 89]. In mammalian cells, the first identified naturally occurring PAgs were IPP and its isomer DMAPP, intermediates of the mevalonate pathway. Although HMBPP is 8,000 times more potent at activating Vγ9Vδ2 T-cells than IPP [90], cancer cells abnormally accumulate IPP due to up-regulation of the mevalonate pathway [91], allowing detection of cancer cells by Vγ9Vδ2 T cells [92]. Statins, a class of drugs used to lower cholesterol, inhibit HMG-COA reductase, the rate limiting enzyme of the mevalonate pathway. This occurs upstream of FPPS, which prevents accumulation of IPP after nBP treatment, preventing activation of γδ T cells [93, 94]. Due to potential inhibition of Vγ9Vδ2 T cell activation, statin use could have negative implications on the efficacy of Vγ9Vδ2 T cell therapy. However, a meta-analysis of over 20 studies including more than 85,000 participants showed that statins had a neutral effect on cancer risk [95].

In addition to naturally occurring PAgs, synthetic compounds including 2-methyl-3-butenyl-1-pyrophosphate (2M3B1PP) [96, 97] and bromohydrin pyrophosphate (BrHPP) [76, 98, 99], are also well-characterised activators of Vγ9Vδ2 T cells. BrHPP (IPH 1101, Innate Pharma) is the most potent known activator of Vγ9Vδ2 T cells *in vitro* [90] and has been tested in Phase I/II clinical trials against a variety of solid tumours [100]. Unfortunately, these trials have been discontinued due to a lack of efficacy, therefore other Vγ9Vδ2 T cell activators must be assessed.

As previously discussed, aminobisphosphonates (nBPs) including alendronate [76], pamidronate [77, 78], and ZOL [75, 78-83] are another group of compounds that can activate and expand Vγ9Vδ2 T cells [reviewed in 101], usually in combination with IL-2 (interleukin-2), a cytokine required for T cell proliferation. After internalisation by monocytes, ZOL inhibits the enzyme farnesyl pyrophosphate (FPP) synthase in the mevalonate pathway, leading to intracellular accumulation of isopentenyl pyrophosphate (IPP), which stimulates and activates Vγ9Vδ2 T cells (Figure 1.5) [102]. From the nBPs, ZOL is the most potent FPPS inhibitor [45], and is considered the best nBP activator of Vγ9Vδ2 T cells. This method for expanding Vγ9Vδ2 T cells *ex vivo* using a low dose of ZOL in combination with IL-2 is well established [83], easily reproducible, and was used to expand Vγ9Vδ2 T cells in this study.

Resembling αβ T cells, Vγ9Vδ2 T cells can be divided into four differentiation phenotypes based on CD27 and CD45RA receptor expression. Stimulation by PAgs results in the expansion of naïve ($T_{naïve}$ $CD27^+/CD45RA^+$) and central memory (T_{CM} $CD27^+/CD45RA^-$) Vγ9Vδ2 T cells, which have a high

Figure 1.5 Expansion of Vγ9Vδ2 T cells from peripheral blood using ZOL.

In cell culture with peripheral blood mononuclear cells (PBMCs), ZOL is internalised by monocytes, resulting in inhibition of farnesyl pyrophosphate synthase (FPPS) of the mevalonate pathway. This results in the accumulation of isopentenyl pyrophosphate (IPP), which activate Vγ9Vδ2 T cells via the Vγ9/Vδ2 TCR (mechanism still unknown, but may occur through BTN3A1 receptors). Activated Vγ9Vδ2 T cells can then mediate cytotoxicity towards target cells such as microbial infected or cancer cells. Figure adapted from [101].

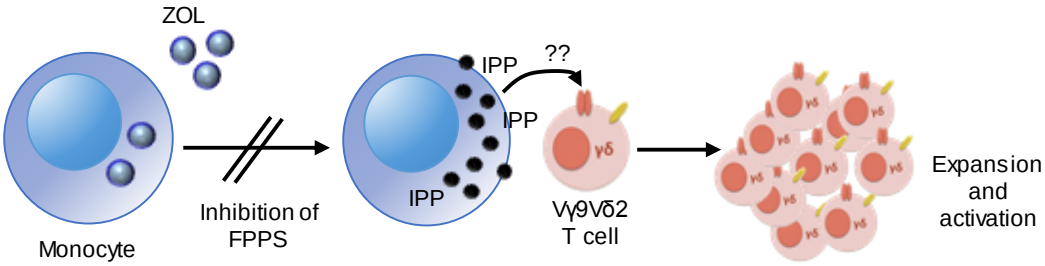
ZOL
Monocyte
Inhibition of
FPPS
IPP
IPP
IPP
??
γδ
Vγ9Vδ2
T cell
Expansion
and
activation

proliferation rate and low effector function, to T_{EM} (effector memory $CD27^-/CD45RA^-$) and eventually T_{ERMA} (terminally differentiated $CD27^-/CD45RA^+$) which have limited proliferation capacity, but high effector function [103, 104]. Not only do different subsets have varying proliferation rates in response to PAg stimulation and effector functions, they also show differences in chemokine secretion and migration [104] (summarised in Figure 1.6). Generally, $T_{naïve}$ and T_{CM} cells are found in the lymph nodes or peripheral blood, while T_{EM} and T_{ERMA} will localise to sites of inflammation where they can exhibit their cytotoxic effects [104]. Monitoring these subtypes is important as it may help predict clinical outcomes. For example, early phase clinical studies showed that cancer patients had depleted levels of T_{EM} Vγ9Vδ2 T cells, which could be increased after *in vivo* activation with ZOL, or adoptive transfer with *ex vivo* expanded Vγ9Vδ2 T cells [105, 106]. As T_{EM} Vγ9Vδ2 T cells exhibit high effector functions such as IFN-γ (interferon-gamma) secretion, it may be beneficial to increase this subtype in patients to maximise anti-cancer efficacy. Also, observations from Noguchi et al., suggest that numbers of $CD27^+$ cells (naïve and central memory) Vγ9Vδ2 T cells can be used to predict how well a patient will respond to expansion conditions, as a larger number of these cells results in a greater Vγ9Vδ2 T cell expansion [105].

1.8 Mechanisms of Vγ9Vδ2 T cell cytotoxicity

Activated Vγ9Vδ2 T cells express markers reminiscent of $CD8^+$ CTL and NK (natural killer) cells, allowing them to kill target cells via a number of mechanisms, including death receptor/ligand interactions with TRAIL (tumour necrosis factor (TNF) related apoptosis inducing ligand) [98], FasL (Fas Ligand) [79], or via the release of perforin/granzymes resulting in the lysis of target cells [75, 98, 104, 107]. Activated Vγ9Vδ2 T cells also release Th1 cytokines, including

Figure 1.6 Differentiation phenotype of Vγ9Vδ2 T cells.

Vγ9Vδ2 T cells can be categorised into four differentiation sub-populations based on CD27 and CD45RA receptor expression. $CD27^+/CD45RA^+$ and $CD27^+/CD45RA^-$ are $T_{naïve}$ and T_{CM} (central memory) cells respectively, which have a high proliferation rate and low effector function and are found in the lymph nodes and peripheral blood. These differentiate into $CD27^-/CD45RA^-$ and $CD27^-/CD45RA^+$ T_{EM} (effector memory) and T_{ERMA} (terminally differentiated) cells which localise to sites of inflammation, and have a high effector function, but limited proliferation capabilities.

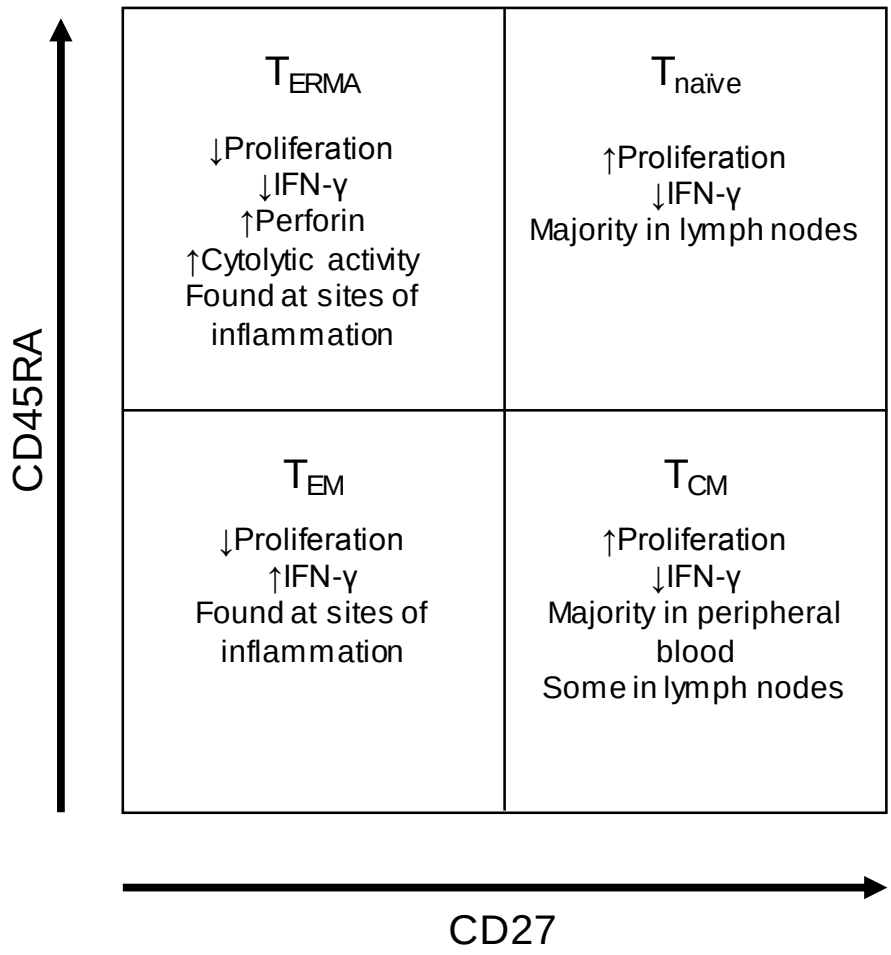
T_{ERMA}
↓Proliferation
↓IFN-γ
↑Perforin
↑Cytolytic activity
Found at sites of inflammation
$T_{naïve}$
↑Proliferation
↓IFN-γ
Majority in lymph nodes
T_{EM}
↓Proliferation
↑IFN-γ
Found at sites of inflammation
T_{CM}
↑Proliferation
↓IFN-γ
Majority in peripheral blood
Some in lymph nodes
CD45RA
CD27

TNF-α (tumour necrosis factor-alpha) and IFN-γ (interferon-gamma) [104, 107, 108] enhancing their anti-cancer activity by inhibiting tumour growth, interacting with the adaptive immune system (reviewed in [109]) and activating NK cells [110].

However, one of the main cytotoxic effects of Vγ9Vδ2 T cells is mediated by NKG2D (Natural killer group 2, member D) expressed by both $CD8^+$ CTL and NK cells. NKG2D on Vγ9Vδ2 T cells can detect the ligands MICA/B (MHC class I polypeptide-related sequence A/B) [111, 112], ULBP1 (UL16 binding protein 1) [113], and ULBP4 (UL16 binding protein 4) [114] on various solid and haematological tumours to mediate killing. Therefore, expression of NKG2D on Vγ9Vδ2 T cells can be used as a marker of cytotoxicity.

Similarly to NK cells, a subpopulation of Vγ9Vδ2 T cells also express CD16 (FcγRIIIA/B). CD16 is a low affinity Fc receptor and upon binding to the Fc portion of IgG antibodies, can stimulate antibody-dependant cellular cytotoxicity (ADCC). CD16 is upregulated on T_{EM} and T_{ERMA} Vγ9Vδ2 T cells, following PAg stimulation [99]. T_{ERMA} effector cells are $perforin^{high}$ but do not produce IFN-γ in response to PAg stimulation, until after cross-linking with CD16 [99]. Cross-linking of the antibodies with CD16 on Vγ9Vδ2 T cells was shown to be important for Vγ9Vδ2 T cell cytotoxicity against various malignancies [115-118].

Ultimately, Vγ9Vδ2 T cells use a number of mechanisms which make them highly cytotoxic towards a variety of solid and haematological cancers (Figure 1.7), including bone [75, 79], breast [82, 111], melanoma [76], lung [78], chronic myeloid leukaemia [98], and multiple myeloma [80], both *in vitro* and in pre-clinical models.

Figure 1.7 Mechanisms of Vγ9Vδ2 T cell mediated killing of cancer cells.

Target cells are recognised by Vγ9Vδ2 T cells via the Vγ9Vδ2^{+} TCR and/or NKG2D. Vγ9Vδ2 T can then induce cytotoxicity of target cells via a variety of mechanisms including through the release of TRAIL and FasL to induce apoptosis, ADCC mediated by antibodies binding to CD16, release of cytotoxic granules containing perforin and granzymes, and through the release of immune modulatory cytokines. Figure adapted from [86] and [119].

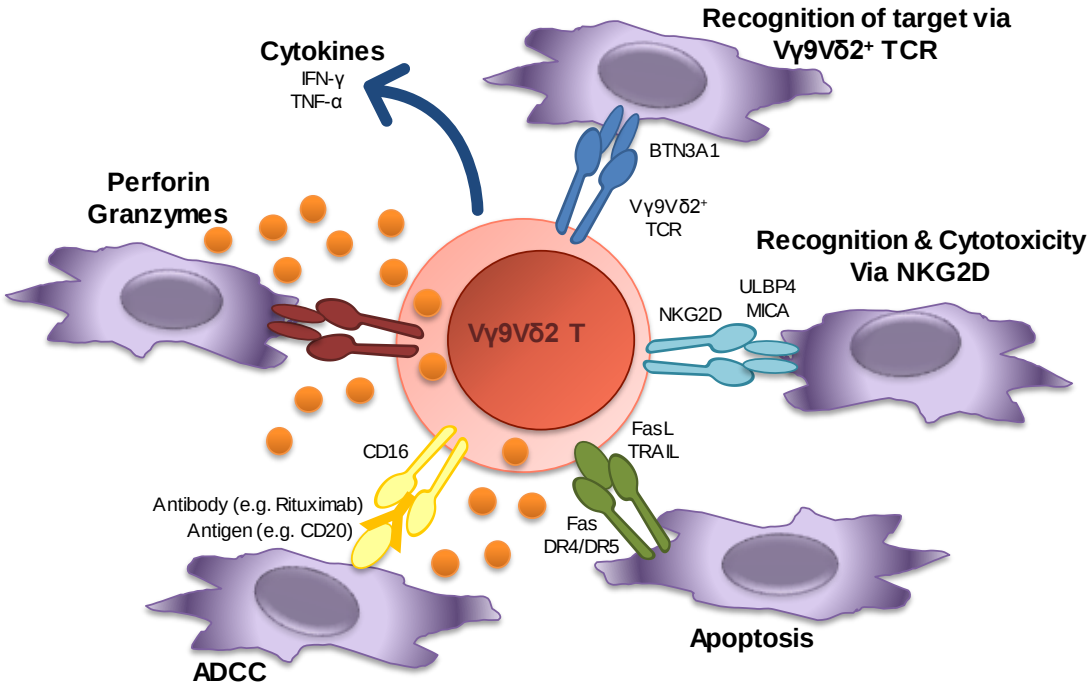
Cytokines
IFN-γ
TNF-α
Recognition of target via
Vγ9Vδ2⁺ TCR
BTN3A1
Vγ9Vδ2⁺
TCR
Perforin
Granzymes
Recognition & Cytotoxicity
Via NKG2D
ULBP4
MICA
NKG2D
Vγ9Vδ2 T
FasL
TRAIL
CD16
Antibody (e.g. Rituximab)
Antigen (e.g. CD20)
Fas
DR4/DR5
ADCC
Apoptosis

1.9 Clinical trials with Vγ9Vδ2 T cells

To date, the potential of γδ T cell immunotherapy has been assessed in more than a dozen early phase clinical trials against a variety of haematological and advanced solid tumours [reviewed in 120, 121]. *In vivo* expansion or adoptive transfer (illustrated in Figure 1.8) are two methods which are being used for Vγ9Vδ2 T cell immunotherapy. The difference between these two methods is where Vγ9Vδ2 T cell expansion occurs. As the name suggest, *in vivo* expansion (Figure 1.8 A) occurs within the patient, where ZOL is infused intravenously (i.v), either alone or often in combination with IL-2. Conversely, adoptive transfer (Figure 1.8 B), involves collecting peripheral blood from the patient, expanding Vγ9Vδ2 T cells *ex vivo* using a variety of culture conditions, then reinfusing expanded Vγ9Vδ2 T cells back into the patient. Both approaches can be used as monotherapies, or in combination with ZOL, IL-2, or other concurrent cancer treatments (e.g. chemotherapy, radiation, hormone therapy etc.).

1.9.1 *In vivo* expansion of Vγ9Vδ2 T cells

In vivo expansion using ZOL and IL-2 has been conducted in several clinical trials in patients with metastatic breast cancer [122], hormone-refractory prostate cancer (HRPC) [123], and advanced renal cell carcinoma [124]. These studies showed patients treated with ZOL and IL-2 had increased numbers of circulating T_{EM} Vγ9Vδ2 T cells, while the infusion itself produced minimal and transient side effects, such as a mild fever or flu-like symptoms, which were easily remedied [122-124]. However, in all studies, Vγ9Vδ2 T cell numbers decreased over time. As the treatment cycles progressed, the frequency of highly proliferating $T_{naïve}$ and T_{CM} Vγ9Vδ2 T cells decreased and did not return to pre-treatment levels, resulting in an overall decrease in Vγ9Vδ2 T cells [122-124]. Additionally,

Figure 1.8 Comparing immunotherapeutic approaches: *in vivo* expansion vs adoptive transfer of Vγ9Vδ2 T cells.

A. During *in vivo* expansion, a Vγ9Vδ2 T cell stimulator e.g. ZOL is infused into the patients' blood stream either alone or in combination with IL-2. Expansion and activation of Vγ9Vδ2 T cells occurs within the peripheral blood, followed by localisation of Vγ9Vδ2 T cells to the tumour. **B.** Conversely, in adoptive transfer, blood from the patient is collected and PBMCs are isolated using a Ficoll gradient. Cells are then stimulated for 7-14 days in the presence of ZOL and IL-2, resulting in a large scale *ex vivo* expansion and activation of Vγ9Vδ2 T cells, which are then re-infused into the patient, either as a monotherapy or in combination with ZOL. Either of these approaches can be used in combination with other treatments such as chemotherapy.

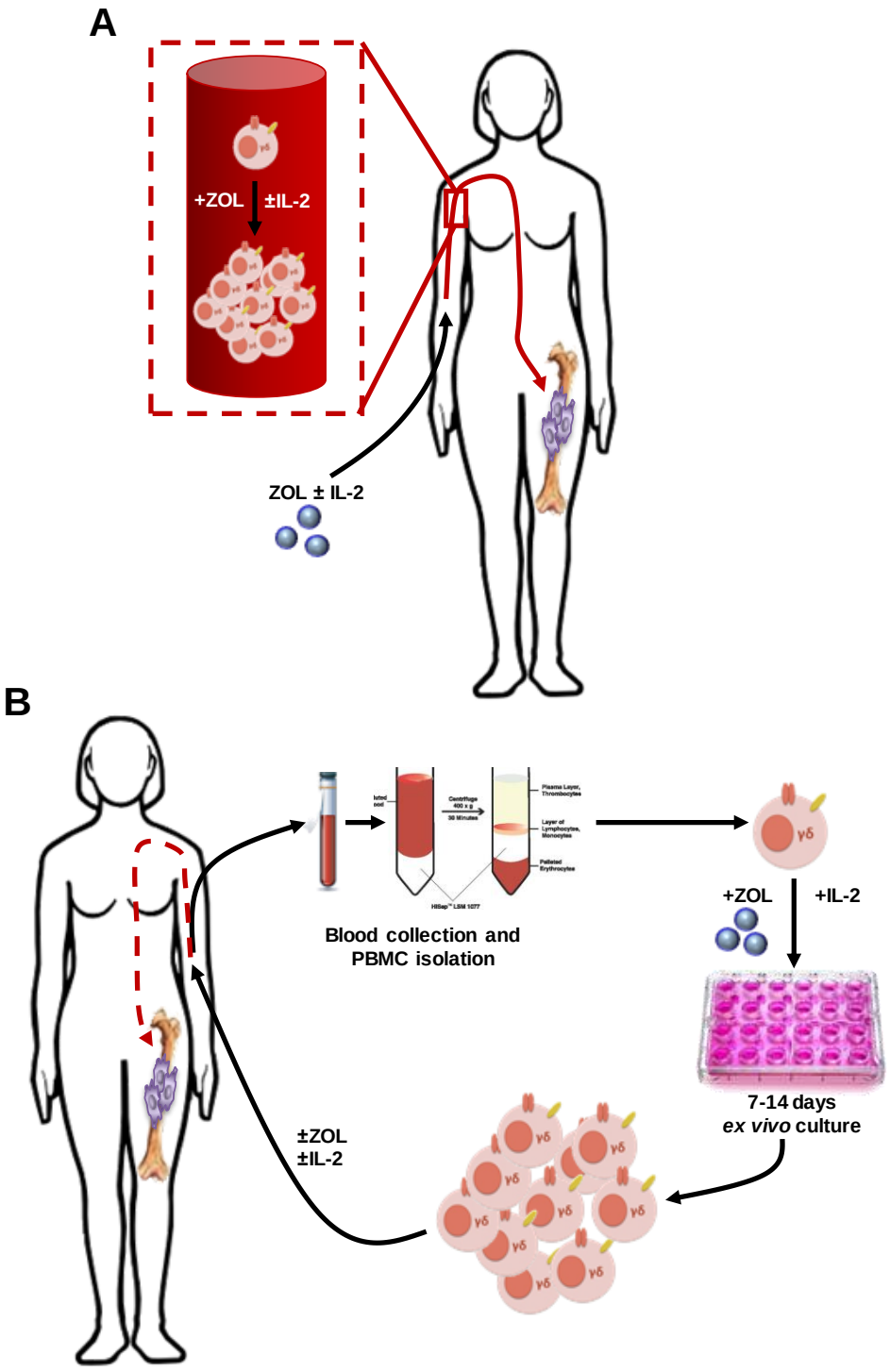
A
+ZOL
±IL-2
ZOL ± IL-2
B
Blood collection and
PBMC isolation
+ZOL
+IL-2
7-14 days
ex vivo culture
±ZOL
±IL-2

deterioration in health correlated with decreasing Vγ9Vδ2 T cell numbers, while patients showing the most robust expansion, had the best prognosis resulting in either stable disease or in some cases remission [122, 123]. These studies highlighted some disadvantages of *in vivo* expansion. Firstly, the observed depletion of Vγ9Vδ2 T cells over time may relate to repeated administrations of nBPs. During chronic exposure to a stimulus, Vγ9Vδ2 T cells can undergo AICD (activation induced cell death), a programmed cell death mechanism mediated by Fas [125], normally responsible for maintaining immune cell homeostasis to avoid over-activation of the immune system which can result in auto-immune disease. However, in the case of immunotherapy, constant infusion of ZOL and IL-2 to activate Vγ9Vδ2 T cells appears detrimental to clinical outcome, with decreasing numbers of $T_{naïve}$ and T_{CM} Vγ9Vδ2 T cells, potentially due to AICD. Secondly, while most patients show increased numbers of Vγ9Vδ2 T cells, there were high levels of interpatient variability, and because Vγ9Vδ2 T cell numbers appeared predictive of response to treatment, any successful immunotherapy must aim to produce as many Vγ9Vδ2 T cells as possible. Now, after many years of trial and error, well-established protocols exist for expanding a large number of Vγ9Vδ2 T cells *ex vivo* [83]. Better and more consistent *ex vivo* expansion protocols may yield greater Vγ9Vδ2 T cell numbers in patients who are poor *in vivo* expanders, such as those undergoing chemotherapy. Together, this suggests that adoptive transfer is a more suitable approach which overcomes some of these disadvantages.

1.9.2 Vγ9Vδ2 T cell adoptive transfer

Adoptive transfer of Vγ9Vδ2 T cells expanded *ex vivo* using ZOL and IL-2 has been examined against a variety of solid and haematological malignancies [105, 126], including non-small cell lung cancer [127] and chemotherapy resistant

malignant ascites from gastric cancer [128]. Apart from mild fever and general fatigue, no serious adverse effects related to adoptive transfer of Vγ9Vδ2 T cells was observed in any of the studies [126-128]. Prior to expansion, the majority of Vγ9Vδ2 T cells from PBMC were $T_{naïve}$ and T_{CM} [127]. Although cancer patients had less of these highly proliferative Vγ9Vδ2 T cells compared to healthy controls [105], they still achieved large expansions, resulting in the majority of adoptively transferred Vγ9Vδ2 T cells to be the effector T_{EM} phenotype [105, 127]. Additionally, patients with the best outcomes were the ones undergoing concurrent treatments with Vγ9Vδ2 T cell adoptive transfer, such as ZOL, chemotherapy, or hormonal therapy [105, 126, 127].

Interestingly, $Vδ1^+$ γδ T cells are considered to have better anti-cancer efficacy and greater resistance to AICD compared to Vγ9Vδ2 T cells [129, 130], however in terms of clinical application, they are more difficult to harness as an immunotherapy. $Vδ1^+$ γδ T cells are more challenging to isolate as they are the minor γδ T cell subset found in peripheral blood and treatment with nBPs only expands Vγ9Vδ2 T cells. The skin is a greater reservoir of $Vδ1^+$ γδ T cells, however additional challenges are involved in isolating substantial numbers of skin resident γδ T cells. Recently, two groups (Bruno Silva-Santos, Instituto de Medicina Molecular, Lisbon and Adrian Hayday, King's College, London) have developed proprietary methods for expanding and activating $Vδ1^+$ γδ T cells from the blood and skin respectively, using clinical-grade materials. Excitingly, expanded $Vδ1^+$ γδ T cells from the blood, termed Delta One T cells (DOT-Cells®) and from the skin produce abundant IFN-γ, TNF-α and are cytotoxic towards a large variety of cancer cells [131, 132]. Additionally, DOT-Cells® have been shown to inhibit chronic lymphocytic leukagrowth in two xenografts models, and as part of a new company

Lymphact, are being assessed against leukaemia, colon, ovarian, and pancreatic cancers *in vivo* [133]. However, as these methods have only been recently developed and are patented by the corresponding groups, at the time of writing, all published human clinical trials for cancer immunotherapy have been focused solely on Vγ9Vδ2 T cells.

1.10 Combination Therapies

While it is well established that Vγ9Vδ2 T cells can target many different cancer types, some cancers, especially advanced solid tumours, appear more resistant. Sensitivity to Vγ9Vδ2 T cell cytotoxicity could depend on several factors, including ligand expression on tumour cells that are targeted by Vγ9Vδ2 T cells. For example, Vγ9Vδ2 T cells express NKG2D, but low expression of its ligand ULBP4 on leukaemia cell lines protected from Vγ9Vδ2 T cell cytotoxicity [114]. Additionally, MICA, another ligand recognised by NKG2D, can be shed by tumour cells therefore evading recognition and cytolysis by immune cells [134]. To overcome resistance and to enhance anti-cancer efficacy, Vγ9Vδ2 T cells can be used in adjuvant to other well-established therapies. This has been reported in a number of clinical trials, where patients treated with adoptive transfer of Vγ9Vδ2 T cells in combination with concurrent treatments such as nBPs, chemotherapy, or hormonal therapy had the best outcomes [105, 126, 127], suggesting that Vγ9Vδ2 T cells may be most effective at targeting advanced cancers in combination with other treatments.

1.10.1 Sensitisation with nBPs

Many cancer types abnormally accumulate PAgs, such as IPP due to up-regulation of the mevalonate pathway [92]. One method to sensitise cancer cells to

killing by Vγ9Vδ2 T cells is to inhibit FPPS in the mevalonate pathway to accumulate even higher levels of IPP. As previously discussed, nBPs are potent inhibitors of FPPS, and many cell types, including cancer cells, can internalise nBPs *in vitro*. It is well-established that osteosarcoma [135], breast [82], glioblastoma [136], lymphoma [81], fibrosarcoma and lung cancer cells [78] are all sensitised to killing by Vγ9Vδ2 T cells following pre-treatment with ZOL.

As well as causing accumulation of IPP to further mediate Vγ9Vδ2 T cell cytotoxicity, pre-treatment with nBPs has also been used to sensitise chemotherapy resistant cancer cells. For example, ZOL pre-treatment could sensitise imatinib-sensitive and resistant chronic myelogenous leukaemia cells to killing by Vγ9Vδ2 T cells *in vitro* [98]. Also *in vitro,* TRAIL-resistant osteosarcoma cells could be sensitised to TRAIL after pre-treatment with the nBP alendronate and overcoming resistance was found to be mediated by the up-regulation of death receptor (DR) 5 (DR5/Apo2L/TRAIL-R2) on resistant cancer cells [137]. Vγ9Vδ2 T cells can release TRAIL, which is a ligand for DR4 and DR5, so upregulation of death receptors could be a mechanism of how the cancer cells became sensitised.

1.10.2 Chemotherapies

Currently, neoadjuvant chemotherapy is frequently used in treatment for osteosarcoma and primary breast cancer. Many chemotherapies have a narrow therapeutic range, where too little drug produces no efficacy, and too much can result in off target toxicity, resulting in severe side effects. Additionally, recurrent and advanced cancers often gain resistance to a range of chemotherapies, making them even more difficult to treat. One way to enhance efficacy, minimise off target toxicity, and to sensitise chemotherapy-resistant cells, is to combine a low dose of chemotherapy with immunotherapy (such as Vγ9Vδ2 T cells), to kill cancer cells

in a synergistic manner. For example, the efficacy of cisplatin and etoposide, were tested in combination with Vγ9Vδ2 T cells, resulting in additive or synergistic cytotoxicity of colorectal, bladder, and prostate cancer cells in an effector: target (E:T) ratio-dependant manner [81]. Additionally, doxorubicin and 5-fluorouracil, sensitised colon cancer initiating cells to Vγ9Vδ2 T cell mediated cytotoxicity via upregulation of DR5 and Fas [138]. Doxorubicin is commonly used for the treatment of both osteosarcoma and breast cancer, however to date, it has not been assessed against either of these cancers in combination with Vγ9Vδ2 T cells.

In recent years, using recombinant human proteins against specific targets on cancer cells has become an attractive alternative to non-specific treatments such as chemotherapies. For example, rhTRAIL (recombinant human TRAIL), a pro-apoptotic receptor agonist (PARA), binds to DR4 (Apo2L/TRAIL-R1) and DR5 on cancer cells, resulting in receptor multimerisation and subsequent recruitment of the FADD (Fas-associated death domain protein) complex, initiating caspases and ultimately resulting in cell death of many cancer types including osteosarcoma and breast cancer [139-141]. Vγ9Vδ2 T cells have the ability to release TRAIL [98] and previously our laboratory has shown that TRAIL reduces tumour burden in a model of osteolytic breast cancer [141]. TRAIL also protects the bone from tumour-associated osteolysis, however prolonged treatment regimens to maximise anti-cancer efficacy result in TRAIL resistance [141]. TRAIL has been previously used in combination with other immunotherapeutic approaches to enhance the anti-cancer efficacy of T cells [142, 143], however it has not been examined in combination with Vγ9Vδ2 T cells.

1.10.3 Antibodies

Another way to enhance the anti-cancer efficacy of Vγ9Vδ2 T cells, is to exploit their expression of CD16, a low affinity receptor which binds to the Fc portion of antibodies [144]. Antibody cross-linking to CD16 mediates antibody-dependant cell-mediated cytotoxicity (ADCC), causing the release of cytolytic granules which result in the eventual apoptosis of target cells via caspase activation (Figure 1.9).

A study by Tokuyama et al. showed that co-treatment of Vγ9Vδ2 T cells and rituximab, an antibody targeting a B-cell marker CD20, lead to increased specific lysis of Daudi cells compared to treatment with Vγ9Vδ2 T cells alone [116]. This study determined that the observed increase in cytotoxicity was due to CD20 cross-linking with $CD16^+$ Vγ9Vδ2 T cells [116]. Similarly, trastuzumab, a humanised monoclonal antibody against HER-2 which is over-expressed on 20-30% of breast cancers, can be used in conjunction with Vγ9Vδ2 T cells to induce greater anti-cancer efficacy against $HER\text{-}2^+$ breast cancer cells [115]. These studies, and others [117, 118] provide evidence to suggest that Vγ9Vδ2 T cells can be successfully used in combination with antibodies to target cancer cells.

Drozitumab (Apomab, Genetech), is a humanized IgG1 monoclonal antibody directed against DR5 and has been shown to require CD16 cross-linking to elicit cytotoxic effects against target cells [145]. Drozitumab binding results in the activation of the extrinsic pathway of apoptosis and consequently cell apoptosis, via caspase activation. In a mouse model of osteolytic breast cancer, drozitumab was shown to decrease tumour burden in the tibia, and reverse osteolysis associated with tumour growth [146]. However, the efficacy of drozitumab in combination with $CD16^+$ Vγ9Vδ2 T cells has not yet been examined.

Figure 1.9 Antibody-dependant cell-mediated cytotoxicity of cancer cells.

Antibodies (e.g. Rituximab) first bind their target receptor on cancer cells (e.g. CD20 on B cell lymphomas). $CD16^+$ Vγ9Vδ2 T cells bind the Fc portion of receptor-bound antibodies, resulting in activation of Vγ9Vδ2 T cells. Activated Vγ9Vδ2 T cells subsequently release perforin and granzymes, indirectly activating caspases, and inducing apoptosis of the cancer cell. Figure adapted from [147].

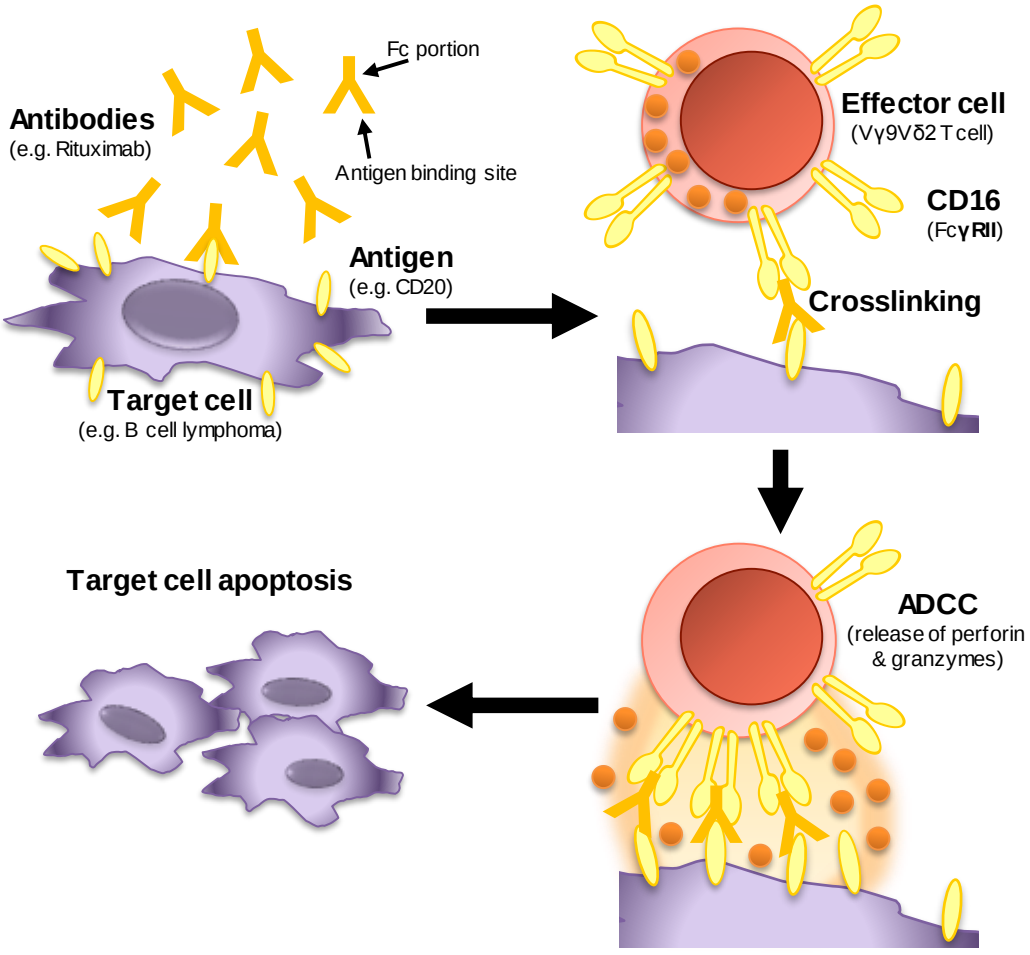
Fc portion
Antibodies
(e.g. Rituximab)
Antigen binding site
Antigen
(e.g. CD20)
Target cell
(e.g. B cell lymphoma)
Effector cell
(Vγ9Vδ2 T cell)
CD16
(FcγRII)
Crosslinking
ADCC
(release of perforin
& granzymes)
Target cell apoptosis

1.11 Role of Vγ9Vδ2 T cells in osteoimmunology

While it has been shown that osteosarcoma cells can be targeted by Vγ9Vδ2 T cells *in vitro* [75, 79, 135], limited studies have investigated the effect Vγ9Vδ2 T cells have on bone, either in the context of cancer in the bone or normal bone homeostasis. The first indication that Vγ9Vδ2 T cells may play an important role in osteoimmunology was that BAONJ observed in osteoporotic patients was correlated with a depletion of Vγ9Vδ2 T cells [73]. *In vitro* studies have shown activated donor-matched human γδ T cells inhibit osteoclast formation from PBMC [148] and Vγ9Vδ2 T cells are cytotoxic towards osteoclasts in co-culture with multiple myeloma cells [80]. Additionally, Vγ9Vδ2 T cells, have been shown to produce IGF-1, and low levels of FGF-2 following antigen stimulation [149]. Under culture conditions, human γδ T cells from peripheral blood have also been shown to release other factors important in bone formation and remodelling such as connective tissue growth factor (CTGF) [150], and matrix metalloproteinase-7 (MMP-7) and MMP-9 [151]. IGF and FGF are osteoblast growth factors, and CTGF also appears to play a role in the proliferation and differentiation of osteoblasts [152, 153] suggesting that if Vγ9Vδ2 T cells are primed to produce these factors following localisation to the bone, in addition to their potential cytotoxicity against osteoclasts, they could possibly stimulate new bone formation or inhibit bone degradation, resulting in a net gain in bone volume. In contrast, murine γδ T cells appear to have a contradictory role in mouse models of fracture repair, where they have been reported to both impair and promote fracture healing [154, 155]. Regardless, these studies overall show that Vγ9Vδ2 T cells have potential to contribute to osteoimmunology, however the net effect they have on normal bone still needs to be elucidated.

1.12 Aims and significance

Osteosarcoma and breast cancer bone metastases are two osteolytic tumour types that result in abnormal osteoclast-mediated bone resorption, causing significant bone degradation and a decline in both patient quality of life and overall survival. Current treatments, including chemotherapy and anti-resorptive agents are only palliative; therefore novel therapies are desperately required.

Adoptive transfer of *ex vivo* expanded cytotoxic Vγ9Vδ2 T cells is emerging as a novel immunotherapeutic approach for solid and haematological malignancies. Based on current knowledge, cytotoxic Vγ9Vδ2 T cells can be successfully expanded from human PMBC using ZOL and IL-2, and target a variety of cancer cells *in vitro* and *in vivo*. However, the anti-cancer efficacy of Vγ9Vδ2 T cells requires enhancing and optimisation. It has been well established that nBPs can sensitise cancer cells to killing by Vγ9Vδ2 T cells both *in vitro* and in pre-clinical animal trials. As nBPs naturally localise to the bone, an elegant approach for targeting cancers in the bone has emerged. A hypothesis has been formed to suggest that treatment with nBPs such as ZOL, followed by adoptive transfer of Vγ9Vδ2 T cells, will sensitise cancer cells in the bone microenvironment, enhancing the anti-cancer efficacy of Vγ9Vδ2 T cells [156]. As osteoclasts are the main target of ZOL in the bone, this would also inhibit the 'vicious cycle' of abnormal osteoclast-mediated resorption associated with osteolytic tumours. To date, this hypothesis has not been examined in an appropriate animal model.

Therefore, the major aim of this thesis was to explore the feasibility of using *ex vivo* expanded human Vγ9Vδ2 T cells for the purpose of adoptive transfer into a xenograft mouse model of osteolytic osteosarcoma and breast cancer, alone and

in combination with ZOL. Also these experiments provided an opportunity to examine the role Vγ9Vδ2 T cells have on bone *in vivo.*

Treatment of advanced cancers is challenging, so multi-therapy approaches are often deemed necessary. Early phase clinical trials with adoptive transfer of Vγ9Vδ2 T cells have shown patients undergoing concurrent treatments obtained the most favourable outcomes. This leads to the secondary aim of this study, which is to enhance the anti-cancer efficacy of Vγ9Vδ2 T cells using PARAs (drozitumab and TRAIL) or chemotherapy (doxorubicin). TRAIL and doxorubicin will be assessed as adjuvant therapies to Vγ9Vδ2 T cells. Drozitumab will be assessed in the context of $CD16^+$ Vγ9Vδ2 T cells, as it requires Fc cross-linking to be biologically active.

Overall, these studies will provide new insights into the anti-cancer efficacy of Vγ9Vδ2 T cells against cancers in the bone, and provide valuable pre-clinical information for the advancement of Vγ9Vδ2 T cell immunotherapy.

The specific aims of these studies are:

1. To expand Vγ9Vδ2 T cells *ex vivo* using ZOL and IL-2, for the purpose of assessing their cytotoxicity *in vitro.* This aim will assess Vγ9Vδ2 T cell cytotoxicity against a panel of cancer cell lines, using Vγ9Vδ2 T cells alone or in combination with ZOL pre-treatment.
2. To adoptively transfer Vγ9Vδ2 T cells alone or in combination with ZOL in a pre-clinical model of osteolytic osteosarcoma and osteolytic breast cancer. Specifically this aim will:
    a. Examine Vγ9Vδ2 T cell *in vivo* localisation

b. Assess the anti-cancer efficacy of Vγ9Vδ2 T cells alone, or in combination with ZOL

c. Assess the treatment effects on tumour-associated bone loss

d. Examine the effects of Vγ9Vδ2 T cells on normal bone.

3. To determine if Vγ9Vδ2 T cell cytotoxicity can be enhanced in combination with:

a. Drozitumab cross-linking to $CD16^{+}$ Vγ9Vδ2 T cells

b. TRAIL

c. Doxorubicin.

Chapter 2

Materials and Methods

2.1 Cell Lines

KHOS, 143B (human osteosarcoma), and ZR-75, T47D (human breast cancer) cell lines were obtained from American Type Culture Collection. The MDA-MB231 human breast cancer derivative cell line MDA-MB231-TXSA was kindly provided by Dr. Toshiyuki Yoneda (University of Texas Health Science Centre, San Antonio, Texas). MDA-MB231-TXSA, KHOS, and 143B cells expressed GFP and luciferase produced by retroviral expression of the SFG-NES-TGL vector, as previously described [146, 157]. All cell lines were cultured as described in Dulbecco's Modified Eagle's Medium (DMEM, Life Technologies, Australia) supplemented with 10% foetal bovine serum (FBS, Life Technologies, Australia), 100IU/mL penicillin (Life Technologies, Australia), 100µg/mL streptomycin (Life Technologies, Australia), and 25mM HEPES (Life Technologies, Australia) at 37°C in a 5% CO_2 humidified atmosphere.

2.2 Antibodies and Reagents

For flow cytometry, the following antibodies conjugated to PE, PeCy5 or PeCy7 were obtained from eBioscience (San Diego, CA, USA): anti-CD3 (clone UCHT1), anti-CD314 (NKG2D) (clone 1D11), anti-CD16 (clone B73.1), anti-CD27 (clone 0323) and anti-CD45RA (clone B73.1). Also for flow cytometry, anti-Vγ9 TCR conjugated to FITC was obtained from BD Biosciences (San Jose, CA, USA). All flow cytometry analysis was performed using the BD FACSCanto II Flow Cytometer (San Jose, CA, USA) and images were created in FlowJo LLC Data Analysis Software v10.1 (Ashland, OR, USA). Affinity Pure Goat Anti-Human IgG Fcγ Fragment was purchased from Jackson Immunoresearch Laboratories, Inc (West Grove, PA, USA). ZOL was generously provided by

Novartis Pharma AG, and Drozitumab and TRAIL were a kind gift from Dr. Avi Ashkenazi (Genentech, Inc., CA, USA).

2.3 *Ex vivo* expansion of Vγ9Vδ2 T cells

Informed consent was obtained prior to collection of peripheral blood from healthy adult donors. 60-80mL of whole blood was obtained by venipuncture using heparin coated collection tubes. PBMC were isolated immediately via density gradient centrifugation using Lymphoprep™ (Axis Shield, Norway) following manufacturer's instructions. PBMCs were resuspended to $1x10^6$/mL in CTS™ OpTmizer™ T Cell Expansion SFM (Life Technologies, Australia) supplemented with OpTmizer™ T cell Expansion Supplement (1:38 dilution) (Life Technologies, Australia), 10% heat-inactivated FBS (HI-FBS), 100IU/mL penicillin, 100µg/mL streptomycin (Life Technologies, Australia), 2mmol L-glutamine (Life Technologies, Australia), 25mM HEPES (Life Technologies, Australia), 0.1% β-mercaptoethanol (Sigma-Aldrich, USA), recombinant human interleukin 2 (rhIL-2) (100IU/mL) (BD Pharmingen, USA) and 5µM ZOL, then seeded into 6-well plates. Cell culture density was maintained at 1-2 x 10^6 cells/mL and replenished with fresh medium containing rhIL-2 (100IU/ml) only (without ZOL) every 2-3 days, as outlined in [83, 157]. The concentrations of ZOL and IL-2 used to activate and expand Vγ9Vδ2 T cells were based on a protocol published by Kondo et al. [83] and used in other studies [75, 78]. Following 7-8 days of culture cells were collected and enriched as described below or phenotyped using flow cytometric analysis.

2.4 Enrichment of Vγ9Vδ2 T cells

Ex vivo expanded Vγ9Vδ2 T cells were enriched by negative selection MACS using the TCR γ/δ+ T cell Isolation Kit (human) (Miltenyi Biotec,

Germany) following manufacture's instruction. Enriched cells consisted of >97% $V\gamma9^+$ and $CD3^+$ double positive lymphocytes and cell viability exceed 95% as determined by trypan blue exclusion.

2.5 Enrichment of $CD16^+$ Vγ9Vδ2 T cells

To test the ability of Vγ9Vδ2 T cells to undergo ADCC with drozitumab (Chapter 7), three populations of Vγ9Vδ2 T cells were assessed; impure, $CD16^-$, and $CD16^+$ Vγ9Vδ2 T cells. Fresh *ex vivo* expanded Vγ9Vδ2 T cells were enriched by positive selection using CD16 MicroBeads (human) (Miltenyi Biotec, Germany) following manufacture's protocols. Enriched cells consisted of >97% $V\gamma9^+$ and $CD3^+$ double positive lymphocytes and cell viability exceed 95% as determined by trypan blue exclusion.

2.6 Cell cytotoxicity assay

Cytotoxicity of Vγ9Vδ2 T cells against cancer cell lines was assessed using a standard lactate dehydrogenase (LDH) release assay (CytoTox 96® Non-Radioactive Cytotoxicity Assay; Promega, USA) according to the manufacturer's directions. Briefly, $1x10^4$ target cells were seeded in triplicate in a 96-well microtiter plate and allowed to adhere overnight. Target cells were then treated with or without 25μM ZOL for 24 hours, and then co-cultured with Vγ9Vδ2 T cells at various Effector: Target (E:T) ratios with Vγ9Vδ2 T cells as the effector cells, and cancer cells as the target cells. After incubation for 9 hours at 37°C, 50μL of supernatant was assayed for LDH activity following the manufactures protocol. The appropriate controls were prepared and cytotoxicity was calculated as:

$$\% \text{ Cytotoxicity} = \frac{\text{experimental release - effector spontaneous release - target spontaneous release}}{\text{target maximum release} - \text{target spontaneous release}} \times 100$$

2.7 Luciferase-based viability assay

MDA-MB231-TXSA, 143B, and KHOS cells expressed luciferase, which was the basis for a luciferase activity viability assay using Dual Luciferase® Reporter Assay kit (Promega, Madison, WI, USA). Briefly, $1x10^4$ target cells were seeded in triplicate in a 96-well microtiter plate and allowed to adhere overnight. Cells were then treated with or without 25μM ZOL for 24 hours, and then co-cultured with Vγ9Vδ2 T cells at various E:T ratios. After incubation for 24 hours, media was removed from the wells and cells were washed in PBS, then lysates were prepared and analysed according to the manufacturer's directions. Viability was calculated as:

$$\% \text{ Viability} = \frac{\text{experimental value}}{\text{untreated control value}} \times 100$$

2.8 Measurement of DEVD-caspase activity

DEVD-caspase activity was assayed by cleavage of zDEVD-AFC (z-asp-glu-val-asp-7-amino-4-trifluoro-methyl-coumarin), a fluorogenic substrate based on the peptide sequence at the caspase-3 cleavage site of poly (ADP-ribose) polymerases (Kamiya Biomedical Company, Seattle, WA, USA). Briefly, cancer cells were seeded at $1x10^4$cells/well in triplicate a 96-well microtiter plate and allowed to adhere overnight. Cells were then treated with or without 25μM ZOL for 18 hours, then co-cultured with Vγ9Vδ2 T cells at a 5:1 E:T ratio. After 2 or 4 hours, media was removed from the wells and cells were washed in PBS, then lysed in caspase lysis buffer containing 5μM EDTA, 5μM TRIS-HCl and 0.5% IGEPAL (Sigma-Aldrich, USA). Caspase activation in the lysates was detected using DEVD-AFC, as previously described [158].

2.9 Western Blotting

Detection of unprenylated small GTPases, including RAP1, were used to indirectly determine the extent of FPPS inhibition by ZOL, which correlates with increased IPP levels, resulting in the increased detection of cancer cells by Vγ9Vδ2 T cells and greater cytotoxicity. To determine the effect of ZOL on the prenylation of small GTPases in the osteosarcoma and breast cancer cells, lysates were analysed by Western blotting for total and unprenylated RAP1. Briefly, $1x10^6$ cancer cells were seeded in a 25-cm^2 flask, allowed to adhere, and then treated with 25μM ZOL for 18 hours or over a 24 hour time course. Lysates were prepared and separated as previously described [158], and immunodetection was performed overnight at 4ºC in PBS/blocking reagent containing 0.1% Tween-20, using the following primary antibodies at the dilutions suggested by the manufacturer: pAb anti-RAP1 (121) for total RAP1 protein, pAB anti-RAP1A (C-17) specifically for unprenylated RAP1 (Santa Cruz Biotechnology, USA), and anti-actin mAb (Sigma-Aldrich, USA) as a loading control. Membranes were then rinsed several times with PBS containing 0.1% Tween-20 and incubated with 1:5,000 dilution of anti-goat or anti-rabbit alkaline phosphatase-conjugated secondary antibodies (Thermo Fisher Scientific, USA) for 1 hour. Visualisation of protein bands was performed using the ECF substrate reagent kit (GE Healthcare, UK) on a LAS-4000 (GE Healthcare, UK).

2.10 Labelling Vγ9Vδ2 T cells with DiR

Vγ9Vδ2 T cells were expanded *ex vivo* and enriched as described above, washed in PBS, and resuspended to $2x10^6$ cells/mL in RPMI-1640 media (Life Technologies, Australia) supplemented with 0.1% HI-FBS. XenoLight DiR Fluorescent Dye (Perkin Elmer, USA) was reconstituted in ethanol and added to cells at a final concentration of 16.6μg/mL. Cells were incubated in the dark for 10-

15 minutes at 37°C, then collected and washed three times in PBS containing 1% HI-FBS. Cell viability was assessed using trypan blue exclusion; labelling efficacy was assessed by flow cytometry using the filter corresponding to PeCy7; and cytotoxicity against cancer cells was assessed using the DEVD-Caspase assay, as outlined above.

2.11 Animals

Female four-week-old non-obese diabetic severe combined immunodeficient (NOD/SCID) mice were purchased from the Animal Resources Centre (Canning Vale, WA, Australia) and housed under pathogen free conditions in The Queen Elizabeth Hospital Experimental Surgical Suite (Woodville, SA, Australia). Mice were acclimatised to the animal housing facility and the general wellbeing of animals was monitored continuously throughout the experiment. All experimental procedures were carried out with strict adherence to the rules and guidelines for the ethical use of animals in research and were approved by the Animal Ethics Committees of the University of Adelaide and the Institute of Medical and Veterinary Science, Adelaide, SA, Australia. If pain relief was required during the course of the study, animals were administered Rimadyl (carprofen) (Pfizer Animal Health, Australia) at 5mg/kg s.c every 24 hours for a maximum of three days.

2.12 *In vivo* fluorescence and bioluminescence imaging

Non-invasive, whole body imaging to monitor DiR-labelled Vγ9Vδ2 T cell localisation and luciferase expressing cancer cell growth *in vivo* was done using the IVIS Spectrum *in vivo* Imaging system (Caliper Life Sciences, Australia). For fluorescent imaging, mice were anaesthetised by isoflurane (Veterinary Companies of Australia, Australia) and fluorescent images were acquired using the optimised settings for DiR dye: f stop: 2, medium binning, ex/em: 745/800nm. Images were

taken at multiple time points, up to 120 seconds. For bioluminescent imaging, mice were injected s.c with 100µL of D-luciferin solution (Perkin Elmer, USA) to a final dose of 3mg/20g mouse body weight and then anaesthetised by isoflurane and bioluminescence was acquired between 0.5 and 30 seconds (images shown at 1 second). Photon emission was quantified as Total Flux measured in [photons/second] using Living Image 4.2 (Caliper Life Sciences, Australia). There was no interference between the DiR dye and the luciferase expressing cancer cells, therefore fluorescent and bioluminescent images could be acquired in succession to assess Vγ9Vδ2 T cell localisation to the tumour site.

2.13 Intratibial injections of cancer cells

Intratibial (i.t) injection of cancer cells is a reproducible method for investigating primary and metastatic cancer in the bone [63, 67, 146, 158]. Injections were performed on either four or five-week old female NOD/SCID mice as the bone at this age has not fully developed, allowing an easier procedure and better tumour inoculation. Animals were anaesthetised by isoflurane (Veterinary Companies of Australia, Australia), then the left leg was shaved, wiped with 70% ethanol and a 27-guage needle coupled to a Hamilton syringe was used to inject luciferase expressing MDA-MB231-TXSA or 143B cells (1×10^5) resuspended in 10µL PBS, through the tibial plateau into the marrow space. The contralateral tibia was not injected.

2.14 *In vivo* localisation

I.t injections were performed as described above for the MDA-MB231-TXSA and 143B cells. Once tumours were established, mice were injected 5×10^6 DiR-labelled Vγ9Vδ2 T cells i.v (n=3-5). Fluorescence and bioluminescence

images were acquired as described above at the time points outlined in the corresponding figures.

2.15 Assessing the *in vivo* anti-cancer efficacy of a single administration of ZOL and Vγ9Vδ2 T cells

I.t injections were performed as described above for the MDA-MB231-TXSA cells. When tumours were established, mice were assigned into four treatment groups (n=2-3): untreated, ZOL alone (100µg/kg s.c), Vγ9Vδ2 T cells alone ($5x10^6$ γδ T cells injected i.v via the tail vein), and ZOL in combination with Vγ9Vδ2 T cells (infusion of γδ T cells 24 hours after ZOL, treatments as above). Treatments were administered once and tumour growth was assessed over three weeks, by bioluminescent imaging using the IVIS Spectrum.

2.16 Assessing the *in vivo* anti-cancer efficacy Vγ9Vδ2 T cells in combination with metronomic ZOL

I.t injections were performed as described above for the MDA-MB231-TXSA cells. When tumours were established, mice were assigned into four treatment groups (n=6-8): untreated, ZOL-M alone (treatment 1: 25µg/kg s.c, treatment 2 and 3: 50µg/kg s.c), Vγ9Vδ2 T cells alone ($5x10^6$ γδ T cells injected i.v via the tail vein), and ZOL-M in combination with Vγ9Vδ2 T cells (infusion of Vγ9Vδ2 T cells 24 hours after ZOL-M, treatments as above). Treatments were repeated three times over a period of 25 days. Tumour growth was assessed by bioluminescent imaging using the IVIS Spectrum and at the conclusion of the study, mice were sacrificed and the tumour bearing and control tibias from each animal were removed for micro-computed tomography, as described below.

2.17 *In vivo* anti-cancer efficacy of ZOL and Vγ9Vδ2 T cells

I.t injections were performed as described above, with MDA-MB231-TXSA cells, and in a second study, with 143B cells. When tumours were established, mice were assigned into four treatment groups (n=5-8): untreated, ZOL alone (100µg/kg s.c), Vγ9Vδ2 T cells alone ($1x10^7$ γδ T cells injected i.v via the tail vein), and ZOL in combination with Vγ9Vδ2 T cells (infusion of Vγ9Vδ2 T cells 24 hours after ZOL, treatments as above). Treatments were repeated three times over a period of three weeks. Tumour growth was assessed by bioluminescent imaging using the IVIS Spectrum and at the conclusion of the study, mice were sacrificed and the tumour bearing and control tibias from each animal were removed for micro-computed tomography, as described below.

2.18 *Ex vivo* micro-computed tomography (µCT) analysis

Tibias for µCT analysis were surgically resected and scanned using the SkyScan-1076 high-resolution µCT Scanner (Bruker). The scanner was operated at 50kV, 110µA, rotation step of 0.5, 0.5-mm aluminium filter, and scan resolution of 7.8µm/pixel. Cross-sections were reconstructed using a cone-beam algorithm in NRecon (V1.6.9.8, Bruker). Images were then realigned in DataViewer (1.5.1.2, Bruker) and imported into CT Analyser (CTAn) (V1.14.4.1+, Bruker, Skyscan). Using the two-dimensional images obtained from the CTAn, the growth plate was identified and 600 sections starting from the growth plate/tibial interface and moving down the tibia were selected for quantification of total bone morphometric parameters and 200 sections starting 25 sections down from the growth plate, were selected for trabecular bone morphometric parameters. Representative three-dimensional images were generated in CTvox (V2.7.0, Bruker).

2.19 Histology

Tibias were fixed in 10% buffered formalin, followed by 6 weeks decalcification in 0.5 M EDTA/0.5% paraformaldehyde in PBS, pH 8.0 at room temperature. Complete decalcification was confirmed by radiography and tibias were then paraffin embedded and sectioned longitudinally at 6μm. Osteoclast-specific tartrate-resistant acid phosphatase (TRAP) staining was conducted following the manufacturer's protocol (386A, Sigma Aldrich). Slides were then imaged using Nanozoomer-HT Digital Pathology (NDP, Hamamatsu) and photos were acquired at 4x and 40x magnification using Nanozoomer software NDP.view (V1.2.33, Hamamatsu). Osteoclast number was determined by counting TRAP positive multi-nucleated (≥3 nuclei) cells in a $1mm^2$ area below the growth plate.

2.20 Data analysis and statistics

In vitro experiments were conducted at least twice using biological triplicates, and data presented is mean ± SEM, unless otherwise specified. A representative experiment is shown for western immunoblot data. A two-tailed unpaired Student's t-test was used to analyse all *in vitro* data and *ex vivo* bone volume analysis. *In vivo,* tumour growth was analysed using a linear mixed effects model with animal treated as a random factor. The data were log transformed prior to analysis. Statistical analysis was done with SAS v9.3 (SAS Institute Inc., USA). All other statistical analysis was done using SigmaPlot v12.5 (Systat Software, Inc). In all cases p-values <0.05 were considered statistically significant.

Chapter 3

Optimising adoptive transfer of *ex vivo* expanded Vγ9Vδ2 T cells

3.1 Introduction

Bone metastases occur in over 75% of patients with advanced breast cancer, however treatment remains palliative. Breast cancer cells in the bone release factors that increase osteoclast number and activity, resulting in cancer-associated osteolysis. During bone degradation there is further release of factors that enhances tumour growth, resulting in what is known as the 'vicious cycle' of metastatic disease [reviewed in 18, 19]. Bone loss contributes to the morbidity of the disease, with patients suffering SREs including fractures, chronic pain, and symptoms associated with hypercalcemia [1, 8]. It is clear that novel therapies developed for the treatment of bone metastases need to target the 'vicious cycle' of cancer growth and bone degradation.

In recent years, the anti-tumour capacity of human Vγ9Vδ2 T cells has become widely recognised [159] and as immunotherapy becomes common, it presents a novel approach for the treatment of advanced breast cancer. Human Vγ9Vδ2 T cells recognise PAgs, metabolites of the mammalian mevalonate pathway, which are accumulated in transformed (cancer), stressed, or infected cells [92]. Recognition of PAgs by Vγ9Vδ2 T cells leads to their activation and results in the release of cytolytic, apoptotic, and immunogenic proteins including perforin, granzyme B [75, 98, 104, 107], TRAIL [98], FasL [79], IFN-γ, and TNF-α [104, 107, 108], which all contribute to cytotoxic potential.

In early phase clinical trials, Vγ9Vδ2 T cell-based immunotherapy has produced encouraging results in terms of good tolerance and safety [reviewed in120, 121]. However the observed anti-cancer efficacy has been relatively underwhelming, especially against advanced solid tumours [122-124, 126-128].

This suggests that Vγ9Vδ2 T cell therapy requires optimisation, potentially in combination with other therapies.

It is well established that treatment of cancer cells with PAg sensitises them to killing by Vγ9Vδ2 T cells [76, 96-99]. nBPs, are a class of FDA approved drugs which inhibit osteoclast mediated bone degradation and increase PAg expression via inhibition of the mevalonate pathway [102]. ZOL is a third generation nBP currently used in the clinic for the treatment of osteoporosis, Paget's disease of the bone, and bone metastases. It is well established that nBPs including ZOL, sensitise cancer cells to killing by Vγ9Vδ2 T cells *in vitro* and *in vivo* [78, 81, 82, 135, 136]. nBPs rapidly localise to the skeleton, where they may be readily available for uptake by cells in the tumour microenvironment, resulting in enhanced Vγ9Vδ2 T cell anti-cancer efficacy.

Additionally, *in vitro* ZOL demonstrates anti-cancer properties and was shown to induce cell death, inhibit proliferation, invasion, and angiogenesis in a variety of cancer cell lines [57-62]. However, studies examining the anti-cancer efficacy of ZOL in pre-clinical models have delivered contradictory outcomes [62-65, 67, 68]. This may be due to ZOL having the highest affinity for bone mineral compared to other nBPs [48], allowing rapid localisation to the bone, potentially limiting any anti-cancer effects it may exert in other tissues.

In the context of breast cancer bone metastases, ZOL in combination with Vγ9Vδ2 T cells would be an ideal two-pronged approach as it has potential to sensitise cancer cells to killing by Vγ9Vδ2 T cells, and inhibit osteoclast mediated bone degradation, a major contributing factor to the morbidity of the disease. While targeting cancer in the bone using Vγ9Vδ2 T cells alone or in combination with

ZOL has been discussed in the literature [156, 160], to date no studies have examined this treatment regimen in a well-characterised pre-clinical model.

Therefore, the aim of this chapter was firstly to optimise and characterise the *ex vivo* expansion of Vγ9Vδ2 T cells from human PBMC using ZOL and IL-2, then to assess the *in vitro* and *in vivo* efficacy of *ex vivo* expanded Vγ9Vδ2 T cells alone and in combination with ZOL in a model of osteolytic breast cancer. This study confirmed that ZOL and IL-2 could be used for large scale *ex vivo* expansions of Vγ9Vδ2 T cells, and that ZOL sensitises breast cancer cells to killing by Vγ9Vδ2 T cells. Pre-clinical studies then examined the efficacy of single and multiple administrations of Vγ9Vδ2 T cells alone, and in combination with ZOL. A single administration of Vγ9Vδ2 T cells transiently decreased tumour growth while multiple infusions were required to prolong this effect. However, in contrast to the *in vitro* observations, when used *in vivo*, ZOL failed to potentiate the anti-cancer efficacy of Vγ9Vδ2 T cells, suggesting that further *in vivo* optimisation is required.

3.2 Results

3.2.1 *Ex vivo* expansion and phenotyping of Vγ9Vδ2 T cells

Numerous reports have shown that Vγ9Vδ2 T cells can be activated and expanded using nBPs including alendronate [76], pamidronate [77, 78], and ZOL [75, 78-83]. The studies in this thesis used 5μM ZOL and 100IU/mL IL-2 to activate and expand Vγ9Vδ2 T cells, based on a protocol published by Kondo et al. [83] and used in numerous other studies [75, 78].

PBMCs were isolated from the blood of healthy donors, then cultured in media containing 5μM ZOL and 100 IU/mL IL-2 for seven days. Flow cytometric analysis was used to phenotype cells immediately following PBMC isolation and

after expansion (Figure 2.1). In total, thirty-seven expansions were carried out to provide sufficient Vγ9Vδ2 T cells for all the experiments conducted in this thesis.

The success of Vγ9Vδ2 T cell expansions was assessed by comparing the percentage of $CD3^+/V\gamma9^+$ cells immediately following PBMC isolation and after expansion. Data was pooled from several expansions to demonstrate a typical analysis. Immediately following PBMC isolation on Day 0, an average of 6% of the viable lymphocytes were $CD3^+/V\gamma9^+$ cells (Figure 3.1 A). By Day 7, this number had increased significantly to approximately 80%. (Figure 3.1 A).

Surface expression of NKG2D and CD16 was assessed using flow cytometry. NKG2D can detect the ligands MICA/B (MHC class I polypeptide-related sequence A/B) [111, 112], ULBP1 (UL16 binding protein 1) [113], and ULBP4 (UL16 binding protein 4) [114] on various solid and haematological tumours to mediate killing by Vγ9Vδ2 T cells. Furthermore, a subpopulation of Vγ9Vδ2 T cells also express CD16 (FcγRIIIA/B), which can stimulate ADCC upon binding [99]. Therefore, NKG2D and CD16 expression on Vγ9Vδ2 T cells can be used as markers of cytotoxicity. Expression of these receptors was measured on the gated $CD3^+/V\gamma9^+$ population immediately following PBMC isolation and after expansion. By Day 7, 99% of Vγ9Vδ2 T cells expressed NKG2D, compared to 82% measured on Day 0 (Figure 3.1 B). In contrast, 25% of Vγ9Vδ2 T cells expressed CD16 on Day 7, compared to 43% measured on Day 0 (Figure 3.1 C).

Based on CD27 and CD45RA receptor expression, flow cytometric analysis was used to assess the differentiation phenotype of Vγ9Vδ2 T cells. Vγ9Vδ2 T cells expressing $CD27^+/CD45RA^+$ and $CD27^+/CD45RA^-$ are $T_{naïve}$ and T_{CM} cells respectively, which have a high proliferation rate and low effector function and are

found in the lymph nodes and peripheral blood [103, 104]. These differentiate into T_{EM} ($CD27^-/CD45RA^-$) and T_{ERMA} ($CD27^-/CD45RA^+$), which localise to sites of inflammation, and have a high effector function, but limited proliferation capabilities [103, 104]. Prior to expansion, the majority of cells (76%) were either $T_{naïve}$ or T_{CM} (Figure 3.1 D), suggesting that many cells had potential to become activated and expand in response to stimulation with ZOL and IL-2. By Day 7, $T_{naïve}$ and T_{ERMA} cells had decreased to 11% of the total cells, and there was an enrichment of T_{CM} and T_{EM} cells (Figure 3.1 D). This suggests that by Day 7, Vγ9Vδ2 T cells were activated and would exhibit cytotoxic activity, while also retaining some proliferative capability.

To evaluate the expansion rate of Vγ9Vδ2 T cells, the number of viable T cells was counted during the expansion period and the fold change compared to Day 0 was calculated. Repeated observations showed that after three days of culture, there was a small decrease in total T cell numbers, followed by a rapid increase between Day 5 and 7, with maximum T cell numbers observed on Day 7 (Figure 3.1 E). The initial decrease in total T cell numbers is due to the death of other cell types for which the Vγ9Vδ2 T cell culture conditions are unsuitable. Following the death of other cells, Vγ9Vδ2 T cells then expand which is reflected by the rapid increase in total T cell numbers between Day 5 and 7. By Day 8, total T cell numbers had greatly decreased and plateaued until Day 11 (Figure 3.1 E). This decrease in total T cells accounts for the exhaustion and subsequent death of the Vγ9Vδ2 T cells.

While the maximum fold change of total T cell numbers showed variation between expansions, on average there was a 4.5-fold increase of T cells by Day 7 (Figure 3.1 E).

Figure 3.1 Expansion of Vγ9Vδ2 T cells from PBMC stimulated with ZOL and IL-2.

PBMC from normal donors were phenotyped immediately following isolation and after 7-8 days *ex vivo* culture with 5μM ZOL and 100IU/mL IL-2. Flow cytometric analysis was conducted to examine expression of **A.** Vγ9/CD3, **B.** NKG2D, **C.** CD16 and **D.** CD27/CD45RA to examine differentiation phenotype. For greater robustness, flow cytometric analysis was pooled from Day 7 and Day 8 expansions as these cells were phenotypically identical. Columns represent the mean of n=4-10, expressed as the percentage of cells from the lymphocyte or $V\gamma9^+/CD3^+$ population. Error bars indicate SD. **E.** Total T cell counts over the expansion culture period were normalised to Day 0 for that expansion and a fold change was calculated. The tabulated data shows the average fold-change increase and SD for fourteen independent expansion.

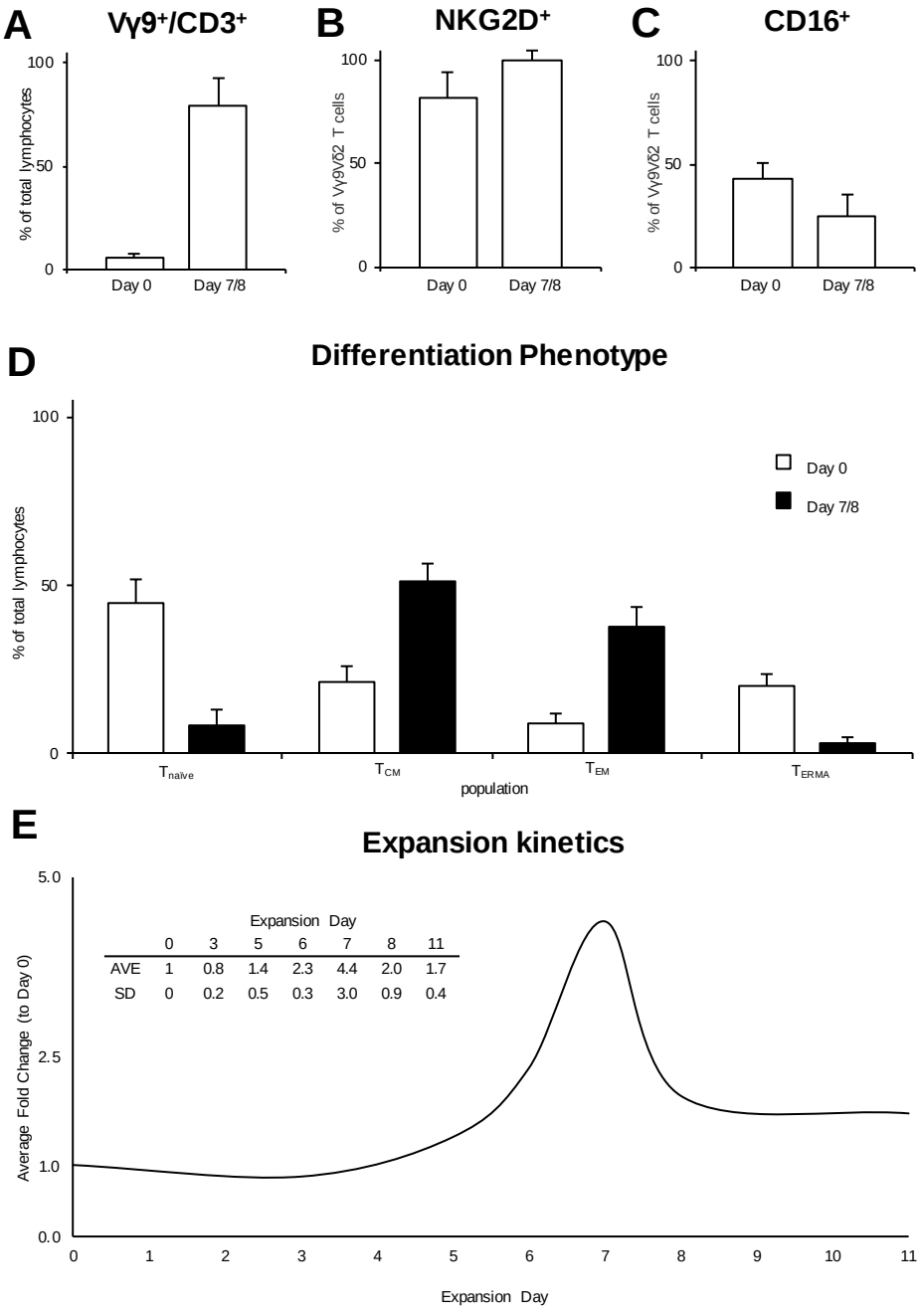
A
Vγ9+/CD3+
% of total lymphocytes
100
50
0
Day 0
Day 7/8
B
NKG2D+
% of Vγ9Vδ2 T cells
C
CD16+
D
Differentiation Phenotype
Day 0
Day 7/8
Tnaïve
TCM
TEM
TERMA
population
E
Expansion kinetics
Expansion Day
0 3 5 6 7 8 11
AVE 1 0.8 1.4 2.3 4.4 2.0 1.7
SD 0 0.2 0.5 0.3 3.0 0.9 0.4
Average Fold Change (to Day 0)
5.0
2.5
1.0
0.0
0 1 2 3 4 5 6 7 8 9 10 11
Expansion Day

3.2.2 ZOL sensitises cancer cells to Vγ9Vδ2 T cell cytotoxicity

It is well established that pre-treatment of cancer cells with ZOL enhances Vγ9Vδ2 T cell cytotoxicity against a wide variety of cancer cell lines [78, 81, 82, 135, 136]. MDA-MB231-TXSA osteolytic breast cancer cells expressing luciferase were pre-treated with 25μM ZOL overnight, followed by co-culture with various E:T (5:1, 10:1, 20:1) of Vγ9Vδ2 T cells (Figure 3.2). After 4 hours, luciferase activity was measured to determine cancer cell viability. Vγ9Vδ2 T cells alone had no effect on cancer cell viability when compared to untreated control (Figure 3.2 A). While ZOL treatment alone showed a small decrease in cancer cell viability, this was significantly enhanced in combination with Vγ9Vδ2 T cells, showing an E:T dependant decrease in viability, reaching a maximum of 45% viable cancer cells after 4 hours co-culture with Vγ9Vδ2 T cells (Figure 3.2 A). Interestingly, after 24 hours, Vγ9Vδ2 T cells alone did show an E:T dependant decrease in cancer cell viability (Figure 4.2). This suggests that 4 hours incubation with Vγ9Vδ2 T cells in not sufficient to completely kill cancer cells, but requires longer incubation periods.

To assess if Vγ9Vδ2 T cells begin apoptosis induction at earlier time points, caspase-3 activation and DAPI staining were assessed after 4 hours induction. Caspase-3 activation was measured in cancer cells that were pre-treated with or without 25μM ZOL overnight, followed by co-culture with Vγ9Vδ2 T cells at 5:1 E:T for 4 hours. ZOL pre-treatment alone did not induce caspase-3 activation compared to untreated (Figure 3.2 B). Caspase-3 activation was significantly increased following treatment with Vγ9Vδ2 T cells alone, and there was a further increase following ZOL pre-treatment in combination with Vγ9Vδ2 T cells (Figure 3.2 B). DAPI staining revealed no differences in cancer cell morphology between

untreated and ZOL pre-treated cells (Figure 3.2 C). Following 4 hours co-culture with Vγ9Vδ2 T cells, some Vγ9Vδ2 T cells were in contact with cancer cells which displayed evidence of apoptosis induction (Figure 3.2 C). Furthermore, cancer cells that were pre-treated with ZOL and Vγ9Vδ2 T cells showed nuclear fragmentation and chromosomes condensation which are typical hallmarks of apoptosis (Figure 3.2 C). Additionally, less cancer cells were observed in the combination treatment overall due to the detachment and loss of dead cancer cells during DAPI staining. This suggests that 4 hours co-culture with Vγ9Vδ2 T cells alone could initiate apoptosis in cancer cells, but this did not yet translate to a decrease in cancer cell viability, however at this time point, ZOL significantly sensitised cancer cells to killing by Vγ9Vδ2 T cells.

3.2.3 A single infusion of Vγ9Vδ2 T cells transiently inhibits tumour growth

Once it was established that ZOL sensitised MDA-MB231-TXSA osteolytic breast cancer cells to Vγ9Vδ2 T cell cytotoxicity *in vitro,* a pilot study was performed to assess this treatment regimen in a pre-clinical model of osteolytic breast cancer. Luciferase tagged MDA-MB231-TXSA osteolytic breast cancer cells were injected directly into the tibial marrow cavity of NOD/SCID mice (n=2-3/group) and treatments were commenced once tumours were established. In the pilot study, ZOL was injected subcutaneously at the conventional dose (ZOL-C) of 100µg/kg. ZOL was administered 24 hours prior to Vγ9Vδ2 T cell infusion in all the studies outlined in this thesis. As nBPs distribute to the skeleton within 24 hours, the rationale for this strategy was to allow ZOL localisation to the bone where it would be made available for uptake by cells in the tumour microenvironment to potentially enhance Vγ9Vδ2 T cell anti-cancer efficacy. Untreated and ZOL-C alone treated animals showed an exponential increase in bioluminescence over 21

Figure 3.2 ZOL sensitises cancer cells to killing by Vγ9Vδ2 T cells *in vitro*.

MDA-MB-231-TXSA were pre-treated with 25μM ZOL overnight at 37°C, then co-cultured with *ex vivo* expanded Vγ9Vδ2 T cells at the outlined E:T for 4 hours at 37°C. Cytotoxicity was measured as **A.** overall viability measured using a luciferase based assay, **B.** caspase-3 activation and **C.** DAPI staining. Arrows indicate Vγ9Vδ2 T cells, arrow heads indicate apoptotic cancer cells. Columns, mean; bars, ±SEM of n=3. *$p<0.05$, **$p<0.01$).

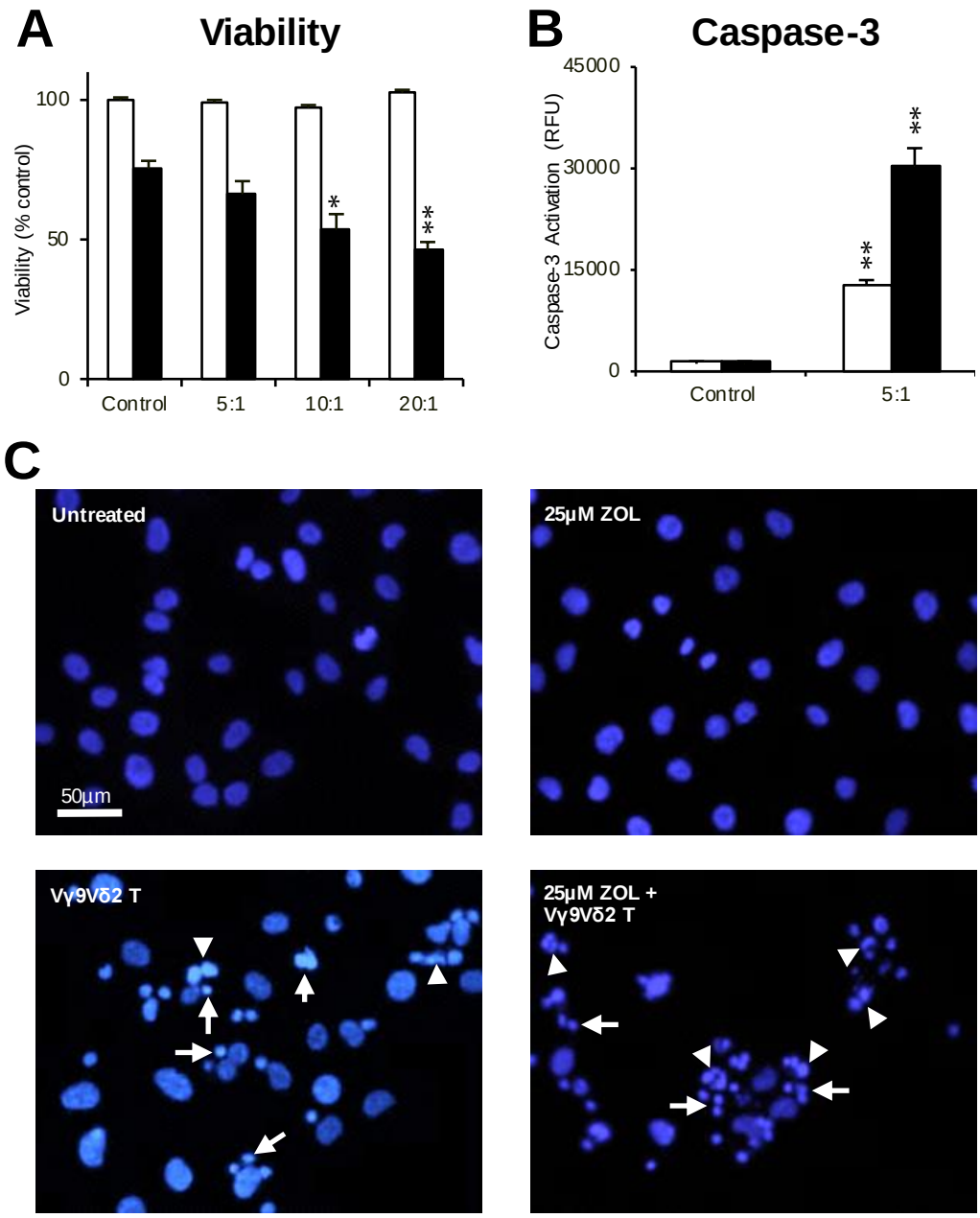
A
Viability
Viability (% control)
100
50
0
Control
5:1
10:1
20:1
*
**
B
Caspase-3
Caspase-3 Activation (RFU)
45000
30000
15000
0
Control
5:1
**
**
C
Untreated
50µm
25µM ZOL
Vγ9Vδ2 T
25µM ZOL +
Vγ9Vδ2 T

Figure 3.3 A single administration of Vγ9Vδ2 T cells shows a trend to transiently inhibit cancer growth.

Luciferase expressing MDA-MB231-TXSA osteolytic breast cancer cells were injected directly into the tibia of 5-week old female NOD/SCID mice. Tumours grew for 12 days, then animals were assigned into four treatment groups. Animals remained untreated (n=2) or were given ZOL-C (100µg/kg s.c) (n=2), $5x10^6$ Vγ9Vδ2 T cells i.v (n=3), or the combination of ZOL-C and Vγ9Vδ2 T cells (same dose as the monotherapy, n=3). ZOL treatment was given on Day 13 and Vγ9Vδ2 T cells supplement with 10IU rhIL-2 were infused 24 hours later. Whole body bioluminescence images were acquired on the IVIS Spectrum *in vivo* imaging system and bioluminescence signal was quantified as Total Radiant Efficiency [p/s]/[µW/cm²]. Images and graphs are shown for one animal per group.

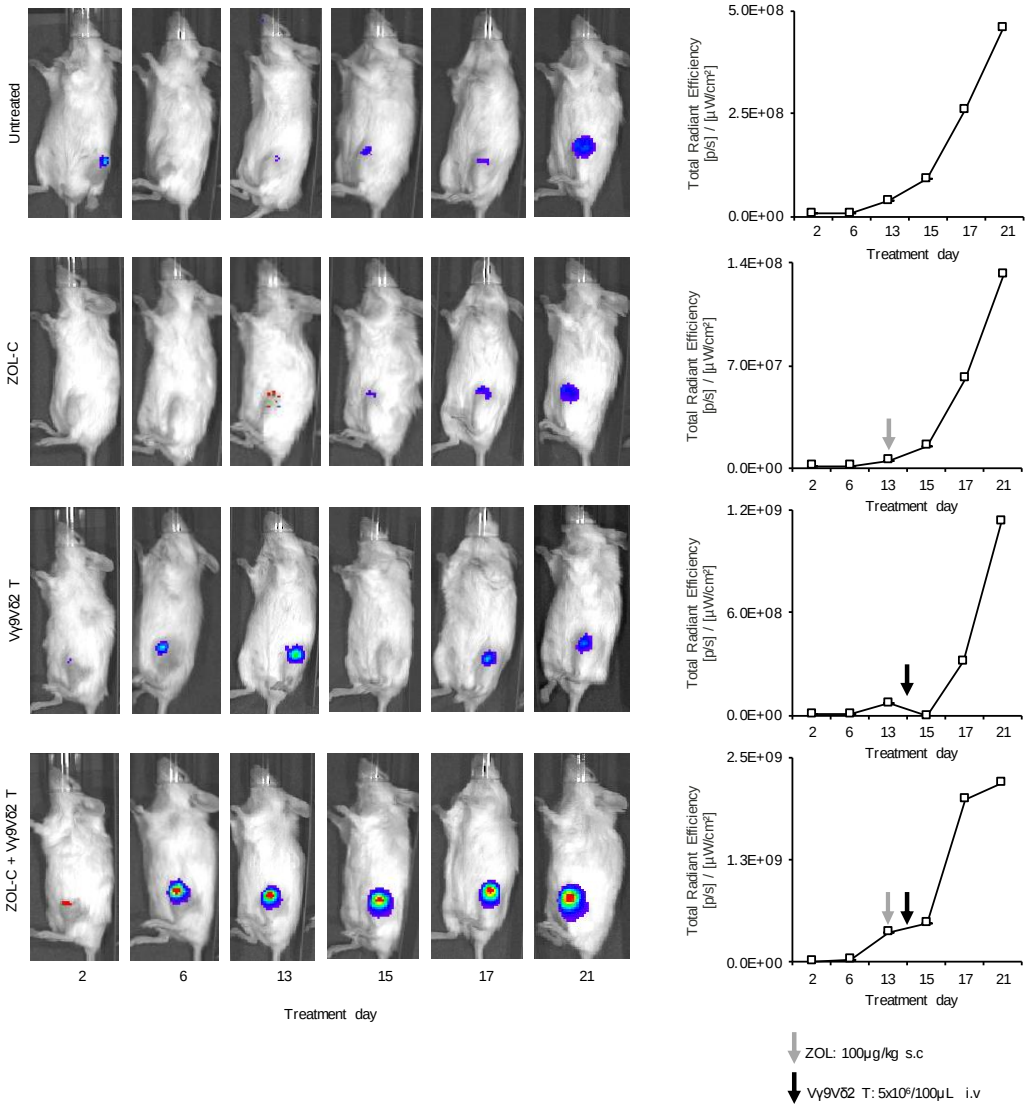
Untreated
ZOL-C
Vγ9Vδ2 T
ZOL-C + Vγ9Vδ2 T
2
6
13
15
17
21
Treatment day
Total Radiant Efficiency [p/s] / [µW/cm²]
5.0E+08
2.5E+08
0.0E+00
1.4E+08
7.0E+07
1.2E+09
6.0E+08
2.5E+09
1.3E+09
ZOL: 100µg/kg s.c
Vγ9Vδ2 T: 5x10⁶/100µL i.v

days (Figure 3.3). In contrast, a single infusion of Vγ9Vδ2 T cells on Day 14 resulted in a small decrease in tumour bioluminescence the following day (Figure 3.3). ZOL-C in combination with Vγ9Vδ2 T also showed a slowing of tumour growth evidenced by the bioluminescence signal on Day 15 (Figure 3.3). However, any effect Vγ9Vδ2 T cells had on tumour growth was only transient and tumour bioluminescence increased thereafter, showing no difference compared to untreated control. This transient effect seen after a single infusion of Vγ9Vδ2 T cells has been previously observed [161], and it has been established that multiple administrations of Vγ9Vδ2 T cells alone or in combination with nBPs are required for sustained anti-cancer efficacy [76, 77, 162].

3.2.4 Metronomic ZOL dosing does not potentiate the anti-cancer efficacy of Vγ9Vδ2 T cells

As sustained tumour inhibition was not observed in the pilot study, a larger study was conducted to assess the anti-cancer efficacy of multiple administrations of Vγ9Vδ2 T cells and when ZOL is administered at metronomic doses. As ZOL was administered more frequently, a lower dose was used (metronomic dosing, ZOL-M), which has been shown previously by our laboratory to reduce tumour burden in nude mice [163]. NOD/SCID mice in this case were inoculated with luciferase tagged MDA-MB231-TXSA osteolytic breast cancer cells and treatments were commenced once tumours were established (n=6-8/group). In this study, animals treated with ZOL-M alone had no effect on tumour burden and tumour bioluminescence increased over the duration of the study similarly to what was seen in the untreated controls (Figure 3.4). Animals treated with multiple infusions of Vγ9Vδ2 T cells showed a trend towards lower tumour bioluminescence at Day 21 and 25 (Figure 3.4). Multiple administrations of ZOL-M followed by Vγ9Vδ2 T

Figure 3.4 Multiple infusions of Vγ9Vδ2 T cells inhibit cancer growth in the tibia.

Luciferase expressing MDA-MB231-TXSA osteolytic breast cancer cells were injected directly into the tibia of 5-week old female NOD/SCID mice. Tumours grew for 8 days, then animals were assigned into four treatment groups. Animals remained untreated (n=6), or were given 25µg/kg (treatment 1) or 50µg/kg (treatment 2 and 3) ZOL-M s.c (n=8), $5x10^6$ Vγ9Vδ2 T cells i.v (n=8), or the combination of ZOL-M and Vγ9Vδ2 T cells (same dose as the monotherapy, n=7). ZOL was administered on Days 8, 14, and 20, and Vγ9Vδ2 T cells were infused 24 hours following each ZOL administration. Whole body bioluminescence images were acquired on the IVIS Spectrum *in vivo* imaging system and bioluminescence signal was quantified as Total Radiant Efficiency [p/s]/[µW/cm²]. A representative bioluminescence image of one animal is shown per group, and lines represent mean bioluminescence and bars indicate ±SEM.

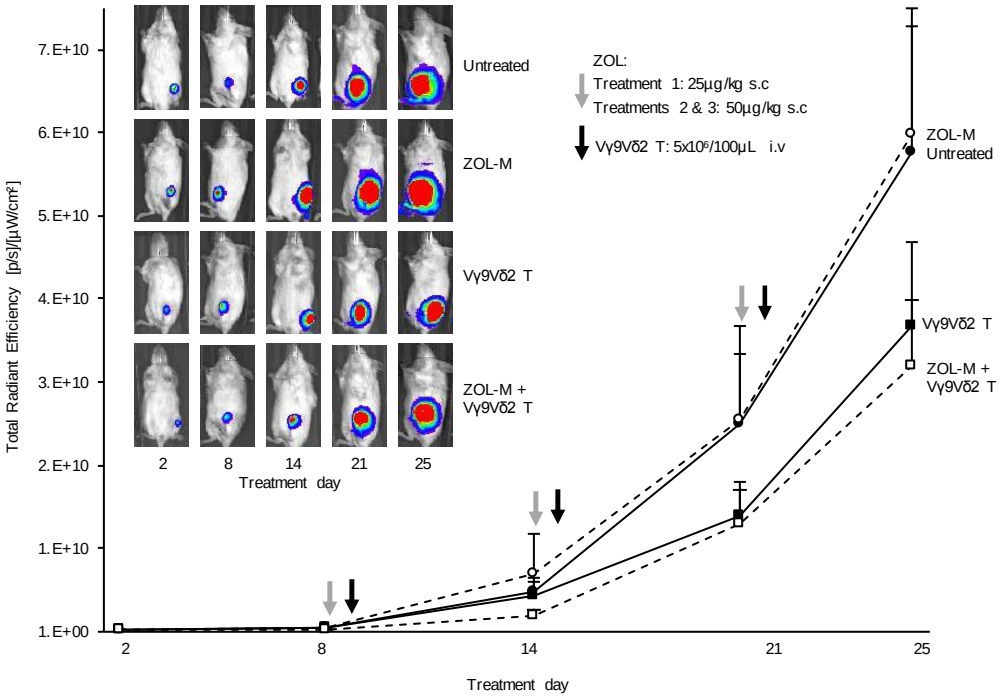
Untreated
ZOL-M
Vγ9Vδ2 T
ZOL-M +
Vγ9Vδ2 T
2
8
14
21
25
Treatment day
ZOL:
Treatment 1: 25µg/kg s.c
Treatments 2 & 3: 50µg/kg s.c
Vγ9Vδ2 T: 5x10⁶/100µL i.v
ZOL-M
Untreated
Vγ9Vδ2 T
ZOL-M +
Vγ9Vδ2 T
Total Radiant Efficiency [p/s]/[µW/cm²]
7.E+10
6.E+10
5.E+10
4.E+10
3.E+10
2.E+10
1.E+10
1.E+00
2
8
14
21
25
Treatment day

cells also showed a trend to towards lower bioluminescence at Day 21 and 25, following the same trend as that seen with Vγ9Vδ2 T cells alone (Figure 3.4), however these treatments did not reach statistical significance due to a large amount of variability between the groups.

3.2.5 ZOL-M shows a trend towards decreasing cancer induced osteolysis

MDA-MB231-TXSA breast cancer cells inoculated directly into the tibia are highly osteolytic [63, 146]. In the literature, it is well established that ZOL inhibits osteoclast activity resulting in reduced bone resorption and an increase in bone volume, however the effect Vγ9Vδ2 T cells have on bone is still unknown. After the study, tibias were surgically resected and bone morphometric parameters were assessed using μCT. Values were expressed as the bone loss percentage, measuring the percentage difference in bone volume between the tumour bearing and non-tumour bearing tibias (Figure 3.5). Animals treated with ZOL-M showed a trend towards smaller bone loss percentage compared to untreated animals (-8% compared to -21%). Vγ9Vδ2 T cells also showed a trend in more bone loss compared to untreated animals, however this difference was small (-25% in Vγ9Vδ2 T cell treated animals compared to -21% in untreated animals). A trend towards less bone loss was also observed in animals treated with ZOL-M + Vγ9Vδ2 T cells compared to untreated (-11% compared to -21%), however it did not differ from treatment with ZOL-M alone (-11% compared to -8%). Trabecular bone loss showed an identical trend. Compared to untreated, which showed -96% trabecular bone loss, ZOL-M alone decreased trabecular bone loss to -67%, while Vγ9Vδ2 T cells alone showed no effect (-93%). Once again, ZOL-M + Vγ9Vδ2 T cells had less trabecular bone loss compared to untreated (-67% compared to -96%), however there was no difference between the combination treatment and ZOL-M alone

Figure 3.5 ZOL-M alone shows a trend towards decreased tumour-associated bone loss.

At the time of sacrifice, the tumour and non-tumour bearing tibias from each mouse were removed and *ex vivo* μCT analysis was performed. **A.** Total bone volume and **B.** trabecular bone volume were measured and the difference between in volume between the tumour bearing and non-tumour was calculated and expressed as percentage bone loss for each treatment group.

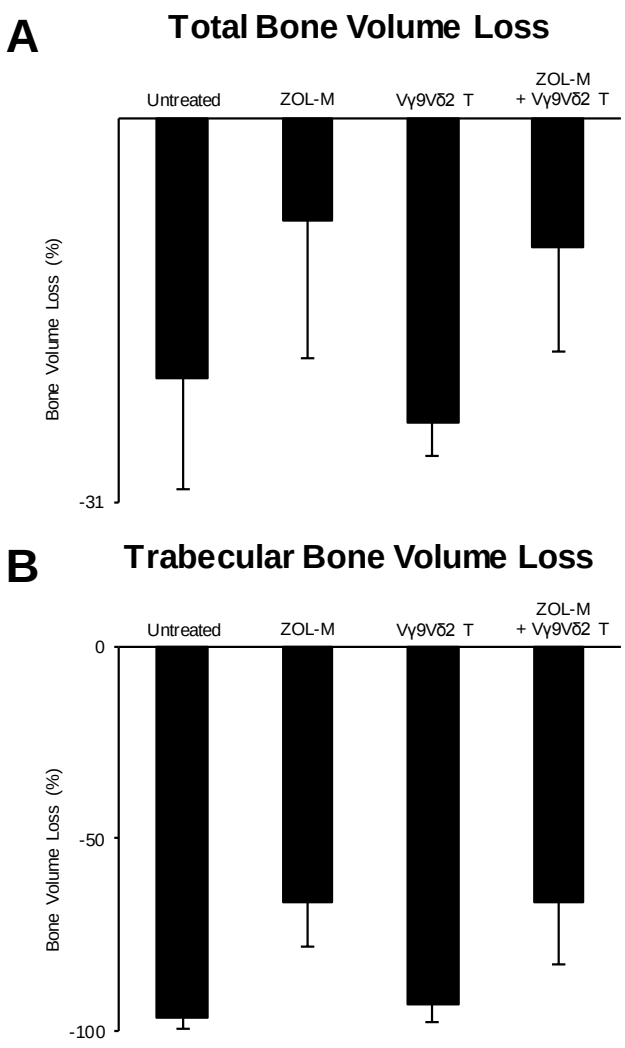
A
Total Bone Volume Loss
Untreated
ZOL-M
Vγ9Vδ2 T
ZOL-M
+ Vγ9Vδ2 T
Bone Volume Loss (%)
-31
B
Trabecular Bone Volume Loss
Untreated
ZOL-M
Vγ9Vδ2 T
ZOL-M
+ Vγ9Vδ2 T
Bone Volume Loss (%)
0
-50
-100

(-67% compared to -67%). None of the differences observed were statistically significant, however a clear trend showed that compared to untreated animals, ZOL-M alone reduce bone loss, while Vγ9Vδ2 T cells had no effect.

3.3 Discussion

In accordance with previous studies, ZOL and IL-2 expanded and activated Vγ9Vδ2 T cells from PBMC, resulting in mostly T_{CM} and T_{EM} Vγ9Vδ2 T cells, which have proliferative capacity and cytotoxic properties respectively [104]. Longer expansions are reported to produce more cytotoxic T_{EM} Vγ9Vδ2 T cells [83], which have been the predominate Vγ9Vδ2 T cells transferred into patients with advanced cancers in a previous early phase clinical trial [105]. However, one of the current obstacles limiting Vγ9Vδ2 T cell therapy in pre-clinical studies is the lack of sustained Vγ9Vδ2 T cell viability which is correlated with a deterioration in health [122-124]. Therefore, this study adoptively transferred a combination of T_{CM} and T_{EM} Vγ9Vδ2 T cells with IL-2 to potentially produce a more sustained anti-cancer efficacy *in vivo*.

This study confirmed that *ex vivo* expanded Vγ9Vδ2 T cells alone were cytotoxic towards breast cancer cells *in vitro,* and cytotoxicity increased following ZOL pre-treatment. This study also showed that a single infusion of Vγ9Vδ2 T cells was not sufficient to inhibit cancer growth and multiple infusions were required for greater efficacy [161]. However, in contrast to previous studies [77, 78], ZOL did not potentiate the anti-cancer efficacy of Vγ9Vδ2 T cells *in vivo.* The lack of ZOL enhancing Vγ9Vδ2 T cell efficacy in this current study may be because the other studies transferred more Vγ9Vδ2 T cells or administrated a higher nBP dose compared to the ZOL-M dosing schedule used in this study [77, 78]. These differences were taken into consideration and the number of Vγ9Vδ2 T cells and

ZOL dose was optimised and increased in the subsequent pre-clinical studies performed in this thesis (Chapter 4 and 5).

Cancer-associated osteolysis contributes to the morbidity of breast cancer bone metastases, hence this study examined the effect each treatment regimen had on bone loss. ZOL alone and in combination with Vγ9Vδ2 T cells showed decreased bone loss, however as the combination showed no additive effect, this increase in bone volume is due to ZOL treatment alone, with Vγ9Vδ2 T cells having no effect on bone. Vγ9Vδ2 T cells alone also had no effect on bone, which was unexpected since previous *in vitro* studies have shown that they can inhibit osteoclast formation [148] and are cytotoxic towards osteoclasts when co-cultured with cancer cells [80]. Additionally, following stimulation with IL-15 and TGF-β, which would be released from the bone matrix during bone degradation, human γδ T cells can produce osteoblast growth factors such as IGF, FGF [149], and CTGF [150]. Overall this suggests that Vγ9Vδ2 T cells have the potential to both inhibit osteoclasts and stimulate osteoblasts, resulting in a net gain in bone volume. No increase in bone volume was observed in this study, potentially due to a lack of supplementation with additional factors, or due to insufficient Vγ9Vδ2 T cells localising to the tumour microenvironment. Therefore, further studies are required to examine the sensitivity of osteoclasts and osteoblasts to Vγ9Vδ2 T cell cytotoxicity, both *in vitro* and *in vivo*.

In conclusion, multiple infusions of Vγ9Vδ2 T cells are required for sustained anti-cancer efficacy, and while ZOL does not exhibit anti-cancer efficacy alone, it protects the bone from cancer-induced osteolysis. Although administration of ZOL and Vγ9Vδ2 T cells requires further optimisation, this treatment regimen shows potential as novel immunotherapy for the treatment of breast cancer bone metastases.

Chapter 4

Adoptive transfer of *ex vivo* expanded Vγ9Vδ2 T cells in combination with zoledronic acid inhibits cancer growth and limits osteolysis in a murine model of osteolytic breast cancer

4.1 Chapter Introduction

In Chapter 3 it was established that neither a single infusion of Vγ9Vδ2 T cells in combination with ZOL nor multiple administrations of Vγ9Vδ2 T cells in combination with metronomic ZOL dosing could significantly decrease tumour burden in a model of osteolytic breast cancer. The following manuscript depicts the experimental results of multiple infusions of Vγ9Vδ2 T cells in combination with a conventional ZOL dose in the same animal model. To provide sufficient *in vitro* justification for the *in vivo* studies conducted for the manuscript, Figure 3.2 from the previous chapter was expanded upon, adapted, and used in the manuscript.

4.2 Statement of Authorship

Title of Paper	Adoptive transfer of ex vivo expanded Vγ9Vδ2 T cells in combination with zoledronic acid inhibits cancer growth and limits osteolysis in a murine model of osteolytic breast cancer
Publication Status	Published
Publication Details	A. Zysk, M.O. DeNichilo, V. Panagopoulos, I. Zinonos, V. Liapis, S. Hay, W. Ingman, V. Ponomarev, G. Atkins, D. Findlay, A. Zannettino, A. Evdokiou, Adoptive transfer of *ex vivo* expanded Vgamma9Vdelta2 T cells in combination with zoledronic acid inhibits cancer growth and limits osteolysis in a murine model of osteolytic breast cancer, Cancer Lett., 386 (2017) 141-150

Principal Author

Name of Principal Author (Candidate)	Aneta Zysk		
Contribution to the Paper	Performed all *in vitro* and *in vivo* experiments, analysed and interpreted all data, created figures and composed manuscript.		
Overall percentage (%)	90%		
Certification	This paper reports on original research I conducted during the period of my Higher Degree by Research candidature and is not subject to any obligations or contractual agreements with a third party that would constrain its inclusion in this thesis. I am the primary author of this paper.		
Signature		Date	14/03/2017

Co-Author Contributions

By signing the Statement of Authorship, each author certifies that:

i. the candidate's stated contribution to the publication is accurate (as detailed above);

ii. permission is granted for the candidate in include the publication in the thesis; and

iii. the sum of all co-author contributions is equal to 100% less the candidate's stated contribution.

Name of Co-Author	Mark O DeNichilo		
Contribution to the Paper	Co-supervisor, assisted with in vitro work, data interpretation, and manuscript evaluation.		
Signature		Date	27/2/17

Name of Co-Author	Vasilios Panagopoulos		
Contribution to the Pape	Assisted with *in vitro* work, animal ethics, and study design.		
Signature		Date	27/02/2017

Name of Co-Author	Irene Zinonos		
Contribution to the Paper	Assisted with animal handling, tissue collections, and micro-CT analysis.		
Signature		Date	01/03/2017

Name of Co-Author	Vasilios Liapis		
Contribution to the Paper	Assisted with *in vitro* experiments, animal handling and tissue collection.		
Signature		Date	27th Feb 2017

Name of Co-Author	Shelley Hay		
Contribution to the Paper	Assisted with *in vitro* experiments, animal handling, tissue collection, and histology.		
Signature		Date	27/2/17

Name of Co-Author	Wendy Ingman		
Contribution to the Paper	Assisted with data interpretation and manuscript evaluation.		
Signature		Date	28/2/2017

Name of Co-Author	Vladimir Ponomarev		
Contribution to the Paper	Provided triple reporter gene construct (SFG-NES-TGL) and assisted with manuscript evaluation		
Signature		Date	2/28/2017

Name of Co-Author	Gerald J. Atkins		
Contribution to the Paper	Assisted with data interpretation and manuscript evaluation.		
Signature		Date	26/02/2017

Name of Co-Author	David M. Findlay		
Contribution to the Paper	Assisted with data interpretation and manuscript evaluation.		
Signature		Date	26/02/2017

Name of Co-Author	Andrew C. Zannettino		
Contribution to the Paper	Assisted with data interpretation and manuscript evaluation.		
Signature		Date	25 February 2017

Name of Co-Author	Andreas Evdokiou		
Contribution to the Paper	Principal supervisor, assisted with data interpretation, and manuscript evaluation.		
Signature		Date	03/03/2017

Adoptive transfer of *ex vivo* expanded Vγ9Vδ2 T cells in combination with zoledronic acid inhibits cancer growth and limits osteolysis in a murine model of osteolytic breast cancer

Aneta Zysk[1], Mark O. DeNichilo[1], Vasilios Panagopoulos[1], Irene Zinonos[1], Vasilios Liapis[1], Shelley Hay[1], Wendy Ingman[2], Vladimir Ponomarev[3], Gerald J. Atkins[4], David M. Findlay[4], Andrew C. Zannettino[5], Andreas Evdokiou[1]

[1]Discipline of Surgery, Breast Cancer Research Unit, Basil Hetzel Institute, University of Adelaide, Adelaide, South Australia, Australia

[2]Discipline of Surgery, Breast Biology Cancer Unit, Basil Hetzel Institute, University of Adelaide, Adelaide, South Australia, Australia

[3]Department of Radiology, Memorial Sloan-Kettering Cancer Centre, New York, USA

[4]Discipline of Orthopaedics and Trauma, University of Adelaide, Adelaide, South Australia, Australia

[5]School of Medical Sciences, Myeloma Research Laboratory Cancer Theme, South Australian Health and Medical Research Institute (SAHMRI), Faculty of Health Science, University of Adelaide, Australia

Current Address of Mark O. DeNichilo: Vascular Biology and Cell Trafficking Laboratory, Centre for Cancer Biology, University of South Australia, Adelaide, South Australia, Australia

Correspondence to:

Professor Andreas Evdokiou,

Breast Cancer Research Unit

Level 1, Basil Hetzel Institute

Queen Elizabeth Hospital

28 Woodville Road, Woodville

South Australia, AUSTRALIA

Fax: 618 8222 7451

E-mail: andreas.evdokiou@adelaide.edu.au

This work was supported by funds from the National Breast Cancer Foundation (NBCF-13-09) and the research fellowships granted to A. Evdokiou by The Hospital Research Foundation (THRF) and Australian Breast Cancer Research (ABCR).

The authors would like to thank Ms Ruth Williams and Dr. Agatha Labrinidis from Adelaide Microscopy at The University of Adelaide for technical assistance with the SkyScan 1076 and related software.

The authors declare no potential conflicts of interest.

Total pages: 10

Total words including references: 7,985

Total figures: 6

Cancer Letters, Impact Factor 5.6

Accepted 8th November 2016

Cancer Letters 386 (2017) 141–150

Contents lists available at ScienceDirect

Cancer Letters

journal homepage: www.elsevier.com/locate/canlet

Original Article

Adoptive transfer of *ex vivo* expanded Vγ9Vδ2 T cells in combination with zoledronic acid inhibits cancer growth and limits osteolysis in a murine model of osteolytic breast cancer

Aneta Zysk [a], Mark O. DeNichilo [a], Vasilios Panagopoulos [a], Irene Zinonos [a], Vasilios Liapis [a], Shelley Hay [a], Wendy Ingman [b], Vladimir Ponomarev [c], Gerald Atkins [d], David Findlay [d], Andrew Zannettino [e], Andreas Evdokiou [a, *]

[a] Discipline of Surgery, Breast Cancer Research Unit, Basil Hetzel Institute, University of Adelaide, Adelaide, South Australia, Australia
[b] Discipline of Surgery, Breast Biology Cancer Unit, Basil Hetzel Institute, University of Adelaide, Adelaide, South Australia, Australia
[c] Department of Radiology, Memorial Sloan-Kettering Cancer Centre, New York, USA
[d] Discipline of Orthopaedics and Trauma, University of Adelaide, Adelaide, South Australia, Australia
[e] School of Medical Sciences, Myeloma Research Laboratory Cancer Theme, South Australian Health and Medical Research Institute (SAHMRI), Faculty of Health Science, University of Adelaide, Australia

ARTICLE INFO

Article history:
Received 6 September 2016
Received in revised form
7 November 2016
Accepted 8 November 2016

Keywords:
Metastasis
Immunotherapy
Bisphosphonate
Osteoclast
Tumour associated macrophage

ABSTRACT

Bone metastases occur in over 75% of patients with advanced breast cancer and are responsible for high levels of morbidity and mortality. In this study, *ex vivo* expanded cytotoxic Vγ9Vδ2 T cells isolated from human peripheral blood were tested for their anti-cancer efficacy in combination with zoledronic acid (ZOL), using a mouse model of osteolytic breast cancer. *In vitro*, expanded Vγ9Vδ2 T cells were cytotoxic against a panel of human breast cancer cell lines, and ZOL pre-treatment further sensitised breast cancer cells to killing by Vγ9Vδ2 T cells. Vγ9Vδ2 T cells adoptively transferred into NOD/SCID mice localised to osteolytic breast cancer lesions in the bone, and multiple infusions of Vγ9Vδ2 T cells reduced tumour growth in the bone. ZOL pre-treatment potentiated the anti-cancer efficacy of Vγ9Vδ2 T cells, with mice showing further reductions in tumour burden. Mice treated with the combination also had reduced tumour burden of secondary pulmonary metastases, and decreased bone degradation. Our data suggests that adoptive transfer of Vγ9Vδ2 T cell in combination with ZOL may prove an effective immunotherapeutic approach for the treatment of breast cancer bone metastases.

Introduction

Breast cancer is one of the most commonly diagnosed cancers in women worldwide. Patients diagnosed with primary breast cancer have higher survival rates compared to those diagnosed with the advanced disease, primarily due to cancer metastases [1]. Bone metastases occur in over 75% of patients with advanced breast cancer, resulting in extensive bone degradation leading to skeletal-related events (SREs) such as hypercalcemia, chronic pain, fracture, spinal cord compression, and impaired mobility, all which greatly affect quality of life [2,3]. Breast cancer bone metastases are predominately osteolytic due to factors secreted by disseminated tumour cells that stimulate osteoclasts [4]. Activated osteoclasts degrade bone and release growth factors from the matrix that further promote tumour growth and bone destruction, perpetuating the 'vicious cycle' of cancer growth and bone destruction [5]. Nitrogen-containing bisphosphonates (nBPs), a class of anti-resorptive drugs, are currently used to inhibit osteoclast-mediated bone degradation in patients with skeletal malignancies, including advanced breast cancer, however, this treatment is only palliative and new therapeutic approaches are required [6,7].

Within the past decade, immunotherapy of cytotoxic gamma delta (γδ) T cells has been gaining momentum as a potential therapeutic approach for targeting cancer. Human γδ T cells comprise a small population (1–10%) of circulating peripheral blood

* Corresponding author. Breast Cancer Research Unit, Level 1, Basil Hetzel Institute, Queen Elizabeth Hospital, 28 Woodville Road, Woodville, South Australia, Australia. Fax: +61 8 8222 7451.
E-mail address: andreas.evdokiou@adelaide.edu.au (A. Evdokiou).

http://dx.doi.org/10.1016/j.canlet.2016.11.013
0304-3835/

lymphocytes [8]. These primarily consist of the Vδ2 chain in combination with Vγ9 (Vγ9Vδ2) which are stimulated and expanded in response of phosphoantigens (PAgs).

Activated Vγ9Vδ2 T cells have the ability to recognise target cells in an MHC-unrestricted manner [9] via detection of PAgs, including isopentenyl pyrophosphate (IPP), an intermediate of the mammalian mevalonate pathway. nBPs, including zoledronic acid (ZOL) inhibit the mevalonate pathway resulting in IPP accumulation which activate and expand Vγ9Vδ2 T cells [10–16].

Due to abnormal upregulation of the mevalonate pathway, tumour cells accumulate PAgs resulting in recognition by Vγ9Vδ2 T cells [17]. Activated Vγ9Vδ2 T cells can then kill cancer cells by releasing Th1 cytokines, including TNF-α (tumour necrosis factor-alpha) and IFN-γ (interferon-gamma) [18–20] and cytolytic granules [10,19–21]. Vγ9Vδ2 T cells also induce target cell death by death receptor/ligand interactions with TRAIL (Apo2L) [21], and FASL (Fas ligand) [11]. As a result, expanded Vγ9Vδ2 T cells exert potent cytotoxicity against a variety of solid and haematological malignancies, *in vitro* and *in vivo* [10–12,15,22,23].

Vγ9Vδ2 T cell immunotherapy has been assessed against a variety of solid and haematological malignancies in early phase clinical trials (reviewed in Ref. [24]). While these trials have deemed Vγ9Vδ2 T cell therapy safe, as a monotherapy the anti-cancer efficacy, especially against advanced tumours has been underwhelming and requires further improvement. In addition to activating Vγ9Vδ2 T cells, ZOL can also sensitise cancer cells to killing by Vγ9Vδ2 T cells both *in vitro* and *in vivo* [13–15,21,25]. Additionally, clinical evidence demonstrates the potential of using Vγ9Vδ2 T cell adoptive transfer in combination with ZOL for the treatment of advanced renal cell carcinoma (RCC), malignant ascites from gastric cancer, and other metastatic tumours [26–28].

As ZOL preferentially localises to the bone, an elegant approach for targeting cancer lesions in the bone has emerged. Discussion in the literature have suggested that nBP administration followed by adoptive transfer of Vγ9Vδ2 T cells would be an ideal two-pronged approach for targeting cancers in the bone [29]. This immunotherapy would allow simultaneous reduction of tumour-associated bone loss in addition to sensitising cancer cells to Vγ9Vδ2 T cell mediated cytotoxicity, inhibiting the vicious cycle of bone destruction and cancer growth. To date, adoptive transfer of Vγ9Vδ2 T cells alone or in combination with ZOL to specifically target cancers in the bone has not been fully investigated. In this study, we used a murine model of osteolytic breast cancer, where breast cancer cells were implanted directly into the tibia in NOD/SCID mice. We showed for the first time, that Vγ9Vδ2 T cells localised to osteolytic breast cancer lesions growing in the bone and that multiple infusions of Vγ9Vδ2 T cells slowed tumour growth. We also showed that ZOL potentiated the anti-cancer efficacy of Vγ9Vδ2 T cells, decreased tumour burden in the bone, inhibited tumour-associated osteolysis, and decreased lung metastases tumour burden.

Materials and methods

Cells and reagents

ZR75 and T47D human breast cancer cell lines were obtained from American Type Culture Collection. The MDA-MB231 human breast cancer derivative cell line MDA-MB231-TXSA was kindly provided by Dr. Toshiyuki Yoneda (University of Texas Health Science Centre, San Antonio, Texas). MDA-MB231-TXSA expressed GFP and luciferase produced by retroviral expression of the SFG-NES-TGL vector, as previously described [30]. All cell lines were cultured in DMEM (Life Technologies, Australia) supplemented with 10% foetal bovine serum (FBS, Life Technologies, Australia), 100 IU/mL penicillin (Life Technologies, Australia), 100 μg/mL streptomycin (Life Technologies, Australia), and 25 mM HEPES (Life Technologies, Australia) at 37 °C in a 5% CO_2 humidified atmosphere. ZOL was generously provided by Novartis Pharma AG.

Ex vivo expansion of Vγ9Vδ2 T cells

Informed consent was obtained prior to collection of peripheral blood from healthy adult donors. PBMC were isolated immediately via density gradient centrifugation using Lymphoprep™ (Axis Shield, Norway) following manufacturer's instructions. PBMCs were resuspended to 1×10^6/mL in CTS™ OpTmizer™ T Cell Expansion SFM (Life Technologies, Australia) supplemented with OpTmizer™ T cell Expansion Supplement (1:38 dilution) (Life Technologies, Australia), 10% heat-inactivated FBS (HI-FBS), 100 IU/mL penicillin, 100 μg/mL streptomycin, 2 mmol L-glutamine (Life Technologies, Australia), 25 mM HEPES, 0.1% β-mercaptoethanol (Sigma–Aldrich, USA), 100 IU/mL recombinant human interleukin 2 (rhIL-2) (BD Pharmingen, USA) and activated with 5 μM ZOL, and seeded into 6-well plates. Cell culture density was maintained at $1–2 \times 10^6$ cells/mL and replenished with fresh medium containing 100 IU/mL rhIL-2 only (without ZOL) every 2–3 days. Following 7–8 days of culture cells were collected and enriched as described below.

Enrichment of Vγ9Vδ2 T cells

Ex vivo expanded Vγ9Vδ2 T cells were enriched prior to *in vitro* and *in vivo* experiments using negative selection MACS with the TCR γ/δ+ T cell Isolation Kit (human) (Miltenyi Biotec, Germany). Cell viability and total cells numbers after enrichment were assessed using trypan blue exclusion. Percentage of Vγ9Vδ2 T cells were determined by flow cytometry using PeCy5 conjugated anti-CD3 (clone UCHT1) (eBioscience, San Diego, CA, USA) and FITC conjugated anti-Vγ9 TCR from BD Biosciences (San Jose, CA, USA). Analysis was performed on the BD FACSCanto II Flow Cytometer (San Jose, CA, USA). Percentages of Vγ9Vδ2 T cells were identified by gating on the lymphocyte population using forward scatter/side scatter then on $Vγ9^+$ $CD3^+$ double positive cells. After enrichment, Vγ9Vδ2 T cell viability was >95%, and the percentage of Vγ9Vδ2 T cells was consistently >97%.

Cell cytotoxicity assay

Cytotoxicity of Vγ9Vδ2 T cells against breast cancer cell lines was assessed using a standard lactate dehydrogenase (LDH) release assay (CytoTox 96® Non-Radioactive Cytotoxicity Assay; Promega, USA). Briefly, 1×10^4 target cells were seeded in triplicate in a 96-well microtiter plate and allowed to adhere overnight. Target cells were then treated with or without 25 μM ZOL for 24 h, and then co-cultured with Vγ9Vδ2 T cells at 1:1, 5:1 and 10:1 effector:target (E:T) ratio, with Vγ9Vδ2 T cells as the effector, and cancer cells as the target. After incubation for 9 h at 37 °C, 50 μL of supernatant was assayed for LDH activity following the manufactures protocol. The appropriate controls were prepared and cytotoxicity was calculated as:

$$\%\,Cytotoxicity = \frac{experimental\ release - effector\ spontaneous\ release - target\ spontaneous\ release}{targetmaximumrelease - targetspontaneousrelease} \times 100$$

Cell viability assay

MDA-MB231-TXSA cells expressed luciferase, which was the basis for a luciferase activity viability assay using Dual Luciferase® Reporter Assay kit (Promega, Madison, WI, USA). Briefly, 1×10^4 luciferase-tagged target cells were seeded in triplicate in a 96-well microtiter plate and allowed to adhere overnight. Cells were then treated with or without 25 μM ZOL for 24 h, and then co-cultured with Vγ9Vδ2 T cells at 1:1, 5:1 and 10:1 E:T ratios. After 24 h incubation, media was removed and cells were washed in PBS, then lysates were prepared and analysed following the manufacturers protocol. Viability was calculated as:

$$\%\,Viability = \frac{experimental\ value}{untreated\ control\ value} \times 100$$

Measurement of DEVD-caspase activity

DEVD-caspase activity was assayed by cleavage of zDEVD-AFC (z-asp-glu-val-asp-7-amino-4-trifluoro-methyl-coumarin), a fluorogenic substrate based on the peptide sequence at the caspase-3 cleavage site of poly (ADP-ribose) polymerases

(Kamiya Biomedical Company, Seattle, WA, USA). Breast cancer cells were seeded at 1×10^4 cells/well in triplicate a 96-well microtiter plate and allowed to adhere overnight. Cells were then treated with or without 25 μM ZOL for 18 h, then co-cultured with Vγ9Vδ2 T cells at a 5:1 E:T ratio for 2 h. Caspase activation was detected using DEVD-AFC, as previously described in [31].

Western immunoblotting

Detection of unprenylated small GTPases, including RAP1, were used to indirectly determine the extent of FPPS inhibition by ZOL, which correlates with increased IPP levels, resulting in the increased detection of cancer cells by Vγ9Vδ2 T cells and greater cytotoxicity. To determine the effect of ZOL on the prenylation of small GTPases in the breast cancer cells, lysates were analysed by Western immunoblotting for total and unprenylated RAP1. Briefly, 1×10^6 breast cancer cells were seeded in a 25-cm^2 flask, allowed to adhere, and then treated with 25 μM ZOL for 18 h or over a 24 h time course. Lysates were prepared and separated as previously described [31] and immunodetection was performed overnight at 4 °C in PBS/blocking reagent containing 0.1% Tween-20, using the following primary antibodies at the dilutions suggested by the manufacturer: pAb anti-RAP1 (121) for total RAP1 protein, pAB anti-RAP1A (C-17) specifically for unprenylated RAP1 (Santa Cruz Biotechnology, USA), and anti-actin mAb (Sigma–Aldrich, USA) as a loading control. Membranes were then rinsed several times with PBS containing 0.1% Tween-20 and incubated with 1:5000 dilution of anti-goat or anti-rabbit alkaline phosphatase-conjugated secondary antibodies (Thermo Fisher Scientific, USA) for 1 h. Visualisation of protein bands was performed using the ECF substrate reagent kit (GE Healthcare, UK) on a LAS-4000 (GE Healthcare, UK).

Labelling Vγ9Vδ2 T cells with DiR

Vγ9Vδ2 T cells were expanded *ex vivo* and enriched as described above, washed in PBS, and resuspended to 2×10^6 cells/mL in RPMI-1640 media (Life Technologies, Australia) supplemented with 0.1% HI-FBS. XenoLight DiR Fluorescent Dye (Perkin Elmer, USA) was reconstituted in ethanol and added to cells at a final concentration of 16.6 μg/mL. Cells were incubated in the dark for 10–15 min at 37 °C, then collected and washed three times in PBS containing 1% HI-FBS. Cell viability was assessed using trypan blue exclusion; labelling efficacy was assessed by flow cytometry using the filter corresponding to PeCy7; and cytotoxicity was assessed using the DEVD-Caspase assay, as outlined above.

Animals

Female four-week-old non-obese diabetic severe combined immunodeficient (NOD/SCID) mice were purchased from the Animal Resources Centre (Canning Vale, WA, Australia) and housed under pathogen free conditions in The Queen Elizabeth Hospital Experimental Surgical Suite (Woodville, SA, Australia). Mice were acclimatised to the animal housing facility and the general wellbeing of animals was monitored continuously throughout the experiment. All experimental procedures were carried out with strict adherence to the rules and guidelines for the ethical use of animals in research and were approved by the Animal Ethics Committees of the University of Adelaide and the Institute of Medical and Veterinary Science, Adelaide, SA, Australia.

In vivo fluorescence and bioluminescence imaging

Non-invasive, whole body imaging to monitor DiR-labelled Vγ9Vδ2 T cell localisation and luciferase-tagged MDA-MB231-TXSA cancer cell growth *in vivo* was performed on the IVIS Spectrum *in vivo* Imaging system (Caliper Life Sciences, Australia). For fluorescence imaging, mice were anaesthetised by isoflurane (Veterinary Companies of Australia, Australia) and fluorescence images were acquired using the optimised settings for DiR dye: f stop: 2, medium binning, ex/em: 745/800 nm. Images were taken at multiple time points, up to 120 s. For bioluminescence imaging, mice were injected s.c with 100 μL D-luciferin solution (Perkin Elmer, USA) to a final dose of 3 mg/20 g mouse body weight and then anaesthetised by isoflurane. Bioluminescence was acquired between 0.5 and 30 s (representative images shown at 1 s). Photon emission was quantified as Total Flux measured in [photons/second] using Living Image 4.2 (Caliper Life Sciences, Australia). There was no interference between the DiR dye and the luciferase-tagged cancer cells, therefore fluorescence and bioluminescence images could be acquired in succession to assess Vγ9Vδ2 T cell localisation.

Intratibial injections of breast cancer cells

Intratibial (i.t) injections were performed as previously described [30]. Briefly, five-week old female NOD/SCID mice were anaesthetised by isoflurane (Veterinary Companies of Australia, Australia). The left leg was shaved, then wiped with 70% ethanol and a 27-guage needle coupled to a Hamilton syringe was used to inject luciferase-tagged MDA-MB231-TXSA (1×10^5 cells) resuspended in 10 μL PBS through the tibial plateau into the marrow space. The contralateral tibia was not injected.

In vivo localisation

I.t injections were performed as described above, and once tumour were established, mice were injected 5×10^6 DiR-labelled Vγ9Vδ2 T cells i.v ($n = 5$). Fluorescence and bioluminescence images were acquired as described above after 20 min, 1 h, 24 h and 6 days.

In vivo anti-cancer efficacy of ZOL and Vγ9Vδ2 T cells

I.t injections were performed as described above and two days post inoculation, tumour growth was assessed by bioluminescence imaging using the IVIS Spectrum. When tumours were established, mice were assigned into four treatment groups ($n = 4–6$): control, ZOL alone (100 μg/kg s.c), Vγ9Vδ2 T cells alone (1×10^7 Vγ9Vδ2 T cells injected i.v via the tail vein), and ZOL in combination with Vγ9Vδ2 T cells (infusion of Vγ9Vδ2 T cells 24 h after ZOL, treatments as above). If pain relief was required, Rimadyl (carprofen) (Pfizer Animal Health, Australia) was administered at 5 mg/kg s.c every 24 h for a maximum of three days. After 3 weeks treatment, mice were sacrificed and the tumour bearing and non-tumour bearing tibia from each animal were surgically resected for micro-computed tomography (μCT).

Ex vivo micro-computed tomography (μCT) analysis

Tibias for μCT analysis were scanned using the SkyScan-1076 high-resolution μCT Scanner (Bruker). The scanner was operated at 50 kV, 110 μA, rotation step of 0.5, 0.5-mm aluminium filter, and scan resolution of 7.8 μm/pixel. Cross-sections were reconstructed using the cone-beam algorithm in NRecon (V1.6.9.8, Bruker). Images were then realigned in DataViewer (1.5.1.2, Bruker) and imported into CT Analyser (CTAn) (V1.14.4.1+, Bruker, Skyscan). Using the two-dimensional images obtained from the CTAn, the growth plate was identified and 600 sections starting from the growth plate/tibial interface and moving down the tibia were selected for quantification of total bone morphometric parameters and 200 sections starting 25 sections down from the growth plate, were selected for trabecular bone morphometric parameters. Representative three-dimensional images were generated in CTvox (V2.7.0, Bruker).

Histology

Tibias were fixed in 10% buffered formalin, followed by 6 weeks decalcification in 0.5 M EDTA/0.5% paraformaldehyde in PBS, pH 8.0 at room temperature. Complete decalcification was confirmed by radiography and tibias were then paraffin embedded and sectioned longitudinally at 6 μm. Osteoclast-specific tartrate-resistant acid phosphatase (TRAP) staining was conducted following the manufacturer's protocol (386A, Sigma Aldrich). Slides were then imaged using Nanozoomer-HT Digital Pathology (NDP, Hamamatsu) and photos were acquired at 4× and 40× magnification using Nanozoomer software NDP.view (V1.2.33, Hamamatsu). Osteoclast number was determined by counting TRAP positive multi-nucleated (≥3 nuclei) cells in a 1 mm^2 area below the growth plate.

Data analysis and statistics

In vitro experiments were conducted at least twice using biological triplicates, and data presented is mean ± SEM, unless otherwise specified. A representative experiment is shown for Western immunoblot data. Two-tailed unpaired Student's t-test was used and in all cases p-values <0.05 were considered statistically significant. All statistical analysis was conducted using SigmaPlot v12.5 (Systat Software Inc., USA).

Results

ZOL sensitises breast cancer cells to Vγ9Vδ2 T cell cytotoxicity in vitro

The cytotoxicity of purified *ex vivo* expanded Vγ9Vδ2 T cells alone and in combination with ZOL was first evaluated against a panel of human breast cancer cell lines. MDA-MB231-TXSA showed cytotoxicity in an E:T dependent manner after 9 h co-culture with Vγ9Vδ2 T cells alone (maximum 28% specific lysis), while T47D and ZR75 cells were relatively resistant. However, after 24 h pre-treatment with ZOL followed by 9 h co-culture with Vγ9Vδ2 T cells, there was a significant increase in cytotoxicity in each cell line which occurred in an E:T dependent manner, resulting in a maximum of 18% (ZR75), 50% (T47D) and 80% (MDA-MB231-TXSA) specific lysis (Fig. 1A). Co-culture of each cell line with Vγ9Vδ2 showed a small but statistically significant increase in caspase-3 activation, with the MDA-MB231-TXSA cells showing a 2-fold increase in caspase-3 activation after Vγ9Vδ2 T cells alone (Fig. 1B). However, after 24 h pre-treatment with ZOL then 2 h co-culture

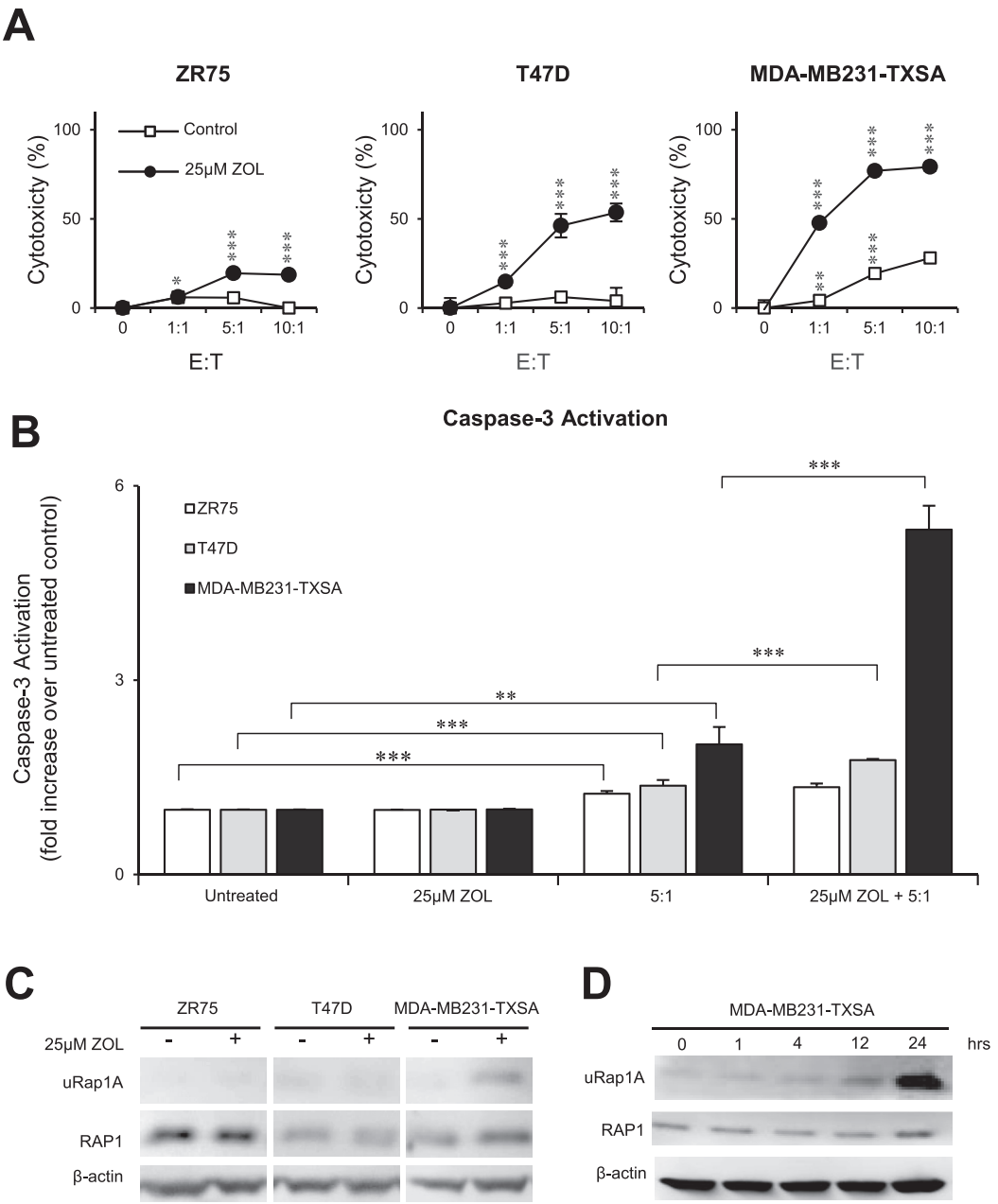

Fig. 1. ZOL sensitises breast cancer cells to Vγ9Vδ2 T cell cytotoxicity *in vitro*. **A**. ZR75, T47D, and MDA-MB231-TXSA breast cancer cell lines were pre-treated with 25 μM ZOL or left untreated for 24 h. Cancer cells were then co-cultured with *ex vivo* expanded Vγ9Vδ2 T cells (E:T, 1:1, 5:1, 10:1). After 9 h, LDH release was measured and expressed as percentage cytotoxicity compared to untreated cells. **B**. Caspase-3 activation of the same cell lines was measured after 24 h pre-treatment with or without 25 μM ZOL, followed by 2 h co-culture with *ex vivo* expanded Vγ9Vδ2 T cells (E:T, 5:1). Caspase-3 activation was expressed as a fold increase over untreated control. For the LDH and Caspase-3 activity assay, data was pooled and normalised from two separate experiments (n = 6). **C**. Western immunoblot analysis showing inhibition of prenylation in breast cancer cell lines after treatment with or without 25 μM ZOL for 24 h, showing unprenylated RAP1A (uRap1A), total RAP1 protein, and β-actin as loading control. **D**. Western immunoblot analysis showing inhibition of prenylation in MDA-MB231-TXSA treated with 25 μM ZOL over a 24 h time course (0, 1, 4, 12, 24 h). Images representative of n = 2–3. $^{*}p < 0.05$, $^{**}p < 0.005$, $^{***}p < 0.001$, ns = non-significant (two-tailed student's t-test, data represent mean ± SEM, n = 3, unless otherwise indicated).

with Vγ9Vδ2 T cells, each cell line except ZR75, showed significantly higher caspase-3 activation compared to Vγ9Vδ2 T cells alone. T47D and MDA-MB231-TXSA showed a 1.7 and 5.3-fold increase in caspase-3 activation respectively (Fig. 1B).

To determine possible reasons for the differential sensitivity to Vγ9Vδ2 T cells after ZOL pre-treatment between the three breast cancer cell lines, we examined inhibition of RAP1 prenylation (a surrogate marker for inhibition of the mevalonate pathway) after 18 h of ZOL treatment using Western immunoblot analysis. This method was used to indirectly determine the extent of FPPS inhibition by ZOL, which leads to increased IPP levels, potentially resulting in the increased detection of cancer cells by Vγ9Vδ2 T cells and greater cytotoxicity. After 18 h pre-treatment with 25 μM ZOL, MDA-MB231-TXSA showed an increase in unprenylated RAP1 compared to untreated control (Fig. 1C), while ZR75 and T47D showed no detectable unprenylated RAP1 compared to untreated. A time course analysis of MDA-MB231-TXSA treated with 25 μM ZOL, showed unprenylated RAP1 was detectable as early as one hour post treatment and peaked at 24 h (Fig. 1D).

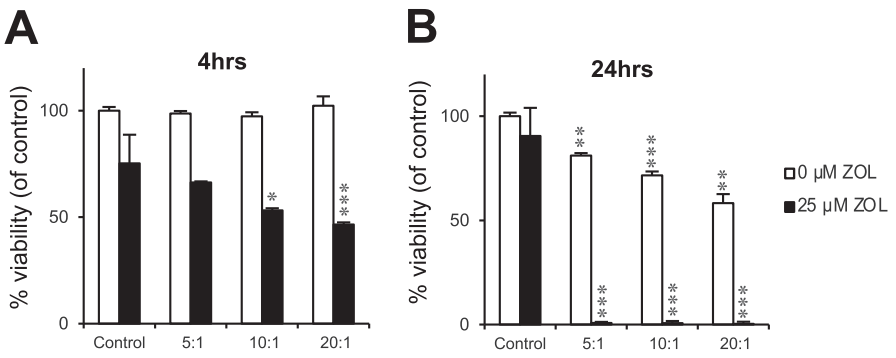

Fig. 2. Vγ9Vδ2 T cell cytotoxicity against breast cancer cells in vitro occurs in a time dependent manner. Luciferase-tagged MDA-MB231-TXSA breast cancer cells were treated with or without 25 μM ZOL for 24 h. Cancer cells were then co-cultured with *ex vivo* expanded Vγ9Vδ2 T cells (E:T, 5:1, 10:1, 20:1) for **A**. 4 or **B**. 24 h, and luciferase activity measured and expressed as percentage viability compared to untreated control. Representative data shown from three experiments.*$p < 0.05$, **$p < 0.005$, ***$p < 0.001$, ns = non-significant (two-tailed student's t-test, data represent mean ± SEM, n = 3, unless otherwise indicated).

Since MDA-MB231-TXSA were consistently the most sensitive breast cancer cell line to Vγ9Vδ2 T cell cytotoxicity, further experiments were conducted to establish an optimal time course for Vγ9Vδ2 T cell cytotoxicity after ZOL pre-treatment. A luciferase-based activity assay was used to determine the viability of cancer cells after 24 h pre-treatment with or without 25 μM ZOL followed by co-cultured with Vγ9Vδ2 T cells for 4 or 24 h. After a 4 h co-culture, Vγ9Vδ2 T cells alone did not reduce MDA-MB231-TXSA viability, however, pre-treatment with ZOL greatly enhanced Vγ9Vδ2 T cell cytotoxicity, resulting in a significant decrease MDA-MB23-TXSA viability in an E:T dependent manner (maximum 46% viable) (Fig. 2A). In contrast, after a 24 h co-culture with Vγ9Vδ2 T cells in the absence of ZOL, an E:T dependent decrease in cancer cell viability (maximum 60% viable) was observed (Fig. 2B). Pre-treatment of MDA-MB231-TXSA with ZOL further potentiated the cytotoxicity of Vγ9Vδ2 T cells resulting in almost 100% death of cancer cells at all E:T tested (Fig. 2B).

Adoptively transfered Vγ9Vδ2 T cells localise to breast cancer lesions in the bone

To date, no studies have demonstrated localisation of Vγ9Vδ2 T cells to tumours in the bone. To examine the potential for Vγ9Vδ2 T cells to co-localise with tumours in the bone microenvironment, a near infrared dye (DiR) was used to fluorescently label Vγ9Vδ2 T cells for live *in vivo* imaging. We established a protocol that allowed consistent labelling of Vγ9Vδ2 T cells, with a labelling efficiency of >80% as analysed by flow cytometry (Fig. 3A). Labelling Vγ9Vδ2 T cells with the fluorescent dye had no effect on the viability of Vγ9Vδ2 T cells (data not shown), or on their ability to induce cell death of MDA-MB231-TXSA cancer cells, compared to unlabelled Vγ9Vδ2 T cells (Fig. 3B). For localisation studies, mice were inoculated with luciferase-tagged MDA-MB231-TXSA cancer cells directly into the bone marrow cavity of the left tibia. After one week, tumours were established as measured by bioluminescence signal from the tibia. Fluorescently labelled Vγ9Vδ2 T cells were injected intravenously into the animals. Within 20 min of infusion, fluorescence signal was detected only in the lungs and liver (data not shown). However, after 24 h, a strong fluorescence signal was also detected in the tumour bearing tibia, corresponding to areas of tumour bioluminescence (Fig. 3C). At this time, fluorescence in the lungs diminished, whereas the fluorescence signal persisted in the liver until the end of the study, six days later. Overall, the fluorescence signal progressively declined over the next six days, at which point, mice were sacrificed and tibias were imaged *ex vivo*. Mice showed fluorescence which corresponded to areas of tumour bioluminescence in the tumour bearing tibias (Fig. 3D), as well as fluorescence in the liver and spleen, which has been previously reported with adoptive transfer of Vγ9Vδ2 T cells [23,32].

ZOL potentiates the anti-cancer efficacy of Vγ9Vδ2 T cells against osteolytic breast cancer and reduces tumour burden of lung metastases

We next examined the *in vivo* efficacy of *ex vivo* expanded Vγ9Vδ2 T cells in a model of osteolytic breast cancer. Mice were inoculated with luciferase-tagged MDA-MB231-TXSA cells directly into the left tibia of mice. Treatments were initiated once tumours had established, as measured by bioluminescence imaging. Animals were pre-treated with ZOL 24 h prior to Vγ9Vδ2 T cell adoptive transfer. This treatment regime was repeated three times over two weeks. Animals treated with ZOL alone had no effect on tumour burden when compared to untreated animals (Fig. 4). A trend showing decreased tumour growth, which did not reach statistical significance, was observed in animals adoptively transferred with Vγ9Vδ2 T cells alone compared to untreated control or ZOL alone treated animals. In contrast, pre-treatment with ZOL, followed by adoptive transfer of Vγ9Vδ2 T cells, potentiated the anti-cancer efficacy of Vγ9Vδ2 T cells. These animals showed the smallest tumours of all treatment groups, which was evident after the third infusion dose of Vγ9Vδ2 T cells. Additionally, Vγ9Vδ2 T cells in combination with ZOL reduced pulmonary tumour burden in those animals that developed lung metastases, compared to animals in the untreated control or ZOL alone treated groups (Fig. 5).

ZOL in combination with Vγ9Vδ2 T cells reduces tumour-induced osteolysis

MDA-MB231-TXSA breast cancer cells growing within the bone give rise to predominantly osteolytic lesions [30,33]. To evaluate the ability of Vγ9Vδ2 T cells alone or in combination with ZOL to protect the bone from tumour-induced osteolysis, tibias were analysed using three-dimensional (3D) μCT imaging and TRAP staining of bone sections was used to visualise and quantify $TRAP^+$ osteoclasts.

Osteolysis was measured as a net loss of total bone volume (T.BV) and trabecular bone volume (Tb.BV) by comparing the tumour bearing tibia to the contralateral non-tumour bearing tibia of the same animal. Qualitative and quantitative μCT showed bone loss in all groups, but with notable differences in the extent of

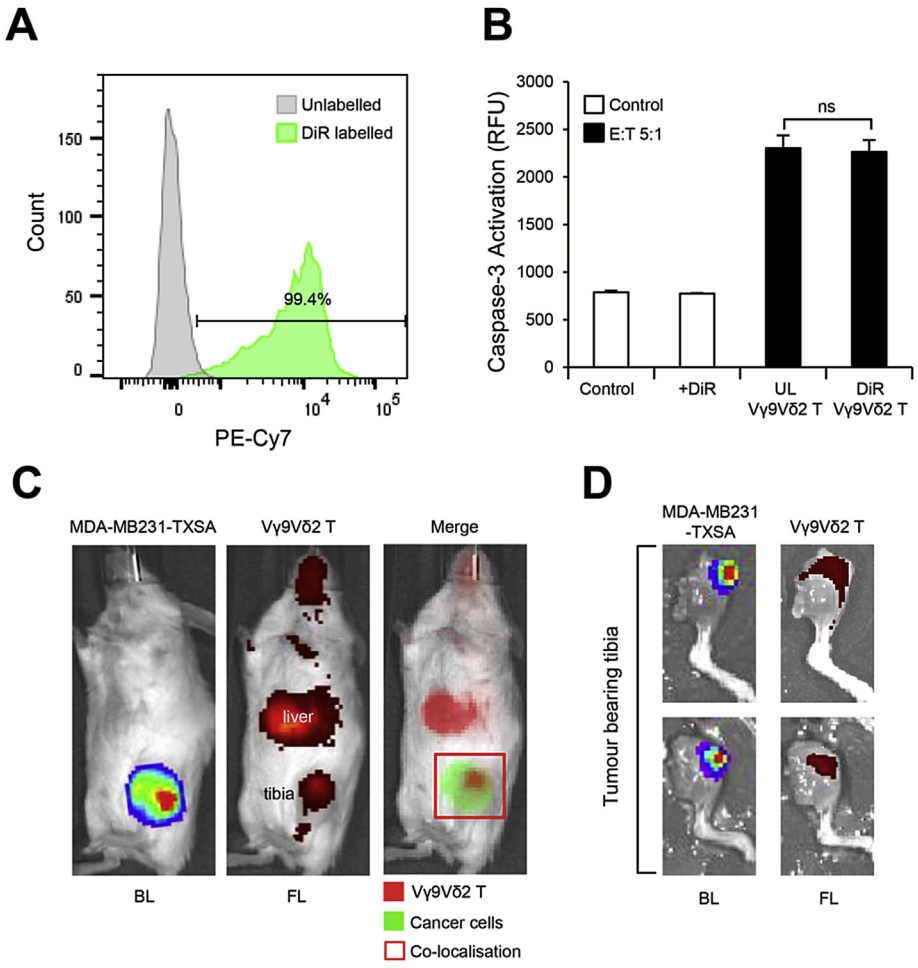

Fig. 3. Fluorescently labelled Vγ9Vδ2 T cells localise to breast cancer lesions in the bone. *Ex vivo* expanded Vγ9Vδ2 T cells were labelled using DiR dye as outlined in the methods. **A**. Flow cytometric analysis of Vγ9Vδ2 T cell DiR labelling efficacy. **B**. Cytotoxicity of DiR-labelled and unlabelled Vγ9Vδ2 T cells against MDA-MB231-TXSA cancer cells (E:T, 5:1) as shown by caspase-3 activation. **C**. *In vivo* localisation of DiR-labelled Vγ9Vδ2 T cells injected via the tail vein into 5-week old female NOD/SCID mice bearing luciferase-tagged osteolytic breast cancer cells (MDA-MB231-TXSA) in the left tibia. Bioluminescence and fluorescence images were acquired on the IVIS Spectrum *in vivo* imaging system 24 h after infusion and **D**. *ex vivo*, 6 days after infusion (representative images of n = 5). UL = unlabelled, BL = bioluminescence, FL = fluorescence. Percentages shown indicate numbers from lymphocyte population. ns = non-significant (Student's t-test, data represent mean ± SEM, n = 3).

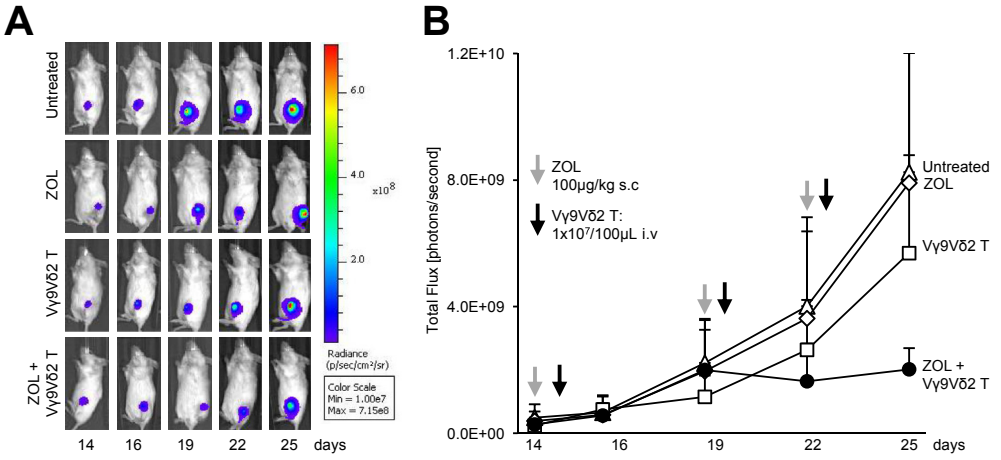

Fig. 4. ZOL potentiates the anti-cancer efficacy of Vγ9Vδ2 T cells against osteolytic breast cancer. Luciferase-tagged MDA-MB231-TXSA breast cancer cells were injected directly into the left tibial cavity of 5-week old NOD/SCID mice. Once tumours were established, treatments were commenced as outlined in the methods. Whole body bioluminescence images were acquired on the IVIS Spectrum *in vivo* imaging system over the course of the study. **A**. A representative bioluminescence image showing a single mouse from each treatment group over the duration of the study. **B**. The line graph shows the quantification of bioluminescence signal over the course of the study and is expressed as total flux [photons/second] (n = 4–6 mice per group).

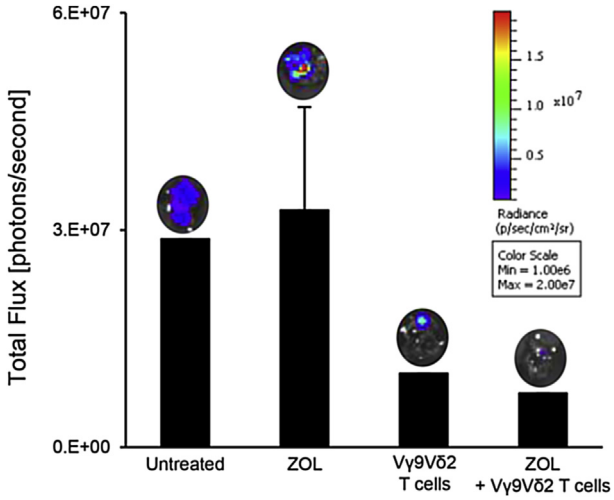

Fig. 5. Vγ9Vδ2 T cells reduce tumour burden of lung metastases. At the time of sacrifice, lungs were removed for bioluminescence quantification of tumour burden. Bioluminescence signal was detected on the IVIS Spectrum *in vivo* imaging system and is expressed as total flux [photons/second]. A representative bioluminescence image of the lungs from each treatment group is shown.

osteolysis (Fig. 6A). Animals that remained untreated showed the greatest osteolysis, with a net loss T.BV of 16% compared to the contralateral non-tumour bearing tibia. As expected, ZOL treatment reduced the extent of osteolysis, to 7% T.BV. Vγ9Vδ2 T cells alone only marginally reduced the T.BV from 16% to 11%. In contrast, treatment with ZOL in combination with Vγ9Vδ2 T cells showed an additive effect in reducing osteolysis, with total BV loss of only 4%. Tb.BV loss was more profound in all treatment groups (Fig. 6B). Animals in the untreated group had a Tb.BV loss of 87%, Vγ9Vδ2 T cells alone increased Tb.BV loss to 65% and ZOL treatment alone increased Tb.BV loss to 49%. ZOL in combination with Vγ9Vδ2 T cells had the least Tb.BV loss at 27%.

Untreated animals showed abundant $TRAP^+$ osteoclasts lining the bone surface, in contrast to animals treated with ZOL alone or ZOL in combination with Vγ9Vδ2 T cells (Fig. 6C). Animals treated with ZOL alone showed a significant decrease in $TRAP^+$ osteoclasts compared to untreated animals (Fig. 6D). A trend showing reduced osteoclast number was observed in the Vγ9Vδ2 T cell alone treated group, however this did not reach statistical significance (Fig. 6D). Furthermore, there were no significant differences in osteoclast number between animals treated with ZOL alone and ZOL in combination with Vγ9Vδ2 T cells (Fig. 6D), suggesting that ZOL alone was responsible for the observed decrease in osteoclasts in the combination treatment group.

Discussion

In this study, we used a well-established murine model of osteolytic breast cancer to examine the anti-cancer efficacy of adoptively transferred *ex vivo* expanded Vγ9Vδ2 T cells alone and in combination with ZOL. The MDA-MB231 derivative cell line, MDA-MB231-TXSA, is a highly osteolytic breast cancer cell line which mimics abnormal osteoclast-mediated bone degradation commonly seen in breast cancer bone metastases [30,33]. *In vitro* pre-treatment of MDA-MB231-TXSA with ZOL lead to a significant augmentation of Vγ9Vδ2 T cell mediated cytotoxicity, which was associated with a time-dependent inhibition of RAP1 prenylation, a surrogate marker of the mevalonate pathway. However, not all breast cancer cell lines were sensitised to Vγ9Vδ2 T cells following ZOL pre-treatment. Observed differences may arise from the ability of cells to uptake nBPs, which varies depending on cell type, and on mevalonate pathway activity [15,34]. Following ZOL pre-treatment, MDA-MB231-TXSA showed the greatest inhibition of RAP1 prenylation, suggesting the sensitivity of cancer cells to killing by Vγ9Vδ2 T cells after ZOL pre-treatment correlated with the accumulation of intracellular PAgs after exposure to ZOL.

In vivo, we have demonstrated for the first time that adoptively transferred Vγ9Vδ2 T cells localised to tumours in the tibia and persisted for up to 6 days following infusion. This is consistent with previous findings in other soft tissue tumours including breast and prostate cancer demonstrating the ability of Vγ9Vδ2 T to localise to tumour lesions [23,32]. Adoptively transferred Vγ9Vδ2 T cells were also observed in the liver. When a substance is injected intravenously via the tail vein, it is directly delivered to the liver, which accounts for this observation.

When Vγ9Vδ2 T cells were infused alone, there was minimal reduction in tumour burden in the bone. However, pre-treatment of mice with ZOL greatly potentiated the anti-cancer efficacy of adoptively transferred Vγ9Vδ2 T cells against tumour growth in bone and also considerably reduced pulmonary metastases burden. This decrease in lung metastases is consistent with similar observations in both pre-clinical studies in prostate cancer [35] and early phase clinical trials in patients with advanced renal cell carcinoma [26].

Given the well-characterised effects of ZOL on the mevalonate pathway and our *in vitro* observations showing inhibition of RAP1 prenylation, our data suggest that cellular accumulation of IPP caused by inhibition of FPPS establishes greater recognition and targeting of cancer cells by Vγ9Vδ2 T cells. Benzaid et al. demonstrated that mice treated with ZOL showed IPP accumulation in mammary fat pad tumours [15]. Additionally, mice that were infused with human PBMC in combination with ZOL and IL-2 showed *in vivo* expansion of Vγ9Vδ2 T cells, and treatment inhibited tumour growth, compared to untreated animals and those treated with ZOL alone or PBMC + IL-2, with the authors' suggesting cancer cells could internalise ZOL *in vivo* [15]. However, following ZOL administration there is a transient peak followed by rapid clearance of ZOL with its permanent retention in bone, thus it is not available for internalisation by cancer cells resident in the bone marrow. Additionally, using real-time intravital imaging within mammary fat pad tumours, Junankar et al. recently showed that fluorescently labelled nBPs were not internalise by cancer cells, but rather by tumour associated macrophages (TAMs) [36], suggesting IPP accumulation within the tumour mass would arise from the TAM population. Macrophages and osteoclasts are derived from the same lineage and both internalise ZOL via fluid-phase endocytosis [37]. Within the bone, osteoclasts and monocytes uptake nBPs [38], therefore it is reasonable to suggest that within the bone tumour microenvironment, these cells uptake ZOL and cancer cells do not. Previously, Ferrero et al. reported that *mycobacterium tuberculosis* pulsed macrophages produce monocyte chemoattractant protein-1 (MCP-1) and IL-8, which promote chemotaxis of γδ T cells *in vitro* [39]. CCR2, a receptor for MCP-1, is expressed on activated Vγ9Vδ2 T cells [20] suggesting that macrophages and/or osteoclasts which have internalised ZOL may attract activated Vγ9Vδ2 T cells to the tumour microenvironment resulting in greater anti-cancer efficacy. However, further studies are required to examine the underlying mechanisms of ZOL sensitisation *in vivo*.

nBPs are well-characterised anti-bone resorptive agents, additionally, they are reported to induce cancer cell death, inhibit proliferation, invasion, and angiogenesis *in vitro* [40–45]. However, the current literature surrounding ZOL *in vivo* anti-cancer efficacy is still contradictory [46–51]. In this current study, frequent ZOL administrations inhibited cancer-associated bone loss, however there

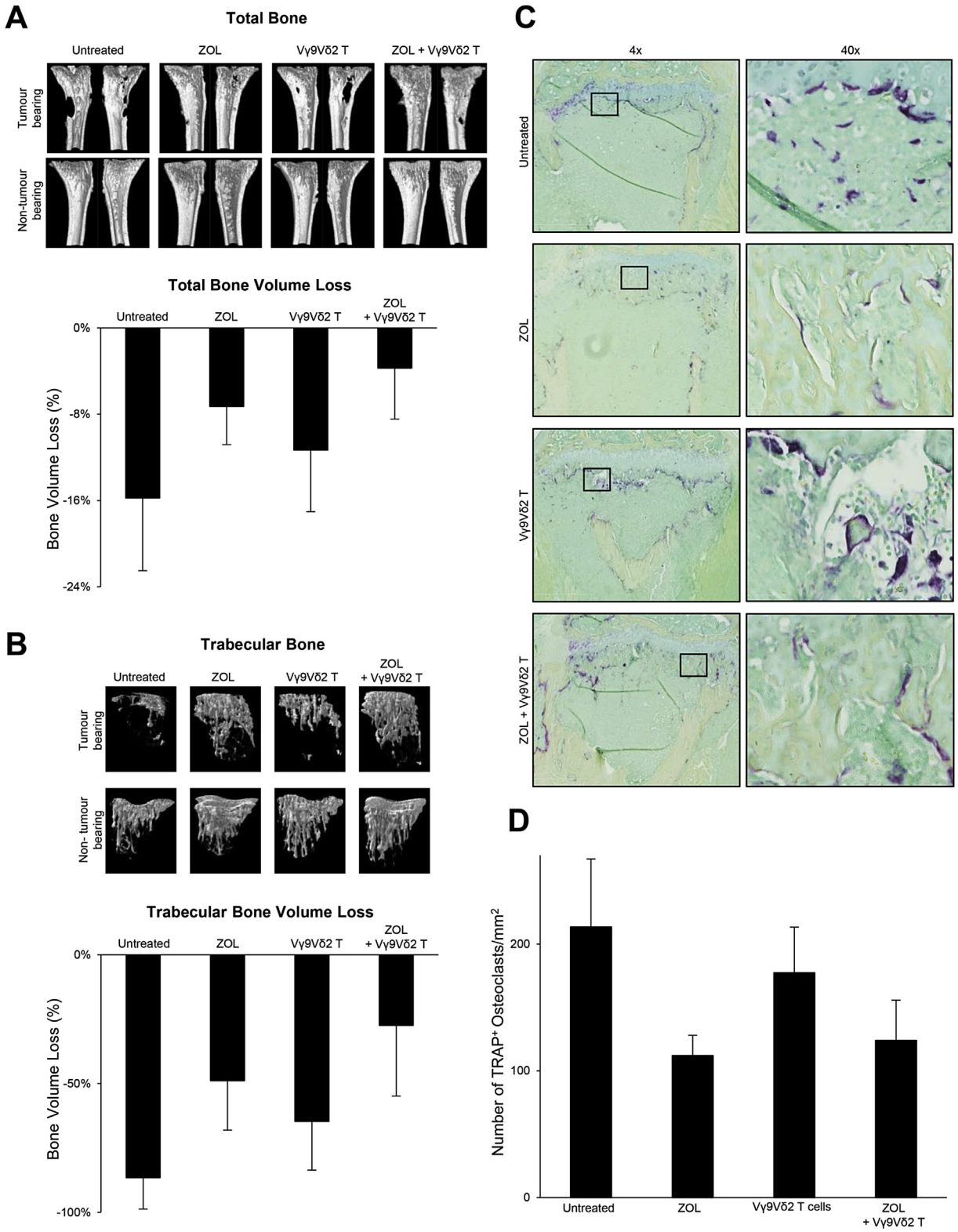

Fig. 6. Vγ9Vδ2 T cells in combination with ZOL reduce tumour-associated osteolysis in total and trabecular bone. The osteolytic nature of MDA-MB231-TXSA breast cancer cells can be seen in the representative qualitative μCT 3D images and in the quantitative assessment of **A**. total and **B**. trabecular bone. Bone loss percentage is calculated as the percentage difference in bone volume between the tumour bearing and contralateral non-tumour bearing control tibia. **C**. Representative histological sections at 4× and 40× magnification showing decalcified tibias from each treatment group stained with TRAP for the detection of osteoclasts. **D**. Quantitative assessment of the number of $TRAP^+$ osteoclasts.

was no effect on tumour burden. These findings are consistent with previous studies from our laboratory using an intratibial model of orthotropic osteosarcoma [50,51]. Interestingly, more frequent ZOL administrations at a lower dose (metronomic dosing), were previously shown to inhibit both tumour growth and protect the bone from tumour-associated osteolysis [48] indicating further *in vivo* optimisation to reduce tumour growth in this model may be required.

In contrast to the well-known anti-bone resorptive effects of ZOL, the effect Vγ9Vδ2 T cells have on bone is still unclear. The first indication that Vγ9Vδ2 T cells may contribute to osteoimmunology was the correlation observed between Vγ9Vδ2 T cell depletion and the incidence of bisphosphonate-associated osteonecrosis of the jaw in osteoporotic patients treated with intravenous nBPs [52]. In this current study, Vγ9Vδ2 T cells alone marginally inhibited tumour-associated bone loss; however, the mechanisms by which this occurs is still unclear. Previous *in vitro* studies demonstrated that activated donor-matched human γδ T cells inhibit osteoclast formation from PBMC [53] and Vγ9Vδ2 T cells are cytotoxic towards osteoclasts in co-culture with multiple myeloma cells [12]. Targeting osteoclasts would result in increased bone volume, as observed in this current study. Vγ9Vδ2 T cells also have the potential to produce IGF-1 and low levels of FGF-2 following antigen stimulation [54]. IGF and FGF are osteoblast growth factors, suggesting that if Vγ9Vδ2 T cells are primed to produce these factors following localisation to the bone, in addition to their potential cytotoxicity against osteoclasts, they could stimulate new bone resulting in a net gain in bone volume. As Vγ9Vδ2 T cells also target cancer cells, they may have an indirect effect on bone loss by reducing tumour growth and subsequently inhibiting the 'vicious cycle'.

Collectively, this study demonstrates that *ex vivo* expanded Vγ9Vδ2 T cells readily localise to osteolytic breast cancer lesions in the bone and exhibit some anti-cancer efficacy, which is enhanced following ZOL pre-treatment. Our data suggests that adoptive transfer of Vγ9Vδ2 T cells in combination with ZOL would be beneficial in reducing tumour growth in bone and tumour-associated osteolysis, while also limiting the potential for metastatic spread in patients with advanced breast cancer, greatly reducing the morbidity of the disease. However, further studies are required to understand the interactions between the bone microenvironment, cancer cells, and *in vivo* ZOL uptake to optimise a treatment regimen that achieves maximal anti-cancer efficacy.

Acknowledgments

This work was supported by funds from the National Breast Cancer Foundation (NBCF-13-09) and the research fellowships granted to A. Evdokiou by The Hospital Research Foundation (THRF) and Australian Breast Cancer Research (ABCR).

The authors would like to thank Ms Ruth Williams and Dr. Agatha Labrinidis from Adelaide Microscopy at The University of Adelaide for technical assistance with the SkyScan 1076 and related software.

Conflict of interest

The authors declare no conflict of interest.

References

[1] N. Howlader, A.M. Noone, M. Krapcho, D. Miller, K. Bishop, S.F. Altekruse, C.L. Kosary, M. Yu, J. Ruhl, Z. Tatalovich, A. Mariotto, D.R. Lewis, H.S. Chen, E.J. Feuer, K.A. Cronin (Eds.), SEER Cancer Statistics Review, 1975–2013, National Cancer Institute, Bethesda, MD, April 2016 based on November 2015 SEER data submission, posted to the SEER web site, http://seer.cancer.gov/csr/1975_2013/.

[2] R.E. Coleman, R.D. Rubens, The clinical course of bone metastases from breast cancer, Br. J. Cancer 55 (1987) 61–66.

[3] R.E. Coleman, Metastatic bone disease: clinical features, pathophysiology and treatment strategies, Cancer Treat. Rev. 27 (2001) 165–176.

[4] G.R. Mundy, Metastasis to bone: causes, consequences and therapeutic opportunities, Nat. Rev. Cancer 2 (2002) 584–593.

[5] G.D. Roodman, Mechanisms of bone metastasis, N. Engl. J. Med. 350 (2004) 1655–1664.

[6] J.R. Ross, Y. Saunders, P.M. Edmonds, S. Patel, K.E. Broadley, S.R. Johnston, Systematic review of role of bisphosphonates on skeletal morbidity in metastatic cancer, BMJ 327 (2003) 469.

[7] J.R. Ross, Y. Saunders, P.M. Edmonds, S. Patel, D. Wonderling, C. Normand, et al., A systematic review of the role of bisphosphonates in metastatic disease, Health Technol. Assess. 8 (2004) 1–176.

[8] S.R. Carding, P.J. Egan, Gammadelta T cells: functional plasticity and heterogeneity, Nat. Rev. Immunol. 2 (2002) 336–345.

[9] A.S. Ensslin, B. Formby, Comparison of cytolytic and proliferative activities of human gamma delta and alpha beta T cells from peripheral blood against various human tumor cell lines, J. Natl. Cancer Inst. 83 (1991) 1564–1569.

[10] M. Muraro, O.M. Mereuta, F. Carraro, E. Madon, F. Fagioli, Osteosarcoma cell line growth inhibition by zoledronate-stimulated effector cells, Cell. Immunol. 249 (2007) 63–72.

[11] Z. Li, Q. Xu, H. Peng, R. Cheng, Z. Sun, Z. Ye, IFN-gamma enhances HOS and U2OS cell lines susceptibility to gammadelta T cell-mediated killing through the Fas/Fas ligand pathway, Int. Immunopharmacol. 11 (2011) 496–503.

[12] Q. Cui, H. Shibata, A. Oda, H. Amou, A. Nakano, K. Yata, et al., Targeting myeloma-osteoclast interaction with Vgamma9Vdelta2 T cells, Int. J. Hematol. 94 (2011) 63–70.

[13] K. Sato, S. Kimura, H. Segawa, A. Yokota, S. Matsumoto, J. Kuroda, et al., Cytotoxic effects of gammadelta T cells expanded ex vivo by a third generation bisphosphonate for cancer immunotherapy, Int. J. Cancer 116 (2005) 94–99.

[14] S.R. Mattarollo, T. Kenna, M. Nieda, A.J. Nicol, Chemotherapy and zoledronate sensitize solid tumour cells to Vgamma9Vdelta2 T cell cytotoxicity, Cancer Immunol. Immunother. 56 (2007) 1285–1297.

[15] I. Benzaid, H. Monkkonen, V. Stresing, E. Bonnelye, J. Green, J. Monkkonen, et al., High phosphoantigen levels in bisphosphonate-treated human breast tumors promote Vgamma9Vdelta2 T-cell chemotaxis and cytotoxicity in vivo, Cancer Res. 71 (2011) 4562–4572.

[16] M. Kondo, T. Izumi, N. Fujieda, A. Kondo, T. Morishita, H. Matsushita, et al., Expansion of human peripheral blood gammadelta T cells using zoledronate, J. Vis. Exp. (2011).

[17] H.J. Gober, M. Kistowska, L. Angman, P. Jeno, L. Mori, G. De Libero, Human T cell receptor gammadelta cells recognize endogenous mevalonate metabolites in tumor cells, J. Exp. Med. 197 (2003) 163–168.

[18] B. Poonia, C.D. Pauza, Gamma delta T cells from HIV+ donors can be expanded in vitro by zoledronate/interleukin-2 to become cytotoxic effectors for antibody-dependent cellular cytotoxicity, Cytotherapy 14 (2012) 173–181.

[19] C. Niu, H. Jin, M. Li, J. Xu, D. Xu, J. Hu, et al., In vitro analysis of the proliferative capacity and cytotoxic effects of ex vivo induced natural killer cells, cytokine-induced killer cells, and gamma-delta T cells, BMC Immunol. 16 (2015) 61.

[20] F. Dieli, F. Poccia, M. Lipp, G. Sireci, N. Caccamo, C. Di Sano, et al., Differentiation of effector/memory Vdelta2 T cells and migratory routes in lymph nodes or inflammatory sites, J. Exp. Med. 198 (2003) 391–397.

[21] M. D'Asaro, C. La Mendola, D. Di Liberto, V. Orlando, M. Todaro, M. Spina, et al., V gamma 9V delta 2 T lymphocytes efficiently recognize and kill zoledronate-sensitized, imatinib-sensitive, and imatinib-resistant chronic myelogenous leukemia cells, J. Immunol. 184 (2010) 3260–3268.

[22] R. Aggarwal, J. Lu, S. Kanji, M. Das, M. Joseph, M.B. Lustberg, et al., Human Vgamma2Vdelta2 T cells limit breast cancer growth by modulating cell survival-, apoptosis-related molecules and microenvironment in tumors, Int. J. Cancer 133 (2013) 2133–2144.

[23] T. Santolaria, M. Robard, A. Leger, V. Catros, M. Bonneville, E. Scotet, Repeated systemic administrations of both aminobisphosphonates and human Vgamma9Vdelta2 T cells efficiently control tumor development in vivo, J. Immunol. 191 (2013) 1993–2000.

[24] J.P. Fisher, J. Heuijerjans, M. Yan, K. Gustafsson, J. Anderson, Gammadelta T cells for cancer immunotherapy: a systematic review of clinical trials, Oncoimmunology 3 (2014) e27572.

[25] T. Nakazawa, M. Nakamura, Y.S. Park, Y. Motoyama, Y. Hironaka, F. Nishimura, et al., Cytotoxic human peripheral blood-derived gammadeltaT cells kill glioblastoma cell lines: implications for cell-based immunotherapy for patients with glioblastoma, J. Neurooncol. 116 (2014) 31–39.

[26] H. Kobayashi, Y. Tanaka, J. Yagi, N. Minato, K. Tanabe, Phase I/II study of adoptive transfer of gammadelta T cells in combination with zoledronic acid and IL-2 to patients with advanced renal cell carcinoma, Cancer Immunol. Immunother. 60 (2011) 1075–1084.

[27] I. Wada, H. Matsushita, S. Noji, K. Mori, H. Yamashita, S. Nomura, et al., Intraperitoneal injection of in vitro expanded Vgamma9Vdelta2 T cells together with zoledronate for the treatment of malignant ascites due to gastric cancer, Cancer Med. 3 (2014) 362–375.

[28] A.J. Nicol, H. Tokuyama, S.R. Mattarollo, T. Hagi, K. Suzuki, K. Yokokawa, et al., Clinical evaluation of autologous gamma delta T cell-based immunotherapy for metastatic solid tumours, Br. J. Cancer 105 (2011) 778–786.

[29] S. Kalyan, W. He, D. Kabelitz, Bone cancer: primary bone cancers and bone metastases, in: D. Heymann (Ed.), Bone cancer: Primary Bone Cancers and Bone Metastases, Elsevier, 2014, pp. 629–636.
[30] I. Zinonos, A. Labrinidis, M. Lee, V. Liapis, S. Hay, V. Ponomarev, et al., Apomab, a fully human agonistic antibody to DR5, exhibits potent antitumor activity against primary and metastatic breast cancer, Mol. Cancer Ther. 8 (2009) 2969–2980.
[31] V. Liapis, A. Labrinidis, I. Zinonos, S. Hay, V. Ponomarev, V. Panagopoulos, et al., Hypoxia-activated pro-drug TH-302 exhibits potent tumor suppressive activity and cooperates with chemotherapy against osteosarcoma, Cancer Lett. 357 (2015) 160–169.
[32] B.H. Beck, H.G. Kim, H. Kim, S. Samuel, Z. Liu, R. Shrestha, et al., Adoptively transferred ex vivo expanded gammadelta-T cells mediate in vivo antitumor activity in preclinical mouse models of breast cancer, Breast Cancer Res. Treat. 122 (2010) 135–144.
[33] M. Thai le, A. Labrinidis, S. Hay, V. Liapis, S. Bouralexis, K. Welldon, et al., Apo2l/Tumor necrosis factor-related apoptosis-inducing ligand prevents breast cancer-induced bone destruction in a mouse model, Cancer Res. 66 (2006) 5363–5370.
[34] F.P. Coxon, K. Thompson, A.J. Roelofs, F.H. Ebetino, M.J. Rogers, Visualizing mineral binding and uptake of bisphosphonate by osteoclasts and non-resorbing cells, Bone 42 (2008) 848–860.
[35] Z. Liu, I.E. Eltoum, B. Guo, B.H. Beck, G.A. Cloud, R.D. Lopez, Protective immunosurveillance and therapeutic antitumor activity of gammadelta T cells demonstrated in a mouse model of prostate cancer, J. Immunol. 180 (2008) 6044–6053.
[36] S. Junankar, G. Shay, J. Jurczyluk, N. Ali, J. Down, N. Pocock, et al., Real-time intravital imaging establishes tumor-associated macrophages as the extraskeletal target of bisphosphonate action in cancer, Cancer Discov. (2014).
[37] K. Thompson, M.J. Rogers, F.P. Coxon, J.C. Crockett, Cytosolic entry of bisphosphonate drugs requires acidification of vesicles after fluid-phase endocytosis, Mol. Pharmacol. 69 (2006) 1624–1632.
[38] A.J. Roelofs, F.P. Coxon, F.H. Ebetino, M.W. Lundy, Z.J. Henneman, G.H. Nancollas, et al., Fluorescent risedronate analogues reveal bisphosphonate uptake by bone marrow monocytes and localization around osteocytes in vivo, J. Bone Miner. Res. 25 (2010) 606–616.
[39] E. Ferrero, P. Biswas, K. Vettoretto, M. Ferrarini, M. Uguccioni, L. Piali, et al., Macrophages exposed to Mycobacterium tuberculosis release chemokines able to recruit selected leucocyte subpopulations: focus on gammadelta cells, Immunology 108 (2003) 365–374.
[40] N. Horie, H. Murata, S. Kimura, H. Takeshita, T. Sakabe, T. Matsui, et al., Combined effects of a third-generation bisphosphonate, zoledronic acid with other anticancer agents against murine osteosarcoma, Br. J. Cancer 96 (2007) 255–261.
[41] K. Koto, H. Murata, S. Kimura, N. Horie, T. Matsui, Y. Nishigaki, et al., Zoledronic acid inhibits proliferation of human fibrosarcoma cells with induction of apoptosis, and shows combined effects with other anticancer agents, Oncol. Rep. 24 (2010) 233–239.
[42] O. Fromigue, L. Lagneaux, J.J. Body, Bisphosphonates induce breast cancer cell death in vitro, J. Bone Miner. Res. 15 (2000) 2211–2221.
[43] S. Boissier, M. Ferreras, O. Peyruchaud, S. Magnetto, F.H. Ebetino, M. Colombel, et al., Bisphosphonates inhibit breast and prostate carcinoma cell invasion, an early event in the formation of bone metastases, Cancer Res. 60 (2000) 2949–2954.
[44] R. Montague, C.A. Hart, N.J. George, V.A. Ramani, M.D. Brown, N.W. Clarke, Differential inhibition of invasion and proliferation by bisphosphonates: anti-metastatic potential of Zoledronic acid in prostate cancer, Eur. Urol. 46 (2004) 389–401 discussion 401–382.
[45] S. Matsumoto, S. Kimura, H. Segawa, J. Kuroda, T. Yuasa, K. Sato, et al., Efficacy of the third-generation bisphosphonate, zoledronic acid alone and combined with anti-cancer agents against small cell lung cancer cell lines, Lung Cancer 47 (2005) 31–39.
[46] J. Jeong, K.S. Lee, Y.K. Choi, Y.J. Oh, H.D. Lee, Preventive effects of zoledronic acid on bone metastasis in mice injected with human breast cancer cells, J. Korean Med. Sci. 26 (2011) 1569–1575.
[47] B. Ory, M.F. Heymann, A. Kamijo, F. Gouin, D. Heymann, F. Redini, Zoledronic acid suppresses lung metastases and prolongs overall survival of osteosarcoma-bearing mice, Cancer 104 (2005) 2522–2529.
[48] K.W. Luo, C.H. Ko, G.G. Yue, M.Y. Lee, W.S. Siu, J.K. Lee, et al., Anti-tumor and anti-osteolysis effects of the metronomic use of zoledronic acid in primary and metastatic breast cancer mouse models, Cancer Lett. 339 (2013) 42–48.
[49] K. Koto, N. Horie, S. Kimura, H. Murata, T. Sakabe, T. Matsui, et al., Clinically relevant dose of zoledronic acid inhibits spontaneous lung metastasis in a murine osteosarcoma model, Cancer Lett. 274 (2009) 271–278.
[50] A. Labrinidis, S. Hay, V. Liapis, V. Ponomarev, D.M. Findlay, A. Evdokiou, Zoledronic acid inhibits both the osteolytic and osteoblastic components of osteosarcoma lesions in a mouse model, Clin. Cancer Res. 15 (2009) 3451–3461.
[51] A. Labrinidis, S. Hay, V. Liapis, D.M. Findlay, A. Evdokiou, Zoledronic acid protects against osteosarcoma-induced bone destruction but lacks efficacy against pulmonary metastases in a syngeneic rat model, Int. J. Cancer 127 (2010) 345–354.
[52] S. Kalyan, E.S. Quabius, J. Wiltfang, H. Monig, D. Kabelitz, Can peripheral blood gammadelta T cells predict osteonecrosis of the jaw? An immunological perspective on the adverse drug effects of aminobisphosphonate therapy, J. Bone Miner. Res. 28 (2013) 728–735.
[53] A. Pappalardo, K. Thompson, Activated gammadelta T cells inhibit osteoclast differentiation and resorptive activity in vitro, Clin. Exp. Immunol. 174 (2013) 281–291.
[54] U. Laggner, P. Di Meglio, G.K. Perera, C. Hundhausen, K.E. Lacy, N. Ali, et al., Identification of a novel proinflammatory human skin-homing Vgamma9V-delta2 T cell subset with a potential role in psoriasis, J. Immunol. 187 (2011) 2783–2793.

Chapter 5

Adoptive transfer of Vγ9Vδ2 T cells in combination with zoledronic acid treatment inhibits tumour growth and lung metastases in a murine model of osteolytic osteosarcoma

5.1 Chapter Introduction

In Chapter 4 it was established that Vγ9Vδ2 T cells in combination with ZOL are shown to decrease osteolytic breast cancer in the bone. To examine that this immunotherapeutic strategy is also viable for other osteolytic cancers, a study was performed using human osteosarcoma cell lines including the osteolytic osteosarcoma cell line 143B, in combination with ZOL and Vγ9Vδ2 T cells. This chapter is presented in manuscript format and will be submitted to Cancer Immunology, Immunotherapy in July 2017.

5.2 Statement of Authorship

Title of Paper	Adoptive transfer of Vγ9Vδ2 T cells in combination with zoledronic acid treatment inhibits tumour growth and lung metastases in a murine model of osteolytic osteosarcoma
Publication Status	Submitted for Publication
Publication Details	To be submitted to Cancer Immunology, Immunotherapy

Principal Author

Name of Principal Author (Candidate)	Aneta Zysk		
Contribution to the Paper	Performed all *in vitro* and *in vivo* experiments, analysed and interpreted all data, created figures and composed manuscript.		
Overall percentage (%)	90%		
Certification	This paper reports on original research I conducted during the period of my Higher Degree by Research candidature and is not subject to any obligations or contractual agreements with a third party that would constrain its inclusion in this thesis. I am the primary author of this paper.		
Signature		Date	14/03/2017

Co-Author Contributions

By signing the Statement of Authorship, each author certifies that:

i. the candidate's stated contribution to the publication is accurate (as detailed above);

ii. permission is granted for the candidate in include the publication in the thesis; and

iii. the sum of all co-author contributions is equal to 100% less the candidate's stated contribution.

Name of Co-Author	Mark O DeNichilo		
Contribution to the Paper	Co-supervisor, assisted with in vitro work, data interpretation, and manuscript evaluation.		
Signature		Date	27/2/17

Name of Co-Author	Vasilios Panagopoulos		
Contribution to the Paper	Assisted with *in vitro* work, animal ethics, and study design.		
Signature		Date	27/02/2017

Name of Co-Author	Irene Zinonos		
Contribution to the Paper	Assisted with animal handling, tissue collections, and micro-CT analysis.		
Signature		Date	01/03/2017

Name of Co-Author	Vasilios Liapis		
Contribution to the Paper	Assisted with *in vitro* experiments, animal handling and tissue collection.		
Signature		Date	27th Feb 2017

Name of Co-Author	Shelley Hay		
Contribution to the Paper	Assisted with *in vitro* experiments, animal handling, tissue collection, and histology.		
Signature		Date	27/2/17

Name of Co-Author	Vladimir Ponomarev		
Contribution to the Paper	Provided triple reporter gene construct (SFG-NES-TGL) and assisted with manuscript evaluation		
Signature		Date	2/28/2017

Name of Co-Author	Andreas Evdokiou		
Contribution to the Paper	Principal supervisor, assisted with data interpretation, and manuscript evaluation.		
Signature		Date	03/03/2017

5.3 Abstract

Osteosarcoma is the most frequent primary malignancy of the bone in children and adolescents. Localised osteosarcoma can be readily treated with the use of pre-operative chemotherapy in combination with surgery, but drug resistance and toxic off-target side effects can occur. Metastatic spread to the lungs occurs in 15-20% of presenting patients, correlating with poor survival. This study examined the anti-cancer efficacy of *ex vivo* expanded human gamma delta (Vγ9Vδ2) T cells, in combination with zoledronic acid (ZOL), using a mouse model of orthotropic osteosarcoma. *In vitro*, Vγ9Vδ2 T cells had low cytotoxicity against osteosarcoma cell lines, however pre-treatment with ZOL enhanced Vγ9Vδ2 T cells mediated killing of osteosarcoma cells. Vγ9Vδ2 T cells adoptively transferred into NOD/SCID mice localised with osteosarcoma lesions in the tibia and also within the developing secondary lung metastases. Multiple infusions of Vγ9Vδ2 T cells alone were not sufficient to reduce tumour burden, however ZOL pre-treatment improved the anti-cancer efficacy of Vγ9Vδ2T cells. The combination treatment also inhibited tumour induced osteolysis, and Vγ9Vδ2T cells alone reduce both the incidence and burden of lung metastases. Our data provides evidence that Vγ9Vδ2 in combination with ZOL may provide a novel immunotherapeutic approach for the treatment of osteolytic osteosarcoma.

5.4 Introduction

Osteosarcoma is the most frequent primary malignancy of the skeleton in children and adolescents [1]. Lesions can be classed into three phenotypes, based on radiographic appearance; osteolytic (abnormal bone degradation) osteoblastic/osteosclerotic (abnormal bone formation), or mixed (abnormal bone degradation linked to abnormal formation). Current treatments including

neoadjuvant chemotherapy followed by tumour resection result in a 10 year overall survival rate of 70-80% for patients with localised osteosarcoma [21]. However, off-target toxicity and the emergence of drug resistance with the use of conventional chemotherapeutics can limit treatment efficacy and impact patient's quality of life. Additionally, metastatic spread, preferentially to the lungs is seen in 15-20% of presenting patients, correlating with poor survival [21-25]. To prolong survival rates, especially in patients with pulmonary metastases, it is clear that novel therapies are required to target tumour burden in the bone, alleviate symptoms associated with bone lysis, and also target pulmonary metastases.

In recent years, adoptive transfer of cytotoxic gamma delta (γδ) T cells has gained momentum as a potential new immunotherapeutic approach for targeting various solid and haematological malignancies [76-79]. The majority of γδ T cells in human peripheral blood are of the $V\gamma9^{+}/V\delta2^{+}$ (Vγ9Vδ2) phenotype but constitute only 1-10% of circulating lymphocytes [84]. They detect target cells, including microbial infected or transformed (tumour) cells in an MHC-unrestricted manner, by recognition of non-peptic antigens, known as phosphoantigens (PAgs). Following target cell recognition, Vγ9Vδ2 T cells kill via a number of mechanisms, including death receptor/ligand interactions with TRAIL and FASL [79, 98], the release of cytolytic granules [98, 104, 107], and Th1 cytokines such as IFN-γ and TNF-α [104, 107, 108]. It is well documented that Vγ9Vδ2 T cells can be activated and expanded by nitrogen-containing bisphosphonates (nBPs), including zoledronic acid (ZOL) [75, 78-81]. nBPs localise specifically to the bone, where they are internalised by osteoclasts during bone resorption. nBPs inhibit a key enzyme in the mevalonate pathway, causing a loss of osteoclast function and subsequently increased bone volume. Inhibition of the mevalonate pathway also

results in the accumulation of the PAg, isopentenyl pyrophosphate (IPP). Extensive evidence has shown that ZOL pre-treatment sensitises various cancer cells, including osteosarcoma [135], breast [82], glioblastoma [136], lymphoma [81], fibrosarcoma and lung cancer cells [78] to Vγ9Vδ2 T cell cytotoxicity. Several early phase clinical trials demonstrate the potential this treatment regimen has against a variety of advanced cancers [126, 128, 181], however, to date, no studies have examined efficacy against osteosarcoma. Recently, we demonstrated that adoptive transfer of Vγ9Vδ2 T cells in combination with ZOL reduced tumour burden, tumour-associated bone destruction, and lung metastases in a model of osteolytic breast cancer [157]. In this current study, we examined if this treatment regimen would produce a similar outcome in a mouse model of osteolytic osteosarcoma. We confirmed that osteosarcoma cells lines were sensitised to Vγ9Vδ2 T cells following ZOL pre-treatment *in vitro* and that when adoptively transferred to osteosarcoma bearing mice, Vγ9Vδ2 T cells readily localised to osteosarcoma lesions in the bone and within the secondary metastases in the lungs. Although multiple infusions of Vγ9Vδ2 T cells alone had no significant impact on tumour burden in the bone, *in vivo* ZOL pre-treatment enhanced the anti-cancer efficacy of Vγ9Vδ2 T cells. Additionally, Vγ9Vδ2 T cells reduced both the incidence and tumour burden of lung metastases, and in combination with ZOL, greatly inhibited tumour-associated bone destruction. Overall, this study demonstrates that adoptive transfer of Vγ9Vδ2 T cells in combination with ZOL has great potential as a novel immunotherapeutic approach for the treatment of osteosarcoma.

5.5 Materials and Methods

5.5.1 Cells and reagents

143B and KHOS human osteosarcoma cancer cell lines were obtained from ATCC (Manassas, VA, USA). Both cell lines expressed GFP and firefly luciferase produced by retroviral expression of the SFG-NES-TGL vector, as previously described [158]. Cancer cells were cultured in Dulbecco's Modified Eagle's Medium (DMEM, Life Technologies, Australia) supplemented with 10% foetal bovine serum (FBS, Life Technologies, Australia), 100IU/mL penicillin (Life Technologies, Australia), 100µg/mL streptomycin (Life Technologies, Australia), and 25mM HEPES (Life Technologies, Australia) at 37°C in a 5% CO_2 humidified atmosphere. ZOL was generously provided by Novartis Pharma AG.

5.5.2 *Ex vivo* expansion and enrichment of Vγ9Vδ2 T cells

Vγ9Vδ2 T cells were expanded as previously described [157]. Informed consent was obtained prior to the collection of peripheral blood from healthy adult donors. Peripheral blood mononuclear cells (PBMC) were isolated by density gradient centrifugation using Lymphoprep™ (Axis Shield, Norway). PBMC were resuspended to $1x10^6$/mL in CTS™ OpTmizer™ T Cell Expansion SFM (Life Technologies, Australia) supplemented with OpTmizer™ T cell Expansion Supplement (1:38 dilution) (Life Technologies, Australia), 10% heat inactivated FBS (HI-FBS), 100IU/mL penicillin, 100µg/mL streptomycin, 2mmol L-glutamine (Life Technologies, Australia), 25mM HEPES (Life Technologies, Australia), 0.1% β-mercaptoethanol (Sigma-Aldrich, USA), recombinant human interleukin 1 (rhIL-2) (100IU/mL) (BD Pharmingen, USA) and activated with 5µM ZOL, then seeded into 6-well plates. Cell culture density was maintained at 1-2 x 10^6 cells/mL and replenished with fresh medium containing rhIL-2 (100IU/ml) only (without

ZOL) every 2-3 days. Following 7-8 days of culture, *ex vivo* expanded Vγ9Vδ2 T cells were enriched prior to *in vitro* and *in vivo* experiments using magnetic activated cell sorting (MACS) system using negative selection with the TCR γ/δ+ T cell Isolation Kit (human) (Miltenyi Biotec, Germany). Cell viability and total cells numbers after enrichment were assessed using trypan blue exclusion and Vγ9Vδ2 T cell percentages were determined by flow cytometry using PeCy5 conjugated anti-CD3 (clone UCHT1) (eBioscience, San Diego, CA, USA) and FITC conjugated anti-Vγ9 TCR from BD Biosciences (San Jose, CA, USA). Analysis was performed on the BD FACSCanto II Flow Cytometer (San Jose, CA, USA). After enrichment, the percentage of Vγ9Vδ2 T cells was consistently <97% (data not shown) and enriched cells were frozen then thawed for future *in vitro* and *in vivo* experiments.

5.5.3 Cell cytotoxicity assay

Cytotoxicity of Vγ9Vδ2 T cells against osteosarcoma cell lines was assessed using a standard lactate dehydrogenase (LDH) release assay (CytoTox 96® Non-Radioactive Cytotoxicity Assay; Promega, USA). Briefly, $1x10^4$ target cells (KHOS or 143B) were seeded in a 96-well microtiter plate and allowed to adhere overnight. Target cells were then treated with or without 25μM ZOL for 24 hours, and then co-cultured with effector cells (Vγ9Vδ2 T cells) at 1:1, 5:1 and 10:1 E:T (effector: target) ratios. After incubation for 9 hours at 37°C, 50μL of supernatant was assayed for LDH activity following the manufactures protocol. The appropriate controls were prepared and cytotoxicity was calculated as:

$$\% \text{ Cytotoxicity} = \frac{\text{experimental release - effector spontaneous release - target spontaneous release}}{\text{target maximum release} - \text{target spontaneous release}} \text{ x } 100$$

5.5.4 Cell viability assay

Both osteosarcoma cell lines were luciferase-tagged, which was the basis for a luciferase activity viability assay using Dual Luciferase® Reporter Assay kit (Promega, Madison, WI, USA). Briefly, $1x10^4$ target cells were seeded in a 96-well microtiter plate and allowed to adhere overnight. Cells were then treated with or without 25µM ZOL for 24 hours, and then co-cultured with Vγ9Vδ2 T cells at 1:1, 5:1 and 10:1 E:T ratios. After incubation for 24 hours, media was removed from the wells and cells were washed in 1x PBS, then lysates were prepared and analysed following the manufacturers protocol. Viability was calculated as:

$$\% \text{ Viability} = \frac{\text{experimental value}}{\text{untreated control value}} \text{ x } 100$$

5.5.5 Western Blotting

Detection of unprenylated small GTPases, including RAP1, are used to indirectly determine the extent of FPPS inhibition by ZOL, which correlates with increased IPP levels, resulting in the increased detection of cancer cells by Vγ9Vδ2 T cells and greater cytotoxicity. To determine the effect of ZOL on the prenylation of small GTPases in osteosarcoma cells, lysates were analysed by Western blotting for total and unprenylated RAP1. Briefly, $1x10^6$ osteosarcoma cells were seeded in a $25cm^2$ flask, allowed to adhere overnight, and then treated with 25µM ZOL for 0, 4, 8, 12 and 24 hours. Lysates were prepared as previously described [158] and immunodetection was performed overnight at 4^oC in PBS/blocking reagent containing 0.1% Tween-20, using the following primary antibodies at the dilutions suggested by the manufacturer: pAb anti-RAP1 (121) for total RAP1 protein, pAB anti-RAP1A (C-17) specifically for unprenylated RAP1 (Santa Cruz Biotechnology, USA), and anti-actin mAb (Sigma-Aldrich, USA) as a loading

control. Membranes were then rinsed several times with PBS containing 0.1% Tween-20 and incubated with 1:5,000 dilution of anti-goat or anti-rabbit alkaline phosphatase-conjugated secondary antibodies (Thermo Fisher Scientific, USA) for 1 hour. Visualisation of protein bands was performed using the ECF substrate reagent kit (GE Healthcare, UK) on a LAS-4000 (GE Healthcare, UK).

5.5.6 Labelling Vγ9Vδ2 T cells with fluorescent DiR dye

Vγ9Vδ2 T cells were expanded and enriched as described above, then labelled with XenoLight DiR Fluorescent Dye (Perkin Elmer, USA) as previously described [157]. Briefly, DiR dye was added to cells at a final concentration of 16.6µg/mL. Cells were incubated in the dark for 10-15 minutes at 37°C, washed three times in DPBS containing 10% HI-FBS, and resuspended to $5x10^7$/mL ($5x10^6$/100µL). Cell viability of labelled cells did not differ to unlabelled cells, as assessed by trypan blue exclusion and labelling efficacy was >90% as assessed by flow cytometry using the filter corresponding to PeCy7.

5.5.7 Animals

Female four-week-old non-obese diabetic severe combined immunodeficient (NOD/SCID) mice were purchased from the Animal Resources Centre (Canning Vale, WA, Australia) and housed under pathogen free conditions in The Queen Elizabeth Hospital Experimental Surgical Suite (Woodville, SA, Australia). Mice were acclimatised to the animal housing facility and the general wellbeing of animals was monitored continuously throughout the experiment. All experimental procedures were carried out with adherence to the rules and guidelines for the ethical use of animals in research and were approved by the Animal Ethics Committees of the University of Adelaide and the Institute of Medical and Veterinary Science, Adelaide, SA, Australia.

5.5.8 *In vivo* localisation

To examine *in vivo* localisation of Vγ9Vδ2 T cells to osteosarcoma lesions, intratibial (i.t) injections were performed as previously described [146, 158]. Briefly, five-week old female NOD/SCID mice were anaesthetised by isoflurane (Veterinary Companies of Australia, Australia). The left leg was shaved, wiped with 70% ethanol, then a 27-guage needle coupled to a Hamilton syringe was used to inject 1 x 10^5 luciferase-tagged 143B osteosarcoma cells resuspended in 10µL PBS, directly through the tibial plateau into the bone marrow space. The contralateral tibia was not injected. Once tumours were established, mice were injected with 5x10^6 DiR labelled Vγ9Vδ2 T cells i.v, prepared as described above. Non-invasive, whole body imaging to monitor Vγ9Vδ2 T cell localisation and tumour growth was done using the IVIS Spectrum *in vivo* imaging system (Caliper Life Sciences, Australia). For fluorescence imaging, mice were anaesthetised by isoflurane (Veterinary Companies of Australia, Australia) and images were acquired using the optimised settings for DiR dye: f stop: 2, medium binning, ex/em: 745/800nm. Images were taken at multiple time points, up to 120 seconds. For bioluminescence imaging, mice were injected s.c with 100µL of D-luciferin solution (Perkin Elmer, USA) to a final dose of 3mg/20g mouse body weight. Mice were then anaesthetised by isoflurane and bioluminescence was acquired between 0.5 and 30 seconds (images shown at 1 second). Photon emission was quantified as Total Flux measured in [photons/sec] using Living Image 4.2 (Caliper Life Sciences, Australia) software. There was no interference between the DiR dye and the luciferase-tagged cancer cells, therefore fluorescence and bioluminescence images could be acquired in succession to form a composite image to assess Vγ9Vδ2 T cell localisation to tumour lesions. After Vγ9Vδ2 T cell infusion, *in vivo*

images were acquired at 20 minutes, 24 hours, 48 hours, and *ex vivo* images were acquired after 3 days.

5.5.9 *In vivo* anti-tumour efficacy of ZOL and Vγ9Vδ2 T cells

I.t injections were performed as described above and once tumours were established, mice were assigned into four treatment groups: control (no treatment, n=5), ZOL alone (100µg/kg s.c, n=6), Vγ9Vδ2 T cells alone ($1x10^7$/100µL injected via the tail vein, n=7), and ZOL + Vγ9Vδ2 T cells (infusion of Vγ9Vδ2 T cells 24hrs after ZOL, treatments as above, n=8). Treatments were given a total of three times. Tumour bioluminescence was monitored over the study period, using the IVIS Spectrum *in vivo* imaging system as outlined above. If pain relief was required, mice were given Rimadyl (carprofen) (Pfizer Animal Health, Australia) at 5mg/kg s.c every 24hr for a maximum of three days. After 3 weeks, mice were sacrificed, and lungs were imaged for *ex vivo* bioluminescence to quantify lung metastases, and tumour bearing and non-tumour bearing control tibia from each animal were surgically resected for micro-computed tomography.

5.5.10 *Ex vivo* micro-computed tomography (µCT) analysis

Tibias for µCT analysis were scanned using the SkyScan-1076 high-resolution µCT Scanner (Bruker). The scanner was operated at 50kV, 110µA, rotation step of 0.5, 0.5-mm aluminium filter, and scan resolution of 7.8µm/pixel. Cross-sections were reconstructed using the cone-beam algorithm in NRecon (V1.6.9.8, Bruker). Images were then realigned in DataViewer (1.5.1.2, Bruker) and imported into CT Analyser (CTAn) (V1.14.4.1+, Bruker, Skyscan). Using the two-dimensional images obtained from the CTAn, the growth plate was identified and 650 sections starting from the growth plate/tibial interface and moving down the tibia were selected for quantification of total bone morphometric parameters

and 250 sections starting 35 sections down from the growth plate, were selected for trabecular bone morphometric parameters. Representative three-dimensional images of total bone were generated in CTvox (V2.7.0, Bruker).

5.5.11 Data analysis and statistics

In vitro experiments were conducted at least twice using biological triplicates, and data presented is mean ± SEM, unless otherwise specified. A representative experiment is shown for Western immunoblot data. Two-tailed unpaired Student's t-test was used, unless otherwise specified and in all cases p-values <0.05 were considered statistically significant. All statistical analysis was conducted using SigmaPlot v12.5 (Systat Software Inc., USA).

5.6 Results

5.6.1 ZOL sensitises osteosarcoma cells to Vγ9Vδ2 T cell cytotoxicity *in vitro*

The *in vitro* cytotoxicity of purified *ex vivo* expanded Vγ9Vδ2 T cells in combination with ZOL was evaluated against two human osteosarcoma cell lines, 143B and KHOS. After 9 hours, both cell lines showed a maximum of 10% specific lysis when cultured with Vγ9Vδ2 T cells alone, and there was no E:T (effector target) dependent increase in lysis (Figure 5.1 A). However, ZOL pre-treatment for 24 hours, followed by co-culture with Vγ9Vδ2 T cells for 9 hours, resulted in a significant increase in cytotoxicity in both cell lines and occurred in an E:T

Figure 5.1 ZOL sensitises osteosarcoma cells to Vγ9Vδ2 T cell cytotoxicity *in vitro*.

Luciferase-tagged 143B and KHOS osteosarcoma cells were pre-treated with 25μM ZOL (●) or left untreated (□) for 24 hours. Cancer cells were then co-cultured with *ex vivo* expanded Vγ9Vδ2 T cells (E:T, 1:1, 5:1, 10:1) for 9 or 24 hours. **A.** After 9 hours co-culture, LDH release was measured and expressed as percentage cytotoxicity using the calculation outlined in the methods. **B.** After 24 hours co-culture, overall cancer cell viability was measured using a luciferase based activity assay. Luciferase activity was measured and expressed as percentage viability using the calculation outlined in the methods. LDH and viability data was pooled and normalised from two separate experiments (n=6). **C.** Western immunoblot analysis showing inhibition of prenylation in 143B and KHOS osteosarcoma cells treated with 25μM ZOL over a 24 hour time course (0, 4, 8, 12, 24 hours). Images representative of n=2-3. Unpaired two-tailed Student's t-test was performed comparing each treatment group to untreated (*$p<0.05$, **$p<0.005$, ***$p<0.001$, non-significant values not shown). Columns and error bars represent mean and ± %SEM

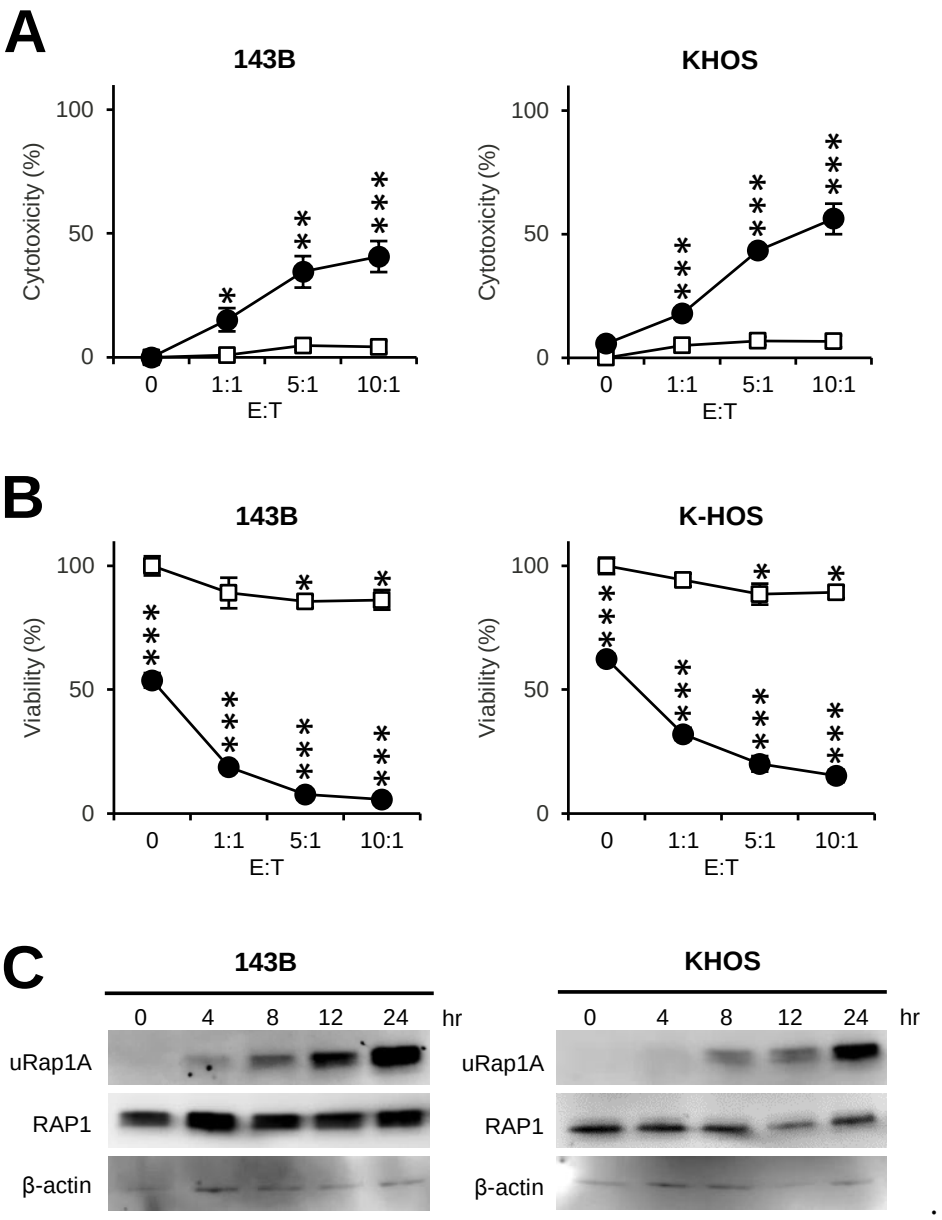
A
143B
KHOS
Cytotoxicity (%)
100
50
0
0
1:1
5:1
10:1
E:T
B
143B
K-HOS
Viability (%)
C
143B
KHOS
0
4
8
12
24
hr
uRap1A
RAP1
β-actin

dependent manner, resulting in a maximum of 40% and 56% lysis of 143B and KHOS cells respectively (Figure 5.1 A). Additionally, osteosarcoma cell viability was assessed using a luciferase based assay following a 24 hour co-culture with Vγ9Vδ2 T cells. After 24 hours treatment with Vγ9Vδ2 T cells, both osteosarcoma cell lines showed a maximum of 10% cell death, which was E:T independent (Figure 5.1 B). However, following 24 hour ZOL pre-treatment and 24 hour co-culture with Vγ9Vδ2 T cells, there was a significant increase in cytotoxicity in both cell lines which occurred in an E:T dependent manner, resulting in a maximum of 95% and 80% cell death of 143B and KHOS cells respectively (Figure 5.1 B). These data indicate ZOL potentiates the cytotoxicity of Vγ9Vδ2 T cells *in vitro*. Both cell lines were sensitive to Vγ9Vδ2 T cells, so we examined inhibition of RAP1 prenylation over 24hr of ZOL treatment. This method was used to indirectly measure the extent of FPPS inhibition by ZOL, which leads to IPP accumulation allowing sensitization of cancer cells to Vγ9Vδ2 T cell cytotoxicity *in vitro.* 143B and KHOS osteosarcoma cells both showed a time dependent increase in unprenylated RAP1A (Figure 5.1 C). Of these two osteosarcoma cell lines, 143B was observed to inhibit FPPS at a faster rate, with unprenylated RAP1 clearly evident after just 4 hours. Greater proliferation or protein synthesis rates of the 143B cell line could account for faster accumulation of unprenylated RAP1A observed, however this was not further investigated.

5.7 *Ex vivo* expanded Vγ9Vδ2 T cells localise to tumours in the bone

We next examined the ability of Vγ9Vδ2 T cells to co-localise to tumour lesions in a model of osteolytic osteosarcoma. We have previously shown that Vγ9Vδ2 T cells can labelled with the DiR fluorescent dye, with >90% labelling efficiency as analysed by flow cytometry, without effecting Vγ9Vδ2 T cell viability

or cytotoxicity [157]. For localisation studies, mice were inoculated with luciferase-tagged 143B cancer cells injected directly into the tibia, and after several days bioluminescence could be detected. Mice were pre-treated with or without 100μg/kg ZOL s.c and 24 hours later, mice were infused with DiR labelled Vγ9Vδ2 T cells via the tail vein. Within 20 minutes of infusion, fluorescence could be detected in the liver and lungs, and in the tibia of mice pre-treated with ZOL (Figure 5.2 A). After 24 and 48 hours, fluorescence was observed in the liver, spleen and tumour-bearing tibia of all mice. Consistently, more fluorescence was observed in the tumour-bearing tibia of mice pre-treated with ZOL (Figure 5.2 A). A composite image overlaying fluorescence and bioluminescence showed fluorescence produced by the Vγ9Vδ2 T cells correlate with bioluminescence produced by tumour cells (Figure 5.2 D). Three days following Vγ9Vδ2 T cell infusion, mice were sacrificed and the legs, liver, lungs, and spleen were imaged *ex vivo*. Strong fluorescence was observed in the imaged organs (Figure 5.2 D). Additionally, fluorescence that was observed in the tibia and lungs corresponded with bioluminescence signal of the tumour bearing tibia and lung, suggesting co-localisation of Vγ9Vδ2 T cells with tumour cells at these sites (Figure 5.2 D).

5.7.1 ZOL potentiates the anti-cancer efficacy of Vγ9Vδ2 T cells against osteosarcoma

To examine the *in vivo* anti-cancer efficacy of Vγ9Vδ2 T cells in a model of osteolytic osteosarcoma, NOD/SCID mice were inoculated with luciferase-tagged 143B cells directly into the left tibia. Once tumours were established as measured by an increase of bioluminescence signal, treatments were commenced. ZOL was administered 24 hours prior to each Vγ9Vδ2 T cell infusion. This treatment regime was repeated three times over two weeks. After three treatments,

Figure 5.2 Fluorescently labelled Vγ9Vδ2 T cells localise to osteosarcoma lesions *in vivo*.

5-week old female NOD/SCID mice were inoculated with luciferase-tagged human osteolytic osteosarcoma cells (143B) directly into the left tibia. Mice were injected with ZOL (100µg/kg s.c) or left untreated. 24 hours later, DiR labelled Vγ9Vδ2 T cells were infused via the tail vein. Fluorescence images were acquired on the IVIS Spectrum *in vivo* imaging system **A.** 20 minutes, **B.** 24 hours, and 48 hours after infusion. Fluorescence and bioluminescence images were acquired to create a composite image after **C.** 24 hours *in vivo,* and **D.** *ex vivo,* 3 days after infusion. *Ex vivo* images show lungs from two mice in the ZOL treated group, one with metastases and one without. BL= bioluminescence, FL= fluorescence.

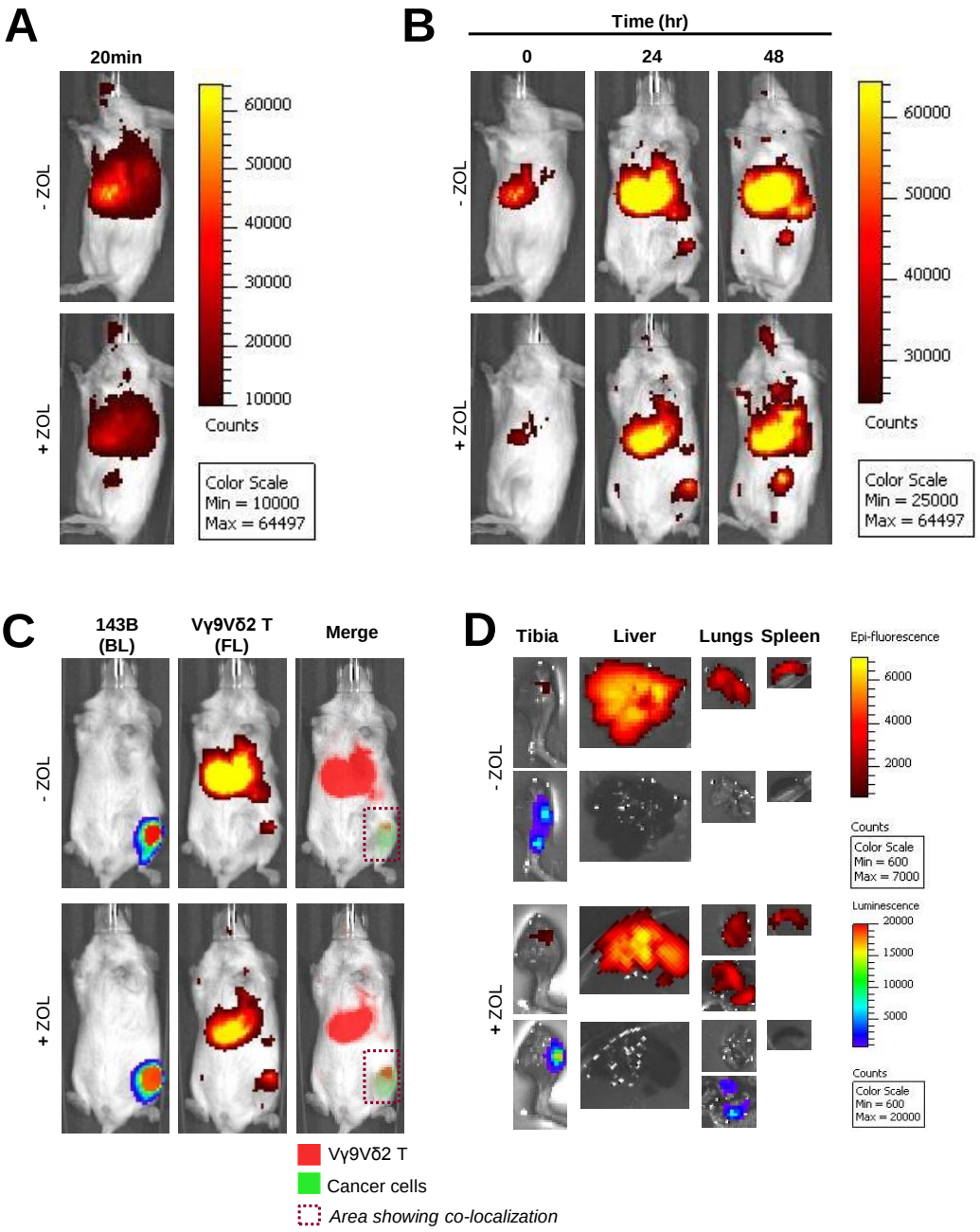
A
20min
- ZOL
+ ZOL
60000
50000
40000
30000
20000
10000
Counts
Color Scale
Min = 10000
Max = 64497
B
Time (hr)
0
24
48
- ZOL
+ ZOL
60000
50000
40000
30000
Counts
Color Scale
Min = 25000
Max = 64497
C
143B (BL)
Vγ9Vδ2 T (FL)
Merge
- ZOL
+ ZOL
Vγ9Vδ2 T
Cancer cells
Area showing co-localization
D
Tibia
Liver
Lungs
Spleen
- ZOL
+ ZOL
Epi-fluorescence
6000
4000
2000
Counts
Color Scale
Min = 600
Max = 7000
Luminescence
20000
15000
10000
5000
Counts
Color Scale
Min = 600
Max = 20000

there was no difference in tumour burden between the untreated, ZOL alone, or Vγ9Vδ2 T cell alone treated groups (Figure 5.3). In contrast, animals treated with ZOL in combination with Vγ9Vδ2 T cells showed a strong trend towards a decrease in tumour bioluminescence (Figure 5.3).

5.7.2 Vγ9Vδ2 T cells reduce the incidence and tumour burden of lung metastases

Lung metastases are frequently seen in patients with osteosarcoma, correlating with poor survival. Analogous to human disease, animals inoculated with the 143B cells develop lung metastases three to four weeks after cancer cell inoculation. To examine the efficacy of Vγ9Vδ2 T cells alone and in combination with ZOL on the incidence and tumour burden of lung metastases, tumour bioluminescence in the lungs was assessed (Figure 5.4). Sixty percent of mice in the untreated group exhibited lung metastases, which was comparable to ZOL treatment alone (66%), however, ZOL reduced tumour burden by approximately half compared to untreated (Figure 5.4). Vγ9Vδ2 T cells alone and in combination with ZOL further reduced tumour incidence to 29% and 25% respectively, and tumour burden was almost undetectable in these treatment groups (Figure 5.4).

5.7.3 ZOL in combination with Vγ9Vδ2 T cells inhibits bone degradation

Orthotropic inoculation of 143B osteosarcoma cells into the tibia results in predominantly osteolytic lesions [158]. Therefore, to evaluate the efficacy of Vγ9Vδ2 T cells alone or in combination with ZOL to protect the bone from tumour-induced osteolysis, tibias were analysed using three-dimensional (3D) μCT imaging (Figure 5.5). Osteolysis was measured as the percentage difference in bone volume between the tumour bearing and non-tumour bearing tibia. Qualitative and quantitative μCT showed bone loss in the untreated, ZOL alone, and Vγ9Vδ2 T cell

Figure 5.3 ZOL enhances the anti-cancer efficacy of Vγ9Vδ2 T cells against osteolytic osteosarcoma.

Luciferase-tagged 143B cells were injected directly into the left tibial cavity of 5-week old female NOD/SCID mice. Once tumours were established, treatments were commenced as outlined in the methods (n=5-8 mice per group). Animals remained untreated (△) or were administered with ZOL alone (◇), Vγ9Vδ2 T cells alone (□) or ZOL in combination with Vγ9Vδ2 T cells (●). Whole body bioluminescence images were acquired on the IVIS Spectrum *in vivo* imaging system over the course of the study. A representative bioluminescence image of a single mouse from each treatment group is shown. The line graph shows the quantification of bioluminescence signal over the course of the study and is expressed as the fold change in total flux [photons/second] from Day 8.

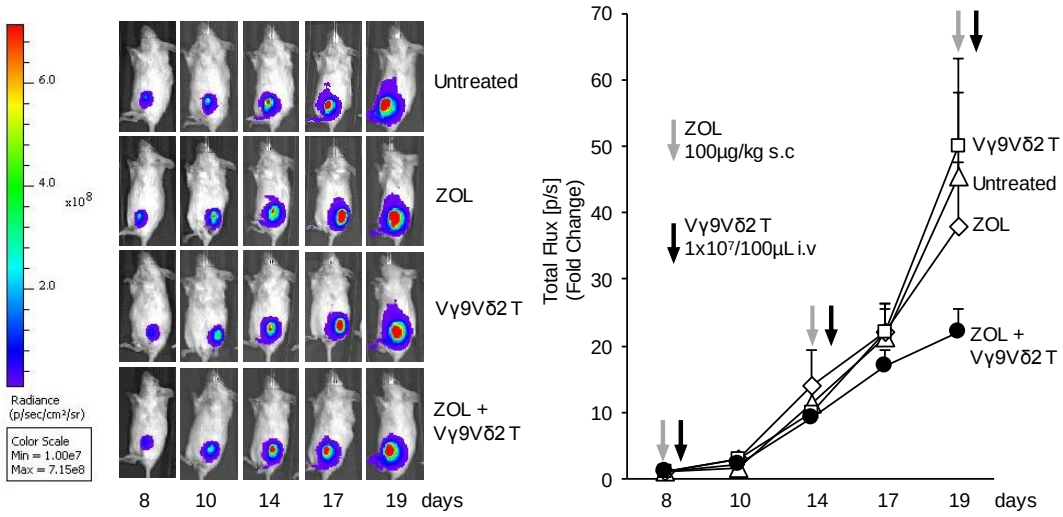
6.0
4.0
x10^8
2.0
Radiance
(p/sec/cm²/sr)
Color Scale
Min = 1.00e7
Max = 7.15e8
Untreated
ZOL
Vγ9Vδ2 T
ZOL +
Vγ9Vδ2 T
8
10
14
17
19
days
Total Flux [p/s]
(Fold Change)
70
60
50
40
30
20
10
0
ZOL
100µg/kg s.c
Vγ9Vδ2 T
1x10⁷/100µL i.v
Vγ9Vδ2 T
Untreated
ZOL
ZOL +
Vγ9Vδ2 T
8
10
14
17
19
days

Figure 5.4 Vγ9Vδ2 T cells reduce the incidence and tumour burden of lung metastases.

At the time of sacrifice, lungs were removed for *ex vivo* bioluminescence quantification of tumour burden. Incidence rate was calculated as the percentage of mice exhibiting pulmonary metastases by observing bioluminescence signal detected on the IVIS Spectrum *in vivo* imaging system. Tumour burden is shown as the average bioluminescence intensity detected for each treatment group expressed as total flux [photons/second]. A corresponding representative bioluminescence image of the lungs from each treatment group is shown. Columns and error bars represent median values and SEM.

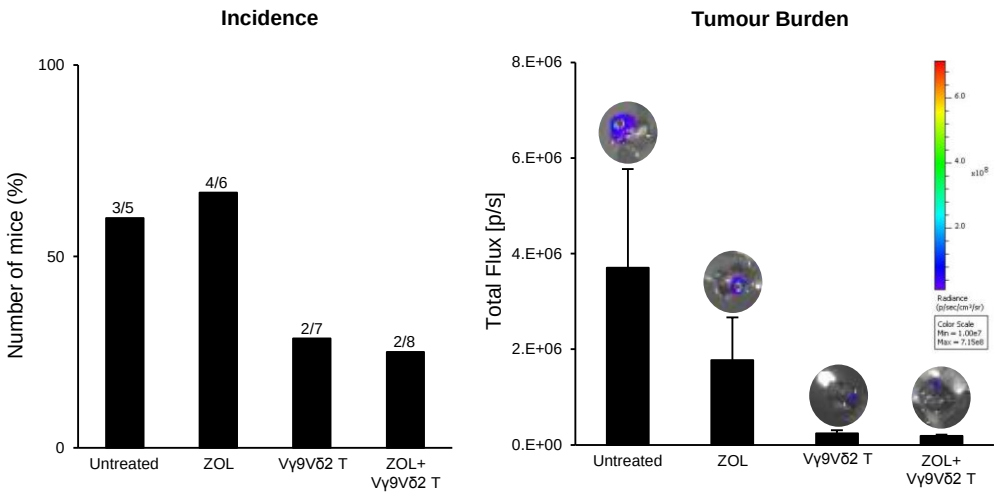
Incidence
Number of mice (%)
100
50
0
3/5
4/6
2/7
2/8
Untreated
ZOL
Vγ9Vδ2 T
ZOL+
Vγ9Vδ2 T
Tumour Burden
Total Flux [p/s]
8.E+06
6.E+06
4.E+06
2.E+06
0.E+00
Untreated
ZOL
Vγ9Vδ2 T
ZOL+
Vγ9Vδ2 T

Figure 5.5 Vγ9Vδ2 T cells in combination with ZOL reduce tumour-associated osteolysis in total and trabecular bone.

A. The osteolytic nature of 143B osteosarcoma cell line can be seen in the representative qualitative μCT 3D images. Quantitative assessment of **B.** total bone and **C.** trabecular bone volume is expressed as a percentage difference between the tumour bearing tibia and non-tumour bearing tibia. A one-tailed student's t-test was performed comparing each treatment group to untreated (*$p<0.05$, **$p<0.005$, ***$p<0.001$, ns= non-significant). Columns and error bars represent mean and %SEM.

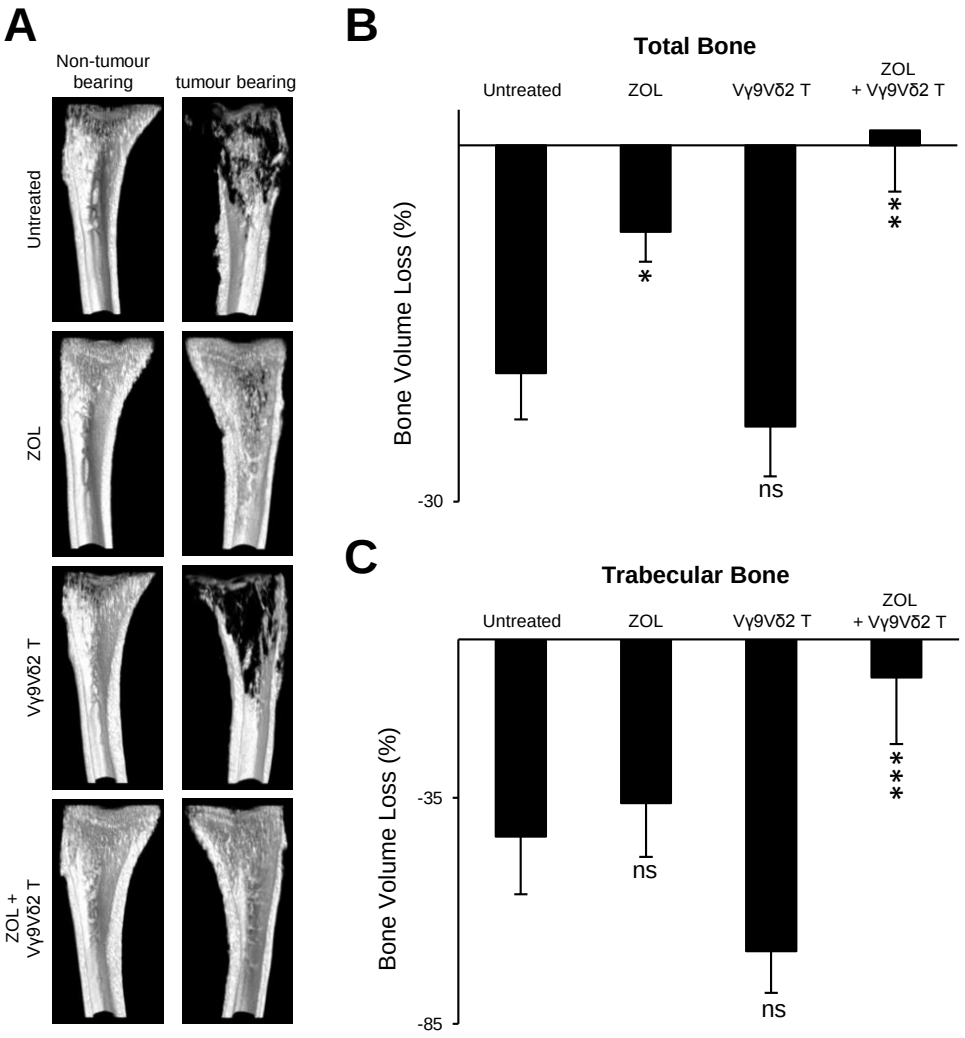
A
Non-tumour bearing
tumour bearing
Untreated
ZOL
Vγ9Vδ2 T
ZOL + Vγ9Vδ2 T
B
Total Bone
Untreated
ZOL
Vγ9Vδ2 T
ZOL + Vγ9Vδ2 T
Bone Volume Loss (%)
-30
*
ns
**
C
Trabecular Bone
Untreated
ZOL
Vγ9Vδ2 T
ZOL + Vγ9Vδ2 T
Bone Volume Loss (%)
-35
-85
ns
ns
***

alone treated groups, but with differences in the extent of osteolysis. Untreated animals showed the greatest osteolysis with 19.2% total bone volume (T.BV) loss and 43.6% trabecular bone volume (Tb.BV) loss. In contrast, ZOL treatment alone increased bone volume and showed 7.3% T.BV loss and 36.2% Tb.BV loss. Animals treated with Vγ9Vδ2 T cells alone showed similar T.BV loss compared with untreated animals (23.7% compared to 19.2%), but greater Tb.BV loss (69.0% compared with 43.6%). However, animals treated with ZOL in combination with Vγ9Vδ2 T cells had the least amount of bone loss, showing a 1.5% gain in T.BV, and only 8.4% Tb.BV loss.

5.8 Discussion

To date, the anti-cancer efficacy of Vγ9Vδ2 T cells in combination with ZOL has not been investigated for the treatment of osteosarcoma. In this study, we used a well-established murine model of osteosarcoma that resembles the human disease [158] and assessed the anti-cancer efficacy of adoptive transfer of Vγ9Vδ2 T cells alone and in combination with ZOL in the context of primary tumour growth in bone and the subsequent lung metastases. We also investigated the effect these treatments had on osteosarcoma induced bone destruction.

Vγ9Vδ2 T cells alone exhibited limited cytotoxicity against both osteosarcoma cell lines *in vitro.* However, pre-treatment with ZOL significantly sensitised cancer cells to Vγ9Vδ2 T cells mediated killing *in vitro,* while *in vivo* ZOL showed a trend towards enhanced anti-cancer efficacy, consistent with previous studies [77, 78, 157]. Currently, the mechanism of *in vivo* ZOL sensitization is unclear, however it is unlikely that cancer cells directly uptake ZOL *in vivo.* It is known that nBPs are preferentially internalised by tumour associated macrophages (TAMs) and not by cancer cells *in vivo* [179]. Under certain

conditions, macrophages have the ability to produce chemotactic factors including monocyte chemoattractant protein-1 (MCP-1) and IL-8 which recruit γδ T cells *in vitro* [180]. We previously proposed that ZOL internalisation by TAMs may result in the recruitment of Vγ9Vδ2 T cells to the tumour microenvironment, thereby enhancing anti-cancer efficacy [157]. In line with our hypothesis, in this study ZOL pre-treated animals were observed to have more Vγ9Vδ2 T cells localisation to the tumour mass compared with untreated animals. However, this data was purely observational, therefore further *in vitro* and *in vivo* studies will be required to fully understand the interactions between TAMs and Vγ9Vδ2 T cells, and potential mechanisms resulting in migration to the tumour microenvironment.

Patients with osteosarcoma frequently experience lung metastases, which contributes to poor survival. This study showed that Vγ9Vδ2 T cells reduced the incidence and tumour burden of lung metastases, consistent with previous findings [157, 178]. Additionally, in two early-phase clinical trials, patients exhibiting metastatic lung lesions from advanced renal cell carcinoma showed decreased growth rate of these lesions and no new lesions detected following Vγ9Vδ2 T cell treatment [97, 181]. Here, we demonstrated that Vγ9Vδ2 T cells are readily detected in the lungs of mice for up to three days following infusion, showing co-localisation with lung tumour lesions. Although Vγ9Vδ2 T cells localise to the lungs, it is still unclear if decreased lung metastases are due to Vγ9Vδ2 T cells directly targeting cancer cells in the lung or circulating Vγ9Vδ2 T cells targeting disseminated cancer cells prior to establishing in the lung, or both. It is also interesting to note that ZOL does not enhance the anti-metastatic effect, suggesting it is due to Vγ9Vδ2 T cells alone.

ZOL is a well-characterised anti-bone resorptive agent approved for the treatment of osteoporosis, Paget's disease of the bone, and skeletal metastases. ZOL administration in patients with primary and metastatic bone cancer inhibits tumour-associated bone loss, increases bone density, and as a result, reduces skeletal related events such as fractures and hypercalcemia [50, 52, 53]. In addition to these anti-bone resorptive effects, studies also suggest ZOL possesses a wide range of anti-cancer properties by inducing cell death, inhibiting proliferation, invasion, and angiogenesis [57-62]. However, the anti-cancer efficacy reported in preclinical models appears to be contradictory 62-65, 67, 68]. This study showed that ZOL alone inhibited tumour-associated bone loss and this is consistent with the well-established role of ZOL on osteoclastic bone resorption. ZOL in combination with Vγ9Vδ2 T cells showed the greatest protection from osteosarcoma induced bone loss, such that the tumour-bearing tibia resembled the non-tumour bearing tibia. However, ZOL alone showed no effect on primary tumour burden, consistent with previous studies in orthotropic osteosarcoma models [67, 68].

In this study, ZOL in combination with Vγ9Vδ2 T cell adoptive transfer showed some anti-cancer efficacy reducing lung metastases, and protecting the bone from osteolysis, however, this treatment regimen did not fully eradicate the primary tumour. Chemotherapy or antibodies in combination with Vγ9Vδ2 T cells have been previously shown to enhance Vγ9Vδ2 T cell cytotoxicity [81, 115, 116, 138]. Pre-clinical studies examining the effects of pro-apoptotic receptor agonists such as recombinant human TRAIL and drozitumab, a monoclonal antibody against DR5, or the hypoxia activated drug, TH-302 (evofosfamide) have shown anti-cancer efficacy against osteosarcoma and osteolytic breast cancer [141, 146, 158]. The efficacy of these compounds in combination with Vγ9Vδ2 T cell adoptive

transfer has not yet been tested, however these combinations could provide new treatment opportunities for osteosarcoma and other cancers that affect the bone.

Overall, this study demonstrates that adoptive transfer of Vγ9Vδ2 T cells in combination with ZOL reduces tumour growth, inhibits tumour-associated bone loss, and limits further lung metastases in a murine model of orthotropic osteosarcoma. Therefore, this two-pronged approach may be appropriate at reducing disease severity in patients with osteosarcoma. However, further studies are required to optimise anti-cancer efficacy, potentially in combination with other therapies.

5.9 Conflict of Interest

The authors declare no conflict of interest.

5.10 Acknowledgments

A. Evdokiou is funded by The Hospital Research Foundation (THRF) and Australian Breast Cancer Research (ABCR). The authors would like to thank Ms Ruth Williams and Dr. Agatha Labrinidis from Adelaide Microscopy at The University of Adelaide for technical assistance with the SkyScan 1076 and related software.

Chapter 6

Adoptive transfer of Vγ9Vδ2 T cells has a neutral effect on normal bone homeostasis

6.1 Introduction

The preceding chapters have examined the anti-cancer efficacy of Vγ9Vδ2 T cells, either alone or in combination with ZOL, and the effect these treatments have on bone homeostasis in the tumour bearing tibia. By examining the contralateral tibia from these studies, the effect these treatments have on normal bone homeostasis can also be assessed.

Vγ9Vδ2 T cells can target and kill osteosarcoma cells *in vitro* and *in vivo* [75, 79, 135], however little is currently known about the role Vγ9Vδ2 T cells have on the cells responsible for normal bone homeostasis. As discussed in the introduction, *in vitro* studies have shown that human γδ T cells can inhibit osteoclast formation [148] and are cytotoxic towards osteoclasts when co-cultured with multiple myeloma cells [80]. Human γδ T cells are known to express factors such as IGF, FGF [149], and CTGF [150], which are important osteoblast growth factors. Additionally, in osteoporotic patients, Vγ9Vδ2 T cells are important in protecting the bone, based on the observation that patients who experienced BAONJ following treatment with intravenous nBPs were severely deficient in Vγ9Vδ2 T cells [73]. Apart from this clinical observation, most *in vivo* studies examining the role of γδ T cells in bone have been conducted using murine γδ T cells, which differ from human Vγ9Vδ2 T cells. Unlike Vγ9Vδ2 T cells, murine γδ T cells do not respond to PAgs and have been reported to both impair and promote bone fracture healing [154, 155]. As more clinical trials are studying Vγ9Vδ2 T cell immunotherapy, it is important to examine their effect on normal bone homeostasis following adoptive transfer.

In addition to examining the effect of Vγ9Vδ2 T cells, the current study also compared two different ZOL dosing schedules and their effect on normal bone

homeostasis. For the treatment of osteoporosis, ZOL is generally administrated as a single yearly infusion of 4mg, equivalent to 100µg/kg in pre-clinical models. However, administrations become more frequent for the treatment for SREs arising from cancerous bone lesions and in Vγ9Vδ2 T cell immunotherapy trials [50, 51, 122-124] Previous pre-clinical studies of osteolytic osteosarcoma and osteolytic breast cancer have shown that multiple ZOL administrations result in increased bone volume to tissue ratio (BV/TV) in both the tumour bearing and non-tumour bearing tibias, compared to a single conventional ZOL administration (ZOL-C; single administration of 100µg/kg) [63, 67]. Pre-clinical studies have shown that multiple nBP administrations are required to potentiate the anti-cancer efficacy of Vγ9Vδ2 T cells [77, Chapters 3-5] and two different ZOL administration schedules were used in these studies: metronomic dosing (ZOL-M, 1st treatment, 25µg/kg, following treatments, 50µg/kg, every 3-5 days) and multiple conventional (ZOL-XC, 100µg/kg every 3-5 days). The effect these two ZOL dosing schedules have on normal bone homeostasis, alone and in combination with Vγ9Vδ2 T cells, has yet to be examined.

As more evidence emerges that ZOL potentiates the anti-cancer efficacy of Vγ9Vδ2 T cell immunotherapy, the aim of this study was to examine the effect these treatments have on normal bone homeostasis. This was achieved by examining and comparing bone morphometric parameters from the contralateral non-tumour bearing tibia of NOD/SCID mice, from three independent pre-clinical studies included in this thesis (summarised in Table 1). Tibias were assessed using quantitative µCT to compare total bone volume (TBV), trabecular bone volume (Tb.BV), trabecular pattern factor (Tb.Pf), trabecular thickness (Tb.Th), trabecular number (Tb.N) and trabecular spacing (Tb.S). The values were then compared

Table 1. Summary of pre-clinical studies compared in Chapter 6.

	Cancer Model	Cell Line	ZOL	Vγ9Vδ2 T cells*	Reference
Study 1	Osteolytic breast cancer	MDA-MB231-TXSA	Treatment 1: 25µg/kg s.c Treatment 2 & 3: 50µg/kg s.c (ZOL-M)	$5x10^6$/100µL i.v	Chapter 3
Study 2	Osteolytic breast cancer	MDA-MB231-TXSA	100µg/kg s.c (ZOL-XC)	$1x10^7$/100µL i.v (purified)	Chapter 4
Study 3	Orthotropic osteolytic osteosarcoma	BTK-143	100µg/kg s.c (ZOL-XC)	$1x10^7$/100µL i.v (purified)	Chapter 5

*supplemented with 10IU IL-2. Abbreviations: i.t, intratibial; i.v, intravenous; s.c, subcutaneous; ZOL-M, metronomic ZOL; ZOL-XC, multiple conventional ZOL.

between appropriate treatment groups to determine the effect Vγ9Vδ2 T cells alone, ZOL alone, and the combination treatment have on normal bone homeostasis.

6.2 Results

6.2.1 Vγ9Vδ2 T cells alone have minimal impact on bone morphometric parameters

To examine the effect Vγ9Vδ2 T cells have on normal bone homeostasis, quantitative µCT analysis was conducted on the contralateral non-tumour bearing tibia of untreated animals and Vγ9Vδ2 T cell treated animals (Table 2). In Study 1 and Study 3, no statistically significant differences were observed when comparing untreated mice with Vγ9Vδ2 T cell treatment alone. Interestingly, Study 2 showed mice treated with Vγ9Vδ2 T cells alone had a modest but statistically significant increase in total bone volume compared to untreated (3.9 mm^3 compared to 3.6 mm^3). These mice also showed a trend towards increased trabecular bone volume compared to untreated mice (0.36 mm^3 compared to 0.23 mm^3), however this did not reach statistical significance. Additionally, there was a significant decrease in the trabecular pattern factor value when comparing these two treatment groups (17.50 mm^{-1} compared to 22.71 mm^{-1}).

6.2.2 ZOL alone has a positive effect on bone morphometric parameters

ZOL is a well-characterised and widely used bone anti-resorptive agent for the treatment of osteoporosis, Paget's disease of the bone, and reversing SREs in patients with cancerous bone lesions [42, 43, reviewed in 44]. To confirm the bone sparing effects of ZOL in these studies, quantitative µCT analysis was conducted on the contralateral non-tumour bearing tibia of mice (Table 3). In all studies, ZOL alone significantly increased total bone volume and trabecular bone volume while significantly decreasing trabecular pattern factor compared to untreated mice. Mice

Table 2. Bone morphometric parameters of the contralateral non-tumour bearing tibiae of untreated and Vγ9Vδ2 T cell treated animals from three studies.

		Study 1			Study 2			Study 3		
		UT	Vγ9Vδ2 T	p-value	UT	Vγ9Vδ2 T	p-value	UT	Vγ9Vδ2 T	p-value
TBV (mm^3)	Mean	2.98	2.83	0.11	3.60	3.93	0.01	3.66	3.57	0.62
	SEM	0.07	0.06		0.12	0.05		0.08	0.15	
Tb.BV (mm^3)	Mean	0.20	0.21	0.50	0.23	0.36	0.10	0.17	0.14	0.30
	SEM	0.02	0.01		0.07	0.05		0.01	0.03	
Tb.Pf (mm^{-1})	Mean	25.37	23.90	0.34	22.71	17.50	0.05	26.23	28.26	0.34
	SEM	1.37	0.77		2.39	1.30		0.97	1.71	
Tb.Th (mm)	Mean	0.05	0.05	0.77	0.06	0.06	0.09	0.05	0.05	0.95
	SEM	0.00	0.00		0.00	0.00		0.00	0.00	
Tb.N (mm^{-1})	Mean	0.11	0.11	0.65	0.54	0.69	0.15	0.36	0.29	0.14
	SEM	0.01	0.01		0.08	0.07		0.04	0.04	
Tb.Sp (mm)	Mean	1.53	1.57	0.45	0.63	0.64	0.61	0.77	0.85	0.06
	SEM	0.02	0.04		0.03	0.01		0.03	0.03	

Bone morphometric parameters were measured by three-dimensional analysis of μCT images of total and trabecular bone. Results are expressed as mean ± SEM. Comparisons were made between Vγ9Vδ2 T cell treated animals and untreated animals. Dark grey shaded cells indicate comparisons determined to be statistically significant (p-value ≤0.05) using the Student's t-test. Abbreviations: TBV, total bone volume; Tb.BV, trabecular bone volume; Tb.Pf, trabecular pattern factor; Tb.Th, trabecular thickness; Tb.N, trabecular number; Tb.Sp, trabecular spacing.

Table 3. Bone morphometric parameters of the contralateral non-tumour bearing tibiae of untreated and ZOL alone treated animals from three studies.

		Study 1			Study 2			Study 3		
		UT	ZOL	p-value	UT	ZOL	p-value	UT	ZOL	p-value
TBV (mm^3)	Mean	2.98	3.51	0.015	3.60	4.73	0.001	3.66	5.04	<0.001
	SEM	0.07	0.16		0.12	0.17		0.08	0.15	
Tb.BV (mm^3)	Mean	0.20	0.37	<0.001	0.23	0.67	<0.001	0.17	1.03	<0.001
	SEM	0.02	0.02		0.07	0.04		0.01	0.11	
Tb.Pf (mm^{-1})	Mean	25.37	12.67	0.001	22.71	11.11	0.001	26.23	0.97	<0.001
	SEM	1.37	2.16		2.39	1.12		0.35	2.80	
Tb.Th (mm)	Mean	0.05	0.06	0.081	0.06	0.12	<0.001	0.05	0.11	<0.001
	SEM	0.00	0.00		0.00	0.01		0.00	0.01	
Tb.N (mm^{-1})	Mean	0.11	0.19	<0.001	0.54	0.74	0.051	0.36	0.95	<0.001
	SEM	0.01	0.01		0.08	0.06		0.04	0.09	
Tb.Sp (mm)	Mean	1.53	1.49	0.417	0.63	0.58	0.062	0.77	0.67	0.030
	SEM	0.02	0.04		0.03	0.01		0.03	0.03	

Bone morphometric parameters were measured by three-dimensional analysis of μCT images of total and trabecular bone. Results are expressed as mean ± SEM. Comparisons were made between Vγ9Vδ2 T cell treated animals and untreated animals. Dark grey shaded cells indicate comparisons determined to be statistically significant (p-value ≤0.05) using the Student's t-test. Light grey shaded cells indicate comparisons determined to be approaching statistical significance (p-value ≈0.05) using the Student's t-test. Abbreviations: TBV, total bone volume; Tb.BV, trabecular bone volume; Tb.Pf, trabecular pattern factor; Tb.Th, trabecular thickness;

treated with ZOL in Study 1 showed a significant increase in trabecular number (0.19 mm^{-1} compared to 0.11 mm^{-1} in untreated mice). Trabecular thickness was significantly increased in Study 2 in the ZOL treatment group compared to untreated (0.12 mm compared to 0.06 mm). Study 3 showed an increase in trabecular thickness (0.11 mm compared to 0.01 mm), trabecular number (0.95 mm^{-1} compared to 0.36 mm^{-1}) and a decrease in trabecular separation (0.67 mm^{-1} compared to 0.77 mm^{-1}) in the ZOL treatment groups compared to untreated animals.

Consistent with the literature, ZOL treated animals had significantly great bone volume compared to untreated animals in each study. While previous studies have shown that multiple ZOL administrations are superior at increasing bone volume compared to a single ZOL dose [63, 67], no studies have examined the difference between metronomic dosing (ZOL-M) and multiple conventional doses (ZOL-XC). To examine the difference in bone volume between metronomic doses (ZOL-M) in Study 1 and multiple conventional doses (ZOL-XC) in Study 2 and 3, the fold change between the untreated and ZOL treated groups for each study were compared (Table 4). Differences between ZOL-M and ZOL-XC were observed in all parameters, but were most noticeable in the trabecular bone parameters. The increase in trabecular bone volume in the ZOL-M treated group in Study 1 was 1.9-fold compared to 2.9-fold and nearly 6-fold in the ZOL-XC treatment in Study 2 and Study 3 respectively. Trabecular thickness in Study 2 and 3 were increased 2-fold compared to a 1-fold increase in Study 1. Interestingly, no differences in trabecular bone pattern factor or trabecular separation were observed between Study 1 and 2, however the values were significantly smaller in Study 3. Additionally, trabecular number was comparable between Study 1 and 2 (1.7 and

1.3-fold increase respectively) compared to a 2.6-fold increase for Study 3. Overall, multiple infusions of ZOL at a higher dose result in a greater bone volume and thicker and well-structured trabecular bone compared with ZOL metronomic dosing.

6.2.3 Vγ9Vδ2 T cells in combination with ZOL have no effect on bone morphometric parameters compared to ZOL alone

To investigate the effect ZOL in combination with Vγ9Vδ2 T cells have on bone homeostasis compared to ZOL alone, quantitative µCT analysis was conducted on the contralateral non-tumour bearing tibia of mice and compared between these two treatment groups (Table 5). In Study 2, no statistically significant differences were observed when comparing mice treated with ZOL alone and ZOL in combination with Vγ9Vδ2 T cells. Study 1 showed that the combination resulted in a greater trabecular volume (0.50 mm^3 compared to 0.37 mm^3) and trabecular number (0.26 mm^{-1} compared to 0.19 mm^{-1}) compared to ZOL alone. In contrast, Study 3 showed that the combination significantly decreased trabecular volume compared to ZOL alone (0.95 mm^3 compared to 1.03 mm^3) however, the trabecular bone volume in the combination was still significantly greater than untreated or Vγ9Vδ2 T cells alone (0.95 mm^3 compared to 0.17 mm^3 and 0.14 mm^3 respectively). The combination also showed a strong trend towards a decrease in trabecular pattern factor (-1.08 mm^{-1} compared to 0.35 mm^{-1}) and an trend towards increased trabecular number (0.99 mm^{-1} compared to 0.95 mm^{-1}) compared to ZOL alone, however these values did not reach statistical significance.

Table 4. Bone morphometric parameters of the contralateral non-tumour bearing tibiae of untreated and ZOL alone treated animals from three studies, expressed as a fold change compared to untreated.

		Study 1			Study 2			Study 3		
		UT	ZOL	Fold-change	UT	ZOL	Fold-change	UT	ZOL	Fold-change
TBV (mm^3)	Mean	2.98	3.51	1.18	3.6	4.73	1.31	3.66	5.04	1.38
Tb.BV (mm^3)	Mean	0.2	0.37	1.9	0.23	0.67	2.94	0.17	1.03	5.97
Tb.Pf (mm^{-1})	Mean	25.37	12.67	0.5	22.71	11.11	0.49	26.23	0.35	0.01
Tb.Th (mm)	Mean	0.05	0.06	1.08	0.06	0.12	2.06	0.05	0.11	2.11
Tb.N (mm^{-1})	Mean	0.11	0.19	1.73	0.54	0.74	1.39	0.36	0.95	2.64
Tb.Sp (mm)	Mean	1.53	1.49	0.97	0.63	0.58	0.92	0.77	0.67	0.86

Bone morphometric parameters were measured by three-dimensional analysis of μCT images of total and trabecular bone. Results are expressed as mean ± SEM. Fold change was calculated as a ratio between the mean of each bone morphometric parameter between untreated and ZOL alone treated animals. Abbreviations: TBV, total bone volume; Tb.BV, trabecular bone volume; Tb.Pf, trabecular pattern factor; Tb.Th, trabecular thickness; Tb.N, trabecular number; Tb.Sp, trabecular spacing.

Table 5. Bone morphometric parameters of the contralateral non-tumour bearing tibiae of animals treated with ZOL alone compared with animals treated with ZOL in combination with Vγ9Vδ2 T cell from three studies.

		Study 1			Study 2			Study 3		
		ZOL	ZOL + Vγ9Vδ2 T	p-value	ZOL	ZOL + Vγ9Vδ2 T	p-value	ZOL	ZOL + Vγ9Vδ2 T	p-value
TBV (mm^3)	Mean	3.51	3.55	0.784	4.73	4.69	0.858	5.04	4.97	0.358
	SEM	0.16	0.12		0.17	0.18		0.15	0.12	
Tb.BV (mm^3)	Mean	0.37	0.5	0.01	0.67	0.69	0.847	1.03	0.95	0.022
	SEM	0.02	0.04		0.04	0.12		0.11	0.08	
Tb.Pf (mm^{-1})	Mean	12.67	11.62	0.682	11.11	10.69	0.849	0.35	-1.08	0.051
	SEM	2.16	0.93		1.12	2.07		2.8	1.67	
Tb.Th (mm)	Mean	0.05	0.06	0.916	0.12	0.13	0.594	0.11	0.1	0.125
	SEM	0.00	0.00		0.01	0.02		0.01	0	
Tb.N (mm^{-1})	Mean	0.19	0.26	0.008	0.74	0.74	0.964	0.95	0.99	0.058
	SEM	0.01	0.02		0.06	0.07		0.09	0.06	
Tb.Sp (mm)	Mean	1.49	1.45	0.379	0.58	0.58	0.906	0.67	0.67	0.823
	SEM	0.04	0.03		0.01	0.03		0.03	0.01	

Bone morphometric parameters were measured by three-dimensional analysis of μCT images of total and trabecular bone. Results are expressed as mean ± SEM. Results are expressed as mean ± SEM. Comparisons were made between animals treated with ZOL alone and animals treated with ZOL in combination with Vγ9Vδ2 T cells. Dark grey shaded cells indicate comparisons determined to be statistically significant (p-value ≤0.05) using the Student's t-test. Light grey shaded cells indicate comparisons determined to be approaching statistical significance (p-value ≈0.05) using the Student's t-test. Abbreviations: TBV, total bone volume; Tb.BV, trabecular bone volume; Tb.Pf, trabecular pattern factor; Tb.Th, trabecular thickness; Tb.N, trabecular number; Tb.Sp, trabecular spacing.

6.3 Discussion

Adoptive transfer of Vγ9Vδ2 T cells in combination with ZOL is gaining momentum as a novel anti-cancer immunotherapy, therefore it is important to examine the effect this treatment has on normal bone homeostasis. This study assessed the non-tumour bearing contralateral tibia of NOD/SCID mice and examined bone morphometric parameters to determine the effect adoptive transfer of Vγ9Vδ2 T cells, ZOL administration and the combination have on bone homeostasis.

Vγ9Vδ2 T cells alone showed minimal impact on bone parameters with only a slight increase in TBV compared to untreated animals observed in one study. Similarly, bone parameters of animals treated with ZOL in combination with Vγ9Vδ2 T cells showed little difference to those treated with ZOL alone. In Chapters 4 and 5, it was shown that following adoptive transfer, fluorescently labelled Vγ9Vδ2 T cells predominately localise to the liver, spleen, and most importantly, the tumour bearing tibia. As Vγ9Vδ2 T cells did not localise to the non-tumour bearing tibia of animals in these studies, it is unlikely they would exert a local effect on normal bone. Vγ9Vδ2 T cells which have localised to the tumour mass however, have the ability to release factors such as IFN-γ in response to cancer cell recognition, which may a have systemic effect on bone homeostasis. IFN-γ is known to interfere with RANK-RANKL signalling resulting in decreased osteoclastogenesis [164] and may be the reason a small bone sparing effect was observed in the non-tumour bearing tibia following Vγ9Vδ2 T cell adoptive transfer. Immunocompromised mice were used in this study, therefore any potential systemic effect may have been dampened, however, this would be comparable to examining the effect Vγ9Vδ2 T cell adoptive transfer has on normal bone

homeostasis in immunocompromised cancer patients. Overall, as the increase in bone volume in the non-tumour bearing tibia is quite subtle, it is difficult to make any inferences until further studies are undertaken and μCT is used to examine bone parameters in patients undertaking Vγ9Vδ2 T cell adoptive transfer.

As multiple nBP administrations are required to potentiate the anti-cancer efficacy of Vγ9Vδ2 T cells [77, Chapters 3-5], this study examined the effect multiple ZOL administrations have on normal bone homeostasis. Consistent with the literature ZOL treatment increased bone volume in the non-tumour bearing tibia, regardless of frequency or dose [63, 67]. Additionally, ZOL-XC had greater bone sparing properties in the non-tumour bearing tibia compared to ZOL-M. It has been previously shown that monthly and weekly administration of 100μg/kg ZOL in ovariectomised mice resulted in increased BV/TV compared to untreated, but the weekly treatment was less effective compared to the monthly treatment [165]. As adoptive transfer of Vγ9Vδ2 T cells in combination with ZOL may be used in post-menopausal women with advanced breast cancer, this suggests frequent ZOL administrations may be less effective than the current ZOL treatment schedule at reducing SREs, however, this has yet to be investigated. Interestingly, ZOL-XC resulted in more bone in the osteosarcoma model (Study 3) compared to the same dosing schedule in the osteolytic breast cancer model (Study 2). As ZOL-M was not examined in the osteosarcoma model, it is difficult to determine if this difference is purely due to the ZOL dosing schedule, or the cell line used, which could have implications on ZOL-XC dosing schedule in different cancer types.

Although increased bone density in the tumour bearing tibia of cancer patients is beneficial for the reduction of SREs, conversely, overall high bone mineral density can be problematic. As observed in osteosclerosis and other high bone

density diseases, disordered bone can be weak, resulting in fractures and other complications [166]. This study observed ZOL-XC predominately increased trabecular bone, implying this is dense, well-structured bone which would be beneficial for patients as it is less likely to fracture.

More concerning is the observation that repeated ZOL administration may led to a greater incidence of BAONJ in immunocompromised patients, which was linked to a decline in Vγ9Vδ2 T cells [73]. Initially the cause was thought to be AICD of Vγ9Vδ2 T cells, until it was discovered that nBP uptake by neutrophils produces reactive oxygen species (ROS) which inhibits Vγ9Vδ2 T cells proliferation and decreases viability [167]. This poses an additional challenge when using frequent ZOL administrations prior to Vγ9Vδ2 T cell adoptive transfer and may be one possible reason why Vγ9Vδ2 T cell clinical trials have shown variability in efficacy.

In conclusion, the data presented here suggests that adoptive transfer of Vγ9Vδ2 T cells may protect bone, however any effect is minor compared to ZOL. Clearly, further clinical studies examining bone parameters are required to fully understand the effects Vγ9Vδ2 T cells and multiple ZOL infusions have in patients receiving this novel immunotherapy.

Chapter 7

Vγ9Vδ2 T cells in combination with pro-apoptotic receptor agonists (PARAs) or chemotherapy enhance killing of breast cancer cells

7.1 Introduction

In the preceding chapters, it was demonstrated that ZOL enhanced the anti-cancer efficacy of Vγ9Vδ2 T cells against osteosarcoma and breast cancer, both *in vitro* and *in vivo*. This treatment regimen also reduced pulmonary metastases, and inhibited tumour-associated osteolysis in pre-clinical models. While decreased tumour burden was observed in the tibia, the tumour was not fully eradicated. This chapter explores the potential of using a combinatorial approach with pro-apoptotic receptor agonists (PARAs) and chemotherapy to enhance the anti-cancer efficacy of Vγ9Vδ2 T cells.

Vγ9Vδ2 T cells recognise PAgs abnormally accumulated in cancer cells [92], resulting in the release of cytolytic granules and T-helper 1 (Th1) cytokines including IFN-γ and TNF-α, causing target cell lysis and immune activation [75, 98, 104, 107, 108]. Activated Vγ9Vδ2 T cells also induce apoptosis by releasing PARAs such as FasL and TRAIL (also called Apo2 ligand) [79, 98]. PARAs bind to death receptors (DR), resulting in receptor multimerisation and subsequent recruitment of the FADD (Fas-associated death domain protein) complex, initiating caspases and ultimately resulting in cell death.

PARAs such as recombinant human TRAIL (rhTRAIL) or drozitumab (Apomab, Genetech), have in recent years become attractive anti-cancer therapeutics because of their high potency and lack of toxicity. TRAIL targets both DR4 (Apo2L/TRAIL-R1) and DR5 (Apo2L/TRAIL-R2), while drozitumab, a humanised monoclonal IgG1 antibody targets DR5 for apoptosis induction. This laboratory has shown these PARAs reduce tumour burden in models of osteolytic breast cancer and can protect the bone from tumour-associated osteolysis [141, 146]. TRAIL has a short serum half-life, and prolonged treatment regimens to

maximise anti-cancer efficacy result in TRAIL resistance [141]. To overcome these disadvantages, TRAIL was also used in combination with other immunotherapeutic approaches to enhance the anti-cancer efficacy of T cells [142, 143], however it was not examined in combination with Vγ9Vδ2 T cells.

For drozitumab to exert its biological effect, it requires Fc-cross linking [145]. A sub-population of Vγ9Vδ2 T cells express CD16 (FcγRIII) a low affinity Fc receptor which binds antibodies of the IgG isotype [144]. Cross-linking of antibodies with CD16 can activate antibody dependant cellular cytotoxicity (ADCC), resulting in the release of perforin and granzymes, subsequently activating caspases that result in target cell death. Previous studies have shown $CD16^{+}$ Vγ9Vδ2 T cells cross-linked to rituximab and trastuzumab enhance cytotoxicity against solid and haematological malignancies [115, 116], however the ability of drozitumab to cross-link CD16 on Vγ9Vδ2 T cells has not been examined.

In addition to PARAs, commonly used chemotherapeutic drugs including cisplatin, etoposide, and 5-flurouracil were shown to enhance the anti-cancer efficacy of Vγ9Vδ2 T cells [81, 138, 168]. The anthracycline compound doxorubicin is a commonly used chemotherapeutic drug which intercalates DNA, resulting in DNA damage and subsequent activation of the mitochondrial mediated (intrinsic) pathway of apoptosis. Doxorubicin is currently used for the treatment of various cancers, including advanced breast cancer, however high doses or long term use are associated with off-target side-effects including cardiotoxicity [reviewed in 41]. These toxic side effects could be avoided by combining low dose chemotherapy in combination with immunotherapy. Indeed, in several early-phase clinical trials, patients with advanced cancers that were treated with adoptive transfer of Vγ9Vδ2 T cells in combination with nBPs, chemotherapy, or hormonal

therapy had the best outcomes [105, 126, 127]. This suggests that using PARAs or conventional chemotherapeutic agents in an adjuvant setting to Vγ9Vδ2 T cell immunotherapy may prove effective in targeting advanced cancers.

This study examined the efficacy of Vγ9Vδ2 T cells in combination with three anti-cancer compounds, drozitumab, TRAIL, and doxorubicin against breast cancer cells *in vitro*. $CD16^+$ Vγ9Vδ2 T cells were assessed for their ability to cross-link drozitumab for apoptosis induction. Although it was shown that drozitumab did not cross-link $CD16^+$ Vγ9Vδ2 T cells, nonetheless, pre-treatment of cancer cells with each of the compounds, including activated Fc cross-linked drozitumab, an additive decrease in breast cancer cell viability was evident. This suggests that Vγ9Vδ2 T cells used in combination with PARAs or chemotherapy represent a favourable treatment regimen to enhance Vγ9Vδ2 T cell immunotherapy.

7.2 Results

7.2.1 Phenotypic analysis of impure, CD16 depleted, and CD16 enriched cells

Prior to examining the ability of $CD16^+$ Vγ9Vδ2 T cells to undergo ADCC with drozitumab, it was required to phenotypically characterise the cell populations. Contrary to previous studies [169], a decline of CD16 expression was observed on the $Vγ9^+/CD3^+$population following 7 days culture (Figure 3.1 C). Therefore, fresh *ex vivo* expanded Vγ9Vδ2 T cells, which were enriched for CD16 prior to ADCC were used for subsequent experiments with drozitumab. Three populations were examined; the whole population of cells prior to purification (impure cells), CD16 enriched cells ($CD16^+$), and CD16 depleted cells ($CD16^-$). CD16 enriched cells had significantly higher levels of CD16 expression, compared to CD16 depleted and impure cells (Figure 7.1 A). There were no differences in the number of $Vγ9^+/CD3^+$

cells, or NKG2D expression between the three populations (Figure 7.1 A). The majority of the cells in the CD16 enriched population were determined to be Vγ9Vδ2 T cells, with a minor population being $V\gamma9^{-}/CD3^{-}/CD16^{+}$.

When examining the differentiation phenotype based on CD27 and CD45RA expression, there were no significant differences in the $T_{naïve}$ ($CD27^{+}/CD45RA^{+}$) and T_{ERMA} ($CD27^{-}/CD45RA^{+}$) populations between the three groups. In contrast, there was an enrichment of T_{EM} ($CD27^{-}/CD45RA^{-}$) and depletion of T_{CM} ($CD27^{+}/CD45RA^{-}$) cells in the CD16 enriched population (Figure 7.1 B), contrary to previous reports which showed the majority of CD16 enriched Vγ9Vδ2 T cells were T_{ERMA} and T_{EM} cells [99].

It is common practice to expand, enrich, and cryogenically store lymphocytes for later use. To verify that thawing frozen cells would have no effect on the three populations of Vγ9Vδ2 T cells, a matched sample was analysed before and after cryogenic freezing. Fresh samples were assessed immediately following MACs isolation using flow cytometric analysis. Cells were cryogenically frozen, thawed after 1 week storage at -80°C, then analysed immediately using flow cytometric analysis.

After thawing, no differences were observed in cell viability, numbers of $V\gamma9^{+}/CD3^{+}$ cells (Figure 7.2 B), NKG2D expression (Figure 7.2 C), or differentiation phenotypes (Figure 7.2 D). There was however, a large decline in the percentage of lymphocytes expressing CD16 in the CD16 enriched population, going from >88% of lymphocytes expressing CD16 to <40% (Figure 7.2 A). Thawed cells were therefore deemed unusable for ADCC experiments with drozitumab, and all subsequent experiments were conducted using freshly isolated cells.

Figure 7.1 CD16 enriched cells are effector memory cells with increased CD16 receptor expression.

After 7-8 days expansion, fresh Vγ9Vδ2 T cells were collected and enriched based on expression of CD16. Flow cytometric analysis was performed on three groups of cells, *ex vivo* expanded Vγ9Vδ2 T cells prior to MACS isolation (impure), CD16 depleted cells ($CD16^-$), and CD16 enriched cells ($CD16^+$). **A.** $CD16^+$, $V\gamma9^+/CD3^+$, and $NKG2D^+$ receptor expression for each of the three populations. **B.** The differentiation phenotype of the cells from each of the three populations, based on CD27/CD45RA. Data was pooled from three independent experiments. Columns represent the mean of n=3, expressed as the percentage of cells from the lymphocyte population. Error bars indicate SEM.

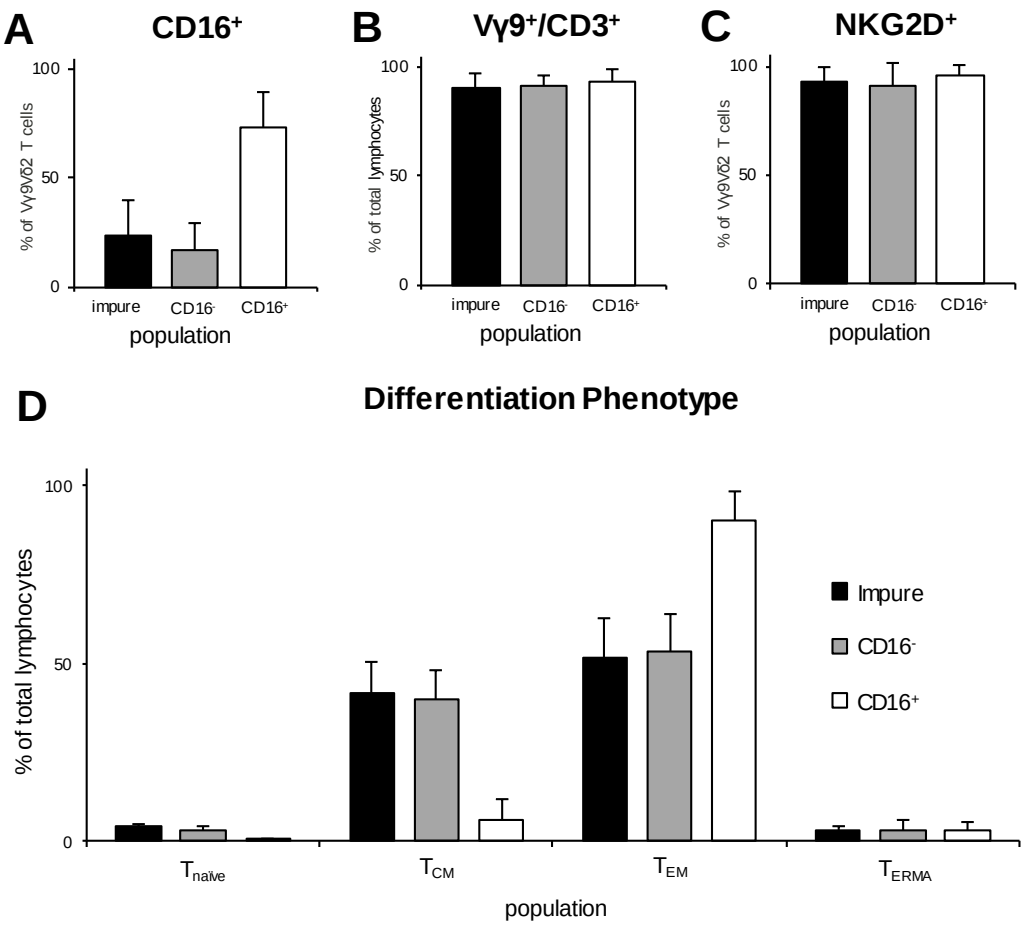
A
CD16+
% of Vγ9Vδ2 T cells
100
50
0
impure
CD16-
CD16+
population
B
Vγ9+/CD3+
% of total lymphocytes
100
50
0
impure
CD16-
CD16+
population
C
NKG2D+
% of Vγ9Vδ2 T cells
100
50
0
impure
CD16-
CD16+
population
D
Differentiation Phenotype
% of total lymphocytes
100
50
0
Impure
CD16-
CD16+
Tnaïve
TCM
TEM
TERMA
population

Figure 7.2 CD16 expression on CD16 enriched cells is lost following cryogenic storage.

After 7 days expansion, fresh Vγ9Vδ2 T cells were collected and enriched based on expression of CD16. Cells were then cryogenically frozen and thawed one week later. Flow cytometric analysis was performed on fresh and thawed cells from three groups, *ex vivo* expanded Vγ9Vδ2 T cells prior to MACS isolation (impure), CD16 depleted cells ($CD16^-$), and CD16 enriched cells ($CD16^+$). Fresh and thawed cells were compared based on **A.** $CD16^+$ **B.** $V\gamma9^+/CD3^+$ **C.** $NKG2D^+$ expression, and **D.** differentiation phenotype, based on CD27/CD45RA expression. Data was from one paired biological sample. Columns represent the percentage of cells from the lymphocyte population expressing the specified receptor/s and no error bars are indicated as n=1.

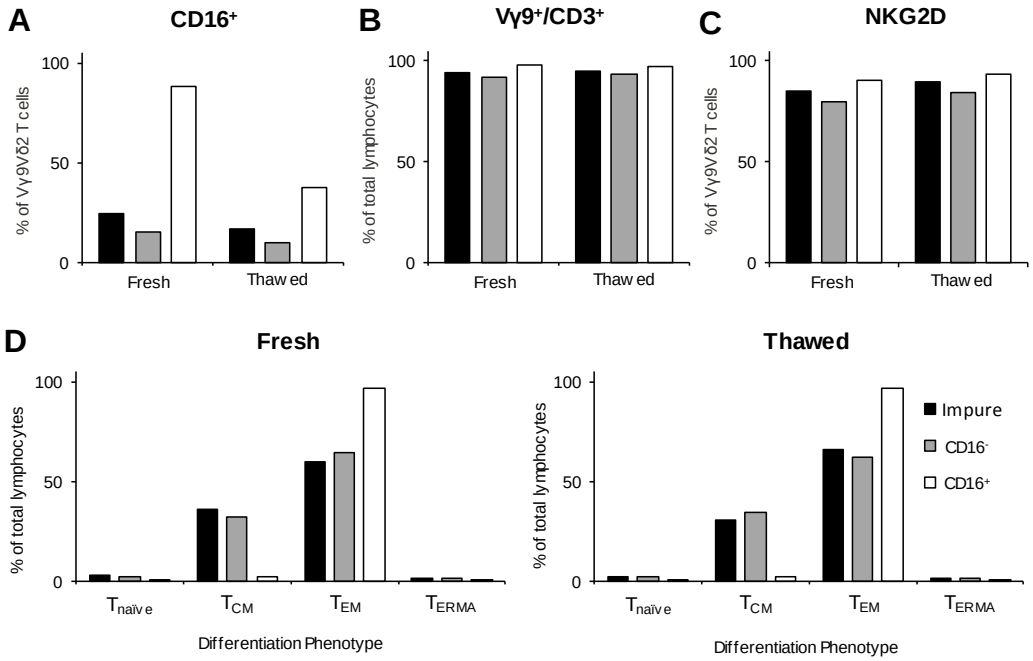
A
CD16+
% of Vγ9Vδ2 T cells
100
50
0
Fresh
Thaw ed
B
Vγ9+/CD3+
% of total lymphocytes
100
50
0
Fresh
Thaw ed
C
NKG2D
% of Vγ9Vδ2 T cells
100
50
0
Fresh
Thaw ed
D
Fresh
% of total lymphocytes
100
50
0
Tnaïve
TCM
TEM
TERMA
Differentiation Phenotype
Thawed
% of total lymphocytes
100
50
0
Tnaïve
TCM
TEM
TERMA
Differentiation Phenotype
Impure
CD16-
CD16+

7.2.2 Drozitumab does not cross-link with CD16 on Vγ9Vδ2 T cells to elicit ADCC against cancer cells

MDA-MB231-TXSA cells are sensitive to drozitumab, which has been cross-linked with an anti-Fc Ab (drozitumab + anti-Fc) [146]. Pre-treatment of MDA-MB231-TXSA with 50ng/mL drozitumab + anti-Fc for 15 minutes could induce caspase-3 activation and reduce cancer cell viability after 24 hours to 85% [146]. However, pre-treatment with 50ng/mL drozitumab alone did not induce caspase-3 activation or reduce cancer cell viability (Figure 7.2). To examine the ability of $CD16^+$ enriched cells to induce ADCC by cross-linking CD16 with drozitumab, cancer cells were pre-treated with or without drozitumab alone, followed by co-culture with impure, $CD16^-$, or $CD16^+$ Vγ9Vδ2 T cells. After 24 hours, there were no differences in caspase-3 activation of cancer cells that were treated with 50ng/mL drozitumab alone or in those that remained untreated, at none of the Vγ9Vδ2 T cell E:T tested (Figure 7.3 A-C). In fact, a mild inhibitory effect was observed with $CD16^-$ cell co-culture in combination with drozitumab alone (Figure 7.3 B)

At the same time point, a luciferase activity-based viability assay was used to determine cancer cell viability. Similar to caspsase-3 activation, there was no difference in the viability of cancer cells that were pre-treated with or without drozitumab alone, between the impure, $CD16^-$, or $CD16^+$ Vγ9Vδ2 T cells (Figure 7.3 D-F). As there were no significant differences between the three populations of cells, further studies were conducted using impure Vγ9Vδ2 T cells.

Figure 7.3 Drozitumab does not cross-link with $CD16^+$ Vγ9Vδ2 T cells to elicit ADCC against breast cancer cells.

Drozitumab-sensitive MDA-MB231-TXSA were pre-incubated with or without 50ng/mL drozitumab (alone or cross-linked with anti-Fc) for 15 minutes, followed by 24 hours co-culture with *ex vivo* expanded Vγ9Vδ2 T cells prior to MACS isolation (impure), CD16 depleted cells ($CD16^-$), and CD16 enriched cells ($CD16^+$), at a 1:1 and 5:1 E:T. After 24 hours co-culture with these cell populations, caspase-3 activation **(A-C)** and luciferase activity **(D-F)** to determine viable cells was measured. The equation used to calcuate cell viability is found in the Materials and Methods chapter. Data points represent a mean of n=3, and error bars indicate ± SEM (**A)** or %SEM (**B)**.

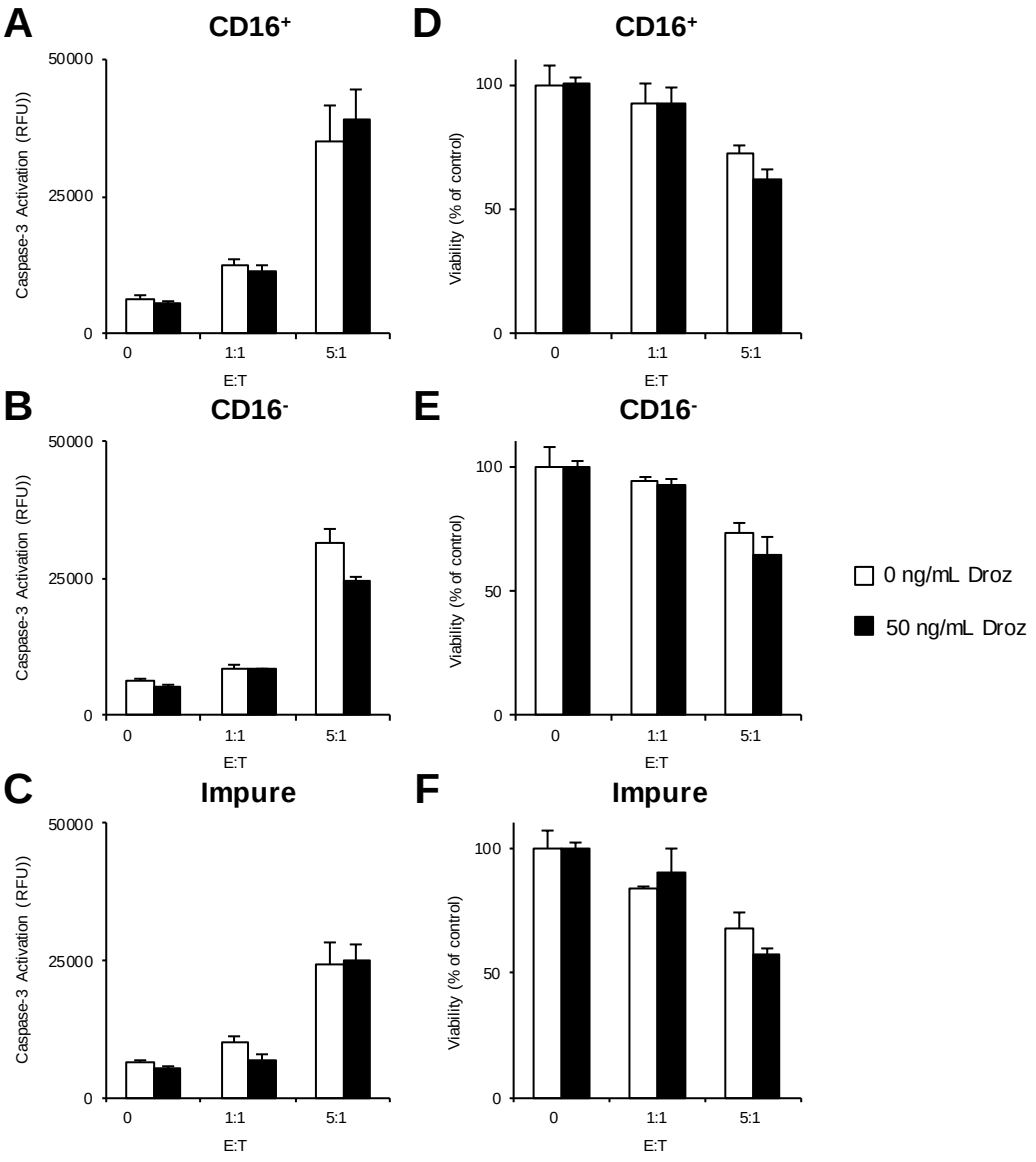
A
CD16+
Caspase-3 Activation (RFU))
50000
25000
0
0
1:1
5:1
E:T
D
CD16+
Viability (% of control)
100
50
0
0
1:1
5:1
E:T
B
CD16-
Caspase-3 Activation (RFU))
50000
25000
0
0
1:1
5:1
E:T
E
CD16-
Viability (% of control)
100
50
0
0
1:1
5:1
E:T
C
Impure
Caspase-3 Activation (RFU))
50000
25000
0
0
1:1
5:1
E:T
F
Impure
Viability (% of control)
100
50
0
0
1:1
5:1
E:T
0 ng/mL Droz
50 ng/mL Droz

7.2.3 Concurrent treatment of Vγ9Vδ2 T cells in combination with PARAs or chemotherapy enhances killing of cancer cells

To determine if drozitumab could be used as an adjuvant agent with Vγ9Vδ2 T cells, MDA-MB231-TXSA cancer cells were treated with drozitumab with or without anti-Fc crosslinking for 4 or 24 hours, followed by 24 hours culture with Vγ9Vδ2 T cells. Cells treated with drozitumab without Vγ9Vδ2 T cells did not show a significant decrease in cancer cell viability compared to untreated cells at both time points. After 4 hours, Vγ9Vδ2 T cells alone decreased viability of cancer cells to 76% and drozitumab showed a trend towards a slight additive effect with Vγ9Vδ2 T cells (66% viability) (Figure 7.4 A). In contrast, cancer cells that were pre-treated with drozitumab + anti-Fc had 40% viability, and this decreased further to 25% after culture with Vγ9Vδ2 T cells (Figure 7.4 A). After 24 hours, a similar trend was observed and there was a slight additive effect using the combination of drozitumab and Vγ9Vδ2 T cells, and after treatment with drozitumab + anti-Fc alone or in combination with Vγ9Vδ2 T cells, nearly 100% of cancer cells were killed (Figure 7.4 B). At both time points, the anti-cancer efficacy of drozitumab + anti-Fc in combination with Vγ9Vδ2 T cells was additive rather than synergistic.

To determine if TRAIL could also be used as an adjuvant therapy with Vγ9Vδ2 T cells, MDA-MB231-TXSA cancer cells were treated with TRAIL for 4 or 24 hours, followed by 24 hours co-culture with Vγ9Vδ2 T cells. After 4 hours treatment with 5ng/mL or 10ng/mL TRAIL alone, cancer cell viability was reduced to 91% and 79% respectively (Figure 7.4 C). Vγ9Vδ2 T cells alone reduced viability to 76%, however in combination with 5ng/mL or 10ng/mL TRAIL, cancer viability decreased to 67% and 56% respectively (Figure 7.4 C). Following 24 hours treatment

Figure 7.4 Concurrent treatment of drozitumab or TRAIL in combination with Vγ9Vδ2 T cells enhances killing of breast cancer cells.

MDA-MB231-TXSA, sensitive to both TRAIL and drozitumab, were treated with or without 25ng/mL drozitumab (alone or cross-linked with anti-Fc) for **A.** 4 hours, or **B.** 24 hours, or with or without TRAIL (5 or 10ng/mL) for **C.** 4 hours, or **D.** 24 hours. Luciferase activity to determine viable cells was measured after a further 24 hours co-culture with or without Vγ9Vδ2 T cells at a 5:1 E:T. The equation used to calculate cell viability is found in the Materials and Methods chapter. Unpaired two-tailed Student's t-test was performed comparing each treatment group to untreated (*$p<0.05$, **$p<0.005$, ***$p<0.001$, non-significant values not shown). Data points represent a mean of n=3, and error bars indicate ± %SEM.

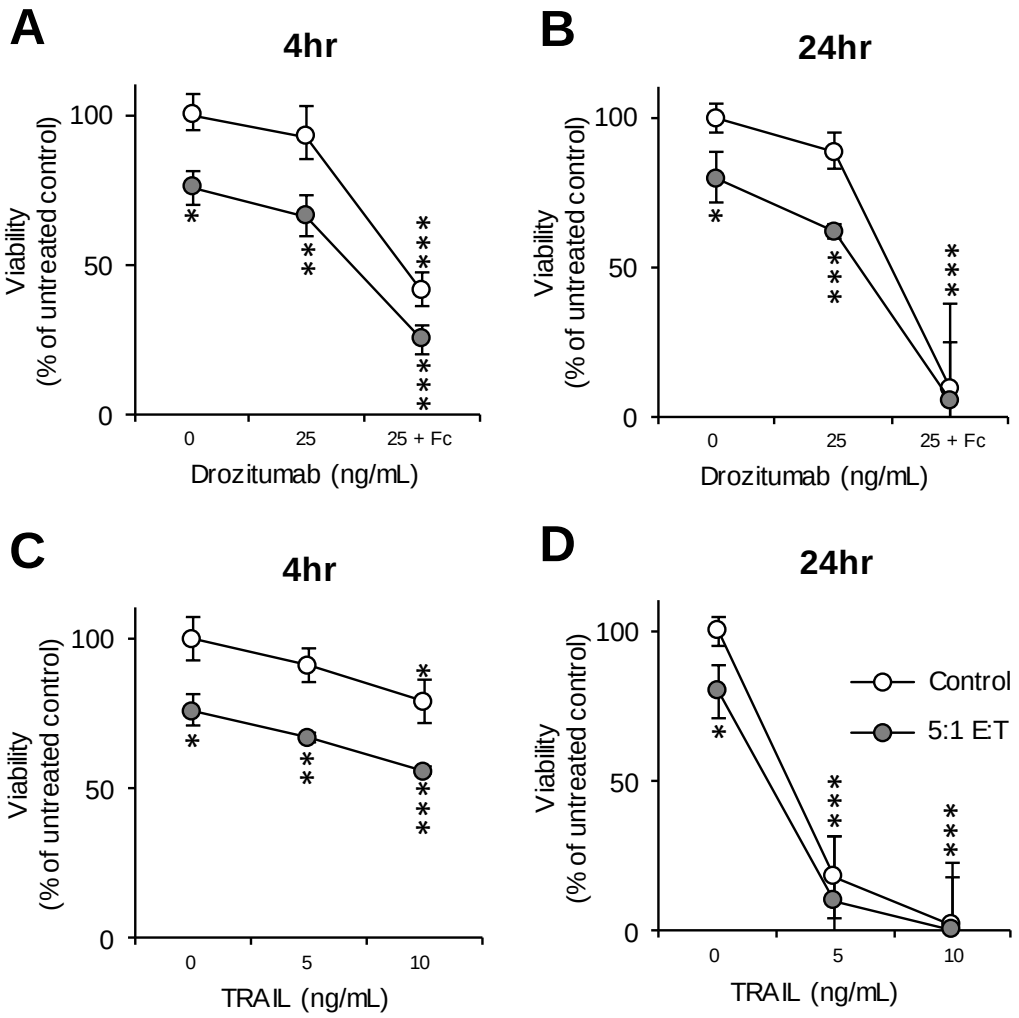
A
4hr
Viability
(% of untreated control)
100
50
0
0
25
25 + Fc
Drozitumab (ng/mL)
B
24hr
Viability
(% of untreated control)
100
50
0
0
25
25 + Fc
Drozitumab (ng/mL)
C
4hr
Viability
(% of untreated control)
100
50
0
0
5
10
TRAIL (ng/mL)
D
24hr
Viability
(% of untreated control)
100
50
0
Control
5:1 E:T
0
5
10
TRAIL (ng/mL)

with 5ng/mL or 10ng/mL TRAIL, cancer cell viability was significantly reduced to 18% and 2% respectively (Figure 7.4 D). When cancer cells were treated with TRAIL then co-cultured with Vγ9Vδ2 T cells, cancer cell viability was <10% for both TRAIL concentrations (Figure 7.4 D). At the time points and TRAIL concentrations examined, the observed decrease in cancer cell viability following TRAIL treatment in combination with Vγ9Vδ2 T cells was purely additive.

Doxorubicin, a chemotherapeutic drug often used to treat breast cancer can result in off target side effects, including cardiotoxicity [reviewed in 41]. Reducing the concentration of doxorubicin is one way to limit its side effects, however, this also decreases the therapeutic efficacy of the drug. Using low-dose chemotherapy in combination with immunotherapy could be a potential method of limiting toxicity, while maximising anti-cancer efficacy. To determine if doxorubicin could be used as an adjuvant therapy with Vγ9Vδ2 T cells, MDA-MB231-TXSA cancer cells were treated with low-dose doxorubicin for 24 hours, followed by co-culture with Vγ9Vδ2 T cells for 24 hours. Doxorubicin alone killed cancer cells in a dose-dependent manner, with 23% viability at the highest dose (Figure 7.5). Vγ9Vδ2 T cells alone reduced cancer cell viability to 37%, but in combination with doxorubicin, there was an even greater decrease in cancer cell viability (Figure 7.5). At the highest dose of 125nM doxorubicin in combination with Vγ9Vδ2 T cells, <4% remained viable (Figure 7.5). However, as previously observed in combination with the PARAs, the anti-cancer efficacy of Vγ9Vδ2 T cells in combination with doxorubicin cells was only additive.

7.3 Discussion

Vγ9Vδ2 T cell-based immunotherapy in combination with other treatments is being explored as a novel approach for targeting advanced cancers. Several *in*

Figure 7.5 Concurrent treatment of doxorubicin in combination with Vγ9Vδ2 T cells enhances killing of breast cancer cells.

Doxorubicin-sensitive MDA-MB231-TXSA breast cancer cells were treated with or without doxorubicin (31, 63 and 125nM) for 24 hours, in low serum (0.5% FCS) media. Luciferase activity to determine viable cells was measured after a further 24 hours co-culture with or without Vγ9Vδ2 T cells at a 10:1 E:T. The equation used to calculate cell viability is found in the Materials and Methods chapter. Unpaired two-tailed Student's t-test was performed comparing each treatment group to untreated (***$p<0.001$, non-significant values not shown). Data points represent a mean of n=3, and error bars indicate ± %SEM.

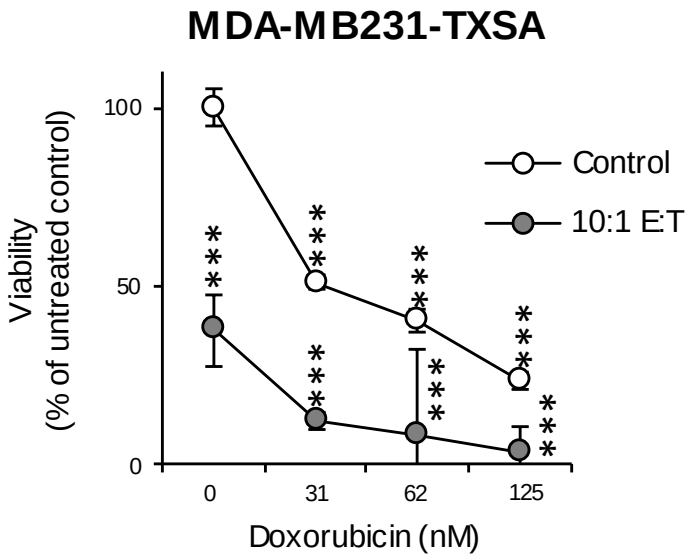
MDA-MB231-TXSA
Viability
(% of untreated control)
100
50
0
0
31
62
125
Doxorubicin (nM)
Control
10:1 E:T
****

vitro studies have demonstrated the therapeutic potential of monoclonal antibodies cross-linked to CD16 on Vγ9Vδ2 T cells to elicit ADCC against solid and haematological malignancies [115-117]. Additionally, in clinical studies, patients treated with adoptive transfer of Vγ9Vδ2 T cells in combination with nBPs, chemotherapy, or hormonal therapy had the best outcomes [105, 126, 127], suggesting a multi-pronged approach is likely to be most beneficial. This study examined the anti-cancer efficacy of Vγ9Vδ2 T cells in combination with three different anti-cancer compounds; drozitumab, TRAIL, and doxorubicin.

Drozitumab, a humanised monoclonal antibody directed against DR5, requires Fc cross-linking with CD16 (FcγRIIIA) to elicit ADCC against target cells [145]. This study has shown that drozitumab does not enhance the anti-cancer efficacy of CD16 enriched Vγ9Vδ2 T cells, suggesting a lack of cross-linking and subsequent ADCC activation. CD16 has two subtypes, FcγRIIIA and FcγRIIIB, which have different roles. FcγRIIIA results in activation, while the role of FcγRIIIB is still unclear, but may act as a decoy receptor [170]. When phenotyping Vγ9Vδ2 T cells in this study, a pan-specific CD16 antibody was used, therefore it was not possible to determine the actual levels of FcγRIIIA and FcγRIIIB. Additionally, pan-specific CD16 microbeads were used to enrich Vγ9Vδ2 T cells. If FcγRIIIB was expressed at higher levels on CD16 enriched Vγ9Vδ2 T cells, drozitumab binding would not induce ADCC to enhance Vγ9Vδ2 T cell cytotoxicity. Since no differences in the cytotoxicity between the impure, CD16 depleted, and CD16 enriched Vγ9Vδ2 T cells were observed, this may be one possible reason why drozitumab did not elicit ADCC against breast cancer cells in these studies. Alternatively, the enrichment of T_{EM} Vγ9Vδ2 T cells in the $CD16^+$ population, which was previously described as less cytotoxic than $CD16^+$ T_{ERMA}

Vγ9Vδ2 T cells [99], suggests the predominance of these cells may have contributed to a lack of ADCC with drozitumab. In contrast to previous studies which showed great success using antibodies to cross-link to Vγ9Vδ2 T cells [115-117], this study demonstrated that attempting to cross-link drozitumab with CD16, a highly specialised receptor on Vγ9Vδ2 T cells to enhance cytotoxicity is unlikely a viable option. Several groups have also arrived at this conclusion and have attempted to circumvent this issue by generating antibodies with the ability to cross-link common receptors such as CD3 or Vγ9 [171, 172].

To overcome the problem of using CD16 to cross-link drozitumab in this study, the cytotoxicity of Vγ9Vδ2 T cells as an adjuvant therapy in combination with anti-Fc cross-linked drozitumab was evaluated in further experiments. Treatment of cancer cells with drozitumab + anti-Fc, TRAIL, or doxorubicin followed by Vγ9Vδ2 T cells, is analogous to using chemotherapy followed by adoptive transfer with Vγ9Vδ2 T cells in a clinical setting. In this study, all of the therapies used in adjuvant with Vγ9Vδ2 T cells showed additive, but not synergistic anti-cancer efficacy. Previous *in vitro* and *in vivo* studies using Vγ9Vδ2 T cells in combination with chemotherapies had similar observations [81, 168]. In regards to the lack of synergy with chemotherapy, Kang et al. suggested this was due to the chemotherapy being toxic to Vγ9Vδ2 T cells [168]. This has implications for the treatment regimens to be used in pre-clinical studies. To minimise off-target toxicity to Vγ9Vδ2 T cells, chemotherapy and immunotherapy would need to be infused in separate cycles. However, the need for this would be overcome with the use of PARAs in combination with Vγ9Vδ2 T cells, as *ex vivo* expanded Vγ9Vδ2 T cells do not express DR4 or DR5 (Supplementary Figure S1), resulting in

potential resistance to TRAIL and drozitumab, and a reduction in off-target toxicity of Vγ9Vδ2 T cells.

Additive cytotoxicity is still of benefit as it reduces treatment dose and may limit adverse effects, however this is in contrast to using other compounds such as ZOL which can sensitises breast [82], osteosarcoma [135], glioblastoma [136], lymphoma [81], fibrosarcoma and lung cancer cells [78] in a synergistic manner. The therapies tested in this study are PARAs which target the same or converging apoptotic pathways as Vγ9Vδ2 T cells, possibly explaining why no synergy is observed. For example, PARAs target death receptors and Vγ9Vδ2 T cells themselves can release TRAIL and other related molecules, all which result in activation of the same pathways.

For adjuvant therapies to produce a synergistic response in combination with Vγ9Vδ2 T cells, compounds need to increase cancer cell recognition by Vγ9Vδ2 T cells or sensitise therapy resistant cancer cells. For example, colon cancer initiating cells were sensitised to Vγ9Vδ2 T cells following chemotherapy pre-treatment by upregulation of death receptors (DR5 and Fas) [138], and nBPs sensitise cancer cells by inhibiting FPPS, resulting in IPP accumulation and enhanced detection by Vγ9Vδ2 T cells. Exploring other novel FPPS inhibitors may provide additional compounds that produce a synergistic anti-cancer response in combination with Vγ9Vδ2 T cells. One such compound that has been examined is N6-isopentenyladenosine (iPA), a novel FPPS inhibitor [173]. iPA was shown to inhibit growth of various cancer cells [174-176], however pre-treatment of breast cancer or osteosarcoma cells with iPA followed by Vγ9Vδ2 T cell co-culture did not result in a synergistic anti-cancer response (Supplementary Figure S2). This

suggests that an additive anti-cancer response remains one of the best possible outcomes.

In conclusion, this *in vitro* study has shown that Vγ9Vδ2 T cells may potentially be used as an adjuvant therapy with PARAs or chemotherapy, resulting in significant additive anti-cancer efficacy. However, further studies are required to fully validate the potential of these treatment regimens in establishing protocols to overcome drug resistance.

7.4 Supplementary Figures

Figure S1 Expanded Vγ9Vδ2 T cells do not express death receptors.

After 7 days expansion, flow cytometric analysis was performed on fresh Vγ9Vδ2 T cells to examine death receptor expression. Histograms show DR4 and DR5 expression on the $V\gamma9^{+}/CD3^{+}$ lymphocyte population, compared to an isotype control and MDA-MB231-TXSA breast cancer cells as a positive control. n=1.

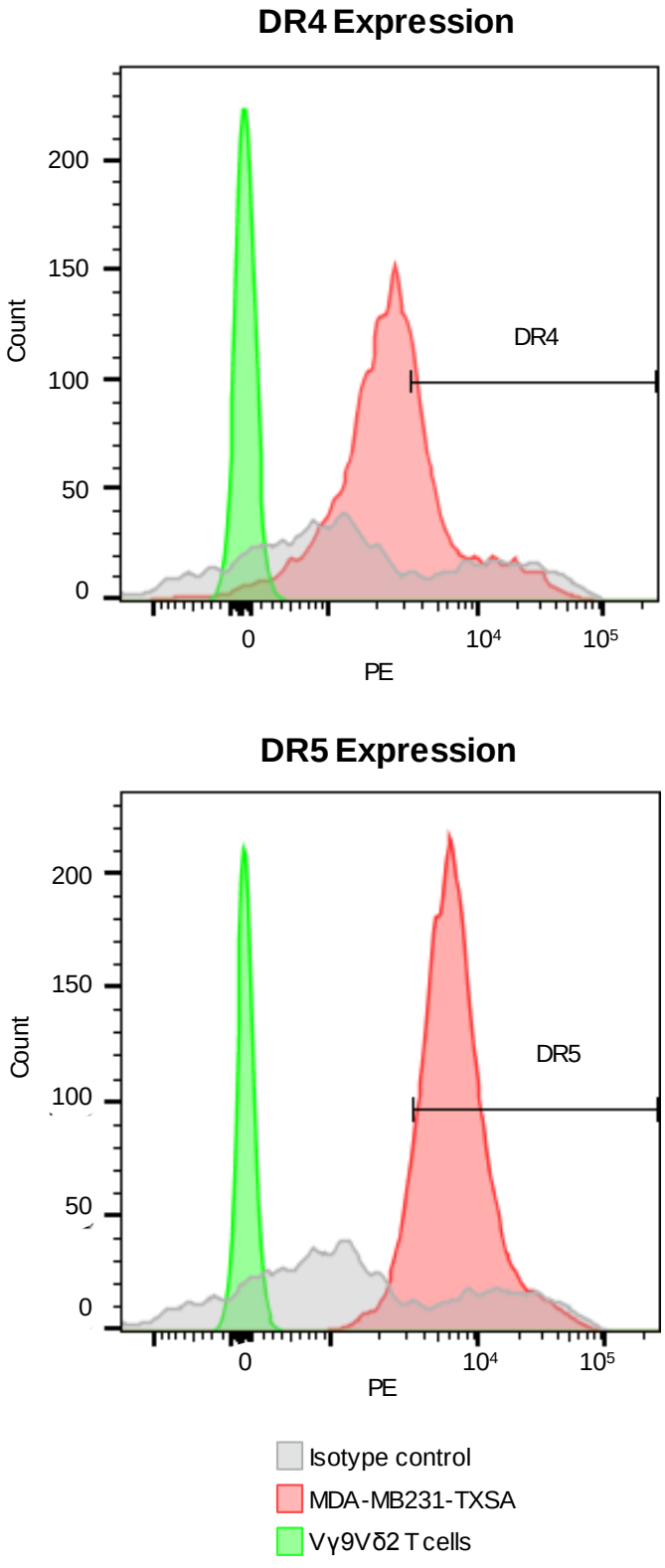
DR4 Expression
Count
200
150
100
50
0
DR4
0
10⁴
10⁵
PE
DR5 Expression
Count
200
150
100
50
0
DR5
0
10⁴
10⁵
PE
Isotype control
MDA-MB231-TXSA
Vγ9Vδ2 T cells

Figure S2 Pre-treatment with FPPS inhibitiors sensitises cancer cells to killing by Vγ9Vδ2 T cells.

A. MDA-MB231-TXSA breast cancer cells **B.** 143B and **C.** KHOS osteosarcoma cells were pre-treated with iPA (0, 1, 5,10 or 20μM) or ZOL (0, 10 or 25μM) for 24 hours. Luciferase activity to determine viable cells was measured after co-culture with or without Vγ9Vδ2 T cells for a further 24 hours (E:T 5:1). The equation used to calculate cell viability is found in the Materials and Methods chapter. Data points represent a mean of n=3, and error bars indicate ± %SEM.

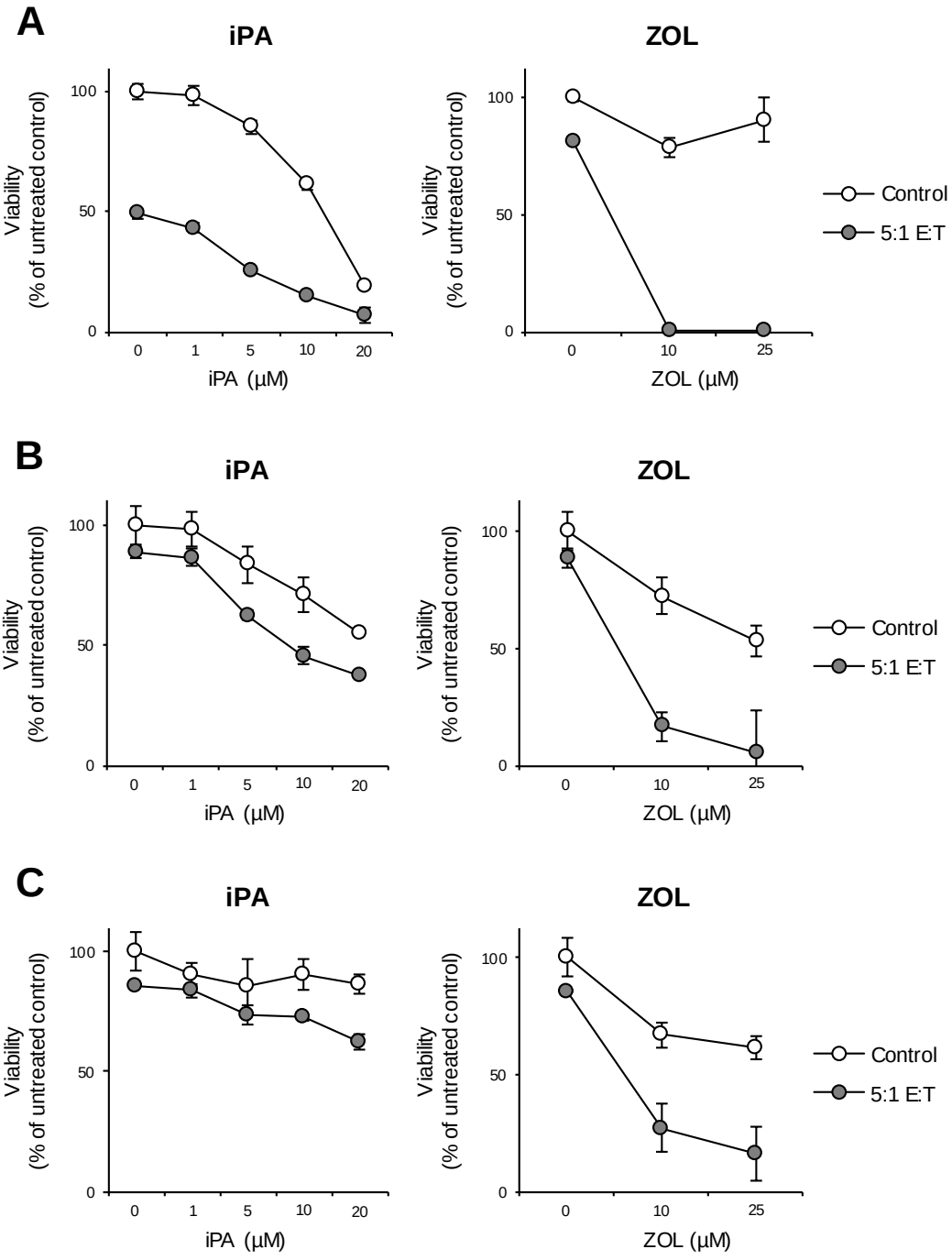
A
iPA
ZOL
Viability
(% of untreated control)
100
50
0
0
1
5
10
20
iPA (μM)
0
10
25
ZOL (μM)
Control
5:1 E:T
B
iPA
ZOL
C
iPA
ZOL

.

Chapter 8

Discussion, Future Directions and Conclusion

8.1 Discussion

In recent years, adoptive transfer of *ex vivo* expanded cytotoxic Vγ9Vδ2 T cells has emerged as a novel immunotherapeutic approach for the treatment of solid and haematological malignancies. However, its clinical utility has been limited due to the wide variation in anti-cancer efficacy, especially in early phase clinical trials for the treatment of advanced tumours. This suggests that combinatorial approaches which provide additive or synergistic actions require optimisation for increased efficacy.

It is well established that nBPs potentiate the anti-cancer efficacy of Vγ9Vδ2 T cells both *in vitro* and in pre-clinical settings. Since nBPs preferentially localise to the bone, an elegant approach for targeting cancers in the bone has emerged. It has been hypothesised that treatment with nBPs such as ZOL followed by adoptive transfer of Vγ9Vδ2 T cells, may potentially sensitise cancer cells in the bone microenvironment to Vγ9Vδ2 T cell cytotoxicity [156]. Using ZOL as a means to sensitise cancer cells in the bone to Vγ9Vδ2 T cells may prove a more amicable approach compared to targeting soft-tissue tumours due to the preferential pharmacological distribution of ZOL to the bone. Additionally, as osteoclasts are the primary target of ZOL in the bone, this treatment regimen would also inhibit the 'vicious cycle' of abnormal osteoclast-mediated bone resorption associated with osteolytic tumours. However, this hypothesis has not yet been examined in an appropriate pre-clinical model.

To test this hypothesis, two cancer models were studied. Osteolytic osteosarcoma and breast cancer bone metastases are two cancers that affect the bone, resulting in abnormal osteoclast-mediated bone resorption that perpetuates the 'vicious cycle' of cancer growth and bone degradation. In the last few decades,

survival rates for osteosarcoma have plateaued, while patients with advanced breast cancer only have palliative care available. This indicates an urgent need for novel therapies which target both tumour growth in the bone and tumour-associated bone degradation. For the first time, the studies in this thesis have examined the anti-cancer efficacy of Vγ9Vδ2 T cells in combination with ZOL against osteolytic cancers using clinically relevant animal models of osteosarcoma and metastatic breast cancer. These studies also examined the potential benefit of combinatorial approaches of using Vγ9Vδ2 T cell adoptive transfer with other adjuvant treatments including drozitumab, TRAIL, and doxorubicin.

Vγ9Vδ2 T cells are cytotoxic against a wide variety of cancer types; however efficacy can be variable [75, 76, 78-80, 82, 98, 111, 157]. In this study, *ex vivo* expanded Vγ9Vδ2 T cells alone induced cell death in the osteolytic breast cancer cell line MDA-MB231-TXSA, but showed limited cytotoxicity against other cancer cell lines (Chapters 3, 4 and 5). Differences in sensitivity to Vγ9Vδ2 T cell mediated cytotoxicity was previously reported [82, 112]. Although this current study does not explore potential mechanisms of resistance, it must be noted that Vγ9Vδ2 T cells engage various mechanisms to kill target cells, and resistance can therefore be multi-faceted. For example, downregulation of MICA/B, the ligand for NKG2D, only partially contributes to cancer cell resistance to Vγ9Vδ2 T cell cytotoxicity [112]. Other mechanisms may include down-regulation of DR4/DR5 expression, which may also inhibit cell death induced by TRAIL produced by Vγ9Vδ2 T cells [98]. Additionally, as further studies explore the role of BTN receptors in the recognition of target cells by Vγ9Vδ2 T cells [88], endogenous levels of BTN receptor expression, downregulation, or mutation of BTN on target cells may also play a role in the differential sensitivity to Vγ9Vδ2 T cells.

While early phase clinical trials have shown Vγ9Vδ2 T cell therapy to be safe, as a monotherapy, the anti-cancer efficacy of this approach, especially against advanced tumours has been underwhelming and due to its limited clinical utility, requires further improvement. Several factors contribute to the failure of Vγ9Vδ2 T cell immunotherapy in clinic. These include the rapid depletion of Vγ9Vδ2 T cells following chronic intravenous nBP treatment, which potentially results in a decrease of Vγ9Vδ2 T cells available for localisation to the tumour site. Therefore, current studies are focused on enhancing Vγ9Vδ2 T cell cytotoxicity and currently, nBP pre-treatment is one approach proven to sensitise various cancer cells to killing by Vγ9Vδ2 T cells [78, 81, 82, 135, 136]. In this current study, most of the cancer cell lines examined, including the osteolytic osteosarcoma (143B) and breast cancer (MDA-MB231-TXSA) cell lines, were highly sensitised to Vγ9Vδ2 T cells following ZOL pre-treatment (Chapters 3, 4 and 5). Interestingly, there were differences in sensitivity to Vγ9Vδ2 T cell cytotoxicity following ZOL pre-treatment. These observed differences may be related to differences in cellular uptake of nBPs and thus differences in the inhibition of the mevalonate pathway and the subsequent accumulation of PAgs [82, 177].

Exploiting the anti-cancer efficacy of Vγ9Vδ2 T cells and the anti-bone resorptive effects of ZOL may be an elegant two-pronged approach to sensitise cancers in the bone to Vγ9Vδ2 T cells [156]. For the first time, the studies outlined in this thesis examined this treatment approach in pre-clinical models of osteolytic osteosarcoma and breast cancer.

For Vγ9Vδ2 T cells to exhibit anti-cancer efficacy, they must first localise to the tumour site. Previous studies have shown that Vγ9Vδ2 T cells localise to solid tumours in soft tissues [77, 162, 178], however none have examined localisation to

lesions in the bone. For the first time, the studies in this thesis demonstrated that intravenously infused Vγ9Vδ2 T cells rapidly co-localised within established tumour lesions in bone (Chapters 4 and 5). The pilot studies using the osteolytic breast cancer model described in this thesis revealed that a single infusion of Vγ9Vδ2 T cells alone transiently decreased tumour burden in the tibia (Chapter 3), however multiple administrations of Vγ9Vδ2 T cells were required to produce sustained anti-cancer efficacy (Chapter 3 and 4). These observations are consistent with the pre-clinical studies assessing Vγ9Vδ2 T cell anti-cancer efficacy against solid tumours [76-78, 111, 161, 162]

Multiple infusions of Vγ9Vδ2 T cells were therefore examined in both the osteolytic osteosarcoma and breast cancer models. Interestingly, while multiple infusions of Vγ9Vδ2 T cells alone reduced tumour burden in the osteolytic breast cancer model, they had no effect on tumour burden in the osteosarcoma model. Intrinsic differences between these two cancers may account for this observation. Indeed, and as previously discussed, the osteosarcoma cell line was less sensitive to Vγ9Vδ2 T cell mediated killing compared to the osteolytic breast cancer cell line when tested *in vitro.*

As shown *in vitro*, ZOL sensitised both osteosarcoma and breast cancer cells to Vγ9Vδ2 T cell cytotoxicity, therefore the pilot study assessed the anti-cancer efficacy of Vγ9Vδ2 T cells in combination with metronomic doses of ZOL (ZOL-M). In contrast to *in vitro* observations, ZOL-M failed to potentiate Vγ9Vδ2 T cell anti-cancer efficacy (Chapter 3). This observation was also contrary to other pre-clinical studies which showed enhanced Vγ9Vδ2 T cell anti-cancer efficacy following nBP treatment in other solid tumour models [76-78] Although different nBPs were used in these studies, they were administrated at the conventional dose,

compared to the metronomic dosing regimen used for ZOL in this pilot study (Chapter 3). Therefore, to examine if a higher ZOL dose could enhance Vγ9Vδ2 T cell *in vivo* efficacy, further studies in this thesis examined multiple administrations of ZOL at the conventional dose (ZOL-XC) in combination with Vγ9Vδ2 T cells.

Multiple administrations of Vγ9Vδ2 T cells in combination with ZOL given at the conventional dose potentiated the anti-cancer efficacy of Vγ9Vδ2 T cells in both the osteolytic breast cancer and osteosarcoma model (Chapter 4 and 5). While this is an important finding, the mechanism of how ZOL sensitises cancer cells to Vγ9Vδ2 T cells *in vivo* is currently unclear. While it was proposed that circulating nBPs may be internalised by cancer cells, resulting in IPP accumulation thereby leading to increased cancer cell recognition by Vγ9Vδ2 T cells, to-date no such evidence exists. Although many cell types readily uptake nBPs *in vitro*, including osteoclasts and cancer cells [177], *in vivo* observations by Junankar et al showed that in the mammary fat pad, fluorescently labelled nBPs were elegantly shown to be internalised by TAMs and not by cancer cells [179]. From the *in vivo* observations in this study a new hypothesis was proposed stating that following ZOL internalisation by TAMs, there is a release of chemotactic factors which may increase Vγ9Vδ2 T cell recruitment to the tumour microenvironment, thereby increasing Vγ9Vδ2 T cell availability at the tumour site while enhancing anti-cancer efficacy. In this context, it was shown that *Mycobacterium Tuberculosis* pulsed macrophages (which would produce IPP), release monocyte chemoattractant protein-1 (MCP-1) and IL-8 which promotes chemotaxis of γδ T cells *in vitro* [180]. Additionally, activated T_{EM} Vγ9Vδ2 T cells express many chemokine receptors necessary for migration, including CCR2, the receptor for MCP-1 [104]. This current study showed that in ZOL pre-treated animals,

adoptively transferred Vγ9Vδ2 T cells (predominately T_{CM} and T_{EM}) localised to the tumour mass within 20 minutes, compared to untreated animals which showed no Vγ9Vδ2 T cell localisation at this time point (Chapter 5). Additionally, ZOL pre-treated animals showed a higher signal of fluorescently labelled Vγ9Vδ2 T cells localising to the tumour mass after 24 hours (Chapter 5). Although this data is purely observational, it supports the proposed hypothesis. Nonetheless, further studies are required to determine if ZOL is sufficient for TAMs to enhance the anti-cancer efficacy of Vγ9Vδ2 T cells *in vivo*, and to fully examine the *in vitro* and *in vivo* migration of Vγ9Vδ2 T cells to ZOL pulsed macrophages and to identify potential chemokines and receptors responsible.

In addition to exhibiting anti-cancer efficacy against tumours in the bone, Vγ9Vδ2 T cells also reduced the incidence and tumour burden of lung metastases in both cancer models (Chapter 4 and 5). This observed decrease in lung metastases is consistent with similar observations in both pre-clinical and early phase clinical trials [97, 178, 181]. In a study by Liu et al. spontaneous lung metastases in a murine model of prostate cancer were reduced with γδ T cell treatment [178]. Additionally, in two early phase clinical trials, some patients exhibiting metastatic lung lesions from advanced renal cell carcinoma showed decreased growth rate of these lesions and no new lesions detected following Vγ9Vδ2 T cell treatment [97, 181]. It is currently unknown whether Vγ9Vδ2 T cells can directly target cancer cells in the lung, or if infused Vγ9Vδ2 T cells instead target disseminated cancer cells prior to lodging in the lung. This study showed that fluorescently labelled Vγ9Vδ2 T cells can be detected in the lungs up to three days following adoptive transfer (Chapter 5), suggesting they are present in the lungs. However, as Vγ9Vδ2 T cells can undergo AICD following FasL engagement [79], which is constitutively

expressed in the lungs [182], this could limit their cytotoxicity at this site. Therefore, it may be more likely that circulating Vγ9Vδ2 T cells are targeting disseminated cancer cells prior to lodging instead. However, as exact mechanisms are still unclear, further studies are necessary to interrogate this process.

While ZOL enhanced Vγ9Vδ2 T cell anti-cancer efficacy against tumours in the bone, the combination had no additive effect on lung metastases, suggesting the reduction in the incidence and tumour burden was due to Vγ9Vδ2 T cells alone. Since nBPs predominately localise to the bone and are rapidly cleared from soft tissue [183], it is unlikely that ZOL would accumulate in the lungs to potentiate the anti-cancer efficacy of Vγ9Vδ2 T cells in that environment.

ZOL is a well-characterised anti-bone resorptive agent, however *in vitro* it is also reported to exhibit a range of anti-cancer effects by inducing cell death, inhibiting proliferation, invasion, and angiogenesis in a variety of cancer cell lines [57-62]. While pre-clinical studies have been numerous, they are often contradictory, therefore the *in vivo* anti-cancer efficacy of ZOL remains unclear. For example, some pre-clinical studies have found ZOL treatment reduced primary tumour growth and inhibited further metastases [63-66], in contrast to other studies where ZOL had no effect [67, 68]. Multiple mechanisms have been proposed by which ZOL may exert anti-cancer efficacy *in vivo*, including direct induction of cancer cell death, indirectly, by inhibiting modulating processes such as angiogenesis, interfering with the 'vicious cycle', and by targeting other cell types that may either enhance or inhibit tumour growth [57-62]. However, in this current study ZOL had no effect on tumour growth in either the osteolytic osteosarcoma or breast cancer model (Chapter 3, 4, 5). Although ZOL alone did not demonstrate anti-cancer efficacy, it did fulfil its role as a bone anti-resorptive agent and reduced

tumour-associated osteolysis in both cancer models. This did not translate to a decrease in tumour burden, suggesting that in these models osteoclast inhibition alone is not sufficient to inhibit cancer cell growth. These findings are in line with previous observations from this laboratory [67, 68].

Although the anti-cancer efficacy of Vγ9Vδ2 T cell adoptive transfer has been examined in early-phase clinical trials for the treatment of advanced cancer, little is known about the role Vγ9Vδ2 T cells may play on bone. Previous studies have implicated the depletion of γδ T cells in osteoporotic patients to be associated with BAONJ [73]. Therefore, to examine the potential effect Vγ9Vδ2 T cell immunotherapy may have on bone, the bone volume of tumour-bearing and non-tumour bearing tibias were compared between untreated animals and those treated with Vγ9Vδ2 T cells. In the osteolytic breast cancer model, there was a small trend showing increased total and trabecular bone volume, in both the tumour and non-tumour bearing tibias (Chapter 6). In contrast, both tibias in the osteosarcoma model showed decreased total and trabecular bone volume (Chapter 6). In both cancer models, localisation studies revealed that Vγ9Vδ2 T cells did not migrate to the non-tumour bearing tibia, therefore the bone modulating effect observed on control bone is unexpected. However, as Vγ9Vδ2 T cells changed bone volume in both the tumour bearing and non-tumour bearing tibias, this suggests that systematic factors may be responsible for modulating bone homeostasis at distant sites. Although the differences in bone volume between untreated animals and those infused with Vγ9Vδ2 T cells was subtle, contrasting effects on net bone volume were observed between the two cancer models. Under certain conditions, γδ T cells are able to produce factors which may either promote bone remodelling or bone formation [150-153]. Potentially, the observed differences between the two cancer

models may arise from the types of factors produced by Vγ9Vδ2 T cells in the tumour microenvironment. This suggests that that cross-talk between different types of cancer cells, the bone microenvironment, and Vγ9Vδ2 T cells will ultimately play a role in determining the effect Vγ9Vδ2 T cell adoptive transfer will have on net bone volume.

These studies are some of the first to examine the effect of Vγ9Vδ2 T cells on bone. However, the limitation here is that human Vγ9Vδ2 T cells were infused into a mouse system, and therefore difficult to assess the translatability in human patients. Until bone parameters are measured in human clinical studies, it will be difficult to definitively conclude the effect Vγ9Vδ2 T cell adoptive transfer will have on bone homeostasis in humans.

While it has been well-established that ZOL sensitises a variety of cancer cells to killing by Vγ9Vδ2 T cells, the effect this treatment has on normal bone cells and overall bone homeostasis is currently unclear. To assess the effect Vγ9Vδ2 T cell immunotherapy in combination with ZOL would have on bone, in the context of osteolytic cancer, the tumour-bearing tibias from all treatment groups were compared to determine which treatment regimen provided the best protection from osteolytic lesions. In the osteolytic breast cancer model, ZOL in combination with Vγ9Vδ2 T cells resulted in the greatest total and trabecular bone volume from all treatment groups, however the observed effects were purely additive of ZOL and Vγ9Vδ2 T cell treatments alone (Chapter 4). Similarly, in the osteosarcoma model, the combination treatment resulted in the greatest total and trabecular bone volume, to the extent where the bone parameters of the tumour-bearing tibia in this treatment group did not differ from the contralateral normal control tibia (Chapter 5). This

was a significant finding as it implies that the combination treatment has a two-pronged effect: it reduces tumour-burden and protects the bone from osteolysis.

The studies outlined in this thesis have shown that ZOL potentiates the anti-cancer efficacy of Vγ9Vδ2 T cells against osteolytic cancers. However, as this treatment regimen does not completely eradicate the tumour, combinatorial approaches are required. To address this need, this current study also briefly examined the use of PARAs (drozitumab and TRAIL) and chemotherapy (doxorubicin) as adjuvant therapies with Vγ9Vδ2 T cells *in vitro*. Vγ9Vδ2 T cells are known to express CD16, an Fc receptor which mediates ADCC. While previous studies have shown that antibodies can enhance the anti-cancer efficacy $CD16^+$ Vγ9Vδ2 T cells [115, 116], drozitumab failed to increase Vγ9Vδ2 T cell cytotoxicity, suggesting cross-linking did not occur. While cross-linked drozitumab, TRAIL, and doxorubicin in combination with Vγ9Vδ2 T cells all showed enhanced cytotoxicity against cancer cells *in vitro*, this was purely additive. Regardless, an additive increase in cytotoxicity may be clinically relevant, therefore further studies are required to assess the anti-cancer efficacy of drozitumab, TRAIL, and doxorubicin in pre-clinical studies.

8.2 Future Directions

While the studies outlined in this thesis provide new insights in the field of Vγ9Vδ2 T cell immunotherapy, further studies are required to optimise treatment that will be clinically beneficial.

8.2.1 Vγ9Vδ2 T cell immunotherapy for other cancers in the bone

Osteolytic osteosarcoma and bone metastases arising from breast cancer are not the only cancer types that affect the bone. Multiple myeloma is the most

frequent primary malignancy of the skeleton, forming osteolytic lesions [1]. Conversely, the majority of osteosarcomas and bone metastases from prostate cancer result in predominately osteoblastic or mixed lesions [1, 12] Studies have shown that all of these cancers are sensitised to Vγ9Vδ2 T cell cytotoxicity following ZOL pre-treatment *in vitro* [77, 80, 135, 184]. Vγ9Vδ2 T cell immunotherapy appears more efficacious in patients with haematological malignancies [185, 186], and nBPs reduce SREs in multiple myeloma patients [187, 188]. It is therefore reasonable to suggest that in a pre-clinical model of multiple myeloma, ZOL in combination with Vγ9Vδ2 T cells would respond in a similar fashion to osteolytic osteosarcoma and osteolytic breast cancer lesions, and may reduce tumour burden and inhibit bone degradation. Conversely, as osteoblastic and mixed lesions behave differently *in vivo* compared to osteolytic lesions it may be more difficult to predict the effect ZOL in combination with Vγ9Vδ2 T cells may have on these tumour types. Previous studies have shown that nBPs inhibits SREs in osteosarcoma and inhibit both osteoblastic and osteolytic lesions in metastatic hormone-refectory prostate cancer (HRPC) patients [50, 51, 189]. Vγ9Vδ2 T cell therapy has also been assessed in patients with HRPC [123], and although clinical trials are yet to be conducted in osteosarcoma patients, many have examined solid tumour patients with bone metastases [105, 126]. Additionally, this current study has demonstrated that multiple infusions of Vγ9Vδ2 T cells in combination with multiple administrations of ZOL are effective at reducing tumour burden and bone degradation in an osteolytic osteosarcoma model (Chapter 5) and a previous study has shown that a similar treatment regimen is effective at reducing tumour burden in a pre-clinical model of prostate cancer [77]. Together, this suggests that ZOL would potentiate the anti-cancer efficacy of Vγ9Vδ2 T cells

against other cancers in the bone. However, further pre-clinical studies are still required to confirm this and to examine the effect treatments have on abnormal bone remodelling and disease progression.

8.2.2 Improving pre-clinical models

It is well established that Vγ9Vδ2 T cell cytotoxicity is partially dependent on immune system activation as demonstrated by their ability to produce potent cytokines such as IFN-γ and TNF-α. Therefore, it is important to study the anti-cancer efficacy of Vγ9Vδ2 T cells within the context of an intact immune system. Currently in the literature the majority of studies assessing adoptive transfer of Vγ9Vδ2 T cells use athymic (nude), NOD/SCID, or NOD/SCID gamma (NSG) pre-clinical models. The studies in this thesis used NOD/SCID mice as they are superior to nude mice due to impaired murine T cell (including γδ T cell) and B cell development, and NK cell deficiency. Normally NOD/SCID mice are highly suitable for studying tumour biology as they lack an intact immune system and will not reject tumour xenografts, however they are not ideal for examining the downstream immune-modulating effects of Vγ9Vδ2 T cells. An ideal pre-clinical model for Vγ9Vδ2 T cell immunotherapy would be to use humanised mouse model, such as NOD/SCD gamma (NSG) inoculated with cancer cells and human peripheral blood (with appropriate growth factors) to mimic an intact human immune system. Future experiments using pre-clinical models with an intact immune system could provide a better understanding of the anti-cancer efficacy of Vγ9Vδ2 T cells in these bone cancer models

8.2.3 Enhancing Vγ9Vδ2 T cell adoptive transfer

Although the studies in this thesis have shown that ZOL potentiates the anti-cancer efficacy of Vγ9Vδ2 T cells, some limitations exist. Currently, one of the

major obstacles contributing to the failure of Vγ9Vδ2 T cell immunotherapy in clinic has been the *in vivo* depletion of Vγ9Vδ2 T cells following intravenous nBP treatment of osteoporotic and cancer patients [73, 122-124, 128]. As a potential method to overcome this, short culture periods were used in this study to ensure a combination of proliferative T_{CM} and cytotoxic T_{EM} Vγ9Vδ2 T cells would be available for infusion following ZOL administration in the pre-clinical models of osteolytic cancer. This would allow T_{EM} Vγ9Vδ2 T cells to immediately target cancer cells and for the T_{CM} Vγ9Vδ2 T cells to undergo further *in vivo* proliferation in response to exogenous rhIL-2 supplementation to prolong anti-cancer efficacy. While this study showed promise in the pre-clinical models, due to the depletion of Vγ9Vδ2 T cells in some early phase clinical trials, this treatment regimen may still not show clinical efficacy. Until recently, it was believed that depletion of Vγ9Vδ2 T cells was due to AICD and while this may partially be the case, Kalyan et al. suggested an alternative theory [167]. The authors showed that in culture, neutrophils uptake nBPs resulting in the release of reactive oxygen species (ROS) which inhibit Vγ9Vδ2 T cell proliferation and activation [167]. This could be reversed following treatment with enzymes which deplete hydrogen peroxide [167]. While this has yet to be examined *in vivo*, in a small clinical study in patients with gastric ascites, the authors observed neutrophil recruitment to the peritoneal cavity following ZOL administration [128]. Interestingly, the majority of patients showed a decrease in Vγ9Vδ2 T cells 7 days after adoptive transfer [128]. While the authors did not propose a link between neutrophil recruitment and a decline in Vγ9Vδ2 T cells, this observation provides some evidence that neutrophils may indeed regulate Vγ9Vδ2 T cells *in vivo*. This suggests that targeting ROS produced by neutrophils with antioxidant drugs such as N-acetylcysteine [190, 191], may

allow further *in vivo* proliferation of transferred T_{CM} Vγ9Vδ2 T cells and as a result, enhanced Vγ9Vδ2 T cell anti-cancer efficacy.

8.2.4 Localised delivery

Another alternative method to improve Vγ9Vδ2 T cell anti-cancer efficacy is to use directed localised delivery to increase the number of Vγ9Vδ2 T cells available directly at the tumour site. Recently, Stephan et al. elegantly demonstrated that scaffolds loaded with tumour reactive T cells were more effective at reducing tumour reoccurrence, compared to adoptive transfer of the same T cells [192]. Scaffolds can also contain growth factors that prolong Vγ9Vδ2 T cell viability and proliferation, such as IL-2, IL-15 [193], and IL-33[194], and are biodegradable, eliminating the need to remove them following treatment. In addition to delivering cells, scaffolds can be engineered to interact strongly with some drugs, and weakly with others, to allow successive drug release. This could be used for the localised release of ZOL to sensitise cancer cells to Vγ9Vδ2 T cells or the successive release of chemotherapeutic drugs as an adjuvant therapy following Vγ9Vδ2 T cell release.

A potential application of this system could be for the treatment of brain tumours, such as glioblastoma multiform (GBM), which is notoriously difficult to treat using conventional chemotherapies as drugs typically cannot pass the blood-brain barrier (BBB). Also, tumour resection surgery is difficult as small margins are required to minimise damage to normal brain tissue, but this can increase the likelihood of leaving behind residual tumour cells. For this reason, biodegradable carmustine-loaded wafers (Gliadel®) have been FDA approved for use following brain tumour resection, so the adjuvant chemotherapy bypasses the BBB and acts directly on residual tumour cells [reviwed in 195]. Vγ9Vδ2 T cells in combination with ZOL have been shown to kill glioblastoma cells *in vitro* [136], and *in vivo*

[196] when injected directly into the tumour site. Combining these approaches with Vγ9Vδ2 T cell loaded scaffolds could be used in a similar manner to eliminate residual cancer cells, while bypassing the BBB. This system could also be used for the treatment of osteosarcoma and primary breast cancer, which are also commonly treated using surgery. Chemotherapy and Vγ9Vδ2 T cell loaded scaffolds could be used following tumour resection with narrower margins, which would minimise the need for limb amputation or mastectomy, while potentially improving efficacy. At the time of writing this thesis, this laboratory has conducted preliminary experiments using Vγ9Vδ2 T cells in hydrogels and others scaffolds for the localised cancer therapy. Results from these preliminary studies have shown that Vγ9Vδ2 T cells are released from hydrogels and scaffolds, and they are as cytotoxic as free Vγ9Vδ2 T cells against breast cancer cells *in vitro* (Kaur and Zysk, unpublished data). Preclinical studies evaluating the potential use of Vγ9Vδ2 T cells embedded in injectable hydrogels for the treatment of localised cancer are well in progress and showing great promise.

8.2.5 Novel antibodies to enhance anti-cancer efficacy

Recently, novel bispecific and tribody antibodies have been designed to enhance Vγ9Vδ2 T cell cytotoxicity. A bispecific antibody which has been developed binds Her-2, commonly over-expressed on a variety of cancer cells including breast and pancreatic cancer, and CD3 or Vγ9, allowing binding to Vγ9Vδ2 T cells or $CD8^+$ CTLs [171]. This bispecific antibody has been shown to enhance the anti-cancer efficacy of Vγ9Vδ2 T cells against pancreatic ductal adenocarcinoma cells *in vitro* and *in vivo* [171]. In addition to targeting Her-2, the tribody also has two additional Vγ9 TCR binding sites, further enhancing cytotoxicity [172]. By modifying existing antibodies such as trastuzumab,

rixitumab, or drozitumab to include CD3 or Vγ9 portions could significantly improve the cytotoxicity of antibodies.

8.3 Conclusion

Collectively, the studies presented in this thesis demonstrate that adoptive transfer of *ex vivo* expanded Vγ9Vδ2 T cells in combination with ZOL is an effective two-pronged approach for targeting osteolytic cancer. These studies suggest this treatment regimen would be beneficial in reducing tumour growth in bone and tumour-associated osteolysis, while also limiting the potential for metastatic spread in osteosarcoma and advanced breast cancer patients. While these new insights into the field of Vγ9Vδ2 T cell immunotherapy have been highly encouraging, further studies particularly those focused on localised Vγ9Vδ2 T cell delivery and combinational therapies, are required to optimise a treatment regimen that achieves maximal anti-cancer efficacy.

Bibliography

[1] M. Campanacci, Bone and Soft Tissue Tumors, 2nd ed., Springer, New York, 1999.

[2] J.D. Mulder, H.E. Schütte, H.M. Kroon, W.K. Taconis, Radiologic Atlas of Bone Tumors. Elsevier, Amsterdam; 1993.

[3] R. Siegel, D. Naishadham, A. Jemal, Cancer statistics, 2013, CA Cancer J. Clin., 63 (2013) 11-30.

[4] I.J. Fidler, The pathogenesis of cancer metastasis: the 'seed and soil' hypothesis revisited, Nat. Rev. Cancer, 3 (2003) 453-458.

[5] K. Polyak, R.A. Weinberg, Transitions between epithelial and mesenchymal states: acquisition of malignant and stem cell traits, Nat. Rev. Cancer, 9 (2009) 265-273.

[6] M.A. Huber, N. Kraut, H. Beug, Molecular requirements for epithelial-mesenchymal transition during tumor progression, Curr. Opin. Cell Biol., 17 (2005) 548-558.

[7] L. Bubendorf, A. Schopfer, U. Wagner, G. Sauter, H. Moch, N. Willi, T.C. Gasser, M.J. Mihatsch, Metastatic patterns of prostate cancer: an autopsy study of 1,589 patients, Hum. Pathol., 31 (2000) 578-583.

[8] G.R. Mundy, Metastasis to bone: causes, consequences and therapeutic opportunities, Nat. Rev. Cancer, 2 (2002) 584-593.

[9] G.R. Mundy, Mechanisms of bone metastasis, Cancer, 80 (1997) 1546-1556.

[10] W. Kozlow, T.A. Guise, Breast cancer metastasis to bone: mechanisms of osteolysis and implications for therapy, J. Mammary Gland Biol. Neoplasia, 10 (2005) 169-180.

[11] L.A. Kingsley, P.G. Fournier, J.M. Chirgwin, T.A. Guise, Molecular biology of bone metastasis, Mol. Cancer Ther., 6 (2007) 2609-2617.

[12] E.T. Keller, J. Brown, Prostate cancer bone metastases promote both osteolytic and osteoblastic activity, J. Cell. Biochem., 91 (2004) 718-729.

[13] G.D. Roodman, Cell biology of the osteoclast, Exp. Hematol., 27 (1999) 1229-1241.

[14] T. Wada, T. Nakashima, N. Hiroshi, J.M. Penninger, RANKL-RANK signaling in osteoclastogenesis and bone disease, Trends Mol. Med., 12 (2006) 17-25.

[15] P.V. Hauschka, A.E. Mavrakos, M.D. Iafrati, S.E. Doleman, M. Klagsbrun, Growth factors in bone matrix. Isolation of multiple types by affinity chromatography on heparin-Sepharose, J. Biol. Chem., 261 (1986) 12665-12674.

[16] J. Pfeilschifter, G.R. Mundy, Modulation of type beta transforming growth factor activity in bone cultures by osteotropic hormones, Proc. Natl. Acad. Sci. U. S. A., 84 (1987) 2024-2028.

[17] J.R. Lieberman, A. Daluiski, T.A. Einhorn, The role of growth factors in the repair of bone. Biology and clinical applications, J. Bone Joint Surg. Am., 84-A (2002) 1032-1044.

[18] T.A. Guise, The vicious cycle of bone metastases, J. Musculoskelet. Neuronal Interact., 2 (2002) 570-572.

[19] G.D. Roodman, Mechanisms of bone metastasis, N. Engl. J. Med., 350 (2004) 1655-1664.

[20] R.E. Coleman, Skeletal complications of malignancy, Cancer, 80 (1997) 1588-1594.

[21] K.R. Duchman, Y. Gao, B.J. Miller, Prognostic factors for survival in patients with high-grade osteosarcoma using the Surveillance, Epidemiology, and End Results (SEER) Program database, Cancer Epidemiol., 39 (2015) 593-599.

[22] M. Hegyi, A.F. Semsei, Z. Jakab, I. Antal, J. Kiss, M. Szendroi, M. Csoka, G. Kovacs, Good prognosis of localized osteosarcoma in young patients treated with limb-salvage surgery and chemotherapy, Pediatr. Blood Cancer, 57 (2011) 415-422.

[23] G.M. Jeffree, C.H. Price, H.A. Sissons, The metastatic patterns of osteosarcoma, Br. J. Cancer, 32 (1975) 87-107.

[24] A. Briccoli, M. Rocca, M. Salone, G.A. Guzzardella, A. Balladelli, G. Bacci, High grade osteosarcoma of the extremities metastatic to the lung: long-term results in 323 patients treated combining surgery and chemotherapy, 1985-2005, Surg. Oncol., 19 (2010) 193-199.

[25] P.A. Meyers, G. Heller, J.H. Healey, A. Huvos, A. Applewhite, M. Sun, M. LaQuaglia, Osteogenic sarcoma with clinically detectable metastasis at initial presentation, J. Clin. Oncol., 11 (1993) 449-453.

[26] H.T. Ta, C.R. Dass, P.F. Choong, D.E. Dunstan, Osteosarcoma treatment: state of the art, Cancer Metastasis Rev., 28 (2009) 247-263.

[27] A. Luetke, P.A. Meyers, I. Lewis, H. Juergens, Osteosarcoma treatment - where do we stand? A state of the art review, Cancer Treat. Rev., 40 (2014) 523-532.

[28] J.K. Anninga, H. Gelderblom, M. Fiocco, J.R. Kroep, A.H. Taminiau, P.C. Hogendoorn, R.M. Egeler, Chemotherapeutic adjuvant treatment for osteosarcoma: where do we stand?, Eur. J. Cancer, 47 (2011) 2431-2445.

[29] A.J. Chou, R. Gorlick, Chemotherapy resistance in osteosarcoma: current challenges and future directions, Expert Rev. Anticancer Ther., 6 (2006) 1075-1085.

[30] R.E. Coleman, R.D. Rubens, The clinical course of bone metastases from breast cancer, Br. J. Cancer, 55 (1987) 61-66.

[31] J. Ferlay, I. Soerjomataram, R. Dikshit, S. Eser, C. Mathers, M. Rebelo, D.M. Parkin, D. Forman, F. Bray, Cancer incidence and mortality worldwide: sources, methods and major patterns in GLOBOCAN 2012, Int. J. Cancer, 136 (2015) E359-386.

[32] Australian Institute of Health and Welfare 2016, Australian Cancer Incidence and Mortality (ACIM) books: breast cancer, in: AIHW (Ed.), Australian Institute of Health and Welfare, Canberra, 2016.

[33] Breast Cancer Network Australia, About Breast Cancer, 2013.

[34] Cancer Australia, Report to the Nation - Breast Cancer 2012, in: A.G.C. Australia (Ed.)Surry Hills, NSW, 2012, 2012.

[35] N. Howlader, A.M. Noone, M. Krapcho, D. Miller, K. Bishop, S.F. Altekruse, C.L. Kosary, M. Yu, J. Ruhl, Z. Tatalovich, A. Mariotto, D.R. Lewis, H.S. Chen,

E.J. Feuer, K.A. Cronin (Eds.), SEER Cancer Statistics Review, 1975–2013, National Cancer Institute, Bethesda, MD (April 2016) based on November 2015 SEER data submission, posted to the SEER web site http://seer.cancer.gov/csr/1975_2013/

[36] A.T. Berman, A.D. Thukral, W.T. Hwang, L.J. Solin, N. Vapiwala, Incidence and patterns of distant metastases for patients with early-stage breast cancer after breast conservation treatment, Clin. Breast Cancer, 13 (2013) 88-94.

[37] National Comprehensive Cancer Network, NCCN Clinical Practice Guidelines in Oncology (NCCN Guidelines) Breast Cancer, 2016.

[38] D.J. Slamon, B. Leyland-Jones, S. Shak, H. Fuchs, V. Paton, A. Bajamonde, T. Fleming, W. Eiermann, J. Wolter, M. Pegram, J. Baselga, L. Norton, Use of chemotherapy plus a monoclonal antibody against HER2 for metastatic breast cancer that overexpresses HER2, N. Engl. J. Med., 344 (2001) 783-792.

[39] C.A. Santa-Maria, W.J. Gradishar, Changing Treatment Paradigms in Metastatic Breast Cancer: Lessons Learned, JAMA Oncol, 1 (2015) 528-534; quiz 549.

[40] A. Coates, V. Gebski, J.F. Bishop, P.N. Jeal, R.L. Woods, R. Snyder, M.H. Tattersall, M. Byrne, V. Harvey, G. Gill, Improving the quality of life during chemotherapy for advanced breast cancer. A comparison of intermittent and continuous treatment strategies, N. Engl. J. Med., 317 (1987) 1490-1495.

[41] K. Chatterjee, J. Zhang, N. Honbo, J.S. Karliner, Doxorubicin cardiomyopathy, Cardiology, 115 (2010) 155-162.

[42] J.R. Ross, Y. Saunders, P.M. Edmonds, S. Patel, K.E. Broadley, S.R. Johnston, Systematic review of role of bisphosphonates on skeletal morbidity in metastatic cancer, BMJ, 327 (2003) 469.

[43] J.R. Ross, Y. Saunders, P.M. Edmonds, S. Patel, D. Wonderling, C. Normand, K. Broadley, A systematic review of the role of bisphosphonates in metastatic disease, Health Technol. Assess., 8 (2004) 1-176.

[44] G. Moriceau, B. Ory, B. Gobin, F. Verrecchia, F. Gouin, F. Blanchard, F. Redini, D. Heymann, Therapeutic approach of primary bone tumours by bisphosphonates, Curr. Pharm. Des., 16 (2010) 2981-2987.

[45] J.E. Dunford, K. Thompson, F.P. Coxon, S.P. Luckman, F.M. Hahn, C.D. Poulter, F.H. Ebetino, M.J. Rogers, Structure-activity relationships for inhibition of farnesyl diphosphate synthase *in vitro* and inhibition of bone resorption *in vivo* by nitrogen-containing bisphosphonates, J. Pharmacol. Exp. Ther., 296 (2001) 235-242.

[46] M.J. Rogers, S. Gordon, H.L. Benford, F.P. Coxon, S.P. Luckman, J. Monkkonen, J.C. Frith, Cellular and molecular mechanisms of action of bisphosphonates, Cancer, 88 (2000) 2961-2978.

[47] S.P. Luckman, D.E. Hughes, F.P. Coxon, R. Graham, G. Russell, M.J. Rogers, Nitrogen-containing bisphosphonates inhibit the mevalonate pathway and prevent post-translational prenylation of GTP-binding proteins, including Ras, J. Bone Miner. Res., 13 (1998) 581-589.

[48] R.G. Russell, N.B. Watts, F.H. Ebetino, M.J. Rogers, Mechanisms of action of bisphosphonates: similarities and differences and their potential influence on clinical efficacy, Osteoporos. Int., 19 (2008) 733-759.

[49] F.P. Coxon, M.J. Rogers, The role of prenylated small GTP-binding proteins in the regulation of osteoclast function, Calcif. Tissue Int., 72 (2003) 80-84.

[50] F. Saad, D.M. Gleason, R. Murray, S. Tchekmedyian, P. Venner, L. Lacombe, J.L. Chin, J.J. Vinholes, J.A. Goas, B. Chen, G. Zoledronic Acid Prostate Cancer Study, A randomized, placebo-controlled trial of zoledronic acid in patients with hormone-refractory metastatic prostate carcinoma, J. Natl. Cancer Inst., 94 (2002) 1458-1468.

[51] F. Saad, D.M. Gleason, R. Murray, S. Tchekmedyian, P. Venner, L. Lacombe, J.L. Chin, J.J. Vinholes, J.A. Goas, M. Zheng, G. Zoledronic Acid Prostate Cancer Study, Long-term efficacy of zoledronic acid for the prevention of skeletal complications in patients with metastatic hormone-refractory prostate cancer, J. Natl. Cancer Inst., 96 (2004) 879-882.

[52] P. Musto, M.T. Petrucci, S. Bringhen, T. Guglielmelli, T. Caravita, V. Bongarzoni, A. Andriani, G. D'Arena, E. Balleari, G. Pietrantuono, M. Boccadoro, A. Palumbo, G.M.M.W. Party, N. the Italian Myeloma, A multicenter, randomized clinical trial comparing zoledronic acid versus observation in patients with asymptomatic myeloma, Cancer, 113 (2008) 1588-1595.

[53] A. Aviles, M.J. Nambo, N. Neri, C. Castaneda, S. Cleto, J. Huerta-Guzman, Antitumor effect of zoledronic acid in previously untreated patients with multiple myeloma, Med Oncol, 24 (2007) 227-230.

[54] R. Coleman, D. Cameron, D. Dodwell, R. Bell, C. Wilson, E. Rathbone, M. Keane, M. Gil, R. Burkinshaw, R. Grieve, P. Barrett-Lee, D. Ritchie, V. Liversedge, S. Hinsley, H. Marshall, A. investigators, Adjuvant zoledronic acid in

patients with early breast cancer: final efficacy analysis of the AZURE (BIG 01/04) randomised open-label phase 3 trial, Lancet Oncol., 15 (2014) 997-1006.

[55] J.R. Green, Antitumor effects of bisphosphonates, Cancer, 97 (2003) 840-847.

[56] M. Caraglia, D. Santini, M. Marra, B. Vincenzi, G. Tonini, A. Budillon, Emerging anti-cancer molecular mechanisms of aminobisphosphonates, Endocr. Relat. Cancer, 13 (2006) 7-26.

[57] N. Horie, H. Murata, S. Kimura, H. Takeshita, T. Sakabe, T. Matsui, T. Maekawa, T. Kubo, S. Fushiki, Combined effects of a third-generation bisphosphonate, zoledronic acid with other anticancer agents against murine osteosarcoma, Br. J. Cancer, 96 (2007) 255-261.

[58] K. Koto, H. Murata, S. Kimura, N. Horie, T. Matsui, Y. Nishigaki, K. Ryu, T. Sakabe, M. Itoi, E. Ashihara, T. Maekawa, S. Fushiki, T. Kubo, Zoledronic acid inhibits proliferation of human fibrosarcoma cells with induction of apoptosis, and shows combined effects with other anticancer agents, Oncol. Rep., 24 (2010) 233-239.

[59] O. Fromigue, L. Lagneaux, J.J. Body, Bisphosphonates induce breast cancer cell death *in vitro*, J. Bone Miner. Res., 15 (2000) 2211-2221.

[60] S. Boissier, M. Ferreras, O. Peyruchaud, S. Magnetto, F.H. Ebetino, M. Colombel, P. Delmas, J.M. Delaisse, P. Clezardin, Bisphosphonates inhibit breast and prostate carcinoma cell invasion, an early event in the formation of bone metastases, Cancer Res., 60 (2000) 2949-2954.

[61] R. Montague, C.A. Hart, N.J. George, V.A. Ramani, M.D. Brown, N.W. Clarke, Differential inhibition of invasion and proliferation by bisphosphonates:

anti-metastatic potential of Zoledronic acid in prostate cancer, Eur. Urol., 46 (2004) 389-401; discussion 401-382.

[62] S. Matsumoto, S. Kimura, H. Segawa, J. Kuroda, T. Yuasa, K. Sato, M. Nogawa, F. Tanaka, T. Maekawa, H. Wada, Efficacy of the third-generation bisphosphonate, zoledronic acid alone and combined with anti-cancer agents against small cell lung cancer cell lines, Lung Cancer, 47 (2005) 31-39.

[63] K.W. Luo, C.H. Ko, G.G. Yue, M.Y. Lee, W.S. Siu, J.K. Lee, W.T. Shum, K.P. Fung, P.C. Leung, G. Li, A. Evdokiou, C.B. Lau, Anti-tumor and anti-osteolysis effects of the metronomic use of zoledronic acid in primary and metastatic breast cancer mouse models, Cancer Lett., 339 (2013) 42-48.

[64] J. Jeong, K.S. Lee, Y.K. Choi, Y.J. Oh, H.D. Lee, Preventive effects of zoledronic acid on bone metastasis in mice injected with human breast cancer cells, J. Korean Med. Sci., 26 (2011) 1569-1575.

[65] B. Ory, M.F. Heymann, A. Kamijo, F. Gouin, D. Heymann, F. Redini, Zoledronic acid suppresses lung metastases and prolongs overall survival of osteosarcoma-bearing mice, Cancer, 104 (2005) 2522-2529.

[66] K. Koto, N. Horie, S. Kimura, H. Murata, T. Sakabe, T. Matsui, M. Watanabe, S. Adachi, T. Maekawa, S. Fushiki, T. Kubo, Clinically relevant dose of zoledronic acid inhibits spontaneous lung metastasis in a murine osteosarcoma model, Cancer Lett., 274 (2009) 271-278.

[67] A. Labrinidis, S. Hay, V. Liapis, V. Ponomarev, D.M. Findlay, A. Evdokiou, Zoledronic acid inhibits both the osteolytic and osteoblastic components of osteosarcoma lesions in a mouse model, Clin. Cancer Res., 15 (2009) 3451-3461.

[68] A. Labrinidis, S. Hay, V. Liapis, D.M. Findlay, A. Evdokiou, Zoledronic acid protects against osteosarcoma-induced bone destruction but lacks efficacy against pulmonary metastases in a syngeneic rat model, Int. J. Cancer, 127 (2010) 345-354.

[69] P.A. Newcomb, M.N. Passarelli, A.I. Phipps, G.L. Anderson, J. Wactawski-Wende, G.Y. Ho, M.J. O'Sullivan, R.T. Chlebowski, Oral bisphosphonate use and risk of postmenopausal endometrial cancer, J. Clin. Oncol., 33 (2015) 1186-1190.

[70] P.A. Newcomb, A. Trentham-Dietz, J.M. Hampton, Bisphosphonates for osteoporosis treatment are associated with reduced breast cancer risk, Br. J. Cancer, 102 (2010) 799-802.

[71] R. Kremer, B. Gagnon, A.N. Meguerditchian, L. Nadeau, N. Mayo, Effect of oral bisphosphonates for osteoporosis on development of skeletal metastases in women with breast cancer: results from a pharmaco-epidemiological study, J. Natl. Cancer Inst., 106 (2014).

[72] V. Kunzmann, E. Bauer, M. Wilhelm, Gamma/delta T-cell stimulation by pamidronate, N. Engl. J. Med., 340 (1999) 737-738.

[73] S. Kalyan, E.S. Quabius, J. Wiltfang, H. Monig, D. Kabelitz, Can peripheral blood gammadelta T cells predict osteonecrosis of the jaw? An immunological perspective on the adverse drug effects of aminobisphosphonate therapy, J. Bone Miner. Res., 28 (2013) 728-735.

[74] A.A. Khan, A. Morrison, D.A. Hanley, D. Felsenberg, L.K. McCauley, F. O'Ryan, I.R. Reid, S.L. Ruggiero, A. Taguchi, S. Tetradis, N.B. Watts, M.L. Brandi, E. Peters, T. Guise, R. Eastell, A.M. Cheung, S.N. Morin, B. Masri, C. Cooper, S.L. Morgan, B. Obermayer-Pietsch, B.L. Langdahl, R. Al Dabagh, K.S. Davison, D.L. Kendler, G.K. Sandor, R.G. Josse, M. Bhandari, M. El Rabbany,

D.D. Pierroz, R. Sulimani, D.P. Saunders, J.P. Brown, J. Compston, J. International Task Force on Osteonecrosis of the, Diagnosis and management of osteonecrosis of the jaw: a systematic review and international consensus, J. Bone Miner. Res., 30 (2015) 3-23.

[75] M. Muraro, O.M. Mereuta, F. Carraro, E. Madon, F. Fagioli, Osteosarcoma cell line growth inhibition by zoledronate-stimulated effector cells, Cell. Immunol., 249 (2007) 63-72.

[76] D. Kabelitz, D. Wesch, E. Pitters, M. Zoller, Characterization of tumor reactivity of human V gamma 9V delta 2 gamma delta T cells *in vitro* and in SCID mice *in vivo*, J. Immunol., 173 (2004) 6767-6776.

[77] T. Santolaria, M. Robard, A. Leger, V. Catros, M. Bonneville, E. Scotet, Repeated systemic administrations of both aminobisphosphonates and human Vgamma9Vdelta2 T cells efficiently control tumor development *in vivo*, J. Immunol., 191 (2013) 1993-2000.

[78] K. Sato, S. Kimura, H. Segawa, A. Yokota, S. Matsumoto, J. Kuroda, M. Nogawa, T. Yuasa, Y. Kiyono, H. Wada, T. Maekawa, Cytotoxic effects of gammadelta T cells expanded *ex vivo* by a third generation bisphosphonate for cancer immunotherapy, Int. J. Cancer, 116 (2005) 94-99.

[79] Z. Li, Q. Xu, H. Peng, R. Cheng, Z. Sun, Z. Ye, IFN-gamma enhances HOS and U2OS cell lines susceptibility to gammadelta T cell-mediated killing through the Fas/Fas ligand pathway, Int. Immunopharmacol., 11 (2011) 496-503.

[80] Q. Cui, H. Shibata, A. Oda, H. Amou, A. Nakano, K. Yata, M. Hiasa, K. Watanabe, S. Nakamura, H. Miki, T. Harada, S. Fujii, K. Kagawa, K. Takeuchi, S.

Ozaki, T. Matsumoto, M. Abe, Targeting myeloma-osteoclast interaction with Vgamma9Vdelta2 T cells, Int. J. Hematol., 94 (2011) 63-70.

[81] S.R. Mattarollo, T. Kenna, M. Nieda, A.J. Nicol, Chemotherapy and zoledronate sensitize solid tumour cells to Vgamma9Vdelta2 T cell cytotoxicity, Cancer Immunol. Immunother., 56 (2007) 1285-1297.

[82] I. Benzaid, H. Monkkonen, V. Stresing, E. Bonnelye, J. Green, J. Monkkonen, J.L. Touraine, P. Clezardin, High phosphoantigen levels in bisphosphonate-treated human breast tumors promote Vgamma9Vdelta2 T-cell chemotaxis and cytotoxicity *in vivo*, Cancer Res., 71 (2011) 4562-4572.

[83] M. Kondo, T. Izumi, N. Fujieda, A. Kondo, T. Morishita, H. Matsushita, K. Kakimi, Expansion of human peripheral blood gammadelta T cells using zoledronate, J Vis Exp, (2011).

[84] S.R. Carding, P.J. Egan, Gammadelta T cells: functional plasticity and heterogeneity, Nat. Rev. Immunol., 2 (2002) 336-345.

[85] D. Hannani, Y. Ma, T. Yamazaki, J. Dechanet-Merville, G. Kroemer, L. Zitvogel, Harnessing gammadelta T cells in anticancer immunotherapy, Trends Immunol., 33 (2012) 199-206.

[86] B. Silva-Santos, K. Serre, H. Norell, gammadelta T cells in cancer, Nat. Rev. Immunol., 15 (2015) 683-691.

[87] A.S. Ensslin, B. Formby, Comparison of cytolytic and proliferative activities of human gamma delta and alpha beta T cells from peripheral blood against various human tumor cell lines, J. Natl. Cancer Inst., 83 (1991) 1564-1569.

[88] C. Harly, Y. Guillaume, S. Nedellec, C.M. Peigne, H. Monkkonen, J. Monkkonen, J. Li, J. Kuball, E.J. Adams, S. Netzer, J. Dechanet-Merville, A. Leger, T. Herrmann, R. Breathnach, D. Olive, M. Bonneville, E. Scotet, Key implication of CD277/butyrophilin-3 (BTN3A) in cellular stress sensing by a major human gammadelta T-cell subset, Blood, 120 (2012) 2269-2279.

[89] H. Sicard, J.J. Fournie, Metabolic routes as targets for immunological discrimination of host and parasite, Infect. Immun., 68 (2000) 4375-4377.

[90] W. Gossman, E. Oldfield, Quantitative structure--activity relations for gammadelta T cell activation by phosphoantigens, J. Med. Chem., 45 (2002) 4868-4874.

[91] M. Thurnher, G. Gruenbacher, O. Nussbaumer, Regulation of mevalonate metabolism in cancer and immune cells, Biochim. Biophys. Acta, 1831 (2013) 1009-1015.

[92] H.J. Gober, M. Kistowska, L. Angman, P. Jeno, L. Mori, G. De Libero, Human T cell receptor gammadelta cells recognize endogenous mevalonate metabolites in tumor cells, J. Exp. Med., 197 (2003) 163-168.

[93] K. Thompson, M.J. Rogers, Statins prevent bisphosphonate-induced gamma,delta-T-cell proliferation and activation *in vitro*, J. Bone Miner. Res., 19 (2004) 278-288.

[94] R.E. Hewitt, A. Lissina, A.E. Green, E.S. Slay, D.A. Price, A.K. Sewell, The bisphosphonate acute phase response: rapid and copious production of proinflammatory cytokines by peripheral blood gd T cells in response to aminobisphosphonates is inhibited by statins, Clin. Exp. Immunol., 139 (2005) 101-111.

[95] K.M. Dale, C.I. Coleman, N.N. Henyan, J. Kluger, C.M. White, Statins and cancer risk: a meta-analysis, JAMA, 295 (2006) 74-80.

[96] M. Murayama, Y. Tanaka, J. Yagi, T. Uchiyama, K. Ogawa, Antitumor activity and some immunological properties of gammadelta T-cells from patients with gastrointestinal carcinomas, Anticancer Res., 28 (2008) 2921-2931.

[97] H. Kobayashi, Y. Tanaka, J. Yagi, Y. Osaka, H. Nakazawa, T. Uchiyama, N. Minato, H. Toma, Safety profile and anti-tumor effects of adoptive immunotherapy using gamma-delta T cells against advanced renal cell carcinoma: a pilot study, Cancer Immunol. Immunother., 56 (2007) 469-476.

[98] M. D'Asaro, C. La Mendola, D. Di Liberto, V. Orlando, M. Todaro, M. Spina, G. Guggino, S. Meraviglia, N. Caccamo, A. Messina, A. Salerno, F. Di Raimondo, P. Vigneri, G. Stassi, J.J. Fournie, F. Dieli, V gamma 9V delta 2 T lymphocytes efficiently recognize and kill zoledronate-sensitized, imatinib-sensitive, and imatinib-resistant chronic myelogenous leukemia cells, J. Immunol., 184 (2010) 3260-3268.

[99] D.F. Angelini, G. Borsellino, M. Poupot, A. Diamantini, R. Poupot, G. Bernardi, F. Poccia, J.J. Fournie, L. Battistini, FcgammaRIII discriminates between 2 subsets of Vgamma9Vdelta2 effector cells with different responses and activation pathways, Blood, 104 (2004) 1801-1807.

[100] J. Bennouna, V. Levy, H. Sicard, H. Senellart, M. Audrain, S. Hiret, F. Rolland, H. Bruzzoni-Giovanelli, M. Rimbert, C. Galea, J. Tiollier, F. Calvo, Phase I study of bromohydrin pyrophosphate (BrHPP, IPH 1101), a Vgamma9Vdelta2 T lymphocyte agonist in patients with solid tumors, Cancer Immunol. Immunother., 59 (2010) 1521-1530.

[101] S. Galluzzo, D. Santini, B. Vincenzi, N. Caccamo, F. Meraviglia, A. Salerno, F. Dieli, G. Tonini, Immunomodulating role of bisphosphonates on human gamma delta T cells: an intriguing and promising aspect of their antitumour activity, Expert Opin. Ther. Targets, 11 (2007) 941-954.

[102] A.J. Roelofs, M. Jauhiainen, H. Monkkonen, M.J. Rogers, J. Monkkonen, K. Thompson, Peripheral blood monocytes are responsible for gammadelta T cell activation induced by zoledronic acid through accumulation of IPP/DMAPP, Br. J. Haematol., 144 (2009) 245-250.

[103] N. Caccamo, S. Meraviglia, V. Ferlazzo, D. Angelini, G. Borsellino, F. Poccia, L. Battistini, F. Dieli, A. Salerno, Differential requirements for antigen or homeostatic cytokines for proliferation and differentiation of human Vgamma9Vdelta2 naive, memory and effector T cell subsets, Eur. J. Immunol., 35 (2005) 1764-1772.

[104] F. Dieli, F. Poccia, M. Lipp, G. Sireci, N. Caccamo, C. Di Sano, A. Salerno, Differentiation of effector/memory Vdelta2 T cells and migratory routes in lymph nodes or inflammatory sites, J. Exp. Med., 198 (2003) 391-397.

[105] A. Noguchi, T. Kaneko, T. Kamigaki, K. Fujimoto, M. Ozawa, M. Saito, N. Ariyoshi, S. Goto, Zoledronate-activated Vgamma9gammadelta T cell-based immunotherapy is feasible and restores the impairment of gammadelta T cells in patients with solid tumors, Cytotherapy, 13 (2011) 92-97.

[106] Y. Abe, M. Muto, M. Nieda, Y. Nakagawa, A. Nicol, T. Kaneko, S. Goto, K. Yokokawa, K. Suzuki, Clinical and immunological evaluation of zoledronate-activated Vgamma9gammadelta T-cell-based immunotherapy for patients with multiple myeloma, Exp. Hematol., 37 (2009) 956-968.

[107] C. Niu, H. Jin, M. Li, J. Xu, D. Xu, J. Hu, H. He, W. Li, J. Cui, *In vitro* analysis of the proliferative capacity and cytotoxic effects of *ex vivo* induced natural killer cells, cytokine-induced killer cells, and gamma-delta T cells, BMC Immunol., 16 (2015) 61.

[108] B. Poonia, C.D. Pauza, Gamma delta T cells from HIV+ donors can be expanded *in vitro* by zoledronate/interleukin-2 to become cytotoxic effectors for antibody-dependent cellular cytotoxicity, Cytotherapy, 14 (2012) 173-181.

[109] Y. He, K. Wu, Y. Hu, L. Sheng, R. Tie, B. Wang, H. Huang, gammadelta T cell and other immune cells crosstalk in cellular immunity, J Immunol Res, 2014 (2014) 960252.

[110] A. Maniar, X. Zhang, W. Lin, B.R. Gastman, C.D. Pauza, S.E. Strome, A.I. Chapoval, Human gammadelta T lymphocytes induce robust NK cell-mediated antitumor cytotoxicity through CD137 engagement, Blood, 116 (2010) 1726-1733.

[111] R. Aggarwal, J. Lu, S. Kanji, M. Das, M. Joseph, M.B. Lustberg, A. Ray, V.J. Pompili, C.L. Shapiro, H. Das, Human Vgamma2Vdelta2 T cells limit breast cancer growth by modulating cell survival-, apoptosis-related molecules and microenvironment in tumors, Int. J. Cancer, 133 (2013) 2133-2144.

[112] J. Lu, R. Aggarwal, S. Kanji, M. Das, M. Joseph, V. Pompili, H. Das, Human ovarian tumor cells escape gammadelta T cell recognition partly by down regulating surface expression of MICA and limiting cell cycle related molecules, PLoS One, 6 (2011) e23348.

[113] T. Lanca, D.V. Correia, C.F. Moita, H. Raquel, A. Neves-Costa, C. Ferreira, J.S. Ramalho, J.T. Barata, L.F. Moita, A.Q. Gomes, B. Silva-Santos, The MHC

class Ib protein ULBP1 is a nonredundant determinant of leukemia/lymphoma susceptibility to gammadelta T-cell cytotoxicity, Blood, 115 (2010) 2407-2411.

[114] Y. Kong, W. Cao, X. Xi, C. Ma, L. Cui, W. He, The NKG2D ligand ULBP4 binds to TCRgamma9/delta2 and induces cytotoxicity to tumor cells through both TCRgammadelta and NKG2D, Blood, 114 (2009) 310-317.

[115] A.H. Capietto, L. Martinet, J.J. Fournie, Stimulated gammadelta T cells increase the *in vivo* efficacy of trastuzumab in HER-2+ breast cancer, J. Immunol., 187 (2011) 1031-1038.

[116] H. Tokuyama, T. Hagi, S.R. Mattarollo, J. Morley, Q. Wang, H.F. So, F. Moriyasu, M. Nieda, A.J. Nicol, V gamma 9 V delta 2 T cell cytotoxicity against tumor cells is enhanced by monoclonal antibody drugs--rituximab and trastuzumab, Int. J. Cancer, 122 (2008) 2526-2534.

[117] M. Otto, R.C. Barfield, W.J. Martin, R. Iyengar, W. Leung, T. Leimig, S. Chaleff, S.D. Gillies, R. Handgretinger, Combination immunotherapy with clinical-scale enriched human gammadelta T cells, hu14.18 antibody, and the immunocytokine Fc-IL7 in disseminated neuroblastoma, Clin. Cancer Res., 11 (2005) 8486-8491.

[118] U.J. Seidel, F. Vogt, L. Grosse-Hovest, G. Jung, R. Handgretinger, P. Lang, gammadelta T Cell-Mediated Antibody-Dependent Cellular Cytotoxicity with CD19 Antibodies Assessed by an Impedance-Based Label-Free Real-Time Cytotoxicity Assay, Front. Immunol., 5 (2014) 618.

[119] M.S. Braza, B. Klein, Anti-tumour immunotherapy with Vgamma9Vdelta2 T lymphocytes: from the bench to the bedside, Br. J. Haematol., 160 (2013) 123-132.

[120] J.P. Fisher, J. Heuijerjans, M. Yan, K. Gustafsson, J. Anderson, gammadelta T cells for cancer immunotherapy: A systematic review of clinical trials, Oncoimmunology, 3 (2014) e27572.

[121] S. Buccheri, G. Guggino, N. Caccamo, P. Li Donni, F. Dieli, Efficacy and safety of gammadeltaT cell-based tumor immunotherapy: a meta-analysis, J. Biol. Regul. Homeost. Agents, 28 (2014) 81-90.

[122] S. Meraviglia, M. Eberl, D. Vermijlen, M. Todaro, S. Buccheri, G. Cicero, C. La Mendola, G. Guggino, M. D'Asaro, V. Orlando, F. Scarpa, A. Roberts, N. Caccamo, G. Stassi, F. Dieli, A.C. Hayday, *In vivo* manipulation of Vgamma9Vdelta2 T cells with zoledronate and low-dose interleukin-2 for immunotherapy of advanced breast cancer patients, Clin. Exp. Immunol., 161 (2010) 290-297.

[123] F. Dieli, D. Vermijlen, F. Fulfaro, N. Caccamo, S. Meraviglia, G. Cicero, A. Roberts, S. Buccheri, M. D'Asaro, N. Gebbia, A. Salerno, M. Eberl, A.C. Hayday, Targeting human {gamma}delta} T cells with zoledronate and interleukin-2 for immunotherapy of hormone-refractory prostate cancer, Cancer Res., 67 (2007) 7450-7457.

[124] J.M. Lang, M.R. Kaikobad, M. Wallace, M.J. Staab, D.L. Horvath, G. Wilding, G. Liu, J.C. Eickhoff, D.G. McNeel, M. Malkovsky, Pilot trial of interleukin-2 and zoledronic acid to augment gammadelta T cells as treatment for patients with refractory renal cell carcinoma, Cancer Immunol. Immunother., 60 (2011) 1447-1460.

[125] Y.H. Gan, M. Wallace, M. Malkovsky, Fas-dependent, activation-induced cell death of gammadelta cells, J. Biol. Regul. Homeost. Agents, 15 (2001) 277-285.

[126] A.J. Nicol, H. Tokuyama, S.R. Mattarollo, T. Hagi, K. Suzuki, K. Yokokawa, M. Nieda, Clinical evaluation of autologous gamma delta T cell-based immunotherapy for metastatic solid tumours, Br. J. Cancer, 105 (2011) 778-786.

[127] J. Nakajima, T. Murakawa, T. Fukami, S. Goto, T. Kaneko, Y. Yoshida, S. Takamoto, K. Kakimi, A phase I study of adoptive immunotherapy for recurrent non-small-cell lung cancer patients with autologous gammadelta T cells, Eur. J. Cardiothorac. Surg., 37 (2010) 1191-1197.

[128] I. Wada, H. Matsushita, S. Noji, K. Mori, H. Yamashita, S. Nomura, N. Shimizu, Y. Seto, K. Kakimi, Intraperitoneal injection of *in vitro* expanded Vgamma9Vdelta2 T cells together with zoledronate for the treatment of malignant ascites due to gastric cancer, Cancer medicine, 3 (2014) 362-375.

[129] G.M. Siegers, L.S. Lamb, Jr., Cytotoxic and regulatory properties of circulating Vdelta1+ gammadelta T cells: a new player on the cell therapy field?, Mol. Ther., 22 (2014) 1416-1422.

[130] D.V. Correia, M. Fogli, K. Hudspeth, M.G. da Silva, D. Mavilio, B. Silva-Santos, Differentiation of human peripheral blood Vdelta1+ T cells expressing the natural cytotoxicity receptor NKp30 for recognition of lymphoid leukemia cells, Blood, 118 (2011) 992-1001.

[131] A.R. Almeida, D.V. Correia, A. Fernandes-Platzgummer, C.L. da Silva, M. Gomes da Silva, D.R. Anjos, B. Silva-Santos, Delta One T cells for immunotherapy

of chronic lymphocytic leukemia: clinical-grade expansion/ differentiation and preclinical proof-of-concept, Clin. Cancer Res., (2016).

[132] O. Nussbaumer, R. Woolf, R. Beatson, A.C. Hayday, Human skin Vδ1+ T cells: Mediators of stress-surveillance and a potential tool for adaptive cell therapy, Gamma Delta Conference 2016, King's College, London, 2016, pp. 85.

[133] PIPELINE | Lymphact - Building the future of healthcare [Internet]. Lymphact.com. 2016 [cited 8 December 2016]. Available from: http://www.lymphact.com/node/34

[134] H.R. Salih, H.G. Rammensee, A. Steinle, Cutting edge: down-regulation of MICA on human tumors by proteolytic shedding, J. Immunol., 169 (2002) 4098-4102.

[135] Z. Li, H. Peng, Q. Xu, Z. Ye, Sensitization of human osteosarcoma cells to Vgamma9Vdelta2 T-cell-mediated cytotoxicity by zoledronate, J. Orthop. Res., 30 (2012) 824-830.

[136] T. Nakazawa, M. Nakamura, Y.S. Park, Y. Motoyama, Y. Hironaka, F. Nishimura, I. Nakagawa, S. Yamada, R. Matsuda, K. Tamura, T. Sugimoto, Y. Takeshima, A. Marutani, T. Tsujimura, N. Ouji, Y. Ouji, M. Yoshikawa, H. Nakase, Cytotoxic human peripheral blood-derived gammadeltaT cells kill glioblastoma cell lines: implications for cell-based immunotherapy for patients with glioblastoma, J. Neurooncol., 116 (2014) 31-39.

[137] M.H. Moon, J.K. Jeong, J.S. Seo, J.W. Seol, Y.J. Lee, M. Xue, C.J. Jackson, S.Y. Park, Bisphosphonate enhances TRAIL sensitivity to human osteosarcoma cells via death receptor 5 upregulation, Exp. Mol. Med., 43 (2011) 138-145.

[138] M. Todaro, V. Orlando, G. Cicero, N. Caccamo, S. Meraviglia, G. Stassi, F. Dieli, Chemotherapy sensitizes colon cancer initiating cells to Vgamma9Vdelta2 T cell-mediated cytotoxicity, PLoS One, 8 (2013) e65145.

[139] S. Bouralexis, D.M. Findlay, A. Evdokiou, Death to the bad guys: targeting cancer via Apo2L/TRAIL, Apoptosis, 10 (2005) 35-51.

[140] S. Bouralexis, D.M. Findlay, G.J. Atkins, A. Labrinidis, S. Hay, A. Evdokiou, Progressive resistance of BTK-143 osteosarcoma cells to Apo2L/TRAIL-induced apoptosis is mediated by acquisition of DcR2/TRAIL-R4 expression: resensitisation with chemotherapy, Br. J. Cancer, 89 (2003) 206-214.

[141] M. Thai le, A. Labrinidis, S. Hay, V. Liapis, S. Bouralexis, K. Welldon, B.J. Coventry, D.M. Findlay, A. Evdokiou, Apo2l/Tumor necrosis factor-related apoptosis-inducing ligand prevents breast cancer-induced bone destruction in a mouse model, Cancer Res., 66 (2006) 5363-5370.

[142] A. Groth, A.V. Salnikov, S. Ottinger, J. Gladkich, L. Liu, G. Kallifatidis, O. Salnikova, E. Ryschich, N. Giese, T. Giese, F. Momburg, M.W. Buchler, G. Moldenhauer, I. Herr, New gene-immunotherapy combining TRAIL-lymphocytes and EpCAMxCD3 Bispecific antibody for tumor targeting, Clin. Cancer Res., 18 (2012) 1028-1038.

[143] M.J. Smyth, K. Takeda, Y. Hayakawa, J.J. Peschon, M.R. van den Brink, H. Yagita, Nature's TRAIL--on a path to cancer immunotherapy, Immunity, 18 (2003) 1-6.

[144] M. Daeron, Fc receptor biology, Annu. Rev. Immunol., 15 (1997) 203-234.

[145] N.S. Wilson, B. Yang, A. Yang, S. Loeser, S. Marsters, D. Lawrence, Y. Li, R. Pitti, K. Totpal, S. Yee, S. Ross, J.M. Vernes, Y. Lu, C. Adams, R. Offringa, B. Kelley, S. Hymowitz, D. Daniel, G. Meng, A. Ashkenazi, An Fcgamma receptor-dependent mechanism drives antibody-mediated target-receptor signaling in cancer cells, Cancer Cell, 19 (2011) 101-113.

[146] I. Zinonos, A. Labrinidis, M. Lee, V. Liapis, S. Hay, V. Ponomarev, P. Diamond, A.C. Zannettino, D.M. Findlay, A. Evdokiou, Apomab, a fully human agonistic antibody to DR5, exhibits potent antitumor activity against primary and metastatic breast cancer, Mol. Cancer Ther., 8 (2009) 2969-2980.

[147] Antibody-dependent cell-mediated cytotoxicity [Internet]. En.wikipedia.org. 2016 [cited 10 December 2016]. Available from: https://en.wikipedia.org/wiki/Antibody-dependent_cell-mediated_cytotoxicity

[148] A. Pappalardo, K. Thompson, Activated gammadelta T cells inhibit osteoclast differentiation and resorptive activity *in vitro*, Clin. Exp. Immunol., 174 (2013) 281-291.

[149] U. Laggner, P. Di Meglio, G.K. Perera, C. Hundhausen, K.E. Lacy, N. Ali, C.H. Smith, A.C. Hayday, B.J. Nickoloff, F.O. Nestle, Identification of a novel proinflammatory human skin-homing Vgamma9Vdelta2 T cell subset with a potential role in psoriasis, J. Immunol., 187 (2011) 2783-2793.

[150] G. Workalemahu, M. Foerster, C. Kroegel, R.K. Braun, Human gamma delta-T lymphocytes express and synthesize connective tissue growth factor: effect of IL-15 and TGF-beta 1 and comparison with alpha beta-T lymphocytes, J. Immunol., 170 (2003) 153-157.

[151] G. Workalemahu, M. Foerster, C. Kroegel, Expression of metalloproteinase-7 (matrilysin) in human blood and bronchoalveolar gamma/delta T-lymphocytes. Selective upregulation by the soluble non-peptidic mycobacterial phosphoantigen (isopentenyl pyrophosphate), J. Cell. Physiol., 207 (2006) 67-74.

[152] Q. Luo, Q. Kang, W. Si, W. Jiang, J.K. Park, Y. Peng, X. Li, H.H. Luu, J. Luo, A.G. Montag, R.C. Haydon, T.C. He, Connective tissue growth factor (CTGF) is regulated by Wnt and bone morphogenetic proteins signaling in osteoblast differentiation of mesenchymal stem cells, J. Biol. Chem., 279 (2004) 55958-55968.

[153] F.F. Safadi, J. Xu, S.L. Smock, R.A. Kanaan, A.H. Selim, P.R. Odgren, S.C. Marks, Jr., T.A. Owen, S.N. Popoff, Expression of connective tissue growth factor in bone: its role in osteoblast proliferation and differentiation *in vitro* and bone formation *in vivo*, J. Cell. Physiol., 196 (2003) 51-62.

[154] N.T. Colburn, K.J. Zaal, F. Wang, R.S. Tuan, A role for gamma/delta T cells in a mouse model of fracture healing, Arthritis Rheum., 60 (2009) 1694-1703.

[155] T. Ono, K. Okamoto, T. Nakashima, T. Nitta, S. Hori, Y. Iwakura, H. Takayanagi, IL-17-producing gammadelta T cells enhance bone regeneration, Nat Commun, 7 (2016) 10928.

[156] S. Kalyan, W. He, D. Kabelitz, Bone Cancer: Primary bone cancers and bone metastases, in: D. Heymann (Ed.) Bone Cancer: Primary bone cancers and bone metastases, Elsevier 2014, pp. 629-636.

[157] A. Zysk, M.O. DeNichilo, V. Panagopoulos, I. Zinonos, V. Liapis, S. Hay, W. Ingman, V. Ponomarev, G. Atkins, D. Findlay, A. Zannettino, A. Evdokiou, Adoptive transfer of *ex vivo* expanded Vgamma9Vdelta2 T cells in combination

with zoledronic acid inhibits cancer growth and limits osteolysis in a murine model of osteolytic breast cancer, Cancer Lett., 386 (2017) 141-150.

[158] V. Liapis, A. Labrinidis, I. Zinonos, S. Hay, V. Ponomarev, V. Panagopoulos, M. DeNichilo, W. Ingman, G.J. Atkins, D.M. Findlay, A.C. Zannettino, A. Evdokiou, Hypoxia-activated pro-drug TH-302 exhibits potent tumor suppressive activity and cooperates with chemotherapy against osteosarcoma, Cancer Lett., 357 (2015) 160-169.

[159] A.J. Gentles, A.M. Newman, C.L. Liu, S.V. Bratman, W. Feng, D. Kim, V.S. Nair, Y. Xu, A. Khuong, C.D. Hoang, M. Diehn, R.B. West, S.K. Plevritis, A.A. Alizadeh, The prognostic landscape of genes and infiltrating immune cells across human cancers, Nat. Med., 21 (2015) 938-945.

[160] Z. Li, Potential of human gammadelta T cells for immunotherapy of osteosarcoma, Mol. Biol. Rep., 40 (2013) 427-437.

[161] B.J. Zheng, K.W. Chan, S. Im, D. Chua, J.S. Sham, P.C. Tin, Z.M. He, M.H. Ng, Anti-tumor effects of human peripheral gammadelta T cells in a mouse tumor model, Int. J. Cancer, 92 (2001) 421-425.

[162] B.H. Beck, H.G. Kim, H. Kim, S. Samuel, Z. Liu, R. Shrestha, H. Haines, K. Zinn, R.D. Lopez, Adoptively transferred *ex vivo* expanded gammadelta-T cells mediate *in vivo* antitumor activity in preclinical mouse models of breast cancer, Breast Cancer Res. Treat., 122 (2010) 135-144.

[163] E. Pasquier, M. Kavallaris, N. Andre, Metronomic chemotherapy: new rationale for new directions, Nat. Rev. Clin. Oncol., 7 (2010) 455-465.

[164] H. Takayanagi, K. Ogasawara, S. Hida, T. Chiba, S. Murata, K. Sato, A. Takaoka, T. Yokochi, H. Oda, K. Tanaka, K. Nakamura, T. Taniguchi, T-cell-mediated regulation of osteoclastogenesis by signalling cross-talk between RANKL and IFN-gamma, Nature, 408 (2000) 600-605.

[165] N. Bonnet, P. Lesclous, J.L. Saffar, S. Ferrari, Zoledronate effects on systemic and jaw osteopenias in ovariectomized periostin-deficient mice, PLoS One, 8 (2013) e58726.

[166] C.L. Gregson, S.A. Hardcastle, C. Cooper, J.H. Tobias, Friend or foe: high bone mineral density on routine bone density scanning, a review of causes and management, Rheumatology (Oxford), 52 (2013) 968-985.

[167] S. Kalyan, V. Chandrasekaran, E.S. Quabius, T.K. Lindhorst, D. Kabelitz, Neutrophil uptake of nitrogen-bisphosphonates leads to the suppression of human peripheral blood gammadelta T cells, Cell. Mol. Life Sci., 71 (2014) 2335-2346.

[168] N. Kang, J. Zhou, T. Zhang, L. Wang, F. Lu, Y. Cui, L. Cui, W. He, Adoptive immunotherapy of lung cancer with immobilized anti-TCRgammadelta antibody-expanded human gammadelta T-cells in peripheral blood, Cancer Biol. Ther., 8 (2009) 1540-1549.

[169] V. Lafont, J. Liautard, J.P. Liautard, J. Favero, Production of TNF-alpha by human V gamma 9V delta 2 T cells via engagement of Fc gamma RIIIA, the low affinity type 3 receptor for the Fc portion of IgG, expressed upon TCR activation by nonpeptidic antigen, J. Immunol., 166 (2001) 7190-7199.

[170] M. Guilliams, P. Bruhns, Y. Saeys, H. Hammad, B.N. Lambrecht, The function of Fcgamma receptors in dendritic cells and macrophages, Nat. Rev. Immunol., 14 (2014) 94-108.

[171] H.H. Oberg, M. Peipp, C. Kellner, S. Sebens, S. Krause, D. Petrick, S. Adam-Klages, C. Rocken, T. Becker, I. Vogel, D. Weisner, S. Freitag-Wolf, M. Gramatzki, D. Kabelitz, D. Wesch, Novel bispecific antibodies increase gammadelta T-cell cytotoxicity against pancreatic cancer cells, Cancer Res., 74 (2014) 1349-1360.

[172] D. Wesch, D. Gonnermann, C. Kellner, M. Peipp, M. Hermes, C. Peters, S. Sebens, D. Kabelitz, H. Oberg, An attractive tool for γδ T cell-based immunotherapy, Gamma Delta Conference 2016, King's College, London, 2016, pp. 135.

[173] C. Laezza, M. Notarnicola, M.G. Caruso, C. Messa, M. Macchia, S. Bertini, F. Minutolo, G. Portella, L. Fiorentino, S. Stingo, M. Bifulco, N6-isopentenyladenosine arrests tumor cell proliferation by inhibiting farnesyl diphosphate synthase and protein prenylation, FASEB J., 20 (2006) 412-418.

[174] M. Bifulco, A.M. Malfitano, M.C. Proto, A. Santoro, M.G. Caruso, C. Laezza, Biological and pharmacological roles of N6-isopentenyladenosine: an emerging anticancer drug, Anticancer Agents Med. Chem., 8 (2008) 200-204.

[175] C. Laezza, M.G. Caruso, T. Gentile, M. Notarnicola, A.M. Malfitano, T. Di Matola, C. Messa, P. Gazzerro, M. Bifulco, N6-isopentenyladenosine inhibits cell proliferation and induces apoptosis in a human colon cancer cell line DLD1, Int. J. Cancer, 124 (2009) 1322-1329.

[176] M. Rajabi, P. Signorelli, E. Gorincioi, R. Ghidoni, E. Santaniello, Antiproliferative activity of N6-isopentenyladenosine on MCF-7 breast cancer cells: cell cycle analysis and DNA-binding study, DNA Cell Biol., 29 (2010) 687-691.

[177] F.P. Coxon, K. Thompson, A.J. Roelofs, F.H. Ebetino, M.J. Rogers, Visualizing mineral binding and uptake of bisphosphonate by osteoclasts and non-resorbing cells, Bone, 42 (2008) 848-860.

[178] Z. Liu, I.E. Eltoum, B. Guo, B.H. Beck, G.A. Cloud, R.D. Lopez, Protective immunosurveillance and therapeutic antitumor activity of gammadelta T cells demonstrated in a mouse model of prostate cancer, J. Immunol., 180 (2008) 6044-6053.

[179] S. Junankar, G. Shay, J. Jurczyluk, N. Ali, J. Down, N. Pocock, A. Parker, A. Nguyen, S. Sun, B. Kashemirov, C.E. McKenna, P.I. Croucher, A. Swarbrick, K. Weilbaecher, T.G. Phan, M.J. Rogers, Real-Time Intravital Imaging Establishes Tumor-Associated Macrophages as the Extraskeletal Target of Bisphosphonate Action in Cancer, Cancer Discov., (2014).

[180] E. Ferrero, P. Biswas, K. Vettoretto, M. Ferrarini, M. Uguccioni, L. Piali, B.E. Leone, B. Moser, C. Rugarli, R. Pardi, Macrophages exposed to Mycobacterium tuberculosis release chemokines able to recruit selected leucocyte subpopulations: focus on gammadelta cells, Immunology, 108 (2003) 365-374.

[181] H. Kobayashi, Y. Tanaka, J. Yagi, N. Minato, K. Tanabe, Phase I/II study of adoptive transfer of gammadelta T cells in combination with zoledronic acid and IL-2 to patients with advanced renal cell carcinoma, Cancer Immunol. Immunother., 60 (2011) 1075-1084.

[182] The Genome Sequencing Consortium, Initial sequencing and analysis of the human genome, Nature, 409 (2001) 860-921.

[183] J.H. Lin, Bisphosphonates: a review of their pharmacokinetic properties, Bone, 18 (1996) 75-85.

[184] R. Uchida, E. Ashihara, K. Sato, S. Kimura, J. Kuroda, M. Takeuchi, E. Kawata, K. Taniguchi, M. Okamoto, K. Shimura, Y. Kiyono, C. Shimazaki, M. Taniwaki, T. Maekawa, Gamma delta T cells kill myeloma cells by sensing mevalonate metabolites and ICAM-1 molecules on cell surface, Biochem. Biophys. Res. Commun., 354 (2007) 613-618.

[185] V. Kunzmann, M. Smetak, B. Kimmel, K. Weigang-Koehler, M. Goebeler, J. Birkmann, J. Becker, I.G. Schmidt-Wolf, H. Einsele, M. Wilhelm, Tumor-promoting versus tumor-antagonizing roles of gammadelta T cells in cancer immunotherapy: results from a prospective phase I/II trial, J. Immunother., 35 (2012) 205-213.

[186] M. Wilhelm, V. Kunzmann, S. Eckstein, P. Reimer, F. Weissinger, T. Ruediger, H.P. Tony, Gammadelta T cells for immune therapy of patients with lymphoid malignancies, Blood, 102 (2003) 200-206.

[187] L.S. Rosen, D. Gordon, M. Kaminski, A. Howell, A. Belch, J. Mackey, J. Apffelstaedt, M. Hussein, R.E. Coleman, D.J. Reitsma, J.J. Seaman, B.L. Chen, Y. Ambros, Zoledronic acid versus pamidronate in the treatment of skeletal metastases in patients with breast cancer or osteolytic lesions of multiple myeloma: a phase III, double-blind, comparative trial, Cancer J., 7 (2001) 377-387.

[188] J.R. Berenson, A. Lichtenstein, L. Porter, M.A. Dimopoulos, R. Bordoni, S. George, A. Lipton, A. Keller, O. Ballester, M.J. Kovacs, H.A. Blacklock, R. Bell, J. Simeone, D.J. Reitsma, M. Heffernan, J. Seaman, R.D. Knight, Efficacy of pamidronate in reducing skeletal events in patients with advanced multiple myeloma. Myeloma Aredia Study Group, N. Engl. J. Med., 334 (1996) 488-493.

[189] R.M. Conry, M.G. Rodriguez, J.G. Pressey, Zoledronic acid in metastatic osteosarcoma: encouraging progression free survival in four consecutive patients, Clin Sarcoma Res, 6 (2016) 6.

[190] M. Benrahmoune, P. Therond, Z. Abedinzadeh, The reaction of superoxide radical with N-acetylcysteine, Free Radic. Biol. Med., 29 (2000) 775-782.

[191] O.I. Aruoma, B. Halliwell, B.M. Hoey, J. Butler, The antioxidant action of N-acetylcysteine: its reaction with hydrogen peroxide, hydroxyl radical, superoxide, and hypochlorous acid, Free Radic. Biol. Med., 6 (1989) 593-597.

[192] S.B. Stephan, A.M. Taber, I. Jileaeva, E.P. Pegues, C.L. Sentman, M.T. Stephan, Biopolymer implants enhance the efficacy of adoptive T-cell therapy, Nat. Biotechnol., 33 (2015) 97-101.

[193] J.C. Ribot, S.T. Ribeiro, D.V. Correia, A.E. Sousa, B. Silva-Santos, Human gammadelta thymocytes are functionally immature and differentiate into cytotoxic type 1 effector T cells upon IL-2/IL-15 signaling, J. Immunol., 192 (2014) 2237-2243.

[194] C. Duault, D.M. Franchini, J. Familliades, C. Cayrol, S. Roga, J.P. Girard, J.J. Fournie, M. Poupot, TCRVgamma9 gammadelta T Cell Response to IL-33: A CD4 T Cell-Dependent Mechanism, J. Immunol., 196 (2016) 493-502.

[195] S.H. Lin, L.R. Kleinberg, Carmustine wafers: localized delivery of chemotherapeutic agents in CNS malignancies, Expert Rev. Anticancer Ther., 8 (2008) 343-359.

[196] C. Chauvin, U. Jarry, N. Joalland, C. Pecqueur, E. Scotet, Human Vγ9Vδ2 T Cells Spontaneously Eliminate Particular Subsets Of Primary Glioblastoma Tumor Cells, Gamma Delta Conference 2016, King's College London 2016, pp. 156.